

The translational relevance of the Annexin A1 pathway in inflammatory pathologies: opportunities for novel therapeutic development

Dalli, Jesmond

The copyright of this thesis rests with the author and no quotation from it or information derived from it may be published without the prior written consent of the author

For additional information about this publication click this link.

<https://qmro.qmul.ac.uk/jspui/handle/123456789/460>

Information about this research object was correct at the time of download; we occasionally make corrections to records, please therefore check the published record when citing. For more information contact scholarlycommunications@qmul.ac.uk

**The translational relevance of the Annexin
A1 pathway in inflammatory pathologies:
opportunities for novel therapeutic
development**

Mr. Jesmond Dalli

A thesis submitted to the University of London (Faculty of Science) for the
degree of Doctor of Philosophy

**Center for Biochemical Pharmacology,
William Harvey Research Institute,
Barts and the London School of Medicine and Dentistry.
Charterhouse Square, London EC1M 6BQ**

**I Jesmond Dalli, confirm that the work presented in this thesis is my own.
Where information has been derived from other sources, I confirm that
this has been indicated and appropriately referenced**

Signed.....

Date.....

ABSTRACT

Endogenous anti-inflammatory mediators form a complex network triggered in the host to dampen cell activation and promote resolution of inflammation. The glucocorticoid-regulated 37-kDa protein Annexin A1 is one such endogenous checkpoint effector, acting on human neutrophils *via* a specific GPCR termed FPR like-1 (FPRL1). FPRL1 belongs to the family of formyl-peptide receptors, of which FPR (the receptor for formylated peptides) is the prototype. However, very little information is available on the mechanisms governing the export of this protein from activated cells, hence the machinery required to activate the counter-regulatory circuit centred on Annexin A1. Furthermore, little data is available describing the status of Annexin A1 and the FPR receptor family in human disease conditions. These questions have been addressed in my thesis.

The analysis of PMNs and monocytes from both Wegener granulomatosis and Giant cell arthritis (GCA) patients provided strong evidence for a deregulation in the Annexin A1 pathway as I observed an increased expression of both FPRL-1 and FPR, along with an elevated cell surface Annexin A1 expression. Moreover, Western blotting against Annexin A1 membrane expression also evidenced elevated protein cleavage suggesting that this is potentially the mechanism responsible for the reported hyper-activated status of the PMNs in these pathologies, a feature I could confirm also in the flow chamber assay, where marked adhesion to endothelial cell monolayers was measured. Significantly, pharmacological manipulation of the Annexin A1 axis could *correct* cell behaviour, further supporting the notion of a deregulated Annexin A1 system in these conditions. Interestingly, very little difference was observed at the mRNA levels for both the FPRL-1 and Annexin A1 genes in samples analysed from patients suffering from Wegener granulomatosis whilst there was a significant increase in expression of both these genes in the GCA samples when compared to aged matched healthy volunteers. An observation, which suggests that the underlying mechanisms governing the regulation in these two conditions, and their potential impact on the Annexin A1 pathway, might be different.

Annexin A1 lacks a signal peptide but nonetheless is abundantly released from activated PMNs; our understanding of the route that is employed for its release is still modest. The analysis of PMN derived microparticles confirmed the presence of the Annexin A1 protein in these microstructures; I was then able to demonstrate that this protein was responsible for microparticle-induced inhibition of PMN recruitment to an

activated endothelium *in vitro* and into the airpouch *in vivo*. Furthermore, when monitoring levels of Annexin A1 positive microparticles in plasma samples from a number of human inflammatory disease, I could observe that both these microparticle subsets were altered when compared to those found in healthy age matched controls, with higher extent of PMN-derived microparticles (CD62L positive) and Annexin A1 positive microparticles. I had the opportunity to monitor these microparticles longitudinally in RA patients treated with prednisolone over a 2-week period: both CD62L and Annexin A1 positive microparticles were restored back to the values (as percentage and median fluorescence intensity) of healthy volunteers. This result occurred in parallel to an amelioration of the clinical symptoms.

The final part of my project involved assessing the anti-inflammatory properties of 5 novel Annexin A1 N-terminal derived peptides developed in collaboration with Unigene (Fairfield, NJ), that are modification of peptide Ac2-26 (which conserves the natural amino acid sequence). *In vitro* analyses of these peptides identified two peptides as the ones with the highest anti-inflammatory capabilities. In radioligand binding assays, I observed these peptides possessed similar binding affinities to the FPRL-1 as the natural peptide. More in detail, peptide 57 did not bind to FPR in a dose dependent fashion as opposed to peptide 84, even though when assessing p-ERK activity it was noted that both peptides equally activated ERK. When tested *in vivo* it was observed that both peptides were able to inhibit PMN recruitment into an inflamed mouse airpouch, with peptide 84 showing the highest potency.

The findings of this thesis provided evidence for a deregulated Annexin A1 system in the human inflammatory pathologies under observation, hence vasculitis and RA. Treatment of patients with an acute glucocorticoid regimen modulated the Annexin A1 pathway suggesting that the re-establishment of this effector of anti-inflammation, likely to occur also at the functional level, could contribute – at least partly – to the positive clinical effect of glucocorticoids in RA patients. Captivatingly, this acute glucocorticoid treatment was also observed to restore the plasma Annexin A1 positive microparticle levels to those observed in healthy age-matched volunteers, suggesting that these microstructures can potentially be used both as biomarkers of disease and also a measure of treatment effectiveness. Finally I have provided evidence for the anti-inflammatory properties of two novel Annexin A1 N-terminal derived peptides that may serve as guidance for the development of novel treatments for inflammatory disorders, depicted on the biology of this intriguing protein that is Annexin A1.

“Before God we are all equally wise – and equally foolish”

Albert Einstein

ACKNOWLEDGEMENTS

I would like to foremost express my gratitude to Professor Mauro Perretti, whose enthusiastic supervision, drive, insight, motivation and dedication made my project exceptionally captivating and instructional, I could not have asked for a better supervisor. I am thankful for always making time to discuss my progress, ideas and questions. I am also extremely thankful for your extensive efforts to secure funding so I could continue with my Ph.D.

I wish to thank Dr. Dianne Cooper, who, although not being my official supervisor, has always found time to discuss questions and ideas, always willing to provide invaluable advice. Furthermore, although being very busy you also made time to correct my manuscript. For all this I am enormously grateful.

I feel fortunate to have worked in such a dynamic, challenging and friendly department. In this regard I wish to thank all the members of the Centre for Biochemical Pharmacology, both past and present, since working with all of you has been a very enjoyable experience. I especially would like to thank my fellow postgraduate students and office buddies for stimulating conversations and a great social environment. In particular I would like to thank Dr. Derek Renshaw for his supervision during my first few months in the lab, making my integration into the new reality easy and pleasurable.

I would like to acknowledge the blood donors, Dr. Baskar DasGupta, Ms Jane Hollywood Prof. Costantino Pitzalis and Dr Stephen Kelly for collecting patient samples and ensuring that they arrive in the timeliest of manners. Furthermore, I would like to thank the midwifery staff at the Royal London Hospital for collecting umbilical cords and most importantly the financial support of the William Harvey Research Foundation and Unigene for making this research possible.

On a more personal note I wish to thank my parents and my sister, whose constant support over all these years has been instrumental in helping me achieve this very important milestone in my career. Thanks mum and dad for always believing in my abilities and supporting me all the way to the furthest of your abilities. An immense thanks goes to my partner Maggie, for all your constant support and encouragement, and for having faith in me, even during those moments when everything was going wrong. Thank you for sticking with me and for your ability to bring back a smile on my face during these difficult times. I do not know if I could have done it without you. I wish to thank my auntie Paul, uncle Joe and my cousin Annette and husband Tim for all their invaluable help and support especially during my first months England, and for supporting me in a crucial time in my career, thank you all very much from the bottom of my heart! Finally, I wish to thank all my friends who have been there for me over the years, all your help and support has not gone unnoticed!

TABLE OF CONTENTS

1. Introduction	18
1.1. Inflammation	19
1.2. Immunity	20
1.3. Annexin A1, a Glucocorticoid inducible anti-inflammatory protein. ...	23
1.3.1. The discovery	23
1.3.2. Annexin A1 and its receptor (s).....	25
1.3.3. Proposed mechanisms of action	27
1.3.4. Annexin A1 and its effect on adhesion molecules	28
1.3.5. Mechanisms of Annexin A1 Externalization.	30
1.3.6. The role of Annexin A1 in human neutrophils.....	32
1.3.7. The Annexin A1 peptides.....	34
1.4. The Formyl Peptide Receptor Family	39
1.4.1. The Discovery of the Formyl Peptide Receptors	39
1.4.2. The FPR family its agonists and the functional domains responsible for their signalling	43
1.5. Mechanisms governing the signalling processes of the FPR family ...	48
1.5.1. Activation similarities and the role of intracellular Ca ²⁺	48
1.6. Microparticles and their potential biological roles.....	54
1.6.1. Composition of microparticle plasma membranes	58
1.6.2. Microparticle cytoplasmic content	59
1.6.3. MP as intercellular transporters.....	60
1.6.4. MP and their role in inflammation	61
1.7. Rheumatic diseases.....	64
1.7.1. Rheumatoid Arthritis- a brief overview	65
1.7.2. Current Treatments for RA.....	66
1.7.3. Wegener's Granulomatosis- a brief overview	68
1.7.4. Giant Cell Arteritis	70
1.8. Aims of the thesis	73
2. Materials & Methods.....	76
2.1. Materials List.....	77
2.2. Isolation and culture of primary HUVEC.	78
2.3. Human blood leukocyte isolation.....	79
2.4. <i>In vitro</i> flow chamber assay.	81
2.5. Flow-cytometric analysis.....	86
2.5.1. Assessment of surface molecule expression on the HEK-FPR, HEK-FPRL1 and HEK-CMV cells by flow cytometry.....	88
2.5.2. Assessment of surface molecule expression on PMNs derived microparticles by flow cytometry.....	89
2.5.3. Assessment of surface molecule expression on PMNs from Wegener granulomatosis, GCA patients and healthy volunteers by flow cytometry	91
2.5.4. Assessment of surface molecule expression on PMNs from RA patients by flow cytometry	91
2.6. Sodium Dodecyl Sulphate - Polyacrylamide Gel Electrophoresis (SDS- PAGE) Western Blotting.	93
2.6.1. Sample Preparation.....	93

2.6.2.	BCA (Bicinchoninic acid) protein assay	99
2.7.	Description of novel Acetyl2-26 derived peptides.	101
2.8.	RadioLigand binding assay.	103
2.9.	Real-Time Reverse Transcription-PCR.....	107
2.9.1.	RNA extraction.....	107
2.9.2.	Reverse Transcription.....	110
2.9.3.	cDNA Quantification.....	112
2.9.4.	Real-Time PCR	113
2.10.	Isolation of Microparticles.	118
2.10.1.	From Purified Neutrophils.....	118
2.10.2.	From whole blood.....	119
2.11.	In-gel Digestion and LC/MS/MS analysis	120
2.12.	Assessment of Reactive Oxygen Species (ROS) production by microparticles.	122
2.13.	Animal experiments.....	123
2.13.1.	Murine Lung Endothelial Cell (MLEC) isolation.	123
2.13.2.	Bone Marrow Neutrophil Extraction and Purification	125
2.13.3.	AirPouch Model of Inflammation	126
2.14.	Statistical Analysis	128
3.	<u>Results.....</u>	129
3.1.	The Annexin A1 system and Rheumatic disease, is there a link?	130
3.1.1.	Role of the Annexin A1 system in Wegener's Vasculitis.	130
3.1.2.	Role of Annexin A1 in Giant Cell Arteritis.....	144
3.1.3.	Understanding the influence of an acute glucocorticoid treatment on the Annexin A1 system in patients with Rheumatoid Arthritis.....	153
3.2.	Annexin A1 in microparticles and its potential role as biomarker.	166
3.2.1.	Exploring a novel mechanism for Annexin A1 release.....	166
3.2.2.	The <i>in vitro</i> anti-inflammatory role on Annexin A1 in PMN derived microparticles	175
3.2.3.	The <i>in vivo</i> anti-inflammatory role on Annexin A1 in PMN derived microparticles	183
3.2.4.	Reactive Oxygen Species production by human PMN-derived Microparticles.....	187
3.2.5.	Stimulus specific expression of the Annexin A1 system in M.P.	194
3.2.6.	Determining the role of the Annexin A1 and FPRL1 positive M.P. in Rheumatic Diseases.....	198
3.2.7.	Exploring the potential of monitoring microparticle populations as biomarkers during disease treatment in Rheumatoid Arthritis.	200
3.3.	Development of novel Ac2-26 derived peptides	208
4.	<u>Discussion</u>	232
4.1.	The Annexin A1 circuit and Rheumatic disease, is there a link?	233
4.1.1.	Evidence for a dysregulated Annexin A1 pathway Wegener Granulomatosis and Giant Cell Arteritis	233
4.1.2.	Modulation of the Annexin A1 system upon glucocorticoid administration in Rheumatoid Arthritis.....	243
4.2.	The biological functions of Annexin A1 in PMN derived microparticles	

4.2.1. The anti-inflammatory action of Annexin A1 in PMN-derived microparticles	257
4.2.2. Reactive oxygen species production by PMN-derived microparticles	260
4.2.3. The potential for use of of Annexin A1 positive PMN-derived microparticles as biomarkers of treatment and disease	262
4.3. Developing and testing of Novel Ac2-26 peptides.....	268
5. <u>Conclusion</u>	277
6. <u>References</u>	283

LIST OF FIGURES

FIGURE 1-1: MOLECULAR STRUCTURE OF ANNEXIN-A1	24
FIGURE 1-2: SITES OF ACTION OF THE ANNEXIN A1 SYSTEM IN THE LEUKOCYTE ADHESION CASCADE.....	30
FIGURE 1-3: NEUTROPHIL EXTRAVASATION AND ANNEXIN A1 EXTERNALIZATION.	34
FIGURE 1-4: FIGURE OUTLINING THE TYPICAL ORGANIZATION OF THE FPR RECEPTOR FAMILY	39
FIGURE 1-5: SCHEMATIC SIGNALLING PATHWAYS OF AN ACTIVATED FORMYL-PEPTIDE RECEPTOR.....	49
FIGURE 1-6: A SCHEMATIC OUTLINING THE PRODUCTION OF MP, OUTLINING THE SEGREGATION OF CELL SPECIFIC ANTIGENS UPON ACTIVATION AND THE RELEASE OF DIFFERENT ANTIGENS DEPENDING ON THE STIMULUS BEING PROVIDED (VANWIJK, VANBAVEL ET AL. 2003).....	55
FIGURE 1-7: SCHEMATIC OUTLINING THE ROLES PLAYED BY MP IN THE PATHOGENESIS OF SOME THE RHEUMATIC DISEASES.	63
FIGURE 1-8: SIZE OF VESSELS AS DEFINED AT THE CHAPEL HILL CONSENSUS CONFERENCE AND ASSOCIATED RHEUMATIC DISEASES..	68
FIGURE 2-1: NEUTROPHIL ISOLATION FROM HUMAN BLOOD USING HISTOPAQUE DOUBLE DENSITY CENTRIFUGATION.	80
FIGURE 2-2: ILLUSTRATION OF THE COUNTING GRID ON A NEUBAUER HAEMOCYTOMETER.....	81
FIGURE 2-3: ASSEMBLY OF THE PARALLEL PLATE FLOW CHAMBER.....	82
FIGURE 2-4: REPRESENTATIVE DOT PLOT OF HUMAN BLOOD LEUKOCYTES.....	87
FIGURE 2-5: LIGHT ABSORBANCE AND LIGHT EMISSION SPECTRA OF FITC.	87
FIGURE 2-6: FIGURE OUTLINING THE SETUP BEING EMPLOYED FOR THE BINDING ASSAYS.....	104
FIGURE 2-7: DETERMINING THE OPTIMAL CONCENTRATION OF TRACER TO BE EMPLOYED IN RADIOLIGAND BINDING ASSAY.	105
FIGURE 2-8: DETERMINING THE OPTIMAL CONCENTRATION OF COLD PEPTIDE TO BE EMPLOYED IN RADIOLIGAND BINDING ASSAY.....	105
FIGURE 2-9: FIGURE OUTLINING A TYPICAL EXPRESSION PROFILE FOR A REAL TIME PCR REACTION.....	115
FIGURE 2-10: FIGURE OUTLINING THE EFFICIENCY PLOT OBTAINED FOR THE GAPDH GENE..	116
FIGURE 2-11: ENDOTHELIAL CELL POSITIVE SELECTION USING MAGNETIC DYNABEADS.....	125
FIGURE 2-12: NEUTROPHIL ISOLATION FROM MOUSE BONE MARROW CELLS USING A PERCOLL GRADIENT.....	126
FIGURE 3-1: ANNEXIN A1 EXPRESSION ON CONTROL (CT) AND WEGENER GRANULOMATOSIS PATIENTS PRE AND POST EDTA WASH.	134
FIGURE 3-2: FPR EXPRESSION ON CONTROL (CT) AND WEGENER GRANULOMATOSIS PATIENTS.....	135
FIGURE 3-3: FPRL1 EXPRESSION ON CONTROL (CT) AND WEGENER GRANULOMATOSIS PATIENTS.....	136
FIGURE 3-4: MEMBRANE PR3 EXPRESSION ON CONTROL (CT) AND WEGENER GRANULOMATOSIS PATIENTS.....	137
FIGURE 3-6: MEMBRANE EXPRESSION OF ANNEXIN A1 IN PMNs FROM CT AND WEGENER VASCULITIS PATIENTS..	138
FIGURE 3-7: CYTOSOLIC EXPRESSION OF ANNEXIN A1 IN PMNs FROM CT AND WEGENER VASCULITIS PATIENTS.....	139
FIGURE 3-8: mRNA EXPRESSION OF ANNEXIN A1 IN WEGENER GRANULOMATOSIS PATIENTS VERSUS CT IN PMNs..	140
FIGURE 3-9: mRNA EXPRESSION OF FPRL1 IN WEGENER GRANULOMATOSIS PATIENTS VERSUS CT IN PMNs..	141
FIGURE 3-10: EFFECT OF WEGENER VASCULITIS ON ACTIVATION OF PMN'S UNDER FLOW, AND THE REVERSAL OF THIS EFFECT THROUGH THE ADMINISTRATION OF HR-ANNEXIN A1.....	143
FIGURE 3-11: FPR EXPRESSION ON CONTROL (CT) AND GCA PATIENTS.	146
FIGURE 3-12: FPRL1 EXPRESSION ON CONTROL (CT) AND GCA PATIENTS.....	146
FIGURE 3-13: ANNEXIN A1 EXPRESSION ON CONTROL (CT) AND GCA PATIENTS.	147
FIGURE 3-14: PR3 EXPRESSION ON CONTROL (CT) AND GCA PATIENTS.....	147

FIGURE 3-15: MEMBRANE EXPRESSION OF ANNEXIN A1 IN PMNS FROM CT AND GCA PATIENTS.....	148
FIGURE 3-16: CYTOSOLIC EXPRESSION OF ANNEXIN A1 IN PMNS FROM CT AND GCA PATIENTS.....	149
FIGURE 3-17: mRNA EXPRESSION OF ANNEXIN A1 IN GCA PATIENTS VERSUS CT IN PMNS.	150
FIGURE 3-18: mRNA EXPRESSION OF FPRL1 IN GCA PATIENTS VERSUS CT IN PMNS.	150
FIGURE 3-19: EFFECT OF GCA ON PMN ACTIVATION UNDER FLOW, AND THE REVERSAL OF THIS EFFECT THROUGH THE ADMINISTRATION OF HR-ANNEXIN A1 (ANNEXIN A1),	152
FIGURE 3-20: REPRESENTATIVE DOT PLOT OF HUMAN BLOOD LEUKOCYTES AS EMPLOYED FOR MONITORING OF ANTIGEN EXPRESSION DURING THIS STUDY.	155
FIGURE 3-21: FLOW CYTOMETRIC ANALYSIS OF BLOOD AND SYNOVIAL PMNS CD11B DERIVED FROM RHEUMATOID ARTHRITIS (RA) PATIENTS PRIOR TO STEROID TREATMENT.	156
FIGURE 3-22: FLOW CYTOMETRIC ANALYSIS OF BLOOD AND SYNOVIAL MONOCYTES CD11B DERIVED FROM RHEUMATOID ARTHRITIS (RA) PATIENTS PRIOR TO STEROID TREATMENT.	157
FIGURE 3-23: WHITE BLOOD PROFILE DURING A 14-DAY STEROID TREATMENT.....	160
FIGURE 3-24: CD11B EXPRESSION ON MONOCYTES AND PMNS DERIVED FROM RHEUMATOID ARTHRITIS (RA) PATIENTS DURING A 14-DAY STEROID TREATMENT.....	161
FIGURE 3-25: CD62L EXPRESSION ON MONOCYTES AND PMNS DERIVED FROM RHEUMATOID ARTHRITIS (RA) PATIENTS DURING A 14-DAY STEROID TREATMENT.....	162
FIGURE 3-26: FPR EXPRESSION ON MONOCYTES AND PMNS DERIVED FROM RHEUMATOID ARTHRITIS (RA) PATIENTS DURING A 14-DAY STEROID TREATMENT.....	163
FIGURE 3-27: FPRL1 EXPRESSION ON MONOCYTES AND PMNS DERIVED FROM RHEUMATOID ARTHRITIS (RA) PATIENTS DURING A 14-DAY STEROID TREATMENT.....	164
FIGURE 3-28: ANNEXIN A1 EXPRESSION IN ON MONOCYTES AND PMNS DERIVED FROM RHEUMATOID ARTHRITIS (RA) PATIENTS DURING A 14-DAY STEROID TREATMENT.....	165
FIGURE 3-29: DETERMINING THE PRESENCE OF MICROPARTICLES FOLLOWING INSTRUMENT CALIBRATION.....	167
FIGURE 3-30: FACS ANALYSIS ON MICROPARTICLES DERIVED FROM ADHERENT PMN.	167
FIGURE 3-31: WESTERN BLOT SHOWING THE PRESENCE OF ANNEXIN A1 IN PMN DERIVED MICROPARTICLES.	170
FIGURE 3-32: LC/MS/MS ANALYSIS OF THE 37kDA IMMUNOREACTIVE BAND.....	170
FIGURE 3-33: FACS ANALYSIS ON MICROPARTICLES DERIVED FROM ADHERENT PMN.	171
FIGURE 3-34: FACS ANALYSIS ON MICROPARTICLES DERIVED FROM ADHERENT PMN.	172
FIGURE 3-35: STAINING FOR MICROPARTICLES DERIVED FROM UNSTIMULATED PMNS.	173
FIGURE 3-36: FLOW-CYTOMETRIC ANALYSIS OF ANNEXIN A1 +VE M.P FOLLOWING EDTA WASH.....	174
FIGURE 3-37: CHARACTERIZATION OF PMN DERIVED M.P. PRIOR TO USE IN FLOW CHAMBER. M.P.	177
FIGURE 3-38: ANNEXIN A1 RICH MICROPARTICLES INHIBIT PMN/HUVEC INTERACTION UNDER FLOW.	178
FIGURE 3-39: CHARACTERIZATION OF PMN DERIVED M.P. PRIOR TO USE IN FLOW CHAMBER..	179
FIGURE 3-40: ROLE FOR ANNEXIN A1 IN THE INHIBITORY PROPERTY OF PMN-DERIVED MICROPARTICLES.	180
FIGURE 3-41: CHARACTERIZATION OF PMN DERIVED M.P. PRIOR TO USE IN FLOW CHAMBER.	181
FIGURE 3-42: CONFIRMING THAT ONLY MICROPARTICLE FROM FMLP STIMULATED PMN POSSESS INHIBITORY PROPERTIES.	182
FIGURE 3-43: ANTI-INFLAMMATORY EFFECTS OF HUMAN PMN-DERIVED MICROPARTICLES.	184
FIGURE 3-44: POSITIVE IDENTIFICATION OF THE MURINE PMN-DERIVED MICROPARTICLES..	185
FIGURE 3-45: ANTI-INFLAMMATORY EFFECTS OF MURINE PMN-DERIVED MICROPARTICLES..	186
FIGURE 3-46: ANALYSIS OF THE MICROPARTICLE POPULATIONS PRODUCED BY DIFFERENTIAL STIMULATION USING FLOW CYTOMETRY.	189
FIGURE 3-47: FLOW CYTOMETRIC DETERMINATION OF FPRL1 IN ROS PRODUCING PMN DERIVED MICROPARTICLES.....	190
FIGURE 3-48: REACTIVE OXYGEN SPECIES PRODUCTION BY PMN DERIVED MICROPARTICLES	191

FIGURE 3-49: REACTIVE OXYGEN SPECIES ANALYSIS USING THE DCFDA ASSAY.....	192
FIGURE 3-50: FLOW CYTOMETRIC DETERMINATION OF ANNEXIN A1, FPRL1, AND CD62L PMN DERIVED M.P.	195
FIGURE 3-51: WESTERN BLOT ANALYSIS OF M.P. RICH SUPERNATANT	196
FIGURE 3-52: WESTERN BLOT ANALYSIS OF MICROPARTICLES DEPLETED SUPERNATANT....	197
FIGURE 3-53: FLOW CYTOMETRIC DETERMINATION OF ANNEXIN A1 AND FPRL1 +VE M.P. IN PLASMA FROM PATIENTS SUFFERING FROM RHEUMATIC DISEASES.	199
FIGURE 3-54: CD62L EXPRESSION ON PLASMA MICROPARTICLES DERIVED FROM RHEUMATOID ARTHRITIS (RA) PATIENTS DURING A 14-DAY STEROID TREATMENT.....	202
FIGURE 3-55: CD62P EXPRESSION ON PLASMA MICROPARTICLES DERIVED FROM RHEUMATOID ARTHRITIS (RA) PATIENTS DURING A 14-DAY STEROID TREATMENT.....	203
FIGURE 3-56: CD54 EXPRESSION ON PLASMA MICROPARTICLES DERIVED FROM RHEUMATOID ARTHRITIS (RA) PATIENTS DURING A 14-DAY STEROID TREATMENT.	204
FIGURE 3-57: CD14 EXPRESSION IN ON PLASMA MICROPARTICLES DERIVED FROM RHEUMATOID ARTHRITIS (RA) PATIENTS DURING A 14-DAY STEROID TREATMENT.	205
FIGURE 3-58: FPRL1 EXPRESSION ON PLASMA MICROPARTICLES DERIVED FROM.....	206
FIGURE 3-59: ANNEXIN A1 EXPRESSION IN ON PLASMA MICROPARTICLES DERIVED FROM RHEUMATOID ARTHRITIS (RA) PATIENTS DURING A 14-DAY STEROID TREATMENT.	207
FIGURE 3-60: FLOW CYTOMETRIC ANALYSIS OF THE THREE TRANSFECTED HEK CELL LINES..	209
FIGURE 3-61: WESTERN BLOTTING ANALYSIS COMPARING THE ACTIVATION POTENCY OF P- ERK BY THE TWO Ac2-26 PEPTIDES.	211
FIGURE 3-62: WESTERN BLOTTING ANALYSIS COMPARING THE ACTIVATION POTENCY OF NOVEL ANNEXIN A1 N-TERMINALLY DERIVED PEPTIDES.....	213
FIGURE 3-63: FLOW CHAMBER ANALYSIS DETERMINING THE INHIBITORY POTENCY OF THE NOVEL Ac2-26 PEPTIDES.	214
FIGURE 3-64: WESTERN BLOTTING ANALYSIS OF THE PEP57 DOSE RESPONSE HIGHLIGHTING ITS P-ERK ACTIVATION POTENCY THROUGH THE FPRL1 RECEPTOR.....	216
FIGURE 3-65: WESTERN BLOTTING ANALYSIS OF THE PEP84 DOSE RESPONSE HIGHLIGHTING ITS P-ERK ACTIVATION POTENCY THROUGH THE FPRL1 RECEPTOR.....	217
FIGURE 3-66: WESTERN BLOTTING ANALYSIS OF THE PEP57 DOSE RESPONSE HIGHLIGHTING ITS P-ERK ACTIVATION POTENCY THROUGH THE FPR RECEPTOR.	218
FIGURE 3-67: WESTERN BLOTTING ANALYSIS OF THE PEP84 DOSE RESPONSE HIGHLIGHTING ITS P-ERK ACTIVATION POTENCY THROUGH THE FPR RECEPTOR.....	219
FIGURE 3-68: WESTERN BLOTTING ANALYSIS DETERMINE IF P-ERK ACTIVATION BY PEP57 IS BEING ACTIVATED BY OTHER RECEPTORS APART FROM THE FPR FAMILY IN THE HEK CELLS.	220
FIGURE 3-69: WESTERN BLOTTING ANALYSIS DETERMINE IF P-ERK ACTIVATION BY PEP84 IS BEING ACTIVATED BY OTHER RECEPTORS APART FROM THE FPR FAMILY IN THE HEK CELLS.	220
FIGURE 3-70: FLOW CHAMBER ANALYSIS DETERMINING THE INHIBITORY POTENCY OF PEP84.	221
FIGURE 3-71: FLOW CHAMBER ANALYSIS DETERMINING THE INHIBITORY POTENCY OF PEP57	222
FIGURE 3-72: DETERMINING THE OPTIMAL CONCENTRATION OF TRACER TO BE EMPLOYED IN RADIOLIGAND BINDING ASSAY.	224
FIGURE 3-73: DETERMINING THE OPTIMAL CONCENTRATION OF COLD PEPTIDE TO BE EMPLOYED IN RADIOLIGAND BINDING ASSAY.	224
FIGURE 3-74: RADIOLIGAND BINDING ASSAYS DETERMINING THE AFFINITY OF PEP84 AND PEP57 TO THE FPRL1 RECEPTOR.	225
FIGURE 3-75: RADIOLIGAND BINDING ASSAYS DETERMINING THE AFFINITY OF PEP84 AND PEP57 TO THE FPR RECEPTOR.....	226
FIGURE 3-76: ANTI-INFLAMMATORY EFFECTS OF THREE NOVEL Ac2-26 DERIVED PEPTIDES.	228
FIGURE 3-77: THE EFFECTS THE NOVEL Ac2-26 DERIVED PEPTIDES ON BLOOD LEUKOCYTE POPULATIONS.	229
FIGURE 3-78: FLOW CYTOMETRIC ANALYSIS ON FPRL1 EXPRESSION ON HEK-FPRL1 CELLS FOLLOWING CO INCUBATION WITH PEPTIDE Ac2-26, PEP57 OR PEP 84.	231

LIST OF TABLES

TABLE 1-1 SUMMARY OF THE AGONISTS AND ANTAGONISTS FOR THE FPR FAMILY MEMBERS.	44
TABLE 2-1: FORMULATIONS FOR SDS-PAGE RESOLVING AND STACKING GELS USING NATIONAL DIAGNOSTIC BUFFERS.	96
TABLE 2-2: PREPARATION OF BSA STANDARDS FOR THE BCA PROTEIN ASSAY.....	100
TABLE 2-3: SEQUENCES, PEPTIDE CONTENTS AND NOMENCLATURE FOR EACH OF THE NOVEL AC2-26 DERIVED PEPTIDES AND THE PARENT PEPTIDE.....	101
TABLE 3-1: TABLE OUTLINING THE DEMOGRAPHIC PARAMETERS FOR THE SUBJECTS EMPLOYED FOR THIS STUDY INCLUDING TREATMENT REGIMES.....	133
TABLE 3-2: TABLE OUTLINING THE DEMOGRAPHIC PARAMETERS FOR THE SUBJECTS EMPLOYED FOR THIS STUDY INCLUDING TREATMENT REGIMES.....	145
TABLE 3-3: TABLE OUTLINING THE DEMOGRAPHIC PARAMETERS FOR THE SUBJECTS EMPLOYED FOR THIS STUDY INCLUDING TREATMENT REGIMES.....	155
TABLE 3-4: TABLE OUTLINING THE ABUNDANCE OF THE DIFFERENT MICROPARTICLE POPULATIONS PRODUCED UPON DIFFERENTIAL STIMULATION.	191
TABLE 3-5 QUANTIFICATION RESULTS FOR REACTIVE OXYGEN SPECIES DETERMINATION IN PMN DERIVED MICROPARTICLES.....	193
TABLE 3-6 TABLE SUMMARISING THE MFI VALUES FOR THE 3 DISTINCT M.P. PREPARATIONS.	193
TABLE 3-7 SUMMARY OF THE FLOW CYTOMETRIC ANALYSIS CONDUCTED ON THE HEK CELL LINES..	210

Work conducted in this thesis has contributed to the following publications:

- Perretti M and **Dalli J**. *Exploiting the Annexin A1 pathway for the development of novel anti-inflammatory therapeutics*. BJP (commissioned review)
- Gastardelo TS, Damazo AS, **Dalli J**, Flower RJ, Perretti M, Oliani SM. *Functional and ultrastructural analysis of annexin A1 and its receptor in extravasating neutrophils during acute inflammation*. Am J Pathol. 2009 Jan;174(1):177-83.
- **Dalli J**, Norling LV, Renshaw D, Cooper D, Leung KY, Perretti M. *Annexin 1 mediates the rapid anti-inflammatory effects of neutrophil-derived microparticles*. Blood. 2008 Sep 15;112(6):2512-9.
- Gavins FN, **Dalli J**, Flower RJ, Granger DN, Perretti M. *Activation of the annexin 1 counter-regulatory circuit affords protection in the mouse brain microcirculation*. FASEB J. 2007 Jun;21(8):1751-8.

ABBREVIATIONS

-/-	knockout
α 1-AT	α 1- antitrypsin
A β ₄₂	42 amino acid form of amyloid β
ABC	ATP binding cassette
ADAM	A disintegrin and metalloprotease
Ac2-26	Acetylated peptide from residues 2-26 of Annexin A1
AF1	Antiflammin-1 peptide from residues 39-47 of uteroglobin
AF2	Antiflammin-2 peptide from residues 246-254 of Annexin A1
APS	Ammonium Persulphate
ANCA	Anti-neutrophil cytoplasmic antibodies
AnxA1	Annexin A1
BCA	Bicinchoninic acid
BAD	BCL2 antagonist of cell death
BSA	Bovine Serum Albumin
BOC2	N-t-butoxycarbonyl-Phe-D-Leu-Phe-D-Leu-Phe
BSS	Buffered Saline Solution
cAMP	Cyclic adenosine monophosphate
CD	Cluster of Differentiation molecule
CaCl ₂	Calcium Chloride
CCR	Chemokine (C-C motif) receptor
CMV	Cytomegalovirus
cPLA ₂	Cytosolic phospholipase A ₂
CXCL	Chemokine (C-X-C motif) ligand
DAG	diacylglycerol
DMARD	Disease modifying anti-rheumatic drugs
DMSO	Dimethylsulphoxide
DNA	Deoxyribonucleic acid
DPBS	Dulbecco's Phosphate Buffered Saline
DTT	Dithiothreitol
EC	Endothelial cell
ECL	Enhanced chemiluminescence
EDTA	Ethylene-(2,2)-diamine-tetracetic acid
EGF	Epidermal growth factor
eNOS	Endothelial nitric oxide synthase
ERK	Extracellular signal-regulated kinase
FCS	Foetal calf serum
FITC	Fluorescein isothiocyanate
fMLP	Formyl-Met-Leu-Phe
FPR	Formyl Peptide Receptor
FPRL	Formyl Peptide Receptor Like
FSC	Forward-scattered light
HEK	Human embryonic kidney
HL	human myeloid leukaemia-cell
HRP	Horseradish peroxidase
GDP	guanosine diphosphate
GCA	Giant cell arthritis
GTP	guanosine triphosphate
GlyCAM-1	glycosylation-dependent cell adhesion molecule-1

GPCR	G-protein coupled receptor
GR	Glucocorticoid receptor
HBSS	Hanks buffered saline solution
HPCA-1	haematopoietic progenitor cell antigen-1
HIV	Human immuno-deficiency virus
HS	Human serum
HUVEC	Human umbilical vein endothelial cells
IC ₅₀	Half maximal inhibitory concentration
ICAM	Intercellular cell adhesion molecule
IgG	Immunoglobulin
IL	Interleukin
iNOS	Inducible nitric oxide synthase
i.p.	Intraperitoneal
IP ₃	inositol 1,4,5-trisphosphate
ITGAM	integrin alpha M
i.v.	Intravenous
JAM	Junctional adhesion molecule
JNK	c-Jun N-terminal kinase
K _d	Dissociation constant
kDa	Kilo Dalton
KO	Knock-out
LPS	Lipopolysaccharid
mAB	Monoclonal antibody
M.P.	Microparticles
Mac-1	Macrophage antigen-1
MAdCAM-1	Mucosal addressin cell adhesion molecule-1
MAPK	Mitogen activated protein kinase
MFI	Median fluorescence intensity
MLEC	Murine lung endothelial cells
MPO	Myeloperoxidase
mRNA	Messenger RNA
L-NAME	Nw-Nitro-L-arginine methyl ester
LXA ₄	Lipoxin A ₄
NK	Natural Killer
NF-kB	Nuclear factor kappa B
NO	Nitric oxide
NSAIDs	Non-steroidal anti-inflammatory drugs
PAF	Platelet activating factor
PAGE	Polyacrylamide gel electrophoresis
PBMC	Peripheral blood mononuclear cells
PBS	Phosphate buffered saline
PECAM-1	Platelet-endothelial cell adhesion molecule-1
PCR	Polymerase chain reaction
PGI ₂	Prostaglandin I ₂ (Prostacyclin)
PI3K	Phosphoinositide-3 kinase
PLA ₂	Phospholipase A ₂
PLCb	phospholipase Cb
PMA	phorbol 12-myristate 13-acetate
PMN	Polymorphonuclear cells
PSGL1	P-selectin glycoprotein ligand-1

Pred	Prednisolone
PR3	Protinease 3
PtIns(4,5)P ₂	Phosphatidylinositol 4,5-biphosphate
PTX	Pertussis toxin
RA	Rheumatoid arthritis
RANTES	Regulated upon activation, normal T-cell expressed and secreted
RBC	Red blood cells
RPMI 1640	Roswell Park Memorial Institute 1640 medium
ROS	Reactive oxygen species
SAA	Serum amyloid protein A
s.c.	Sub-cutaneous
SCR	Short consensus repeat
SDS	Sodium dodecylsulphate
SLE	Systemic lupus erythematosus
sLe ^a	Sialyl Lewis ^a
sLe ^x	Sialyl Lewis ^x
SSC	Side-scattered light
TACE	TNF- a converting enzyme
TBS	Tris buffered saline
TEMED	Tetramethylethlenediamine
TIMP	tissue inhibitor of metalloprotinease
TNF-a	Tumor necrosis factor -a
VCAM	Vascular cell adesion molecule
VE-Cadherin	Vascular endothelial cadherin
WT	Wildt-type
WRW ₄	Try-Arg-Try-Try-Try-Try peptide

1. Introduction

1.1. Inflammation

Inflammation (Latin, *inflamatio*, to set on fire) is a complex biological response of vascular tissues to harmful stimuli, such as irritants, pathogens or damage. This is a process initiated by the organism as a response to tissue injury or infection in an attempt to remove the invading pathogens as well as initiate the healing process. Inflammation can be classified as either acute or chronic. Acute inflammation is the initial response of the body to harmful stimuli and is achieved by the increased movement of plasma and leukocytes from the blood into the injured tissues. A cascade of biochemical events propagates and matures the inflammatory response, involving the local vascular system, the immune system, and various cells within the injured tissue. Acute inflammation is a short-term process, usually appearing in a few minutes or hours and ceasing once the injurious stimulus has been removed. It is characterised by five cardinal signs: loss of function, increased temperature, redness, swelling, and pain. Cells already present in all tissues initiate the process of acute inflammation, mainly tissue macrophages called dendritic cells, endothelial cells and mastocytes. Once activated by an insult (infection, burn, etc.), they undergo activation and release inflammatory mediators responsible for the signs of inflammation. In acute inflammation, removal of the stimulus halts the recruitment of monocytes into the inflamed tissue, and existing macrophages exit the tissue via lymphatics.

If the inflammatory insult is not cleared within the short term it leads to chronic inflammation. This is a pathological condition characterised by concurrent active inflammation, tissue destruction, and attempts at repair. This condition is

not characterised by the classic signs of acute inflammation listed above. Instead, chronically inflamed tissue is characterised by the infiltration of mononuclear immune cells including monocytes, macrophages, lymphocytes, and plasma cells; tissue destruction and attempts at healing, which include angiogenesis and fibrosis. Unlike in acute inflammation, in chronically inflamed tissue the stimulus is persistent, and therefore recruitment of monocytes is maintained, existing macrophages are tethered in place, and proliferation of macrophages is stimulated.

1.2. Immunity

The term immunity describes a state of having sufficient biological defences to avoid infection, disease, or other unwanted biological invasion. Immunity involves both specific and non-specific components. The non-specific components, or the innate branch of the immune response, play a role in preventing the infection by eliminating a wide range of pathogens irrespective of antigenic specificity. It involves local cells in the affected tissue, such as macrophages and mast cells that act as “alarm systems” and triggers leading to the co-activation of the ensuing events.

Adaptive immunity conveys a pathogen-specific response to each new assault/pathogen encountered and is subdivided into two major subtypes depending on how the response was induced. Naturally acquired immunity results from contact with a disease-causing agent, when the contact was not deliberate, whereas artificially acquired immunity develops only through deliberate actions such as vaccination. Both naturally and artificially acquired

immunity can be further subdivided depending on whether immunity is induced in the host or passively transferred from an immune host. Passive immunity is acquired through transfer of antibodies or activated T-cells from an immune host, and is short lived, usually lasting only a few months, whereas active immunity is induced in the host itself by antigen, and lasts much longer, sometimes life-long.

Once leukocytes arrive at a site of infection or inflammation, they release mediators that control the later accumulation and activation of other cells. However, in inflammatory reactions initiated by the immune system, the antigen itself exerts the ultimate control.

Inflammatory mediators are soluble, diffusible molecules that act locally at the site of tissue damage and infection, and at more distant sites. They can be divided into exogenous and endogenous mediators. Bacterial products and toxins can act as exogenous mediators of inflammation. Notable among these is endotoxin, or lipopolysaccharide (LPS) of Gram-negative bacteria. The immune system of higher organisms has probably evolved around in a veritable sea of endotoxin, so it is perhaps not surprising that this substance evokes powerful responses. In fact endotoxin can trigger complement activation, resulting in the formation of anaphylatoxins C3a and C5a, which cause vasodilatation and increase vascular permeability. Endotoxin also activates the Hageman factor, leading to activation of the coagulation and fibrinolytic pathways as well as the kinin system. In addition, endotoxins elicit T cell proliferation, and have been described as superantigen for T cells.

Endogenous mediators of inflammation are produced from within the (innate and adaptive) immune system itself, as well as other systems. For example, they can be derived from molecules that are normally present in the plasma in an inactive form, such as peptide fragments of some components of complement, coagulation, and kinin system(s) components. Mediators of inflammatory responses are also released at the site of injury by a number of cell types.

Thus the modulation of inflammation through the inhibition of an immune response can provide beneficial effects in chronic inflammatory responses where the inflammatory insult is self-propagating, in this context glucocorticoids are currently the most potent immunomodulators available. Glucocorticoids, first used therapeutically in 1950 (Hench 1950), regulate the immune system by modulating the expression of pro-inflammatory genes and the expression of transcription factors.

1.3. Annexin A1, a Glucocorticoid inducible anti-inflammatory protein.

1.3.1. The discovery

In the early 1980's data generated from different laboratories showed that glucocorticoid inhibition of arachidonic acid production was dependent on the synthesis and release of inhibitory proteins which down-regulated phospholipase A₂ (PLA₂) activity. This in turn repressed the prostaglandin [PG] generation from perfused lungs and activated macrophages. Glucocorticoid treatment resulted in the production of a factor that mimicked the inhibitory action of the steroid itself. The factor was then identified as a protein of 37 kDa and named 'lipocortin' (nowadays referred to as Annexin A1 (Flower 1988)).

Annexin A1 (ANXA1) was the first characterized member of the annexin superfamily of proteins, so called since their main property is to bind (i.e. to *annex*) to cellular membranes in a Ca²⁺-dependent manner (Crumpton and Dedman 1990).

The 13 members of this family show a high degree of structural homology, with each possessing four (or 8 in the case of Annexin A6) repeated units of approximately 70 amino acids within the core and C-terminal regions. These units are believed to confer their Ca²⁺ and phospholipid binding properties. The N-terminal region of each family member is, however, unique and is considered to confer the biological specificity of the individual proteins. The basic structure of ANXA1 is shown in Figure 1-3. Crystallographic studies indicate that the

four repeated sequences are arranged around a pore, giving the protein a “doughnut” appearance.

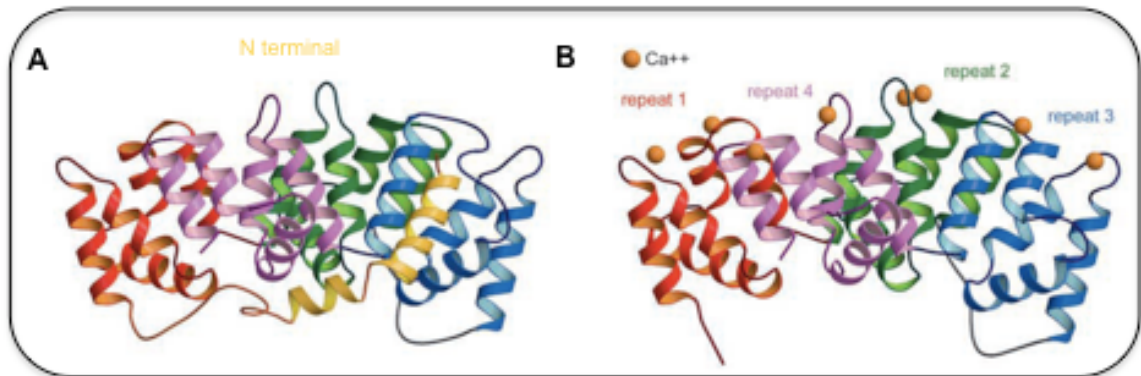


Figure 1-1: Molecular structure of Annexin-A1. Ribbon diagram of (A) Annexin A1, showing the N-terminal domain (yellow) and the protein core, consisting of four annexin repeats (1-4). (B) In response to calcium binding (indicated by the orange spheres), the N-terminal domain. Adapted from (Rosengarth and Luecke 2003).

Furthermore, the N-terminal 26 amino acid residues form two α -helices with a bend at amino acid 16 that causes the first residues to insert within the protein core. This N-terminal domain is embedded within the pore at low Ca^{2+} concentrations, but elevations in Ca^{2+} levels expose this region and may thereby influence the biological activity of the protein. In this context studies have highlighted the fact that the Glu-255, which is present on the D-helix of repeat 3 is essential for calcium binding to take place (Rosengarth and Luecke 2003).

Annexin A1 expression and localization within the cell varies between cell types. In human neutrophils Annexin A1 is predominantly localised in gelatinase granules (Perretti, Christian et al. 2000) on the other hand in mast cells Annexin A1 is found in the α -granules (Oliani, Christian et al. 2000). This confined distribution does not seem to be a common trend however since in

macrophages and most of other cell types investigated, Annexin A1 was observed to be either in the cytoplasm, attached to the plasma membrane or in the nucleus depending upon the state of activation. Under resting conditions a large proportion of the protein is found intracellularly (Peers, Smillie et al. 1993) however following a short stimulation, such as exposure (10 min) to glucocorticoid (Solito, Kamal et al. 2003) or LPS (Solito, Christian et al. 2006), Annexin A1 translocates from the cytoplasm to the cell surface where it is retained in a Ca^{2+} -dependent manner (Solito, Christian et al. 2006). Longer stimulations, such as a 1-h glucocorticoid exposure, has been shown to enhance the translocation of Annexin A1 both *in vivo* and *in vitro* from the cytoplasm to the nucleus with an induction of Annexin A1 *de novo* synthesis (Buckingham 1996).

1.3.2. Annexin A1 and its receptor (s)

Initial studies have outlined that Annexin A1 binds to human monocytes in a saturable and trypsin-sensitive manner suggesting that this protein could be binding to a specific protein site and not merely to membrane anionic phospholipids. Further studies highlighted that in fact Annexin A1 binding is also sensitive to collagenase, cathepsin G and elastase, where treatment of the cells with any of these enzymes lead to an almost complete loss of Annexin A1 binding capacity to monocytes (Goulding, Pan et al. 1996). Analysis of surface radioiodinated human monocytes by SDS PAGE and autoradiography demonstrated that recombinant Annexin A1, in conjunction with a monoclonal antibody directed against Annexin A1 (clone 1B), immunoprecipitated two molecules with molecular masses of 15 kDa and 18 kDa respectively however no data is available on the nature of these two proteins (Goulding, Pan et al.

1996).

Other later studies have demonstrated that Annexin A1 and/or the N-terminal peptides derived from this protein (Annexin A1 peptido-mimetics) bind to various extents all three members of the Formyl Peptide Receptor (FPR) family (as will be discussed further in subsequent sections). Moreover, recent data has showed that this protein and its peptides exert the majority of their anti-inflammatory action through the FPR-Like 1 (FPRL1) receptor (Hayhoe, Kamal et al. 2006; Kamal, Hayhoe et al. 2006). In fact, it was demonstrated through the use of competitive binding assays, that both the Annexin A1-derived peptide Acetyl (Ac) 2-26 (corresponding to amino acids 2-26 of the N-terminal portion of Annexin A1) and a shorter peptide denoted Ac2-12 (Ac- AMVSEFLKQAW) competed for specific [³H]LXA₄ binding with similar affinities (50% inhibitory concentration; IC₅₀ ~0.3 μM) in HEK 293 cells transfected with the FPRL1 receptor. This point was further highlighted by the co-incubation of [¹²⁵I-Tyr] Ac2- 26 peptide with the HEK293 transfected with the recombinant FPRL1 receptor; which gave a specific and saturable binding with a K_d value of ~0.9 μM (Hayhoe, Kamal et al. 2006). Furthermore, the full-length Annexin A1 protein also competed for [¹²⁵I-Tyr] Ac2-26 binding with similar affinity, whereas the Ac2-12 peptide gave an IC₅₀ of ~20 μM. A scrambled sequence peptide Ac2-26 did not compete for specific [¹²⁵I-Tyr] Ac2-26 binding (Perretti, Chiang et al. 2002; Hayhoe, Kamal et al. 2006)

The direct interaction between Annexin A1 and FPRL1 was further substantiated via immunoprecipitation of both the proteins from activated

human polymorphonuclear (PMN) cell lysates. Activation of PMNs with either PMA or fMLF induces adhesion and mobilization of Annexin A1 on to the cell surface. Following lysis proteins were co-immunoprecipitated (IP) from this soup using an anti-Annexin A1 specific antibody. Analysis of the IP by SDS-PAGE revealed a band of approximately 70kDa, which was immunoreactive to the FPRL1 specific antibody in a western blot analysis. Furthermore, immunoreactive bands of ~36 kDa, consistent with molecular mass of Annexin A1, were obtained by co-immunoprecipitation with anti-FPRL1 antibody (Perretti, Chiang et al. 2002), thus confirming the interaction between Annexin A1 and the FPRL1 in human cells.

1.3.3. Proposed mechanisms of action

Low affinity FPR (or FPRL) ligands play a very important role in leukocyte recruitment toward the focus of inflammation where high concentrations of chemo-attractant are met and in which high affinity ligand-receptor interactions result in receptor saturation, desensitization and/or sequestration. This scenario requires high (micromolar) extracellular Annexin A1 concentrations in close proximity to the focus of inflammation; concentrations that are higher than the Annexin A1 levels reported in normal serum. However, a number of mechanisms have been proposed which could lead to the localized increase of extracellular Annexin A1 levels including: glucocorticoid administration (Flower 1988), inflammatory and infectious diseases (Goulding, Jefferiss et al. 1992; Cuzzocrea, Taylor et al. 1997) and tissue or cell damage (Rescher, Goebeler et al. 2006). In such cases the released Annexin A1 is proteolytically cleaved generating the active N-terminal peptides. A substantial degree of N-terminal Annexin A1 proteolysis also occurs within cells, e.g., in neutrophils

upon extravasation into the sub-endothelium (Perretti, Croxtall et al. 1996). Thus, suggesting that the N-terminal Annexin A1 peptides are the physiologically active entity released from cells or generated extracellularly at sites of inflammation.

Apart from a role in inflammation Annexin A1 has also been shown to have a role in the control of cardiovascular function. Studies conducted by Wu and colleagues have demonstrated Annexin A1 has beneficial haemodynamic effects through inhibition of inducible nitric oxide synthase (iNOS) expression when rats suffering from septic shock were treated with dexamethasone (Wu, Croxtall et al. 1995). In addition, dexamethasone and the N-terminal fragment of Annexin A1 inhibited the induction of cyclooxygenase-2 (COX-2) and interleukin (IL)-12 mRNA, as well as the release of PGE₂, in a dose-dependent manner, whilst augmenting the release of IL-10 in a number of macrophage cell lines activated with LPS. Furthermore, suppression of nitric oxide and PGE₂ release could also be important in the neuroprotective properties described for Annexin A1, since inflammatory metabolites may participate in the establishment of neurone and oligodendrocyte damage in ischaemic and neurodegenerative disorders (Merrill, Ignarro et al. 1993; Ferlazzo, D'Agostino et al. 2003).

1.3.4. Annexin A1 and its effect on adhesion molecules

The leukocyte adhesion process is very important in the context of inflammation, playing an integral part in the extravasation of inflammatory cells from the microvasculature to the sites of insult. A number of recently published reports conducted both *in vivo* and *in vitro* have shown that exogenous and

endogenous Annexin A1 strongly inhibit this process (Perretti, Getting et al. 2001; Hayhoe, Kamal et al. 2006).

A mechanism that has been put forward to explain the observed regulation of cell migration is the interference of Annexin A1 with adhesion molecules that mediate leukocyte-endothelium interactions. In support of this theory is the observation that Annexin A1 colocalizes with the $\alpha_4\beta_1$ integrin on the surface of monocytic cells. It is known that $\alpha_4\beta_1$ integrin interacts with vascular cell adhesion molecule (VCAM)-1 expressed by endothelial cells to mediate several neutrophil functions such as tethering, rolling and firm adhesion (Meerschaert and Furie 1995); a process that could be reversed by the extracellular domain of VCAM-1. Moreover, co-immunoprecipitation experiments demonstrated that Annexin A1 and VCAM-1 competed for binding to the $\alpha_4\beta_1$ integrin in a pro-monocytic cell line (Solito, Romero et al. 2000) (Figure 1-2).

Another adhesion molecule, which seems to be under the regulation of Annexin A1 is L-selectin, whereby this protein promotes L-selectin shedding (Strausbaugh and Rosen 2001). A process which has recently been confirmed by de Coupade *et al.* (de Coupade, Solito et al. 2003) who have proposed that endogenous Annexin A1, externalized on the cell surface of monocytic cells by treatment with glucocorticoids, could facilitate CD62L shedding through a calcium-dependent interaction the adhesion molecule. However, the details of the mechanism governing this process are still elusive.

Work conducted by Lim and colleagues along with that done by Das and colleagues suggests that Annexin A1 also has an influence on CD11b expression. It was in fact observed that CD11b protein expression but not mRNA levels in eosinophils were altered in a number of *in vivo models* upon post glucocorticoid treatment (Lim, Flower et al. 2000), an effect that was, at least in part, mediated by Annexin A1 (Das, Lim et al. 1997).

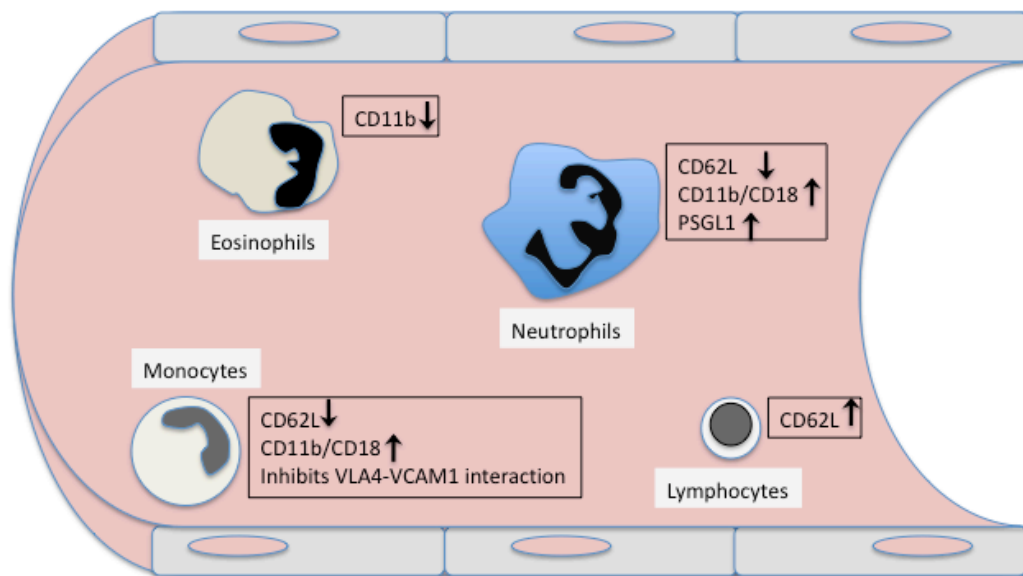


Figure 1-2: Sites of action of the Annexin A1 system in the leukocyte adhesion cascade.

1.3.5. Mechanisms of Annexin A1 Externalization.

As previously described this protein's main site of action appears to be at the cell surface, at least with respect to its actions on inflammatory cells, thus understanding the mechanisms responsible for its externalization is of great importance.

Initial studies have shown that Annexin A1 does not possess a signal sequence, a property it shares with other proteins such as IL-1 and galectin-1, as opposed to most pre-secretory proteins that have a sequence of about 13 to 30

hydrophobic amino acids, which allow transport across the membrane of the endoplasmic reticulum. This will then lead to the direction of the protein to the endoplasmic reticulum-Golgi system and hence permits vesicular packaging for release by exocytosis (Milstein, Brownlee et al. 1972) Furthermore, its gene does not include a nucleotide sequence which would encode for an appropriate amino acid sequence (Raynal and Pollard 1994)

The specific localization of Annexin A1 within the neutrophil gelatinase granules was thought for some time to be the only pathway by which this protein is externalized from this cell type, as these granules and their contents can be exported to the cell surface by a process of exocytosis, similar to that described by Borregaard and colleagues (Sengelov, Follin et al. 1995; Borregaard and Cowland 1997).

However, only neutrophils contain these gelatinase granules, thus limiting the functionality of this mechanism to this cell type, leaving the question on the mechanism/s governing the transport of Annexin A1 to the cell membrane in other cell types unanswered. It thus seems likely that Annexin A1 can also be exported via an alternative pathway at least in other cell types. This hypothesis was confirmed when it was shown that brefeldin A, monensin and nocodazole, three drugs which block the classical pathway of protein secretion had no effect on the capacity of dexamethasone to induce the cellular exportation of Annexin A1 in brain (cortex, hippocampus, hypothalamus), anterior pituitary tissue and peritoneal macrophages (Philip, Flower et al. 1998).

Recent data have started to shed some light into one possible mechanism of Annexin A1 exportation, at least in folliculo-stellate cells. In these cells, Annexin A1 is secreted through a non-classical pathway that is dependent on the ABCA1 transporter. This was shown by the pharmacological blockade of the ABCA1-transporter with geranyl-geranyl pyrophosphate and sulfobromophthalein, which in turn lead to a significant reduction Annexin A1 externalization. Partial silencing of ABCA1 expression in TtT/GF cells by siRNA also significantly decreased the amount of cell surface Annexin A1. Further information can be obtained by looking into the secretory pathways described for other annexin family members, where for example Annexin A2 secretion in human umbilical endothelial cells is dependent on S100A10 protein expression (Omer, Meredith et al. 2006).

1.3.6. The role of Annexin A1 in human neutrophils

Annexin A1 is expressed in relatively large amounts (between 2% and 4%) in the cytosol of human neutrophils (Francis, Balazovich et al. 1992; Rosales and Ernst 1997). The pattern of expression appears to be punctuate with patches of immunoreactivity seen throughout the cell within a specific subset of neutrophil organelles. Other studies conducted with human resting neutrophils *in vitro* (Perretti, Christian et al. 2000) and with rat neutrophils within an inflamed vascular bed *in vivo* (Oliani, Paul-Clark et al. 2001) found that a majority (~50%) of intracellular Annexin A1 colocalized with gelatinase granules, whereas a much smaller proportion was detected on the plasma membrane (Figure 1-3).

In parallel studies, it was demonstrated that treatment with glucocorticoids increased Annexin A1 content in circulating leucocytes in man (Goulding, Godolphin et al. 1990) and rodents (Perretti and Flower 1996). As cytosolic Annexin A1 is actively mobilized when the neutrophil adheres to the endothelium, glucocorticoid-dependent increase in cellular Annexin A1 content would increase the amount of the protein externalized on the cell surface once the leukocyte adheres to the inflamed vascular endothelium. A survey of human donors indicated that between 50% and 70% of total Annexin A1 is externalized onto the neutrophil surface upon adhesion to endothelial cell monolayers (Perretti 1997). It is likely that the Annexin A1 system in the neutrophil can be finely regulated by post-translational mechanisms. The Annexin A1 N-terminal region, which is unique to this member of the family, contains several putative phosphorylation sites. For instance, epidermal growth factor receptor activation leads to Annexin A1 phosphorylation on tyrosine 21 (Hollenberg, Valentine-Braun et al. 1988). More recently, protein kinase C (PKC)-dependent serine/threonine phosphorylation has been reported in a pituitary cell line, and this event was essential to externalization of the protein (John, Cover et al. 2002).

Recent data indicates the existence of a phenylmethylsulfonyl fluoride-sensitive enzymatic activity responsible for Annexin A1 cleavage (Rescher, Goebeler et al. 2006). However, a metalloprotease has also been proposed to cleave the first seven amino acid of the Annexin A1 N-terminus (Movitz, Sjolín et al. 1999). A more recent publication has showed that proteinase 3 is another enzyme, which can cleave Annexin A1 in a similar way to that observed *in vivo* (Vong,

D'Acquisto et al. 2007). Whereas this aspect warrants further analysis, it is already conceivable that Annexin A1 cleavage might be of clinical relevance.

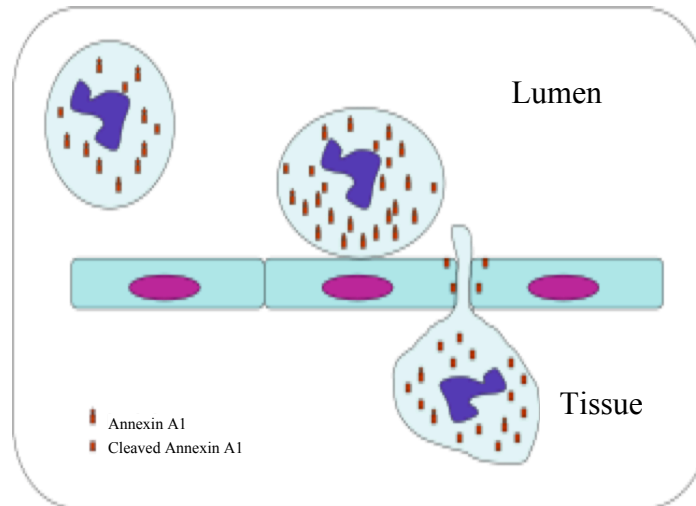


Figure 1-3: Neutrophil extravasation and Annexin A1 externalization. Neutrophil adhesion to the post capillary venule leads to the externalization and cleavage of the Annexin A1 protein on the neutrophil cell membrane along with the transfer of this protein to the endothelium (Adapted from Perretti 2002).

In fact, bronchoalveolar lavage fluids obtained from patients suffering from cystic fibrosis and other lung pathologies display a marked degree of Annexin A1 proteolysis (Tsao, Meyer et al. 1998). These studies proposed a role for elastase as the proteolytic Annexin A1-cleavage enzyme. In line with the data just discussed, Annexin A1 (intact and cleaved) is often recovered from inflammatory exudates, and inflamed tissues, in correspondence to the peak of neutrophilia (Vergnolle, Comera et al. 1997).

1.3.7. The Annexin A1 peptides

A number of peptides mainly derived from the unique N-terminal portion of the Annexin A1 protein have been shown to possess anti-inflammatory properties. The first peptide to be synthesized is that derived from the first 188 amino acid sequence of the Annexin A1 protein. This was in the first instance shown to

inhibit Thromboxane A₂ production in perfused guinea pig lungs when stimulated with fMLF (Cirino, Flower et al. 1987). Its anti-inflammatory properties were then highlighted in various models of inflammation where the administration of this peptide was shown to reduce PMN recruitment following ischaemia reperfusion injury in the rat brain (Relton, Strijbos et al. 1991) and into an inflamed airpouch (Perretti, Ahluwalia et al. 1993). Apart from its anti-inflammatory effects, the Ac1-188 fragment has also been shown to display antipyretic properties when administered into the rat brain stimulated with INF- γ and IL1- β . Interestingly, this antipyretic effect was not observed in the same model when the brain was stimulated with PGE₂, indicating that its effects are probably exerted on cytokine synthesis upstream prostaglandin synthesis (Carey, Forder et al. 1990).

One of the most extensively studied Annexin A1 peptides is peptide Ac2-26, which mimics the 2nd to the 26th amino acids of the 54-aa N-terminal region, and like the Ac1-188 fragment (and the native protein) has an N-terminal acetylation to increase its stability, and possibly its half-life. When employed in an *in vitro* model of leukocyte/endothelium interaction, the flow chamber model, it was observed that this peptide was able to reduce the number of rolling neutrophils on to the activated endothelial cells. Interestingly, no effect was observed on the number of adherent cells suggesting that this peptide selectively inhibits one portion of the leukocyte recruitment cascade. Furthermore, apart from reducing the rolling on neutrophils this peptide was also able to increase the clearance rate of apoptotic neutrophils by human macrophages *in vitro* (Maderna, Yona et al. 2005), suggesting that the Ac2-26 peptide also has pro-resolving properties.

In vivo the Ac2-26 peptide has been shown to exert an anti-inflammatory effect in models of myocardial ischaemia reperfusion (I/R) (La, D'Amico et al. 2001), mesentery I/R (Gavins, Yona et al. 2003), glycogen peritonitis (Teixeira, Das et al. 1998) and IL1 β airpouch (Perretti, Ahluwalia et al. 1993), where it was reported to significantly reduce the recruitment of neutrophils to the site of injury/inflammation (Perretti and Flower 1993). In other more complex acute models such as zymosan peritonitis apart from a reduction in PMN recruitment at an early time point (4h) a reduction of monocyte recruitment into the peritoneal cavity after 24h was also reported (Getting, Flower et al. 1997). Furthermore, in models of tissue injury such as glacial acetic acid induced gastric ulcers (Martin, Perretti et al. 2008), contusive spinal chord injury (Liu, Zhang et al. 2007), septic shock (Ritchie, Sun et al. 2003) and mouse skin oedema (Perretti, Ahluwalia et al. 1993) the administration of the Ac2-26 peptide has been shown to partially - and in some cases completely - reverse the damage. This effect is, at least in part, mediated through down regulation of pro-inflammatory factors such as TNF- α , IL1 β and Cox2. However, the anti-inflammatory properties of this peptide are not just restricted to acute models of inflammation. In a number of chronic models, including, the carrageenan induced arthritis, intra-articular administration of the Ac2-26 peptide was shown to reduce disease severity through a reduction in neutrophil recruitment (Yang, Leech et al. 1997).

Shorter versions of the Ac2-26 peptide, the Ac2-12 and the Ac2-6 peptides, have also been shown to produce some degree of anti-inflammatory effects *in*

in vivo in acute models of inflammation. The administration of peptide Ac2-12 in models of inflamed mouse dorsal airpouch (Perretti, Chiang et al. 2002), myocardial I/R (La, D'Amico et al. 2001) and inflamed mesenteric microvasculature reduced PMN recruitment (La, D'Amico et al. 2001), infarct size and the number of adherent PMN to the inflamed vascular endothelium respectively. On the other hand, the latter peptide has only been reported to exert anti-inflammatory properties in the mouse inflamed airpouch model where it reduced PMN recruitment into the airpouch (Perretti, Chiang et al. 2002). Thus, although not as potent as the longer peptide Ac2-26, these shorter mimetics still retain some of the anti-inflammatory properties characteristic of the parent protein, further highlighting the importance of this region in the resolution of inflammation.

Work conducted by a number of laboratories has shown that a peptide derived from a region completely independent of the N-terminal of the Annexin A1 protein, more precisely amino acids 247-253 – in the third repeat of the core region of the protein - referred to as antinflammin-2 (AF2), also possesses anti-inflammatory properties. Of interest this region is also the portion of the Annexin A1 protein that is of highest sequence similarity to uteroglobin (Miele, Cordella-Miele et al. 1988). In fact this sequence corresponds to the amino acids 40-46 on the uteroglobin monomer a region that corresponds to the C-terminal part of the third α -helix (Vostal, Mukherjee et al. 1989). This peptide has been shown to reduce the number of rolling cells but not the number of adherent cells in the flow chamber model, as was observed for the Ac2-26 peptide, thus suggesting that it might be acting through a similar pathway as the N-terminal

derived peptide (Kamal, Hayhoe et al. 2006). Furthermore, AF2 was effective in inhibiting Leukotrine C₄ and Thromboxane B₂ production in unsensitized and ovalbumin-sensitized guinea pig lungs *in vitro*, whilst it had no effect in histamine or bradykinin sensitized lungs, pointing to a stimulus specific response by the AF2 peptide (Sautebin, Cirino et al. 1992). On the other hand, *in vivo*, this nona-peptide has been shown to inhibit eosinophil recruitment in a model of allergic conjuvitis (Sohn, Kim et al. 2003). AF2 has also been shown to suppress endotoxin-induced uveitis in rats and murine allergic conjuvitis with potencies similar to those observed for glucocorticoids (Chan, Ni et al. 1991). Moreover, this peptide is effective in reducing vascular permeability and PMN infiltration in a model of carrageenan-induced rat footpad oedema (Camussi, Tetta et al. 1990).

1.4. The Formyl Peptide Receptor Family

1.4.1. The Discovery of the Formyl Peptide Receptors

Chemoattractant receptors comprise a single 350–370 amino acid polypeptide chain, which spans the cell membrane seven times (Figure. 1-4). The N-terminus and three loops, believed to be essential for interaction with the ligand, are exposed extracellularly, and the carboxyl terminus and three additional loops of importance for intracellular signalling, are facing the cytosolic side of the membrane (Murphy 1994; Murphy 1997). Neutrophil chemoattractant GPCRs all share sequence similarities in some of the transmembrane domains as well as in the cytosolic signalling domains. In contrast, the surface-exposed regions which confer the ligand specificity of the GPCRs show a lower degree of sequence similarity (Miller and Falke 2004).

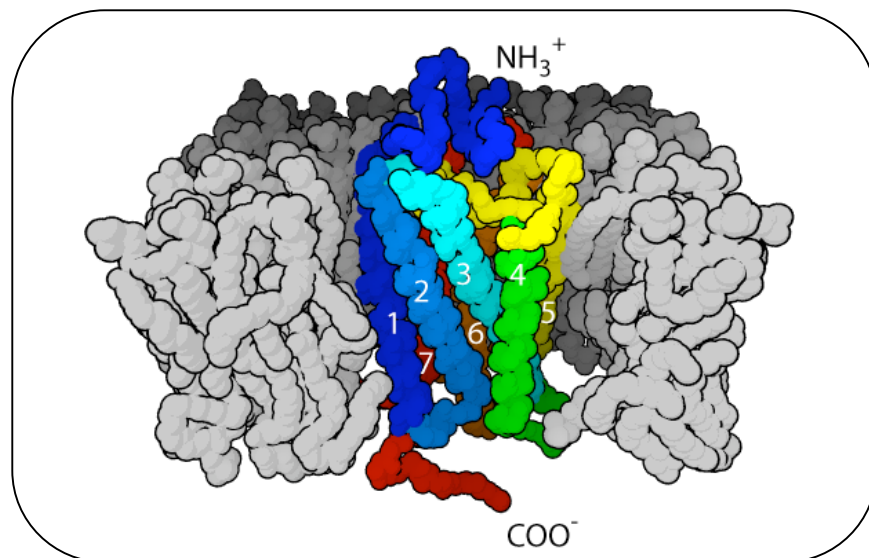


Figure 1-4: Figure outlining the typical organization of the FPR receptor family

The N-formylated peptides, derived from Gram-negative bacteria and human cell mitochondria, were initially identified as chemoattractants for human phagocytes (Chen, Bernstein et al. 1995; Su, Gong et al. 1999; Gavins, Yona et

al. 2003; Bellner, Thoren et al. 2005). Ligand binding and chemical cross-linking allowed the identification of distinct high-affinity cell surface binding proteins for fMLF, which migrated as a broad band on SDS-PAGE with an apparent molecular mass between 55 and 70 kDa (Walther, Riehemann et al. 2000; Perretti, Chiang et al. 2002). Boulay and co-workers isolated two human cDNAs encoding a 350 amino acid protein from a cDNA library prepared from differentiated HL-60 cells (Boulay, Tardif et al. 1990; Boulay, Tardif et al. 1990). These two cDNAs differ in the organization of their 5' and 3' flanking regions as well as by two nucleotides in the coding sequence, yet both encode a functional protein that belongs to the G protein-coupled receptor family. This receptor, termed FPR by its high affinity interaction with the bacterial formyl peptide, is encoded by a 6 kb single copy gene (Perez, Holmes et al. 1992; Haviland, Borel et al. 1993; Murphy, Tiffany et al. 1993). The open reading frame is intronless, but the 5' untranslated region resides on three exons. The *FPR* gene contains three *Alu* repeats, one in each intron, and a third in the 3' flanking region, indicating that the different cDNA clones originally isolated may be derived by alternative polyadenylation (Haviland, Borel et al. 1993). The proposed promoter contains a non-consensus TATA box and an inverted CCAAT element. Two mRNAs are produced in HL-60 myeloid cells and human monocytes by alternative splicing of exon 2 (Murphy, Tiffany et al. 1993). The presence of this exon permits the potential formation of stem-loop structures that could affect mRNA stability (Boulay, Tardif et al. 1990; Murphy and McDermott 1991).

Sequence analysis of cDNA clones isolated from different sources revealed amino acid differences that do not alter the pharmacological profile (Boulay, Tardif et al. 1990; Perez, Holmes et al. 1992), suggesting that there are allelic forms of FPR and a polymorphism of the *FPR* gene. FPR binds and is activated by picomole to low nanomole concentrations ($K_d < 1$ nM) of fMLF, and was thus defined as the high-affinity fMLP receptor.

The cellular distribution of FPR is not restricted to neutrophils and monocytes, as previously thought. It is also expressed in hepatocytes, dendritic cells, astrocytes, microglia cells, and the tunica media of coronary arteries (Lacy, Jones et al. 1995; McCoy, Haviland et al. 1995). More recently, by using an antiserum directed against the carboxyl terminus of human FPR receptor, it was shown that the FPR receptor, or an antigenically similar receptor, is widely localized in different human tissues and organs, including thyroid, adrenals, liver, and the nervous system. It is therefore speculated that FPR may have broader functions than host defence against bacterial infection (Becker, Forouhar et al. 1998).

Two additional human genes, designated *FPRL1* (FPR-like 1) and *FPRL2* (FPR-like 2), were subsequently isolated by low-stringency hybridization using FPR cDNA as a probe (Klein, Paul et al. 1998; Le, Gong et al. 1999; Hu, Le et al. 2001; Tiffany, Lavigne et al. 2001) and shown to cluster with *FPR* on human chromosome 19q13.3 (Le, Gong et al. 1999; Tiffany, Lavigne et al. 2001). *FPRL1* is defined as a low-affinity fMLP receptor, based on its activation only by high concentrations of fMLP (μ M range) *in vitro* (Gao, Lee et al. 1999; Le,

Murphy et al. 2002). However, it is unclear whether such concentrations of fMLP could be generated at sites of bacterial infection or tissue injury. Therefore, the role of FPRL1 as another *bona fide* functional fMLP receptor *in vivo* remains to be determined. This receptor exhibits an amino acid sequence similarity of 69% to FPR (Fig. 1), but the degree of identity differs in different regions of the receptors. A high degree of identity is found in the three cytosolic loops of the receptors, whereas the carboxyl tail and the extracellular domains have lower degrees of identity. Taken together, this suggests that the ligand-binding epitopes as well as the signalling properties might differ between the two receptors.

The *FPRL2* gene has a 56% sequence identity to human FPR and 83% sequence identity to FPRL1. The expression profile of this gene is different to that of FPRL1, in fact it is expressed in monocytes, mature and immature dendritic cells but not in neutrophils (Durstin, Gao et al. 1994). Furthermore very little is known about its function and only a few ligands most of which are synthetic have been identified for this receptor. To date, the only endogenous ligand described for this receptor is the F2L ligand, which is an acetylated amino-terminal peptide derived from the cleavage of the human haeme-binding protein (Migeotte, Riboldi et al. 2005). This peptide binds and activates the receptor in the low nanomolar range, triggering a cascade of events through the G_i class of heteromeric G proteins leading to intracellular Ca²⁺ release and cAMP accumulation. Peptide Ac2-26, activates FPRL2 mediated chemotaxis in cells transfected with the receptor (Ernst, Lange et al. 2004). In contrast, the

expression of the FPRL2 in *Xenopus* oocytes did not result in any functional responses to fMLP (Durstin, Gao et al. 1994).

1.4.2. The FPR family its agonists and the functional domains responsible for their signalling

Due to the limited knowledge on the FPLR2 receptor the remainder of my summary will concentrate on FPR and FPRL1; furthermore, the latter receptors are co-expressed in neutrophils, the cell type of interest in this study, thus unless otherwise stated the term FPR family will refer to FPR and FPRL1.

The FPR is a high-affinity pattern recognition receptor with the ability to recognize a number of N-formylated peptides, formed as part of prokaryotic protein synthesis (Fu, Dahlgren et al. 2003; Rabiet, Huet et al. 2005), supporting the idea that this receptor evolved to mediate trafficking of phagocytes to sites of bacterial invasion or tissue damage. The receptor also binds formylated peptides of mitochondrial origin (Fu, Dahlgren et al. 2003), and based on studies with free amino, desamino, and acetylated derivatives of the potent model peptide fMLP, it was believed that the formyl group was of utmost importance for the binding affinity and function of the chemoattractant. However, recent work reveals that FPR also recognizes nonformylated peptides as well as peptides with several other modifications, which all bind with high affinity and activate the receptor (Gao, Becker et al. 1994; Chen, Bernstein et al. 1995). In addition, FPRL-1 recognizes and is activated by peptides that lack all sequence similarities with the peptides originally isolated from bacteria. Important examples of such proteins and peptides are, the GP-41 envelope protein of the human immunodeficiency virus type 1 (Le, Jiang et al. 2000), a

member of the annexin family of calcium-regulated proteins (Perretti, Chiang et al. 2002; Gavins, Yona et al. 2003) and proteins linked to the onset of Alzheimer's (Table 1-1) (De, Chen et al. 2000).

Although no defined structure has been identified as the determinant for FPR binding and activation, the close relationship between structural variation and function is illustrated by the fact that substitution of the carboxyterminal D-methionine in W-peptide (WKYMVm), which is a hexa-peptide that uses both FPR and FPRL1, for the L-isomer generates a peptide that loses most of the FPR-binding affinity (Freer, Day et al. 1980; Christophe, Karlsson et al. 2001), and replacement of the formyl group in fMLP by a tert-Boc (tBoc) group generates a receptor-specific antagonist with low receptor affinity (Freer, Day et al. 1980).

Functional domains on the FPR receptor have been extensively analyzed using receptor chimeras and site-directed mutations. Chimeric receptors constructed between C5aR and FPR suggested the involvement of multiple FPR domains in recognition of the agonist fMLP, including the first, second, and third extracellular loops. The transmembrane domains in FPR are also implicated in contributing to the formation of a ligand binding structure (Mills, Miettinen et al. 2000). Studies with chimeric receptors composed of segments from FPR and FPRL1 suggested that the first and third extracellular loops with adjacent transmembrane domains in FPR were essential for its high-affinity binding for fMLP (Le, Ye et al. 2005).

Table 1-1 Summary of the agonists and antagonists for the FPR family members.

Expressing Cell Types	Ligands	Receptor	Antagonist (s)
Cortical Cells of the adrenal, As, DC, EC, H, LC, M, N, NB, NS	fMLP and other formyl peptides from bacteria and mitochondria, WKYMVm, WKGVMm, WKRMVm, Annexin 1 ₁₋₂₆ , Annexin 1 ₉₋₂₃ , T20 (DP176), fMIVIL, fMIVTFL, gG-2p20	FPR	BOC-PLPLPL, Boc-MLF, Several N-Ureido peptides, cyclosporine H, CHIPS
As, iDC, L, M, Mi, N, T, Ep, NB, SF, spleen, testis	fMLP and other formyl peptides from bacteria and mitochondria, WKYMVM WKYMVm, Annexin A1 and related peptides, SAA, Hp(2-20), LL-37, Ab ₄₂ , HIV envelope protein fragments -T20, T21 (DP107), F peptide, V3 peptide, -N36, LXA ₄ , MMK1, D2D3 _[x1-247] , PrP ₁₀₆₋₁₂₆ , MHC binding peptide, Compound 43, sCKb8-1, fMIVIL, fMIVTFL, PACAP27	FPRL1	WRWWWW, FLIPr, PBP10, BOC-PLPLPL, Boc-MLF
M, iDC, DC	Annexin 1 ₁₋₂₅ , F2L, WKYMVM, Hp(2-20)	FPRL2	

Cell abbreviations: As, Astrocytes; DC, dendritic cell; EC, endothelial cell; Ep, epithelial cells; H, hepatocytes; iDC, immature DC; L, lung; LC, lung carcinoma cell; M, monocyte; Mi, microglia; N, neutrophil; NB, neuroblastoma; NS, nervous system; SF, synovial fibroblasts; T, T cells.

Agonist abbreviations: Ab, amyloid b; fMLF, formylmethionyl-leucyl-phenylalanine; F2L, FPL2 Ligand; LXA4, lipoxin A4; MHC, major histocompatibility complex; SAA, serum amyloid A; WKYMVm, Trp-Lys-Tyr-Met-Val-D-Met; WKYMVM, Trp-Lys-Tyr-Met-Val-L-Met, CHIPS, chemotaxis inhibitory protein secreted by *Staphylococcus aureus*; FLIPr 105-AA protein isolated from *S. aureus*; fMIVIL, fMIVTFL, putative degradation fragments from *Listeria monocytogenes* components, PACAP27 pituitary adenylate cyclase-activating polypeptide 27 for FPR, FPRL1, and FPRL2.

In addition, three noncontiguous clusters of amino acid residues in the first extracellular loop and the adjacent transmembrane domains in FPR are important for its high-affinity interaction with fMLP (Quehenberger, Pan et al. 1997). Consistent with these results, in a study where HEK293 cells were transfected with a number of chimaeric receptors in which one or more of the transmembrane domains of FPR were replaced by the sequences from FPRL1, the cells either did not migrate or showed greatly reduced efficacy in response to fMLP (Le, Ye et al. 2005).

On the other hand, an intriguing observation was obtained when these cells were incubated with the W-peptide to stimulate phagocytes with a certain degree of preference for FPRL1 (Le, Gong et al. 1999; Dahlgren, Christophe et al. 2000). In fact, in this case the peptide induced migration of the HEK293 cells

expressing all chimeric receptors, including those chimeras that had failed to show any chemotactic response to fMLP. These results further highlight the possibility that different peptides can exploit different, possibly unrelated domains of the receptor to activate it.

A recent search for new FPR antagonists, using a ligand-based virtual screening technique, identified 30 different FPR antagonistic compounds belonging to nine distinct chemical families (Edwards, Bologna et al. 2005), suggesting that there will be an increasing number of antagonists also identified for FPRL1. The only FPRL1-specific antagonist described so far is the recently identified hexapeptide, WRWWWW. This peptide has no effect on FPR signalling but blocks activation by most (but not all) FPRL1 agonists (Bae, Lee et al. 2004). The WRWWWW peptide also affects cellular activities mediated by FPRL2, the FPR family member expressed selectively in cells of the monocytic lineage (Shin, Lee et al. 2006).

LXA₄ was the first high-affinity ligand described for FPRL1, where initially it was shown to activate monocytes through FPRL1, to induce adherence and migration. However, its most prominent activity was then shown to be inhibition of neutrophil functions using the same receptor (Serhan 2002; Levy and Serhan 2003). The dichotomy in responses elicited by this lipid and the fMLP peptide upon activation of the FPRL1 receptor has been linked to a differential activation of the receptor. In fact, some data suggest that LXA₄ competes with activating agonists for binding to FPRL1, and that the binding of LXA₄ switches the function of FPRL1 towards the generation of an inhibitory

signal suggested to involve a novel polyisoprenyl phosphate signalling pathway (Levy, Fokin et al. 1999; Chiang, Fierro et al. 2000; Fierro, Colgan et al. 2003; Levy, 1999). Furthermore, it has been shown that whereas N-glycosylation of the receptor is essential for its recognition of peptide sequences this is not true for LXA₄ where recognition is independent of glycosylation. Moreover, more recent data has shown that the seventh transmembrane and adjacent regions are essential for LXA₄ recognition (Le, Ye et al. 2005), in contrast to signalling by other peptide agonists where their high affinity recognition and signalling has been shown to be independent of these regions.

Recently, a number of novel peptide agonists of diverse origin and distinct chemical entities have been identified that selectively activates FPRL1. Amongst these agonists one finds the peptide domains derived from the envelope proteins of human immunodeficiency virus type 1 (HIV-1) (Miller and Falke 2004) and at least three amyloidogenic polypeptides, SAA (Rabiet, Huet et al. 2005), Ab42 (Murphy 1994) and a 21 amino acid fragment of human prion (PrP 106–126) (Dalpiaz, Pecoraro et al. 1999) (Table 1-1 on page 45).

1.5. Mechanisms governing the signalling processes of the FPR family

1.5.1. Activation similarities and the role of intracellular Ca²⁺

The biology of FPR and the downstream signalling pathways it activates have been studied extensively as a model system in GPCR research. In contrast, little is known about signalling from FPRL1, however it is reasonable to assume that this receptor uses similar signalling pathways as the FPR, since, apart from these two receptors being structurally similar, the cellular responses they induce are almost identical. Receptor signalling upon chemoattractant stimulation through FPR and FPRL1 starts with a rapid, conformational change of the occupied receptor followed by a dissociation of G proteins into two parts: G $\beta\gamma$ and G α subunits, which then mediate the activation of phospholipase C β (PLC β) and phosphoinositide 3-kinase (PI3K) (Le, Li et al. 2000; Le, Oppenheim et al. 2001). The dissociated protein subunits activate multiple downstream second messengers, including various phospholipases and protein kinases (Figure 1-5) (Rane, Carrithers et al. 1997; Miller and Falke 2004).

An immediate consequence of the production of inositol 1,4,5-trisphosphate (IP₃) upon cleavage of membrane phosphatidylinositol 4,5 bisphosphate (PIP₂) by phospholipase C (PLC) is the transient elevation of intracellular Ca²⁺, characterized by a release of Ca²⁺ from intracellular Ca²⁺ storage organelles exposing IP₃ receptors (Ptasznik, Traynor-Kaplan et al. 1995). In resting cells, the cytosolic Ca²⁺ concentration is kept at low levels (~100 nM) as compared with the level outside of the cells. However, the cytosolic concentration can rise

up to μM levels upon chemoattractant stimulation and then return to basal levels quite rapidly.

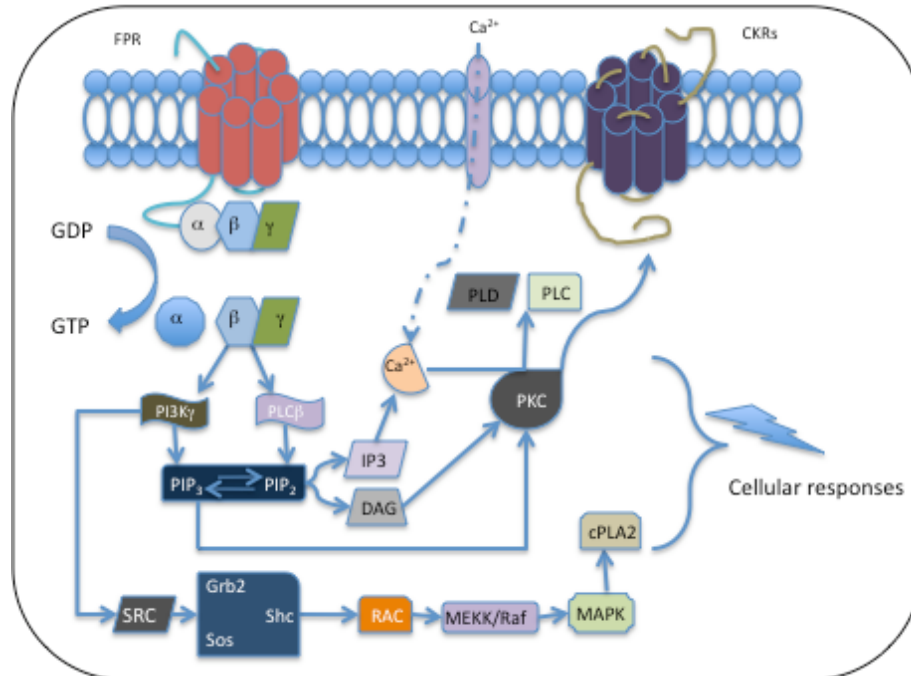


Figure 1-5: Schematic signalling pathways of an activated formyl-peptide receptor. Adapted from (Le, Li et al. 2000)

Such a transient rise in Ca^{2+} has long been considered essential for various neutrophil functions; however, recent evidence indicates that an elevation of Ca^{2+} alone is neither sufficient nor required for certain FPR family mediated responses. In fact, although cytoskeletal remodelling protein activity has been shown to be Ca^{2+} dependent (Janmey 1994), cytoskeleton-dependent cellular processes such as neutrophil polarization, membrane ruffling, chemotaxis, and phagocytosis can also occur in Ca^{2+} -depleted cells (Zaffran, Lepidi et al. 1993). Furthermore in the activation of processes such as the superoxide-generating system, an increase of intracellular Ca^{2+} alone is not sufficient (Dahlgren 1987), and can occur independently of cytosolic Ca^{2+} elevation (Bylund, Bjorstad et al.

2003; Bylund, Pellme et al. 2004; Fu, Bylund et al. 2004).

Another process elicited by the FPR family of receptors, which has been shown to be Ca^{2+} mediated, is the exocytosis of neutrophil secretory vesicles induced by fMLF or LTB₄ that occurs to the same extent even in a Ca^{2+} free buffer (Sengelov, Kjeldsen et al. 1993). Moreover, a transient elevation of Ca^{2+} alone is not sufficient for the low level of neutrophil azurophilic granule mobilization induced during fMLP stimulation; a second synergistic signal is required (Hattori, Komoda et al. 1998).

1.5.1.1. Receptor desensitization and internalization

When neutrophils encounter increasing concentrations of a chemoattractant, they gradually become nonresponsive to further stimulation by the same agonist. This process, known as homologous desensitization (Ali, Richardson et al. 1999), is also important to limit or terminate the response to higher concentrations of an attractant, avoiding prolonged activation and thereby a continuation of an inflammatory event. Cells desensitized to FPR or FPRL1 agonists are also desensitized to a second stimulation with the GPCR agonists IL-8 or PAF, suggesting the existence of a hierarchical receptor cross-talk within the GPCR receptor family (Heit, Tavener et al. 2002; Fu, Bylund et al. 2004). This type of hierarchy may be of importance in guiding the neutrophils to the site of bacterial infections when facing multiple gradients of different chemoattractants.

Cross-desensitization experiments with specific FPR and FPRL1 agonists have suggested that these receptors are hierarchically, equally strong. The phosphorylation of occupied GPCRs by specific GPCR kinases, β -arrestin binding, phosphorylation of nonoccupied GPCR by second messengers, and physical GPCR coupling to the cytoskeleton are proposed mechanisms by which these receptors are desensitized (Klotz and Jesaitis 1994; Miller and Falke 2004).

In the context of receptor recycling very little work has been done on the FPRL1 receptor and thus I will concentrate on the FPR receptor, however until further data becomes available one can hypothesize that due to the high structural homogeneity found between these two receptors, some of these processes might be similar.

Unlike other extensively investigated GPCRs such as the β 2 adrenergic and angiotensin 1A receptors, FPR internalization occurs in an arrestin-, dynamin-, and clathrin-independent manner, despite the fact that the FPR forms stable endosomal complexes with arrestin (Dalpiaz, Ferretti et al. 2002). FPR internalization is, however, dependent upon receptor phosphorylation (Dalpiaz, Pecoraro et al. 1999) and as opposed to internalization, receptor recycling to the surface is dependent on arrestin binding (Bae, Lee et al. 2004). Recent studies have shown that the eight residues located between and including Ser³²⁸ and Thr³³⁹, at the C-terminal end of the receptor, are critical for internalization and desensitization of the receptor (Dalpiaz, Pecoraro et al. 1999). These eight residues are arranged as two clusters of four serines or threonines with acidic

residues preceding each cluster, which are characteristic of G protein-coupled receptor kinase (GRK)-mediated phosphorylation sites (Miller and Falke 2004).

1.5.1.2. Distinct differences between FPR and FPRL1 signalling

The plasma membranes of many cells, including neutrophils, contain lipid rafts which are liquid-ordered microdomains enriched in cholesterol and suggested to be of prime importance in the outside-in signalling, leading to priming or a direct cellular activation (Lambert, Barlow et al. 1998). Treatment of cells with cholesterol-depleting reagents disrupts the integrity of the rafts, and such an approach has been used to determine the importance of the microdomains in signalling through FPR and FPRL1. Cholesterol depletion had little effect on the neutrophil response to high concentrations of an FPR agonist, whereas the response induced by a FPRL1 agonist was greatly impaired. The exact mechanism involved is yet to be determined, but the proposed hypothesis suggests a difference between the two receptors in their ability to couple to the signalling G protein, a process affected by the disruption of the lipid rafts (Pachter 1997).

Furthermore, in attempts to investigate the role of the cytoskeletal protein gelsolin in neutrophil activation, there was an up to 50% inhibition of reactive oxygen species production and granule mobilization triggered by the FPRL1-specific agonist WKYMVM and the more general agonist fMLP by PBP10, a selective inhibitor of the PIP₂ binding region of gelsolin. Treatment of neutrophils with PBP10 prior to WKYMVM stimulation did not alter the Ca²⁺ response, suggesting that the PBP10-mediated, inhibitory effect on the FPRL1

response is independent of PLC and affects a signal generated in a PLC-independent signalling pathway. On the other hand, PBP10 was without effect when another FPR-specific agonist replaced fMLP. Apparently, this PBP10-sensitive pathway is essential and selective for FPRL1-mediated responses in human neutrophils (Fu, Bylund et al. 2004).

1.6. Microparticles and their potential biological roles

The first report of microparticles (MP), also referred to as microvesicles, is from 1967, when Wolf described the presence of fragments derived from platelets in human plasma (Wolf 1967). Analysis of these fragments demonstrated that they were small membrane-coated vesicles. At that time, these vesicles were considered to be a residue or by-product of platelet activation and were therefore named “platelet dust.” Subsequent studies have demonstrated that these particles, like the cells from which they arise, have potent activities in clotting and are not inert (Combes, Simon et al. 1999). Since the first report by Wolf it has been shown that MP can be released from multiple cell types, including macrophages, monocytes, B and T cells, neutrophils, erythrocytes, endothelial cells, vascular smooth muscle cells, epithelial cells, and tumour cell lines.

MP are a heterogeneous population of small, membrane-coated vesicles with a size varying between 0.1 and 1.5 μm , that represent subcellular elements for cell signalling and intercellular communication in inflammation, bearing on their surfaces at least some of the antigenic markers distinctive of the parent cell. Several circumstances occurring in many disease states are known to stimulate their release such as (i) activation or apoptosis induced by numerous agents, (ii) partial or complete lysis by for example complement, (iii) oxidative injury, or (iv) other insults such as high shear stress (Miyazaki, Nomura et al. 1996) (Figure 1-6).

Stimuli that trigger the release of MP increase the intracellular calcium levels, leading to a rearrangement of the cytoskeleton and the budding of MP from the plasma membrane (Wiedmer and Sims 1991).

Studies in a variety of *in vitro* systems have demonstrated that MP are potentially important mediators of cellular interactions. Thus, these subcellular structures can transfer bioactive molecules between cells as well as regulate diverse processes, such as inflammation, coagulation, vascular function, apoptosis, and cell proliferation. In view of these activities, MP play a role in the pathogenesis of rheumatologic diseases such as rheumatoid arthritis (RA) (Berckmans, Nieuwland et al. 2005), systemic vasculitis (Daniel, Fakhouri et al. 2006), and antiphospholipid syndrome (Joseph, Harrison et al. 2001).

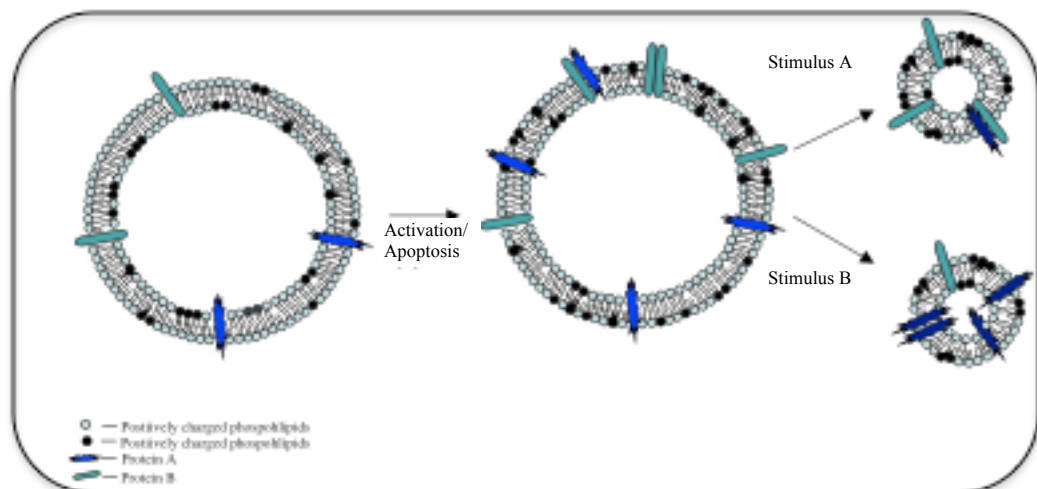


Figure 1-6: A schematic outlining the production of MP, outlining the segregation of cell specific antigens upon activation and the release of different antigens depending on the stimulus being provided (VanWijk, VanBavel et al. 2003).

Although arising during apoptosis, MP are distinct from apoptotic bodies. After the induction of apoptosis, the cell shrinks and shows chromatin condensation and cellular rearrangement, leading to formation of blebs. Eventually, the apoptotic cell collapses and fragments, which leads to the formation of

membrane-coated structures, the so-called apoptotic bodies. In contrast to MP, which are released early during apoptosis, apoptotic bodies form in the final stages of programmed cell death. In addition to the kinetics of their generation, MP and apoptotic bodies differ in composition and size, with apoptotic bodies being many times larger in diameter and volume (Hristov, Erl et al. 2004).

MP also differ from exosomes, another type of vesicle released from eukaryotic cells either spontaneously or during activation. Unlike MP, exosomes are preformed vesicles. Exosomes are stored intracellularly in multivesicular bodies and are secreted when the multivesicular bodies fuse with the cell membrane (Gasser, Hess et al. 2003). Although they arise from the inside of cells, exosomes, nevertheless can be functionally active. For example, exosomes derived from B lymphocytes can bind to follicular dendritic cells and function in antigen presentation (Denzer, Kleijmeer et al. 2000), while exosomes from cytotoxic T cells may mediate target cell killing (Monleon, Martinez-Lorenzo et al. 2001). As shown in morphologic studies, exosomes range in size from 50 to 100 nm and are coated by a lipid bilayer. Exosomes also display certain surface receptors of the parental cell (Stein and Luzio 1991).

Another term used to characterize vesicles released from cell membranes is ectosomes. Stein and Luzio coined the expression “ectocytosis” for the process of releasing vesicles with a “right-side-out” orientation (Stein and Luzio 1991). Most MP that are released by monocytes, neutrophils, platelets, and fibroblasts correspond to the definition of ectosomes. While the terms MP and ectosomes

may not be synonymous, there is evidence for a structural and functional similarity of these structures.

It had been known for a long time that many, if not all, proteins of the plasma membrane exhibit a high degree of lateral mobility (White 1993), manifested in such phenomena as receptor clustering, dimerization and capping of leukocytes (Nurden 1997). Recently, the concept of lipid rafts has emerged, in part to account for aspects of this mobility being floating islands of distinctive lipid composition bearing restricted sets of proteins (such as GPI-anchored proteins), and are studied by their differential solubility in detergents (Simons and Ikonen 1997; Czech 2000). Erythrocytes (RBC) have been good models for study and their rafts assisted in understanding earlier findings amongst which the selective shedding of RBC MP enriched in acetyl cholinesterase (Butikofer, Kuypers et al. 1989). It was also observed that in some cells the clustering (capping) of platelet endothelial cell adhesion molecule (PECAM)-1 occurs as a prelude to the shedding of MP enriched in it (Jy, Jimenez et al. 2002), suggesting that specific kinds of rafts are preferentially shed as MP. This could also explain another finding, that of endothelial MP with multiple phenotypes (Jimenez, Jy et al. 2003), since it would mean that the same cell could be the origin of distinctive raft species the content of which depend on stimulus and environment.

Yet another interesting observation was the fact that the shedding of endothelial MP *in vivo* is highly sensitive to the blood lipid profile, consistent with the fact

that the composition and stability of rafts are very sensitive to levels and compositions of particular plasma lipid particles and transfer proteins.

1.6.1. Composition of microparticle plasma membranes

MP expose membrane antigens that are specific for the 'parent cell' they originate from. These identification antigens are always present on the surface, irrespective of the activation or apoptosis status of the parent cell, and enable the determination of their cellular source, e.g., CD62L for neutrophil derived MP (Gasser, Hess et al. 2003). MP however, can differ in the expression of cell surface molecules from their parental cells. This phenomenon has been analyzed in the most detail for RBCs. MP derived from erythrocytes upon treatment with calcium and ionophore A23187 are enriched for glycosyl phosphatidylinositol-anchored proteins, such as acetylcholinesterase and decay accelerating factor (Butikofer, Kuypers et al. 1989). Erythrocyte-derived MP are also enriched for the membrane protein stomatin and for the proteins synexin and sorcin, which translocate from the cytosol to the plasma membrane upon calcium binding (Salzer, Hinterdorfer et al. 2002).

Furthermore, the expression of surface molecules on MP may vary with parent cell activation state, with levels of PECAM-1 and E-selectin significantly higher on MP from activated endothelial cells than on those from resting cells (Abid Hussein, Meesters et al. 2003) and cellular origin.

The microparticle composition is also agonist dependent. T-cells produce MP that are enriched in CD3 ϵ - and ζ -chains only upon activation of the T-cell antigen receptor and not upon activation by ionomycin plus *p*-methoxyamphetamine hydrochloride (Blanchard, Lankar et al. 2002). MP from thrombin- or collagen-activated platelets expose glycoprotein IIb–IIIa complexes that bind fibrinogen, in contrast to MP produced by platelets incubated with C5b-9, which do not bind fibrinogen (Martinez, Tesse et al. 2005). Finally, even MP released by one cell type in response to a single agonist still can form a heterogeneous population. For instance, MP released from platelets after stimulation with serum from patients with heparin-induced thrombocytopenia are heterogeneous in size and in exposure of glycoprotein IIb–IIIa (Hughes, Hayward et al. 2000).

1.6.2. Microparticle cytoplasmic content

In contrast to the characterization of surface molecules, little is known about the intracellular contents of MP. They and colleagues demonstrated that MP from dendritic cells contain histones (They, Boussac et al. 2001), whilst MP released by THP-1 monocytic cells upon activation of the ATP receptor P2X₇ contain IL-1 β (MacKenzie, Wilson et al. 2001).

Based on the mechanism of microparticle release, it is possible that cytosolic and even nuclear proteins from the parental cells are present within the MP. These internal molecules could contribute to biological activity of the particles, although this has not been investigated extensively.

1.6.3. MP as intercellular transporters

MP may have various (patho-) physiological functions, namely transport of membrane components from the parent cell to other cells and (in-)direct activation of inflammation, coagulation or vascular function.

Among their pro-inflammatory activities, MP can transport biologically active compounds such as lipid mediators and cell surface receptors between different cells. Barry and coworkers demonstrated that MP can alter cellular functions through transcellular lipid metabolism (Barry, Pratico et al. 1997; Barry, Kazanietz et al. 1999).

Recently, it has also been shown that MP can mediate the intercellular transfer of cell surface receptors. The transferred receptors can be integrated into the plasma membrane of the acceptor cells rendering them responsive to new stimuli. Horizontal transfer of proteins via MP could also play a role in the pathogenesis of human immunodeficiency virus (HIV) infection. While receptor transfer provides a novel regulatory mechanism, the integration of receptors from MP into the plasma membrane of the acceptor cells may not lead to new function. One example is that although when MP containing the chemokine (C-C motif) receptor (CCR)-5 were incubated with T-cells and the receptor was observed to be incorporated into the cell membranes, the incubation with a CCR5 agonist was not observed to lead to down stream signalling by this receptor. This finding suggests that the functional integration of chemokine receptors may be limited to certain cell types. In addition, the transfer of cell surface molecules by MP has been demonstrated only for chemokine receptors. It remains unknown whether other cell surface proteins can be exchanged

between different cells through this mechanism (Mack, Kleinschmidt et al. 2000).

1.6.4. MP and their role in inflammation

As shown in a few *in vitro* studies, MP can display a variety of proinflammatory activities that could contribute to the pathogenesis of rheumatic disease. Thus, these particles can promote adhesion and rolling of leukocytes, contain proinflammatory cytokines, and trigger the release of MP from various cell types *in vitro* (Mesri and Altieri 1998). Further evidence for a potential role in disease pathogenesis comes from observations of increased numbers of MP during inflammatory states *in vivo* (Nieuwland, Berckmans et al. 2000; Knijff-Dutmer, Koerts et al. 2002; Amabile, Guerin et al. 2005).

Similar to the events promoted by damaged cells, MP can trigger inflammation by activating the complement cascade. In fact, C1q bound to MP can activate the classical complement pathway, as demonstrated by deposition of C3 and C4 on the surface of MP (Nauta, Trouw et al. 2002).

In their interactions with cells, platelet-derived MP can enhance the binding of neutrophils to other neutrophils prebound to the surface of a flow chamber. In these experiments, even when L-selectin is blocked, platelet-derived MP allow neutrophils to aggregate and adhere to prebound cells. In this model, the interaction between P-selectin on platelet-derived MP and P-selectin-glycoprotein ligand 1 (PSGL1) on neutrophils has been suggested to be responsible for this interaction. Furthermore, platelet-derived MP can promote

cell–cell contact by inducing adhesion molecules expression on recipient cells (Forlow, McEver et al. 2000).

Interestingly, a recent study suggests that MP can, under certain circumstances, exert anti-inflammatory effects. In these experiments, MP derived from fMLP-stimulated polymononuclear cells up-regulated the expression of the anti-inflammatory cytokine transforming growth factor β 1 (TGF β 1) in macrophages. In contrast, the release of the proinflammatory cytokines TNF α , IL-8, and IL-10 induced by zymosan and lipopolysaccharide was reduced by these MP in a dose-dependent manner (Gasser and Schifferli 2004). MP may also exert anti-inflammatory effects by the induction of apoptosis in immunocompetent cells. Jodo and colleagues showed that cells were able to release MP that bear Fas ligand (FasL) on their surface. Unlike soluble FasL, which is a relatively poor mediator of cytotoxicity, the efficacy of microparticle-associated FasL was similar to that of cellular FasL in killing B and T cell lines (Jodo, Xiao et al. 2001). In similar experiments, it was demonstrated that T cell MP can induce apoptosis in RAW 264.7 macrophages, thereby triggering the release of MP from dying macrophages (Distler, Huber et al. 2005).

MP appear to play an important role in the pathogenesis of coronary artery disease. Endothelial cell– and platelet-derived MP are significantly increased in coronary artery disease, especially in patients with acute events, whilst MP derived from monocytes and lymphocytes are found in atherosclerotic plaques (Figure 1.6) (Distler, Pisetsky et al. 2005).

These structures have also been implicated to play a role in rheumatic diseases, were in a number of studies it was observed that there was an elevated number of MP in plasma samples from patients suffering from these diseases (Figure 1.7). Consequently it was suggested that MP could function in disease pathogenesis by acting systemically on the vasculature as well as locally in the joint. Since cell death and activation are ubiquitous events at sites of inflammation, microparticle release could be a common occurrence, with these structures further stimulating inflammation (e.g., T cell activation leading to fibroblast activation *via* transferred particles) (Knijff-Dutmer, Koerts et al. 2002).

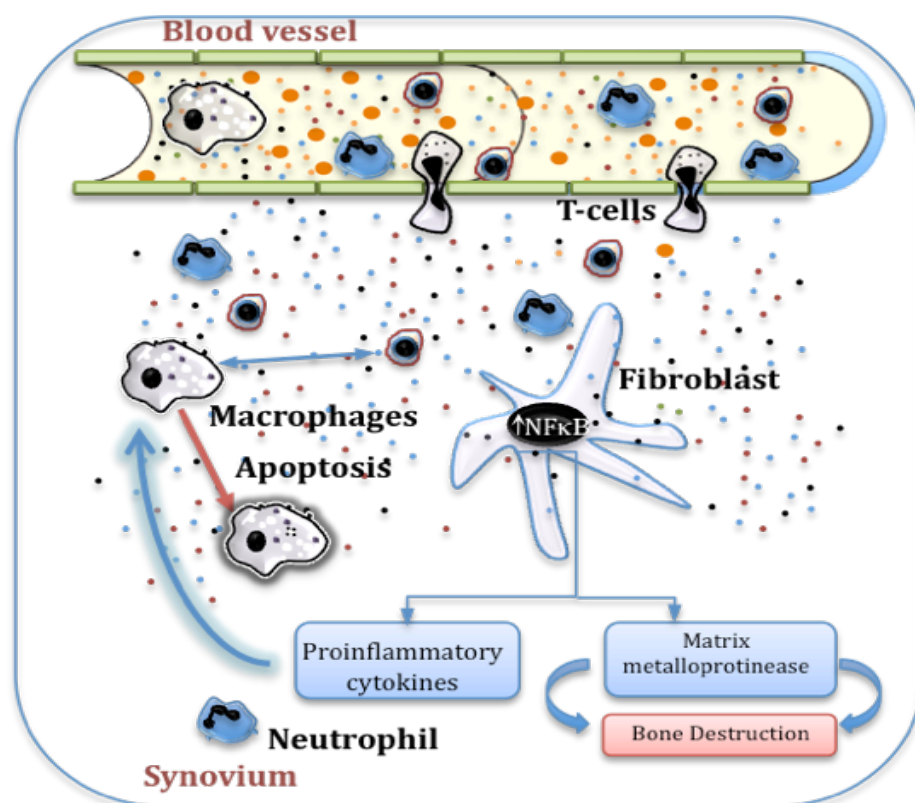


Figure 1-7: Schematic outlining the roles played by MP in the pathogenesis of some the rheumatic diseases. In the synovium MP from various sources primarily T-cells and macrophages activate the fibroblasts leading to the release of proinflammatory cytokines, which attract more cells into the synovium. These cytokines in turn also activate the newly attracted cells leading to a further activation of the synovial fibroblasts. In the vessels, MP are involved in the formation of atherosclerotic plaques (Distler, Pisetsky et al. 2005).

1.7. Rheumatic diseases

Rheumatic diseases may cause pain, stiffness, and swelling in the joints and other supporting body structures, such as muscles, tendons, ligaments, and bones, however, other areas of the body, including internal organs may also be affected. Some rheumatic diseases involve connective tissues (called connective tissue diseases), while others may be caused by an autoimmune disorder. Rheumatic diseases can affect anyone, at any age, or of any race. However, certain diseases are more common in specific populations, some examples are: osteoarthritis in the elderly; rheumatoid arthritis in women; ankylosing spondylitis and gout in men; scleroderma and lupus in women.

The cause of most types of rheumatic diseases remains unknown and, in many cases, it may vary depending on the type of rheumatic disease. However, it is believed that some if not all of the following factors may play a role in the development or aggravation of one or more types of rheumatic diseases: genetic predisposition and family history (i.e., inherited cartilage weakness); lifestyle choices (such as being overweight); trauma; infection; neurogenic disturbances; metabolic disturbances; excessive wear and tear along with stress on a joint(s); environmental trigger and the influence of certain hormones on the body. Increasing evidence is highlighting the role of auto-antibodies in the propagation of at least a subset of these diseases, where they can have either organ-specific or generalized autoreactivity.

There are a number of symptoms reported for rheumatic disease with some of the most common being: pain, swelling, early morning stiffness, chronic pain,

tenderness, warmth, redness and limited movement in the joints and fatigue. However, each individual may experience symptoms differently, and different types of rheumatic diseases present different symptoms.

1.7.1. Rheumatoid Arthritis- a brief overview

The first recognized description of rheumatoid arthritis (RA) was made in 1800 by Dr Augustin Jacob Landré-Beauvais (1772-1840) of Paris. The name is based on the term "rheumatic fever", an illness which includes joint pain and is derived from the Greek word rheumatosis ("flowing"). The suffix -oid ("resembling") gives the translation as joint inflammation that resembles rheumatic fever.

RA is a chronic, systemic autoimmune disorder that most commonly causes inflammation and tissue damage in joints (arthritis) and tendon sheaths, together with anaemia. It can also produce diffuse inflammation in the lungs, pericardium, pleura, the sclera of the eye, and also nodular lesions most common in subcutaneous tissue under the skin. Extra-articular manifestations other than anaemia (which is very common) are clinically evident in about 15-25% of individuals with rheumatoid arthritis (Gabriel, Crowson et al. 2003; Turesson, O'Fallon et al. 2003). It can be difficult to determine whether disease manifestations are directly caused by the rheumatoid process itself, or from side effects of the medications commonly used to treat it for example methotrexate has been limited to lung fibrosis and corticosteroids to osteoporosis (Guler-Yuksel, Bijsterbosch et al. 2008).

1.7.2. Current Treatments for RA

A number of treatments have been developed using an array of medications. The first subset is referred to as non-pharmacological treatment, which includes physical therapy and occupational therapy. Pharmacologically, analgesics and anti-inflammatory drugs, as well as steroids, are used to suppress the symptoms with the former only being effective in reducing pain and stiffness without effecting joint damage or disease progression. Disease-modifying anti-rheumatic drugs (DMARDs) are often required to inhibit or halt the underlying immune process and prevent long-term damage. The DMARDs originally meant a drug that affects biological measures such as erythrocyte sedimentation rate (ESR), haemoglobin and autoantibody levels. However nowadays this definition has been expanded to also encompass those drugs that reduce the rate of damage to bone and cartilage. DMARDs have been found to produce both durable symptomatic remissions and to delay or halt progression of the disease.

Among the chemically synthesised DMARDs one finds: azathioprine, cyclosporin (cyclosporine A), D-penicillamine, gold salts, hydroxychloroquine, leflunomide and methotrexate (MTX).

The most important and most common adverse events of these drugs relate to liver and bone marrow toxicity (MTX, SSZ, leflunomide, azathioprine, gold compounds, D-penicillamine), renal toxicity (cyclosporine A, parenteral gold salts, D-penicillamine), pneumonitis (MTX), allergic skin reactions (gold compounds, SSZ), autoimmunity (D-penicillamine, SSZ, minocycline) and infections (azathioprine, cyclosporine A). Hydroxychloroquine may cause

ocular toxicity, although this is rare, and because hydroxychloroquine does not affect the bone marrow or liver it is often considered to be the DMARD with the least toxicity. Unfortunately hydroxychloroquine is not very potent, and is usually insufficient to control symptoms on its own and is normally used as part of a combination therapy with other DMARDs such as methotrexate and sulfasalazine (Weaver, Lautzenheiser et al. 2006; Walker-Bone and Farrow 2007).

In late 1980 it was suggested that TNF- α was a pivotal cytokine in the development of RA and a number of companies amongst which Centocor, Inc. started working on the development of anti-bodies to block this cytokine. Subsequent work lead to the development of an anti-TNF Receptor (TNFR) – Ig fusion protein and the starting of clinical trials in the US, where by the late 1990 this was approved as method of therapy for RA in both the US and Europe. The development of this novel therapy represented a tremendous advance in the management of RA. Furthermore their use meant that those patients whose disease was previously resistant to conventional DMARDs could usually be satisfactorily controlled, and remission of disease became an increasingly realistic aim. However, these therapies are expensive in comparison with conventional DMARDs and, in countries with socialized healthcare, their unrestricted use would be unaffordable (Ledingham J, Deighton C. et al 2001).

1.7.3. Wegener's Granulomatosis- a brief overview

Small-vessel vasculitides are defined as selective inflammation of the arterioles, venules, and capillaries (Figure 1-8).

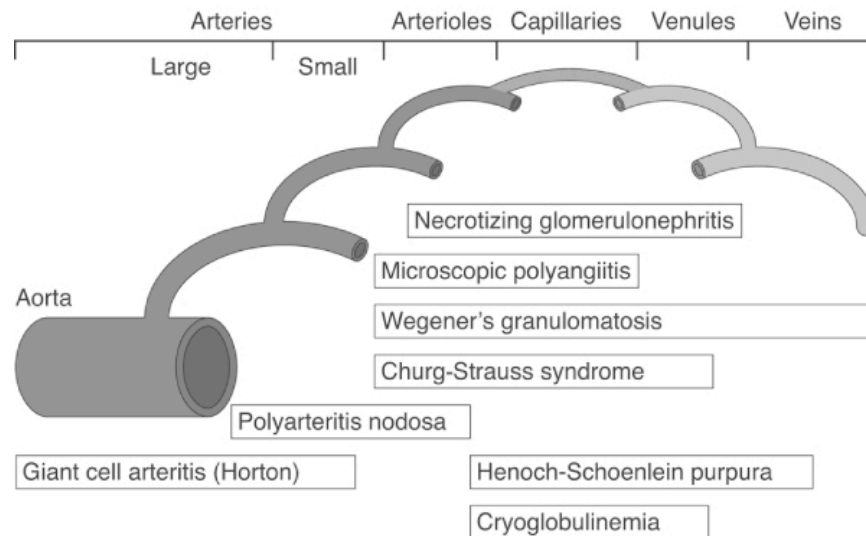


Figure 1-8: Size of vessels as defined at the Chapel Hill consensus conference and associated rheumatic diseases. (Taken from (Jennette et al 1994).

The identification of anti-neutrophil cytoplasmic antibodies (ANCA) about two decades ago in patients with pauci immune small-vessel vasculitis proved a breakthrough in the classification, diagnosis, monitoring, and understanding of the vasculitides. ANCA were found to be associated with four vasculitides: microscopic polyangiitis, Wegener granulomatosis, Churge-Strauss syndrome, and necrotizing crescentic glomerulonephritis. The incidence of ANCA-associated vasculitides is rising; it has been estimated at more than 20/106 population, with a peak between 65 and 75 years of age (Seo and Stone 2004).

Scottish otolaryngologist Peter McBride first described the condition in 1897, Heinz Karl and Ernst Klinger would add information on the anatomical pathology, but the full picture was presented by Friedrich Wegener, a German pathologist, in two reports in 1936 and 1939.

The upper and lower respiratory tract and the kidneys are the main targets of Wegener granulomatosis. About 90% of patients experience otolaryngological involvement that may manifest as episodes of rhinitis, sinusitis, epistaxis or nasal crusting. The pathology of Wegener granulomatosis combines vasculitis of the small vessels or, less often, the medium-sized vessels; irregularly contoured foci of ischaemic necrosis with the development of sterile abscesses; and formation of granulomas composed of neutrophils, lymphocytes, and giant multinuclear cells. ANCA against PR3 are found in 80-90% of patients with systemic Wegener granulomatosis, of whom only 10% have anti-MPO ANCA (Gross, Schmitt et al. 1993).

Histology may show granulomatous airway inflammation in addition to small vessel vasculitis. Only 60% of these patients have detectable titers of ANCA, specifically cytoplasmic (c) ANCA, in contrast to perinuclear (p) ANCA (normally targeted against MPO). The presence of these antibodies leads to the activation of neutrophils, an increase in their adherence to endothelium leading to degranulation. This causes extensive damage to the vessel wall, particularly of arterioles. The exact cause for the production of ANCAs is unknown, although some drugs have been implicated in secondary forms of Wegener's granulomatosis (Csernok, Lamprecht et al. 2006; Jennette, Xiao et al. 2006).

1.7.3.1. Current treatment for Vasculitides

Before steroid treatment became available, mortality within one year was over 90%, with average survival being 5 months. Since the introduction of glucocorticoids and immunosuppressants to treat ANCA-associated

vasculitides, 5-year survival has exceeded 80%. The introduction of cyclophosphamide (CYC) in the 1970s was a major breakthrough. However, early mortality due to alveolar haemorrhage or severe renal failure remains common, most notably in older patients. Infection is also a major cause of early death. Despite the improved survival, some patients fail to achieve long-term remissions where about 50% of patients experience one or more relapses within the first 4-5 years. Relapses are more common in Wegener granulomatosis than in the other ANCA-associated vasculitides. They may be related to the presence of granulomas and to colonization of the airways by pathogens such as *Staphylococcus aureus*. As relapses occur in more than 50% of patients with Wegener granulomatosis, prolonged immunosuppressant therapy is often required, at the cost of frequent and severe adverse events. With regimens involving long-term oral cyclophosphamide therapy, a risk increase of 33-fold occurred for urinary bladder carcinoma, 11-fold for lymphoma, and 2.4-fold for solid tumours. Although relapses are often less severe than the initial presentation, they may add to the burden of sequelae thereby worsening the functional impairment (Stegeman, Tervaert et al. 1994; Cruz, Ramanoelina et al. 2003; Jayne 2003).

1.7.4. Giant Cell Arteritis

Giant cell arteritis (GCA) is a chronic granulomatous vasculitis of unknown aetiology occurring in the elderly. It affects the cranial branches of the arteries originating from the aortic arch including the temporal artery and the ocular nerve where is usually associated with markedly elevated acute-phase reactants. This disease is more commonly found in females by a 3:1 ratio. The mean age of onset is about 70 years and is rare in those less than 50 years of age. Patients

present with a number of symptoms amongst which: fever, headache, tenderness and sensitivity on the scalp, jaw claudication (pain in jaw when chewing), tongue claudication (pain in tongue when chewing), reduced visual acuity and acute visual loss (Wang, Hu et al. 2008).

GCA of large- and medium-sized peripheral arteries typically leads to long tapering and occlusion of the arterial lumen due to concentric intimal thickening, sometimes accompanied by spontaneous dissection (Devauchelle-Pensec, Jousse et al. 2008). Depending on the extent of the arterial obliteration and on the anatomy of the involved arterial segment, this may result in severe ischaemia of the limbs during the acute phase of the disease. GCA of the aorta usually remains asymptomatic for many years, and leads to a markedly increased risk of aneurysms and dissections, particularly of the thoracic aorta. In 76% of cases involving the eye, the inflammatory condition effects the ophthalmic artery causing anterior ischemic optic neuropathy. Loss of vision in both eyes may occur very abruptly and this disease is therefore a medical emergency (Devauchelle-Pensec, Jousse et al. 2008; Tato and Hoffmann 2008; Wang, Hu et al. 2008).

The diagnosis is relatively straightforward in the presence of cranial manifestations, but it may be challenging in the case of a normal erythrocyte sedimentation rate that may occult the disease or in patients with isolated extra-cranial features. Temporal artery biopsy still represents the gold standard for diagnosis, while the role of ultrasonography, high-resolution magnetic

resonance imaging and positron emission tomography should be better addressed (Devauchelle-Pensec, Jousse et al. 2008).

1.7.4.1. GCA Treatment

Treatment of this condition involves corticosteroids, typically high-dose prednisone (40-60mg bd), which must be started as soon as the diagnosis is suspected (even before the diagnosis is confirmed by biopsy) to prevent irreversible blindness secondary to ophthalmic artery occlusion. Steroids do not prevent the diagnosis from later being confirmed by biopsy, although certain changes in the histology may be observed towards the end of the first week of treatment and are more difficult to identify after a couple of months (Moutray, Williams et al. 2008). The dose of prednisone is lowered after a few days, although treatment may continue for up to two years.

1.8. Aims of the thesis

In previously conducted studies it was shown that MP derived from human neutrophils might produce anti-inflammatory effects on human monocyte-derived macrophages *in vivo*. Furthermore it was also described that primed PMN export Annexin A1 to their cell surface thus it was deemed important to determine what role Annexin A1 is playing in the inhibitory effect described above:

Thus I set out to determine the presence of Annexin A1 on PMN derived MP.

- In order to fulfil this aim I propose to produce PMN derived MP by stimulation of PMNs with fMLP and determine their presence by using the flow-cytometry, and subsequently I intend establishing the presence of Annexin A1 in these microstructures by flow cytometry, Western Blotting and Q-ToF LC/MS/MS

After determining the presence of Annexin A1 on these MP it is important to determine if this Annexin A1 is playing a role in the observed anti-inflammatory effects.

- In order to fulfil this aim I intend incubating the PMN derived MP with PMN and then flowing these cells over and activated endothelial cell monolayer. Then blocking either the Annexin A1 protein or its specific receptor to further elucidate the anti-inflammatory role of Annexin A1. Furthermore I intend extracting PMN MP from Annexin A1 *-/-* and WT mice to further outline the role of microparticle Annexin A1 in and *in vivo* model of inflammation.

Upon determining the role of Annexin A1 in MP the next step is to understand the clinical importance of these Annexin A1 positive MP and their potential use as biomarkers:

- In order to achieve this I intend analyzing MP obtained from the plasma of patients suffering from rheumatic diseases mainly, MPO and PR3 ANCA positive, GCA and RA patients to determine if there is any alteration in levels of the Annexin A1 - FPRL1 axis on these MP. Further more in order to further validate the robustness of using Annexin A1 and FPRL1 positive MP as biomarkers, I intend analyzing the levels of these two proteins on plasma samples obtained from RA patients pre, during and post steroidal treatment.

The third area of my research involves the development of novel Ac2-26 derived peptides as potential anti-inflammatory drugs. A panel of peptides has been synthesized based on previously published data in our lab highlighting PR3 cleavage sites on the N-terminal portion of the Annexin A1. Two of these amino acids, amino acid 11 and 22, of the Ac2-26 peptide were substituted with 5 different amino acids resulting in 5 distinct peptides.

- In order to achieve this aim, a screening process will be conducted where first the ability of each of the peptides to activate ERK 1/2 through the FPRL1 receptor will be assessed by western blotting.
- The next step will be to determine the ability of each of these peptides to inhibit neutrophil recruitment to an activate HUVEC monolayer. Based upon the data obtained from this set of experiment and the ERK 1/2

activation 2 peptides showing properties similar to the parent peptide will be chosen for further analysis.

- After identifying the two peptides to take forward, the binding affinity to the FPR and FPRL1 receptors will be assessed using transfected HEK cell lines expressing the two receptors. Furthermore their ability to activate the MAPK pathway will be further assessed by conducting a dose response curve on the activation of ERK 1/2 along with their ability to reduce neutrophil recruitment to an activated HUVEC monolayer.
- Finally the anti-inflammatory properties of the two peptides will be assessed in a pre-clinical model of inflammation where the ability of these peptides to inhibit neutrophil recruitment into an airpouch inflamed using IL-1 β will be investigated.

2. Materials & Methods

2.1. Materials List

Distributor	Material		Tris-Base
Serotec	Star9b		Tween 20
	IgG1 Isotype		p-Coumaric acid
	Anti-CD62P (clone:Psel.KO.2.12)		Luminol
	Anti-CD62L (clone: FMC64)		Hydrogen peroxide
	Anti-CD14 (TUK14)		DEPC water
	IgG2b Isotype		fMLP
	Anti-CD11b (clone:MCA551)		Ethanol
Oxoid	PBS		Coomassie Blue
Astra-Zeneca	Anti-FPRL1 (clone:6C7-3-A)		Lucigenin
<i>In-house</i>	Anti-Annexin A1 (clone:1b)		DCFDA
	hr-Annexin A1		PMA
CRB	Ac2-26 peptide	BD Pharmingen	IL1 β
	W-peptide		Anti-mouse CD102 (clone 3C4)
	Anti-Flammin 2		Anti-FPR (clone: 5F1)
Pierce	BCA-protein assay kit	Cell Signalling Tech	Anti-total ERK ½ (clone: E10)
Sigma	Penicillin		Anti-phospho-ERK ½ (clone: 137F5)
	Streptomycin	DakoCytomation	Anti-mouse-HRP conj.
	Fugizone		Anti-rabbit-HRP conj.
	L-Glutamine	Amersham	Hyperfilm ECL
	Meidum 199		Percoll
	Trypsin	Qiagen	18s Quantitec Primer Assay
	Gelatin		GAPDH Quantitec Primer Assay
	HEPES buffered saline		FPRL1 Quantitec Primer Assay
	EDTA solution		AnxA1 Quantitec Primer Assay
	RPMI 1640 medium		RNA mini-kit
	Histopaque 1077	Phoenix-Pharma	W-peptide I ¹²⁵
	Histopaque 1119	Bioline	dNTP
	Sodium Chloride	Invitrogen	Foetal Calf serum
	Sodium Citrate		Trizol
	TNF- α		Oligo-dt ₂₀
	HBSS		Superscript III
	Human γ -Globulins		RNAse OUT
	Bovine serum albumin		Ham's F-12 media
	DDT		Collaginase type IS
	Sodium orthovanadate		Collaginase type II
	Sodium fluoride		
	PMSF	Ambion	Turbo DNase I
	Tris-HCl	ABi bioscience	POWET SYBR Green
	SDS	Calbiochem	Lipoxin A ₄
	Glycerol	<i>Gift</i>	Anti-PR3 (clone:CLB-12.8)
	Bromophenol blue	VWR	Acetic Acid
	Pepstatin	eBioscience	Anti-Gr1-PE (clone rb6-8c5)
	β -glycerolphosphate		Ig2a Isotype-PE
	Leupeptin		
	Triton-X 100		
	DMSO		
	Ammonium persulphate		
	TEMED		

2.2. Isolation and culture of primary HUVEC.

Primary HUVEC cells were employed for the studies conducted during my PhD, these were isolated from umbilical cords as will be detailed below. Human cells were prepared according to a protocol approved by the local Research Ethics Committee (P/00/029 ELCHA).

Umbilical cords were kindly supplied by the midwifery staff of the Maternity Unit, Royal London Hospital. Cords were placed in cord buffer (PBS containing penicillin (100U) streptomycin (100mg/ml) and fungizone (2.5µg/ml)] and stored at 4°C until endothelial isolation. Endothelial cells were isolated from umbilical cords by collagenase digestion of the interior umbilical vein (Jaffe, Nachman et al. 1973). The veins were perfused with approximately 50 ml of cord buffer using a sterile syringe, to wash out the residual blood. The other end of the cord was then clamped and approximately 20ml of 0.1% collagenase type II in serum free medium 199 containing penicillin (100U), streptomycin (100mg/ml), fungizone (2.5µg/ml) and L-glutamine (2mM) was added. Another clamp was then placed at the top end of the cord and the vein was incubated in a humidified chamber in 5% CO₂ at 37°C for 15min. Following incubation, the collagenase solution was collected into a 50ml centrifuge tube and the vein was flushed with 30ml of cord buffer, and once with air to remove endothelial cells. The cells were centrifuged at 560g for 5min, supernatant removed, and the pellet was re-suspended in 15ml of complete medium (M199 containing 20% human serum (FCS), penicillin (100U), streptomycin (100mg/ml), fungizone (2.5µg/ml) and L-glutamine (2mM)) and transferred to a T75 flask. Typically the yield from this procedure was in the range of 0.5-1.5x10⁶ cells per cord.

Cells were seeded into T75 flasks and 35mm plates precoated in 0.5% bovine gelatine prior to use. Gelatine (2%) was diluted 1:4 with PBS and tissue culture plastics were coated with the 0.5% solution for 20min. Following the coating procedure, gelatine was aspirated before seeding. The cells or dishes were incubated in a humidified chamber in 5% CO₂ at 37°C, medium was replaced after 24h and changed every 48h thereafter. When the cells cultured in the flask had reached approximately 80% confluency, they were rinsed once with HEPES buffered saline solution (BSS) and subcultured using room temperature (RT) 0.025% trypsin/0.01% EDTA solution (4ml for a 75cm² flask). When 90% of the cells had rounded and started to detach, the flask was tapped firmly on the side to release the cells and an equal volume of trypsin neutralizing solution (TNS) was added. Cells were transferred to a 15ml centrifuge tube, flasks rinsed with HEPES-BSS added to tube, and spun at 220xg for 5min to pellet the cells. The HUVEC were never cultured beyond passage 3.

2.3. Human blood leukocyte isolation.

Experiments with healthy volunteers were approved by the local research committee, and informed consent was provided according to the Declaration of Helsinki.

Blood was collected from healthy volunteers with a 21-gauge needle and transferred to a 50ml centrifuge tube containing 1/10 volume of 3.2% sodium citrate. Blood was first diluted 1:1 with warm Roswell Park Memorial Institute (RPMI) 1640 medium before addition to a double density gradient. The double gradient is formed by layering an equal volume (3ml) of Histopaque 1077 over

Histopaque 1119. This was prepared immediately before use to avoid any diffusion occurring between the two layers. Pre-diluted blood was carefully added to the top layer using a sterile Pasteur pipette and centrifuged at 400g for 30min at room temperature.

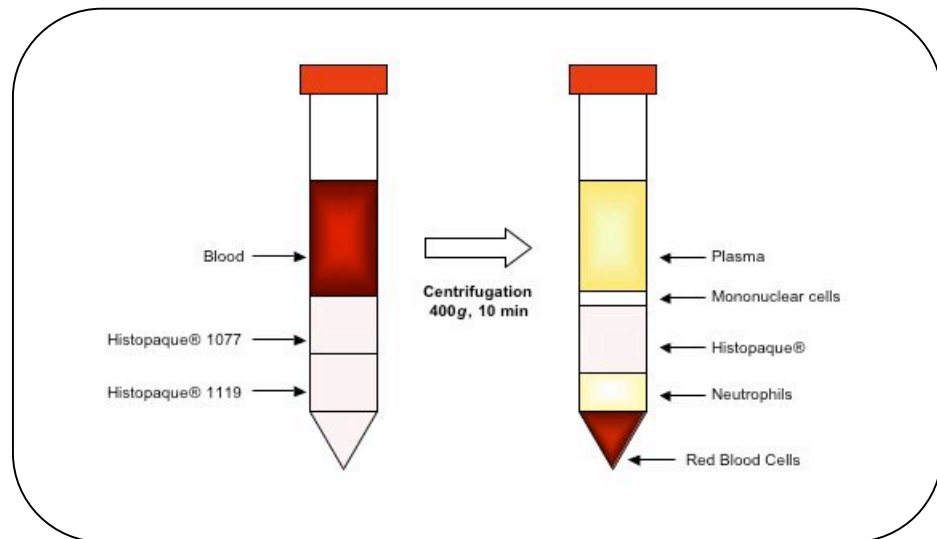


Figure 2-1: Neutrophil isolation from human blood using histopaque double density centrifugation.

Two distinct layers of leukocytes can be seen after centrifugation, with red blood cells (RBCs) pelleted to the bottom of the centrifuge tube. Polymorphonuclear cells (PMNs) are found above the RBCs whereas peripheral blood mononuclear cells (PBMCs) are found at the plasma/histopaque interphase (Figure 2-1). In order to reduce cross contamination between the two cell populations the PBMC layer was isolated first and the cells discarded. Then the PMNs were removed and placed in 6ml aliquots in 15ml centrifuge tubes to which an equal volume of RPMI 1640 was added. Samples were centrifuged at 300g for 15min, supernatant discarded and cells re-suspended gently with a Pasteur pipette in 7.5ml of ice-cold water and subsequently 2.5ml of 3.6%

sodium chloride solution were added. The ice-cold water was employed to lyse any erythrocytes which were present along with the PMN pellet, whilst the sodium chloride was immediately added to preserve the PMNs. Cells were then centrifuged at 300xg for another 10 min and then resuspended in 3ml of RPMI medium supplemented with 10% heat inactivated foetal calf serum (FCS), L-glutamine (2mM), penicillin (100U) and streptomycin (100mg/ml) (complete media) to count. Cells were counted in all four large squares outlined in red in Figure 2-2, and divided by 4 to obtain the average. The total number of cells per ml was calculated according to the formula below:

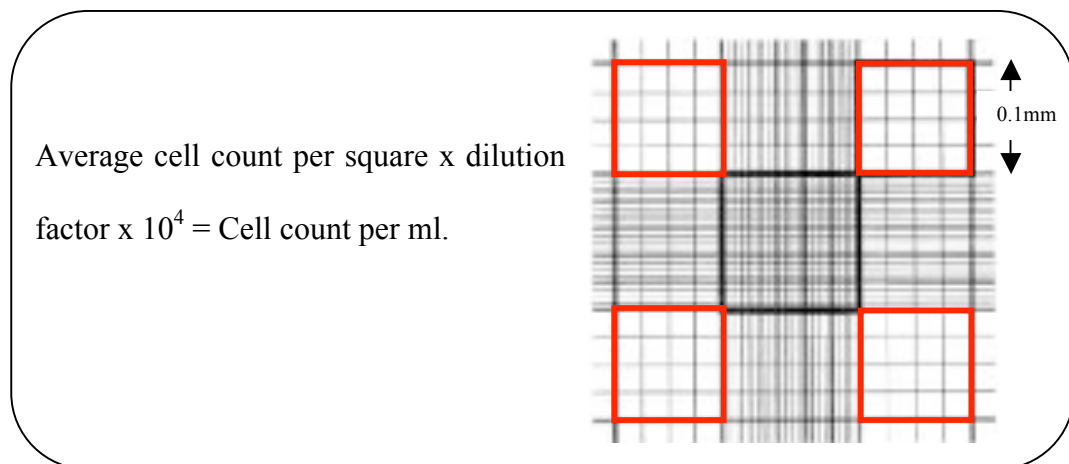


Figure 2-2: Illustration of the counting grid on a Neubauer haemocytometer. Cells were counted in the four large squares highlighted and an average was obtained.

2.4. *In vitro* flow chamber assay.

HUVECs were seeded in 35mm² coated-coated dishes at a density of 3×10^5 cells in complete media, and used two days after plating, at confluence. Confluent monolayers were stimulated with TNF- α (10ng/ml; Sigma-Aldrich) for 4h to up-regulate adhesion molecules such as E-Selectin, ICAM-1 and VCAM-1. Human PMNs were isolated as outlined in section 2.2, centrifuged at 300g for 5min and resuspended to 1×10^7 cells/ml in Dulbecco phosphate

buffered saline (DPBS) containing 0.1% bovine serum albumin (BSA) and kept on ice before use. Immediately prior to flow, 5×10^6 (0.5ml) PMNs were diluted to 5ml (1×10^6 cells/ml) in DPBS supplemented with Ca^{2+} and Mg^{2+} (as integrins on the PMNs require these divalent cations for their adhesive function). The PMNs were then incubated for 10min at 37°C following which the endothelium was rinsed with PBS prior to attachment to the parallel plate laminar flow chamber (GlycoTech) as shown in Figure 2-3 and the cells were flowed for 8 min prior to recording.

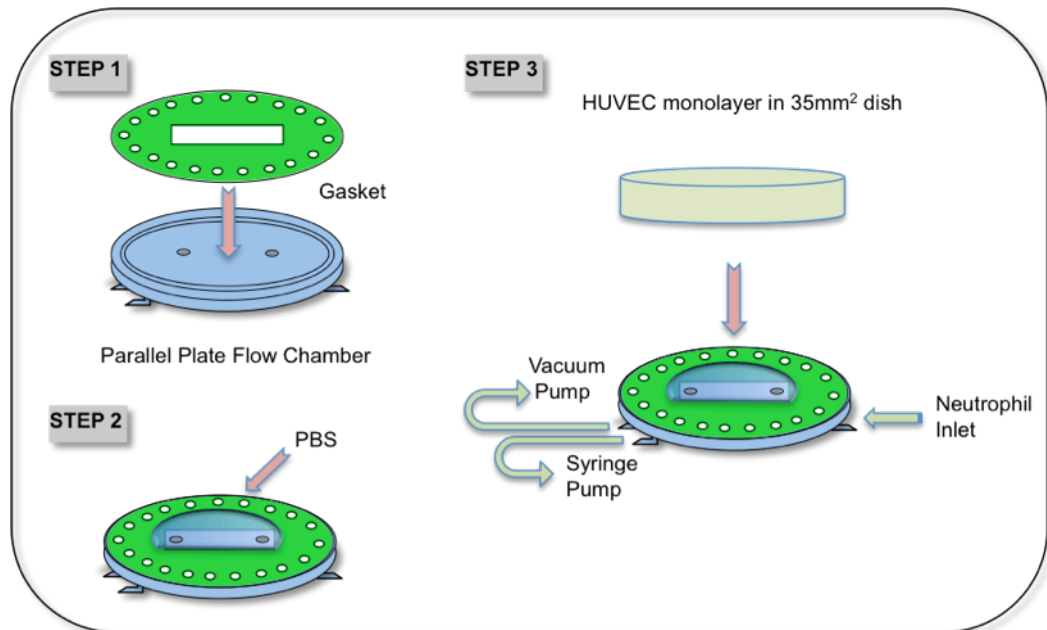


Figure 2-3: Assembly of the parallel plate flow chamber. The chamber was first covered in vacuum grease to hold the gasket in place, and residual grease was removed using an alcohol wipe. PBS was then added to the window in the gasket to cover both the inlet and outlet, ensuring no air bubbles are present. Finally, the HUVEC monolayer was added to the vacuum-sealed chamber, inverted and placed under a Nikon microscope.

A shear stress of 1 dyne/cm^2 was generated using an automated syringe pump (Harvard Apparatus, South Natick, MA). This was calculated according to an adaptation of Poiseuille's law that states:

Wall shear stress (dyne/cm²) = Mean flow velocity (mm/s) x [8/tube diameter (mm)] x viscosity (Poise).

This takes into account the flow rate through a cylindrical vessel; the equation relating wall shear stress to volumetric flow rate through the chamber is given by (Lawrence, McIntire et al. 1987):

$$\tau_w = \frac{6\mu Q}{a^2 b}$$

Where:

τ_w = Wall shear stress (dynes/cm²)

μ = Coefficient of viscosity (Poise)

Q = Volumetric flow rate (ml/s)

a = Channel height (i.e. gasket thickness, cm)

b = Channel width (i.e. gasket width, cm)

Experiments were performed at a constant volumetric flow rate of 0.00707ml/s. The coefficient of viscosity is determined by the fluid in which the PMNs are resuspended and the temperature of the solution. For PBS at a constant temperature of 37°C, the viscosity is 0.0076 Poise. The flow channel was a set size determined by the dimensions of the gasket; the channel height relates to the thickness of the gasket, which was of 0.0254cm and the channel width was of 0.5cm. These conditions create a wall shear stress of precisely 0.9994172 dyne/cm².

The entire flow chamber was placed under a Nikon Eclipse TE3000 microscope fitted with x10 and x20 phase contrast objectives (Nikon, Melville, NY). Neutrophils were perfused over HUVEC monolayers for a period of 8min, and six, 10s frames were chosen from random fields of view using a Q-imaging Retiga EXi digital video camera (Q-imaging) and recorded in Streampix capture software (Norpix) ready for off-line analysis. Sequences were loaded into ImagePro-Plus software (Media Cybernetics, Wokingham), PMNs were manually tagged and their migration monitored. Three measurements were made in the analysis: the total number of interacting cells were quantified as number of cells initially captured during the 10s frame, which were further classified as either rolling or firmly adherent (those which remain stationary for the 10s observation period) (Patel 1999). Experiments were repeated at least three times using various blood donors and various sources of HUVEC. The total number of interacting cells for each category (capture, rolling and adhesion) was converted to number of cells/mm².

In some experiments the PMNs were pre-incubated with either a monoclonal anti-FPRL1 (clone: 6C7-3-A, Kind gift of Dr. Duncan Anderson, Astra Zeneca) or microparticles previously generated from isolated PMN, as described in section 2.10, for 10min at 37°C prior to perfusion of the PMNs. Alternatively, the microparticles were pre-incubated with the monoclonal anti-Annexin A1 (clone 1B) prior to the preincubation of these microparticles with the PMN and the perfusion over the HUVEC monolayer, with the pre-incubations being both conducted for 10min at 37°C. In a separate set of experiments the PMNs were

preincubated for 10mins at 37°C with microparticles generated from either unstimulated or adherent PMNs prior to flowing over the HUVEC monolayer.

Additional experiments were performed in order to determine, initially, which of the novel Ac2-26 derived peptides (sequences illustrated in Table 1.3) possessed inhibitory properties similar to those observed for the parent Ac2-26 peptide. In this case the PMNs were pre-incubated for 10 min at 37°C with 10µM of peptide prior to flowing over the HUVEC monolayer.

In a distinct set of experiments a dilution series was prepared for both Pep57 and Pep84 (sequences illustrated in Table 1.3) ranging from 10µM down to 0.01nM.

These dilutions were then employed to determine the inhibitory potential of each of these peptides on PMN adhesion to an activated endothelial monolayer. To do so, each of the prepared dilution was pre-incubated with PMNs for 10min at 37°C with and then perfused over the activated HUVEC monolayer.

In another separate set of experiments PMNs isolated from Wegner and GCA patients were flowed over an activated HUVEC monolayer in order to determine their level of activation when compared to healthy volunteers. In another set of experiments these PMNs were pre-incubation with 10nM hr Annexin A1 for 10 min (Hayhoe, Kamal et al. 2006) prior to perfusion in order ascertain the pharmacological effect of hr-Annexin A1 protein in this subset of rheumatic conditions.

2.5. Flow-cytometric analysis.

Flow-cytometry is a versatile tool that allows various characteristics of a cell to be analyzed. Cell suspensions are aspirated in single file through a narrow chamber (the flow cell) and illuminated by a laser (incident beam). This light will either be scattered or absorbed when it hits the cell. Absorbed light of the appropriate wavelength may be re-emitted as fluorescence if the cell contains a naturally fluorescent substance (autofluorescence) or if fluorochrome-labelled antibodies are attached to the cell. Light scatter is dependent on the internal structure of the cell, its size and shape. The amount of light scattered at small angles ($0.5\text{-}5^\circ$) or forward scattering (FSC) gives a rough measure of cell size, whereas the light scattered at large angles ($15\text{-}150^\circ$) or side scattering (SSC) increases with the cells' internal granularity. This data alone can be very useful as it discriminates between distinct cell types. This is demonstrated in the dot plot below, where larger cells with a big nucleus and granular cytoplasm (granulocytes) are gated in blue, small cells with a large nucleus (lymphocytes) are gated in green, and monocytes, which have intermediate properties are gated in red (Figure 2-4).

These groups can be confirmed using antibodies specific for each of the cell types, CD11b, CD3 and CD14 respectively. To excite the fluorescence of a fluorochrome, an intense light source that provides the necessary excitation wavelengths is needed. Fluorescein isothiocyanate (FITC) for example, is stimulated by blue wavelengths of light around 490nm (therefore the blue Argon-ion laser is used which excites at 488nm) and re-emits light at a longer wavelength (emission spectra).

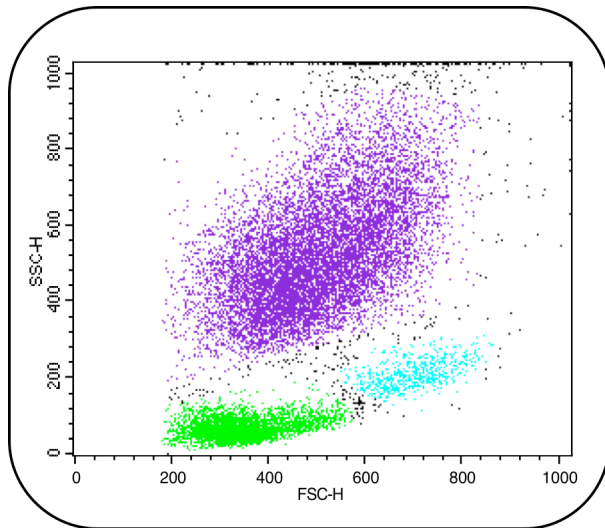


Figure 2-4: Representative dot plot of human blood leukocytes. Granulocytes (purple), lymphocytes (green) and monocytes (light blue) are gated according to size and granularity.

FITC emits light over the range 475-700nm peaking at 525nm, which falls in the green spectrum, shown in the spectral diagram (Figure 2.5). Photomultiplier-based detectors placed in line or perpendicular to the axis of the laser beam collect the emitted or scattered light. Typically, 10,000 cells from each sample are analyzed for statistically valid results. Flow-cytometry data was acquired using a FACScan II analyser (Becton Dickinson, Cowley) and analyzed with CellQuest software (BD Biosciences).

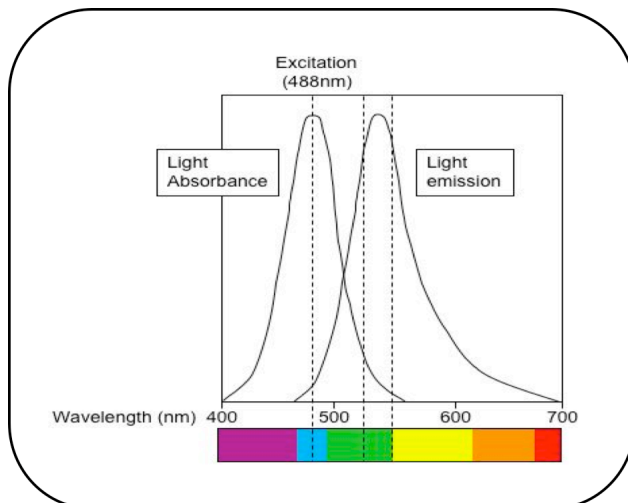


Figure 2-5: Light absorbance and light emission spectra of FITC.

2.5.1. Assessment of surface molecule expression on the HEK-FPR, HEK-FPRL1 and HEK-CMV cells by flow cytometry

Three human embryonic kidney (HEK) cell lines were thawed from the cryogenic stocks by placing the cryovial in a water bath at 37°C for 2mins, following which the cells were immediately re-suspended in 15ml Minimum Essential Medium Eagle (MEM) supplemented 10% heat inactivated foetal calf serum (FCS), L-glutamine (2mM), gentamycin (1µg/ml) and geneticin (200µg/ml). The medium was initially changed after 24h following which it was changed after 48h. Cells were cultured till 90% confluency after which they were trypsinized and counted, 1×10^5 cells were seeded per well in 96-well plates. Cells were incubated with blocking IgG (at a concentration of 16mg/ml) and purified mouse anti-human monoclonal antibodies (mAb) at 5µg/ml final concentration: FPRL1 (clone 6C7-3-A: kind gift Dr Duncan Anderson, Astra Zeneca), FPR (clone 5F1: BD Pharmingen) for 1h on ice. The cells were then washed twice with PBC (which is PBS + 0.15% BSA and 1mM CaCl₂) prior to staining with fluorescein isothiocyanate (FITC)-conjugated F(ab')₂ rabbit anti-mouse IgG (1:200; AbD Serotec). An IgG1 isotype and unstained controls were also prepared for accurate calibration of the FACS machine. Surface protein expression was recorded as Mean Fluorescence Index (MFI) units measured in the FL1 green channel.

In a separate set of experiments HEK-FPRL cells were seeded in a 24 well plate and incubated with 1µM of either Pep84, Pep57 and Ac2-26 (sequences illustrated in Table 1.3) for the following time points 15, 30, 60 and 120 min. At the end of each time point a metabolic inhibitor cocktail containing 1mM 2-4 dinitrophenol and 45mM 2-deoxy-D-glucose was added to each well to stop any

further receptor trafficking. This inhibitor cocktail interferes with mitochondrial function blocking respiration and this metabolic activity. The cells were incubated with this metabolic inhibitor cocktail for 10 min then washed twice with PBC counted and seeded at a concentration of 1×10^5 cells per well in 96-well plates. Following which they stained using a mouse monoclonal anti-human FPRL1 antibody and anti-mouse FITC conjugated secondary antibody as outlined above. An IgG1 isotype and unstained controls were also prepared for accurate calibration of the FACS machine. Surface protein expression was recorded as MFI units and percentage positive cells measured in the FL1 green channel.

2.5.2. Assessment of surface molecule expression on PMNs derived microparticles by flow cytometry

Microparticles derived from patients suffering from a number of rheumatic conditions, healthy volunteers and wild type (WT) and Annexin A1 knock out mice (Annexin A1 $-/-$) were produced as will be subsequently outlined in section 2.10. These were then re-suspended and counted using the forward and side scatter parameters on the flow-cytometer, which had been previously calibrated using $1 \mu\text{m}$ size beads (Gasser, Hess et al. 2003). After counting the microparticles were seeded into 1.2 ml FACS tubes at a concentration of 4×10^4 microparticles per tube. Subsequently, they were incubated with purified mouse anti-human monoclonal antibodies (mAb) at $5 \mu\text{g/ml}$ final concentration: Annexin A1 (clone 1B), FPRL1 (Clone 6C7-3-A, Astra Zeneca), CD62L (Clone: FMC46, Serotec), CD62P (clone: Psel.KO.2.12, Serotec), CD14 (TUK4, Serotec) for 1h on ice, and concomitantly they were stained with FITC-conjugated $\text{F(ab}')_2$ rabbit anti-mouse IgG (1:200; AbD Serotec). Whilst the

mouse microparticles were co-incubated with rat anti-mouse anti bodies against CD62L (clone: MEL14, Serotec) along with an annexin-V FITC conjugated protein (also used for the human microparticles). IgG1, IgG2b isotypes and unstained controls were also prepared for accurate calibration of the FACS machine. Surface antigen expression was recorded as MFI units and percentage positive MP measured in the FL1 green channel.

The FPRL1 and Annexin A1 levels in plasma microparticles derived from healthy volunteers, Wegner and GCA patients were assessed using flow-cytometry. This was done by incubating 10µl of plasma to 10µl of primary antibody for 30 min at 4°C following which 2µl of secondary anti-mouse FITC conjugated antibody (1:200 final dilution) was added for a further 20 min. Finally 200 µl of PBC were added to the reaction mixture and the antigen expression was determined by flow-cytometry.

In a further separate set of experiments the effect of a daily prednisolone (14mg oral) treatment on the Annexin A1 and FPRL1 levels in MPs was assessed. Blood was collected in collaboration with Dr. Stephen Kelly at the Mile End Rheumatology Clinic, the plasma separated as described in section 2.10 and stained as highlighted above.

2.5.3. Assessment of surface molecule expression on PMNs from Wegener granulomatosis, GCA patients and healthy volunteers by flow cytometry

PMN's from were isolated as detailed in section 2.2, after isolation and counting, 1×10^5 cells were seeded per well in 96-well plates. Cells were incubated with purified mouse anti-human monoclonal antibodies (mAb) at $5 \mu\text{g/ml}$ final concentration: Annexin A1 (clone 1B), FPRL1 (Clone 6C7-3-A, Astra Zeneca), FPR (clone 5F1: BD Pharmingen) CD62L (Clone: FMC46, Serotec), PR3 (clone CLB-12.8: kind gift Dr Valerie Witko-Sarsat) for 1h on ice, prior to staining with FITC-conjugated F(ab')₂ rabbit anti-mouse IgG (1:200; AbD Serotec) for a further 30min. IgG1, IgG2b isotypes and unstained controls were also prepared for accurate calibration of the flow-cytometer. Surface protein expression was recorded as MFI units and percentage positive cells measured in the FL1 green channel.

2.5.4. Assessment of surface molecule expression on PMNs from RA patients by flow cytometry

Monocytes and PBMC's were isolated as detailed in section 2.2, from patients enrolled in a clinical study to determine the efficacy of an oral daily prednisolone(15mg) treatment on disease control in Rheumatoid Arthritis patients in collaboration with Dr Stephen Kelly, Rheumatology Clinic, Mile End. Blood was collected on days 0 (i.e. prior to commencement of glucocorticoid treatment) and after, at days 1, 3, 7 and 14. Where cells were isolated, counted and seeded at a concentration of 1×10^5 cells per well in 96-well plates. Cells were incubated with purified mouse anti-human monoclonal antibodies (mAb) at $5 \mu\text{g/ml}$ final concentration: Annexin A1 (clone 1B), FPRL1 (Clone 6C7-3-A, Astra Zeneca), FPR (clone 5F1: BD Pharmingen) CD62L

(Clone: FMC46, Serotec) and CD11b (clone: MCA551 Serotec), for 1h on ice, prior to staining with FITC-conjugated F(ab')₂ rabbit anti-mouse IgG (1:200; AbD Serotec) for a further 30min. IgG1, IgG2b isotypes and unstained controls were also prepared for accurate calibration of the flow-cytometer. Surface protein expression was recorded as MFI units and percentage positive cells measured in the FL1 green channel.

Staining of the synovial cells was also conducted, in this case the synovial fluids obtained from the patients at day 0 were centrifuged at 400xg for 10 min and the supernatant removed. The cells were then washed twice with HBSS and re-suspended in PBC, after which the staining protocol outlined above was followed and the level of antigen expression observed on the synovial monocyte and neutrophil populations was determined.

2.6. Sodium Dodecyl Sulphate - Polyacrylamide Gel Electrophoresis (SDS-PAGE) Western Blotting.

In principle, electrophoresis separates molecules according to their molecular weight, shape and intrinsic charge using an electric field. Using SDS-PAGE proteins are resolved primarily by their size. The anionic detergent SDS denatures proteins by disrupting hydrogen bonds and also causes them to become negatively charged by covering the polypeptide backbone of the protein in its hydrophobic tail. SDS binds to most proteins at a constant ratio of 1.4g per gram of protein resulting in a negative uniform charge-to-mass ratio. Consequently, the charge of the protein becomes insignificant compared to the overall net negative charge of the bound SDS, and proteins migrate in the gel according to size, with the smallest proteins moving furthest through the gel.

2.6.1. Sample Preparation

Microparticles were extracted and washed, supernatants were aspirated and, for analysis of total cellular proteins, 50µl per $\sim 6 \times 10^4$ microparticles of 1x hot Laemmli sample buffer (50mM Tris-HCl (pH 6.8), 2% SDS, 10% glycerol) were added directly to the pellet. This solution was syringed twice with a 25G needle to fully lyse the microparticles. Protein concentration was determined using the BCA protein assay (Pierce) as described below and samples were equalized by dilution with sample buffer. The reducing agent, 100mM DTT was added to cleave disulphide bonds to completely unfold the protein structure, and 0.01% bromophenol blue was added to identify the protein front as they migrate through the gel, prior to boiling the samples. 40µl of sample containing 20-30µg

of protein was boiled for 5 min before loading and running on a polyacrylamide gel.

In a separate set of experiments microparticles were produced from PMNs and pelleted as will be subsequently highlighted and the supernatant collected. This supernatant was then concentrated 40x by loading on to the receiving part of a 10kDa cut of concentration column (Millipore) and centrifugating for 45mins at 13000xg. Subsequently, 8 μ l of lamelli buffer were added to 42 μ l of the concentrated sample this solution was boiled for 5mins loading and running on a polyacrylamide gel

To determine the subcellular localization of Annexin A1 in PMNs derived from Wegner, and GCA patients along with healthy aged matched controls, membrane and cytoplasmic extracts were obtained using a protocol adapted from (Hilgenberg and Miles 1995). Cells were washed with ice cold PBS and 100 μ l of Lysis Buffer (20mM Tris-HCL (pH7.5), and the following protease inhibitors: 10 μ M Leupeptin, 1 μ M Pepstatin A, 200 μ M Phenylmethyl-sulfonyl fluoride, 1mM Sodium Fluoride and 1mM β -glycerolphosphate) per 3×10^6 PMNs and homogenized through a 25G needle 5 times. Homogenates were centrifuged at 300g for 2 min at 4°C to remove cell debris and the supernatants were transferred to a new eppendorf. These were centrifuged at 100, 000xg for 45min at 4°C, and the new supernatants were collected as the cytosolic fraction. 1% Triton X-100 was added to the lysis buffer and 100 μ l was added to the pellet, re-suspended and incubated on ice for 15min to obtain the membrane fraction.

In the quest to determine the affectivity of the Ac2-26 derived peptides, the HEK-FPR and FPRL1 cells were seeded in 12 well plates and grown to 90% confluency, following which 10 μ M of each of the five peptides, the parent peptide, W-peptide or DMSO was added to each well and the cells incubated in a humidified chamber at 37°C and 5% CO₂ for 8 min. Subsequently, the supernatant was aspirated and the cells transferred to -80°C for 2 min. The plate was then taken out and then 100 μ l of lysis buffer containing the protease inhibitors described above was added following which, the cells were scraped off and transferred into eppendorfs where subsequently the protein content for each sample was determined using the BCA protein assay described in section 2.5.2.

Subsequently, a concentration range for Pep84 and Pep57 was prepared by diluting the original stock of each of these peptides 1:10 in DMSO for a final concentration range between 10 μ M and 0.1nM. The cells were incubated with various concentrations of these peptides and the proteins prepared for western blotting analysis as outlined above.

Two types of buffer system can be used for protein electrophoresis, a continuous and a discontinuous system; the former uses only one buffer whereas the latter uses two buffers to make the gel. The discontinuous (Laemmli) buffer system, constructed of a low percentage (4%) stacking and a higher percentage (6-15%) resolving gel, allows proteins to concentrate prior to separation resulting in a far greater resolution. The percentage of the resolving gel depends

on the molecular weight of the protein of interest, the formulations of which are shown in Table 2.1. The resolving and stacking gels were prepared by combining all reagents except for the polymerisation catalysts ammonium persulfate (APS) and TEMED, which were added immediately before pouring the gels. A gel cassette was assembled using a Bio-Rad casting frame, spacer plate and short plate, and was placed in a casting stand with pressure levers that seal the bottom of the cassette.

Resolving Gel Formula						
% Gel	Size Range (kD)	Volume of Reagents				
		Protogel	1.5M Tris pH8.8	dH₂O	10% APS	Temed
6%	60-200	10ml	12.5ml	26.5ml	250µl	25µl
7.5%	40-140	12.5ml	12.5ml	24.5ml	250µl	25µl
10%	20-80	16.7ml	12.5ml	19.8ml	250µl	25µl
12%	15-70	20ml	12.5ml	16.5ml	250µl	25µl
15%	10-30	25ml	12.5ml	11.5ml	250µl	25µl
Stacking Gel Formula						
		Protogel	0.5M Tris pH6.8	dH₂O	10% APS	Temed
4%		2.5ml	3.9ml	12ml	125µl	25µl

Table 2-1: Formulations for SDS-PAGE resolving and stacking gels using National Diagnostic buffers.

A 1.5mm spacer plate, and either a 10 or 15-well comb were used allowing a maximum of 66µl and 40µl of sample to be loaded respectively. The glass plate was marked 1cm below the teeth of the comb, the level to which the resolving gel was poured using a Pasteur pipette. This was overlaid with water and allowed to polymerise for 30min, after which the water was poured off and blotted with filter paper. The stacking gel was poured to the top of the short plate and the comb was carefully inserted to avoid bubbles forming. After polymerisation, the gel cassettes were placed into the electrode assembly, which

in turn was placed into the Mini Tank of the Hoefer Mini Blotting Electrophoresis System. Running buffer (25mM Tris base, 200mM glycine and 0.1% SDS) was added to the inner chamber and approximately 200ml was added to the lower chamber of the tank. Combs were removed and samples as well as pre-stained protein markers (GE Healthcare) were added using gel loading tips. The lid was added and connected to a power supply, and the gel was run at 100 constant volts for approximately 90min until the dye front reached the bottom of the gel.

Once electrophoresis was complete, gels were removed from between the plates, the stacking gel was discarded, and the resolving gel was placed in transfer buffer (25mM Tris base, 192mM glycine and 20% methanol). Protein was transferred onto Polyvinylidene Fluoride (PVDF) membrane (GE Healthcare) by wet transfer (Hoefer). A gel sandwich was made using 1 sheet of blotting paper, PVDF membrane, the gel and 1 sheet of blotting paper on top, all of which were first soaked in transfer buffer. The sample set was then placed in a transfer chamber filled with transfer buffer and was run at a constant voltage. For Annexin A1 and extracellular signal-regulated kinases (ERK) analysis, the transfer was conducted at a 110 constant volts for 90min, for other proteins.

For western blotting, membranes were blocked overnight at 4°C on a plate rocker in either 5% non-fat dried milk solution (1g in 20ml) made up in Tris-buffered saline (TBS) (150mM sodium chloride, 2mM Tris base, pH7.4) containing 0.1% Tween 20 (TBS-T). Membranes were then incubated for 1h at room temperature (RT) in TBS-T with the mouse monoclonal anti-Annexin A1

Ab (clone 1B: 1:2,000 dilution, 10- μ l in 20ml). Following three 5-min washes, with TBS-T, the membrane was incubated for 1h at RT with a horseradish peroxidase (HRP) conjugated goat anti-mouse IgG secondary Ab (1:2,000 dilution) (DakoCytomation). Membranes were washed three times for 5min and excess buffer drained prior to incubation with enhanced chemoluminescence (ECL) solution for protein detection. In principle, the HRP/ H_2O_2 oxidises the luminol within the ECL solution under alkaline conditions, resulting in an excited state, which then decays to its ground state by emitting light at a peak wavelength of 428nm that can be detected by autoradiography film. An equal volume of ECL solution 1 was mixed with ECL 2 according to the manufacturer's instructions (Amersham Pharmacia Biotech), 4ml was poured onto each membrane and incubated for 90s at RT. Excess reagent was drained off and membranes were wrapped in SaranWrap, placed protein side up in an X-ray film cassette, and transferred to the dark room. A sheet of Hyperfilm ECL (Amersham Pharmacia Biotech) was placed on top of the membrane, the cassette was closed and film was exposed for a minimum of 15s and up to 15min in most instances. Films were placed in developer solution until bands were visible, rinsed with H_2O , placed in fixer, rinsed again with H_2O and left to dry.

After determining presence of annexin A1 immunoreactivity in these samples, blots were stripped using 1mM glycine for 15 min and then thoroughly washed for 1 hour with TBS-T in order to ensure adequate removal of any glycine traces. Then the blot was incubated in the presence of an anti- β actin anti body

for 1 hour at room temperature as outlined above. Then the anti- β actin content was determined as previously mentioned.

In a separate set of experiments, where the ability to activate the Mitogen-activated protein kinase (MAPK) pathway through either the FPRL1 or FPR receptors as a measure of activity for the Ac2-26 derived peptides was being assessed, the blot was blocked using a 3% BSA solution for 2h then probed first with an anti-phospho (p)-ERK, 1:2000 dilution in 3% BSA (clone: E10; Cell Signalling Technologies), overnight at 4°C. Subsequently the membrane was washed three times with TBS-T and incubated with a goat anti-mouse HRP conjugated anti-body for 1 hour at room temperature, after which the p-ERK levels were assessed using ECL chemistry as outlined above.

Following the determination of the p-ERK levels in each of these samples, the blot was stripped for 15mins with 1mM glycine following which the membrane was washed for 2 hours in T-BST. Subsequently the blot was then re-incubated for 1h with an anti-total ERK anti-body, 1:2000 dilution in 3% BSA (clone: 137F5; Cell Signalling Technologies), which provided a positive control to the protein concentration loaded. The blot was then probed with an anti-rabbit

2.6.2. BCA (Bicinchoninic acid) protein assay

This assay is based on a colorimetric detection of protein reduction from Cu^{2+} to Cu^+ . Bicinchoninic acid is highly sensitive and specific for Cu^+ and rapidly forms an intense purple colour complex.

A set of standards was prepared for each protein assay using a stock concentration of 2mg/ml BSA. Dilutions were made using the same diluent as the samples (lysis or sample buffer) ranging from 25-2000 μ g/ml (Table 2-2). 10 μ l of each standard or unknown sample were pipetted in duplicate into a 96-well plate. Working Reagent (WR) was prepared by mixing BCA Reagent A to B at a ratio of 50:1, and 200 μ l of WR was added to each well. The plate was incubated at 37°C for 30min and the absorbance was measured at 570nm on an optical plate reader. An average absorbance value of the blank standards was subtracted from all other absorbance measurements, a standard curve was plotted from each BSA standard versus its concentration, yielding a linear response curve ($r^2 > 0.95$). This curve was used to interpolate the protein concentrations of the unknown samples.

Vial	A	B	C	D	E	F	G	H	I
Final BSA Conc. (μ g/ml)	2000	1500	1000	750	500	250	125	25	0
Volume of Diluent (μ l)	0	125	325	175	325	325	325	400	400
Volume and Source of BSA (μ l)	300 Stock	375 Stock	300 Stock	175 Vial B	325 Vial C	325 Vial E	325 Vial F	100 Vial G	0

Table 2-2: Preparation of BSA standards for the BCA protein assay.

2.7. Description of novel Acetyl2-26 derived peptides.

The Acetyl 2-26 peptide is derived from peptides 2-26 of the n-terminal portion of Annexin A1, which has been acetylated on the n-terminal in order to increase its stability and thus its half-life (peptide sequence highlighted in Table 1.3). Modifications were made in the synthesis of this peptide with the aim to produce a more potent peptide with an extended half-life *in vivo*. This modification consisted of substituting amino acids 11 and 22 during the chemical synthesis process, by either two non charged amino acids labelled as α and ϵ corresponding to peptides 84 and 57. Two charged amino acids labelled as χ and δ corresponding to peptides 59 and 60 and an amino acid with a tertiary structure labelled as β corresponding to peptide 83. I cannot declare the real sequences of these novel peptides, as not provided by the Company that sponsored this work (Unigene Corp, Fairfield, New Jersey). These substitutions at the 3 dimensional level could possibly lead to the alterations of the peptide structure or otherwise depending on the charge and bulkiness of the amino acids being substituted.

Amino-Acid Sequence	% pep content	Reference
acetyl-AMVSEFLKQAWFIENEEQEYVQTVK (CRB)	90.1	Ac2-26 CRB
acetyl-AMVSEFLKQAWFIENEEQEYVQTVK (Uni)	83.1	Ac2-26 Uni
acetyl-AMVSEFLKQ α WFIENEEQEY α QTVK	88.1	Pep84
acetyl-AMVSEFLKQ β WFIENEEQEY β QTVK	86.1	Pep83
acetyl-AMVSEFLKQ χ WFIENEEQEY χ QTVK	50.7	Pep59
acetyl-AMVSEFLKQ δ WFIENEEQEY δ QTVK	64.8	Pep60
acetyl-AMVSEFLKQ ϵ WFIENEEQEY ϵ QTVK	73.3	Pep57

Table 2-3: Sequences, peptide contents and nomenclature for each of the novel ac2-26 derived peptides and the parent peptide.

The peptides were received in a lyophilized form, following which they were reconstituted in DMSO at a concentration of 10mM. The volume of DMSO added to each individual vial was calculated taking into consideration the peptide content of each preparation in order to ensure a homogenous final

peptide concentration for each sequence. After reconstitution these peptide solution was aliquoted into 15 μ l volumes and stored at -80°C until required.

2.8. RadioLigand binding assay.

The HEK-FPRL1 or HEK-FPR cells were grown in a T175 flask up to approximately 90% confluency in complete MEM as described in section 2.4.1. Upon reaching ~90% confluency, the cells were washed with PBS and then trypsinized using 3ml of 0.05% trypsin with EDTA for 5mins at 37°C. Subsequently, the flask was gently tapped to detach the cells and 10ml of complete MEM media was added to neutralize the trypsin. The cell suspension was then transferred to a 15ml flacon from which a 100µl aliquot was taken for cell count, whilst the remaining cells were centrifuged at 400 x g for 5 min. The supernatant was then aspirated and the cells re-suspended in 1 ml of PBS containing Ca²⁺ and Mg²⁺. From this cell suspension 31x10⁶ cells were taken, re-suspended at a concentration of 10x10⁶ cells per ml in PBS containing Ca²⁺ and Mg² and then placed on ice until needed, whereas the remaining cells were reseeded in a T175 flask.

The tracer was prepared following manufacturer's instructions, whereby it was re-suspended in 1ml of distilled water. The concentration was calculated using the specific activity (1507.17 Ci/mmol), quantity provided (10µCi) and the relative molecular mass of the peptide (856.11) and was determined to be of 7ng/ml (82pM). With this information the following 1:10 serial dilutions were prepared from: 82pM down to 82fM.

The cold peptide was also prepared by resuspension in distilled water to a final concentration of 1µM. Subsequently a 500µM working stock was prepared, this

was then employed to determine the extent of Non Specific Binding (NSB) by the radio labelled tracer.

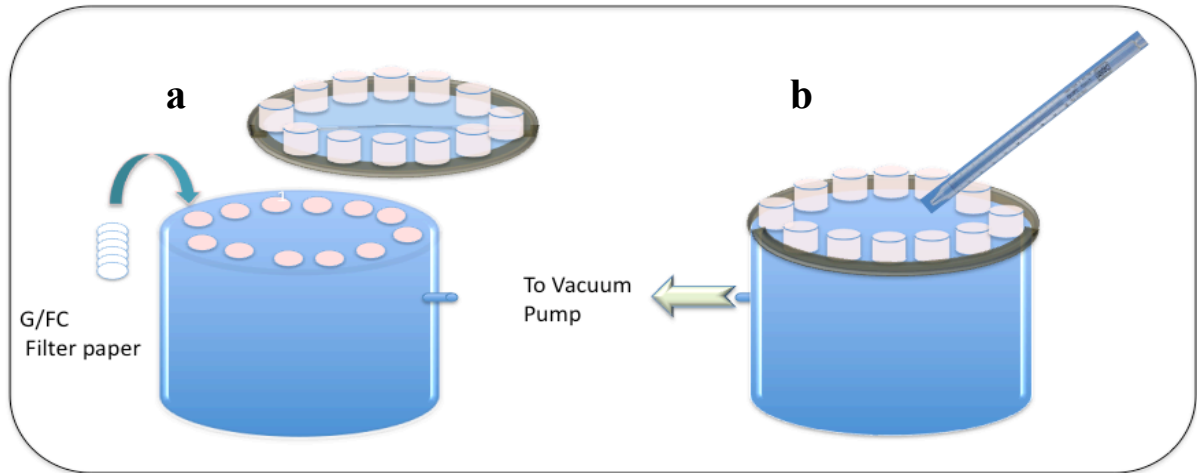


Figure 2-6: Figure outlining the setup being employed for the binding assays (a) outlined the position of the G/FC filters employed to trap the cells along with any bound tracer (b) the setup as employed to wash off any unbound tracer.

The first step in this protocol was to determine the optimal tracer concentration to be employed for the subsequent assays. The criteria employed to identify this concentration involved having a significant difference in the number of counts recorded on a gamma counter between the Total Binding (TB) and Non-Specific binding (NSB) group. In order to achieve this a concentration range of tracer was prepared which ranged from 82pM down to 82fM, whilst the concentration of cold peptide in the NSB group was maintained constant at 1 μ M.

Following the preparation of the tracer dilutions the various experimental conditions (i.e. TB and NSB) were setup as follows in triplicate in 1.5ml eppendorfs:

Total Binding (TB) - 800 μ l PBS (with Ca²⁺ and Mg²⁺), 100 μ l of one of the tracer dilutions previously prepared and 100 μ l of the cell suspension

Non Specific Binding (NSB) - 700 μl PBS (with Ca^{2+} and Mg^{2+}), 100 μl of one of the tracer dilutions previously prepared, 100ul of cold peptide at 1 μM (final concentration) and 100 μl of the cell suspension.

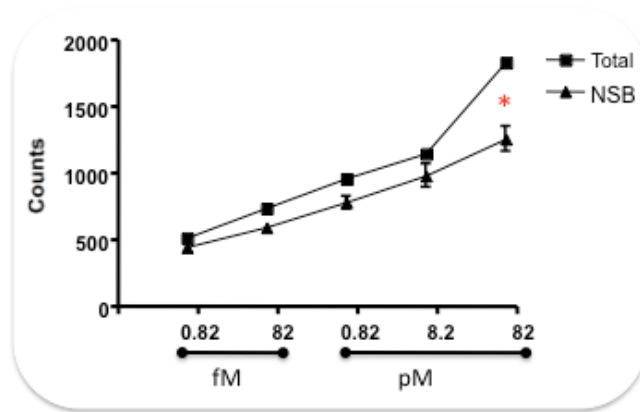


Figure 2-7: Determining the optimal concentration of tracer to be employed in Radioligand Binding assay. Following the resuspension of the HEK-FPRL1 cells at a concentration of 1×10^6 cells were incubated with $10 \mu\text{M}$ of cold peptide and various concentrations of tracer. The highest concentration of tracer is the one that shows a significant difference between Total and nonspecific binding (NSB). Data are mean \pm SEM of 3 independent experiments. * = $P < 0.05$ vs. CT group

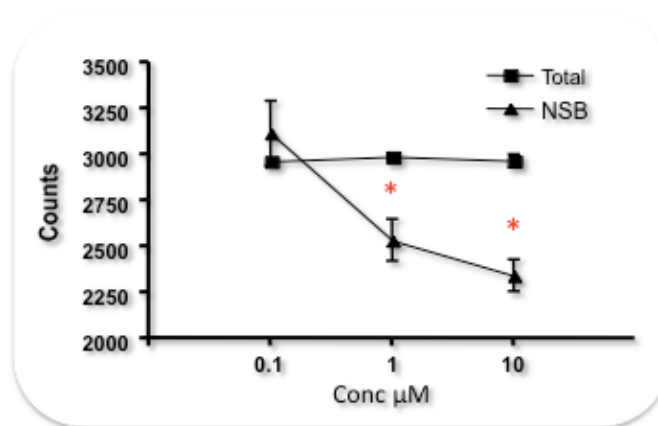


Figure 2-8: Determining the optimal concentration of cold peptide to be employed in Radioligand Binding assay. Following the resuspension of the HEK-FPRL1 cells at a concentration of 1×10^6 cells were incubated with 7pM of cold peptide and 10, 1 or $0.1 \mu\text{M}$ of cold peptide. In this set of experiments the highest concentration of cold peptide was shown to be the most effective at displacing the tracer from the FPRL1 receptor. Data are mean \pm SEM of 3 independent experiments * = $P < 0.05$ vs. CT group.

The reaction mixture was then incubated for 1 hour on ice after which it was transferred on to a vacuum filtration unit equipped with 25mm GF/C filter membranes on to which any cells and bound tracer would be retained. The

filters were then washed 3 times using 4ml aliquots of 10mM ice cold Tris-HCL, to remove any unbound tracer (Figure 2-6). Following the wash step the filter paper was transferred into recipient tubes and the amount of bound tracer was determined using a γ -counter. This experiment was repeated 3 times in order to confirm the reproducibility of the results obtained.

After identifying the optimal tracer concentration (Figure 2.7), the next step was to determine the optimal cold peptide concentration that best displaces the tracer from its binding to the FPR and FPRL1. For this purpose 3 cold peptide dilutions were prepared at a final concentration of, 10 μ M, 1 μ M and 0.1 μ M (Figure 2.8). Then following the procedure outlined above and using the optimal tracer concentration previously determined of 82pM the optimal cold peptide concentration was determined; once again the experiment was repeated 3 times in order to ensure reproducibility of the results obtained.

Subsequently, the binding affinities of Pep84 and Pep57 to both the FPRL1 and FPR receptors, using the HEK-FPRL1 and the HEK-FPR cell lines, were determined following the protocol outlined above and employing a dilution series ranging in concentration between 10 μ M and 0.1nM. Once again, experiments were repeated 3 times in order to ensure the reproducibility of the obtained results.

2.9. Real-Time Reverse Transcription-PCR

2.9.1. RNA extraction

A number of RNA extraction protocols have been developed and in order to determine the optimal extraction method for my studies, I initially compared two of these techniques previously employed in the lab. The first technique employed a charged membrane that traps the RNA from the samples using electrostatic charges on the RNA molecule. This methodology allows for the purification of the RNA by sequential washes and then by reversing the charge of the solution and consequently of the RNA one can elute it off the membrane. The protocol followed was that supplied with the Quiagen RNA mini-kit. This RNA extraction protocol was then compared to a more classical phenol-chloroform derived protocol whereby the sample is homogenised in a phenol-guanidine isothiocyanate containing solution, marketed under the name of TRIZOL®. Following the homogenisation step the RNA was extracted from the aqueous phase obtained upon centrifugation of the TRIZOL®-cell solution, following isopropanol was added to reversing the charge on the RNA molecules leading to the precipitation of the RNA. The RNA was pelleted by centrifugation and then washed in 75% ethanol in DEPC water (protocol outlined in further detail below). The resulting RNA was then assessed for integrity, purity and yield. The integrity was assessed by reverse transcribing the RNA using Oligo-dt, as described below, and the cDNA yield measured using a Nano-Drop spectrophotometer. The rationale behind this step was that the Oligo-dt binds to poly-A tails on the mRNA, which in turn is very susceptible to degradation. Thus by assessing the amount of cDNA produced a measure of the poly-A tail integrity and thus mRNA integrity is obtained. The purity and yield of the RNA were assessed using a Nano-Drop spectrophotometer; purity could

be assessed using the absorbance in 230, 260 and 280nm ranges. This is because the 230/260 ratio provides a measure of assessing the amount of phonetics present in the RNA solution whilst the 260/280 ratio provides a measure of protein contamination in the sample. Thus, after assessing all these parameters it was observed that the integrity and purity of for both protocol employed were comparable. However, the yield obtained using the TRIZOL® (Invitrogen) protocol was superior especially when extracting RNA from tissues. Furthermore, the cost per reaction was much less for this method over the Quigen kits, thus I decided to employ the TRIZOL® method for all the RNA extractions conducted during my PhD

Using TRIZOL® reagent (Invitrogen) cells were rinsed with PBS and lysed directly by adding 1ml of reagent to every 5×10^6 cells, and pipetting several times to lyse the cells. At this point samples could be stored at -80°C until required. The homogenized samples were incubated for 5min at RT to allow complete dissociation of nucleoprotein complexes, and 0.2ml of chloroform (per ml of TRIZOL) was added. Tubes were shaken vigorously by hand for 15s, left at RT for 2-3min before centrifuging at $12,000 \times g$ for 15min at 4°C . This procedure separates the solution into a colourless aqueous phase containing the RNA, an interphase and a lower organic phase. The aqueous phase was transferred to a new tube and the RNA was precipitated with 0.5ml of isopropyl alcohol (per ml of TRIZOL). Samples were incubated for 10min at RT, centrifuged at $12,000 \times g$ for 10min at 4°C to pellet the RNA, supernatants carefully aspirated, and washed with 1ml of 75% ethanol (per ml of TRIZOL). Samples were vortexed, centrifuged at $7,500 \times g$ for 5min at 4°C , supernatants

carefully aspirated and pellets briefly air-dried at 50°C. RNA was dissolved in 20µl of RNase-free water, and stored at -20°C until further use.

The first step when extracting RNA from the human cells using the RNeasy kits (Qiagen) was to pellet $\sim 1 \times 10^6$ cells, by centrifuging for 5min at 300g, after which the supernatant was removed. The cell membranes were then disrupted by re-suspending the cell pellet in 350 µl RLT buffer. Subsequently, the cell pellet was homogenised by passing the lysate 5 times thorough a blunt 20 gauge needle fitted with an RNase free syringe. 350 µl of 70% ethanol were then added and the solution was mixed well. Following which the sample was transferred, including any precipitate that may have formed, to an RNeasy spin column placed in a 2 ml collection tube. The lid was then closed, and centrifuge for 15 s at 8000g. The flow-through was then discarded and 700 µl Buffer RW1 was added to the RNeasy spin column once again the column was spun for 15 s at 8000g to wash the spin column membrane. The flow through was then discarded and the RNeasy spin column was then carefully removed from the collection tube so that the column does not contact the flow-through. 500 µl of the RPE Buffer were again added to the RNeasy spin column the lid gently closed, and the column centrifuge for 15 s at 8000g to wash the spin column membrane followed by another 500 µl Buffer RPE and 2 min at 8000g centrifugation to wash the spin column membrane. The longer centrifugation dries the spin column membrane, ensuring that no ethanol is carried over during RNA elution following which the RNeasy spin column was carefully removed ensuring that the membrane did not come in contact with the flow-through. This is due to that fact that residual ethanol may interfere with downstream reactions.

The RNeasy spin column was subsequently placed in a new 2 ml collection tube, the lid gently closed, and centrifuged at 13000g for 1 min. This step was performed in order to eliminate any possible carryover of Buffer RPE, or if residual flow-through remains on the outside of the RNeasy spin column. Subsequently the RNeasy spin column in a new 1.5 ml collection tube. 30–50 µl RNase-free water was then directly added to the spin column membrane that was then centrifuge for 1 min at 8000g to elute the RNA. The removal of any contaminating DNA was done following the protocol outlined above.

2.9.2. Reverse Transcription

The next step was to identify the optimal reverse transcription protocol for my investigation. Thus I conducted a literature review that pointed out that for this purpose the M-MLV H- RT enzyme would be the better choice since its complementary DNA (cDNA) synthesis rate is up to 40-fold greater than that of AMV. Furthermore, newly available thermostable RNase H- RT maintains its activity up to 70°C, thus permitting increased specificity and efficiency of first primer annealing. Thus, due to its higher specificity and extensive used in the literature it was decided to employ this enzyme to produce my cDNA (Bustin, Benes et al. 2005). Subsequently I also evaluated the various options available for priming the reverse transcription reaction, primarily sequence specific primers, Oligo-dt and random hexameres. Target gene-specific primers work well in conjunction with elevated RT-reaction temperatures to eliminate spurious transcripts. The same reverse primer is used for subsequent PCR assay in conjunction with the corresponding gene-specific sense primer (forward primer). However, the use of gene specific primers limits the number of genes

that can be analysed per sample to the primer sets employed in the RT reaction. Furthermore it cannot be assumed that different reactions have the same cDNA synthesis efficiency, the result can be a high variability during multiple RT reactions.

To circumvent the high inter-assay variations in RT, target gene unspecific primers e.g. random hexameres, octameres or decameres can be used and a cDNA pool can be synthesized. Similarly poly-T oligonucleotides (Oligo-dt), consisting of 16-26 deoxythymidine residues can anneal to the polyadenylated 3' poly-A tail found in the large majority of mRNA. cDNA pools produced with unspecific primers can be split into a number of different target-specific kinetic PCR assays. This maximizes the number of genes that can be assayed from a single cDNA pool, derived from one small RNA sample (Bustin 2002; Bustin and Nolan 2004). Studies comparing the efficacy of the different priming methods have outlined that the best results were obtained with gene specific priming, with Oligo-dt priming ranking next and the random hexameres being the least efficient (Bustin, Benes et al. 2005).

Since for my studies I did not want to restrict myself to a small number of genes, I decided to employ Oligo-dt as the primer of choice for the RT reaction. After deciding on the RT system to be employed, it was important to clean the RNA from any contaminating genomic DNA. This was achieved by incubating the extracted RNA solution with DNase 1, where (20µl) RNA were treated with 2U (1µl) of TURBO DNase 1 (Ambion, Austin, TX) and incubated for 30min at 37°C to remove any contaminating genomic DNA. 4µl of DNase Inactivation

Reagent slurry (Ambion) was added, mixed thoroughly, and left at RT for 2min prior to centrifuging at 1250g for 2min. The RNA solution was then transferred to a new RNase-free tube. RNA was then ready for reverse transcription into cDNA using an Abgene thermal cycler. For each sample, 1µl of Oligo-dt (a poly-T strand annealing to the poly-A tails of the mRNA) 1µl 10mM dNTP Mix, and 11.8µl of RNA were first incubated at 65°C for 5min (to denature RNA secondary structure) and placed on ice for 2min (to allow primers to anneal). Tubes were then briefly centrifuged at 1250g for 30s and the other components for reverse transcription were added, including 4µl 5X first-strand buffer, 1µl 0.1M DTT, 1µl RNaseOUT (a recombinant RNase inhibitor), and 1µl of Superscript™ III Reverse Transcriptase (200U/µl) (Invitrogen). Samples were gently mixed and incubated at 55°C for 1h (for cDNA extension) and then heated at 70°C for 15min to inactivate the enzyme and hence the reaction.

2.9.3. cDNA Quantification

cDNA was then quantified using a Nanodrop ND-1000 Spectrophotometer. With the sampling arm open, 1µl of sample was pipetted onto the lower measurement pedestal, the sampling arm was closed and spectral measurement made using the operating software on the PC; for cDNA quantification, the nucleic acid option was selected. When the measurement was complete, the sampling arm was opened and wiped gently from both the upper and lower pedestals using a soft tissue. The next sample was then measured and procedure repeated. The 260/280 ratio of the sample absorbance was used to assess the purity of the sample, a ratio of approximately 1.8 is generally accepted as 'pure' for DNA and a ratio of 2 generally accepted as pure for RNA. If the ratio is

lower, this indicates that protein/phenol or other contaminants are present that absorb near 280nm. The concentration of cDNA was measured in ng/ μ l from the absorbance at 260nm. cDNA was diluted to 40ng/ μ l in new tubes using molecular biology H₂O, ready for loading into 384-well plates for Real-Time PCR.

2.9.4. Real-Time PCR

The next step was to determine what type of detection chemistry I was to employ in my analysis, since this also influenced the primer design. Two general methods for the quantitative detection of the amplicon have become established: gene specific fluorescent probes or specific double strand (ds) DNA binding agents based on fluorescent energy transfer (FRET). The best-known probe based system is the ABI's TaqMan, which makes use of the 5'-3' exonuclease activity of *Taq* polymerase to quantitative target sequences in the samples. Probe hydrolysis separates fluorophore and quencher and results in an increased fluorescence signal referred to as 'Foerster type energy transfer'. The alternative is a non-sequence specific fluorescent intercalating dsDNA binding dye such as SYBR Green 1 or POWER SYBR Green. For single PCR product reactions with well-designed primers, the SYBR Green chemistry has been shown to work extremely well, with spurious non-specific background only showing up in very late cycles. For my studied I decided to employ an intercalating dye: Power SYBR green. The SYBR Green reporter system consists of an asymmetrical cyanine dye, which binds to double-stranded DNA. The resulting DNA-dye-complex absorbs blue light ($\lambda_{\text{max}} = 488 \text{ nm}$) and emits green light ($\lambda_{\text{max}} = 522 \text{ nm}$). This decision was taken following reports in the literature where comparisons between labelled probes and SYBR green showed

that the two chemistries did produced similar outcomes when it came to dynamic range, sensitivity and selectivity of the signal produced as long as the primers employed for detection were selective and sensitive. Furthermore, SYBR Green detection was more precise and produced a more linear decay plot than the TaqMan probe detection.

Subsequently it was important to identify a primer set of each gene under investigation: GAPDH, 18s, FPRL1 and Annexin A1, which also show an elevated sensitivity. The process for primer design involved first of all identifying a region for amplification, preferably one that is intron-spanning, since this would help in reducing interference by any genomic DNA that is found in the sample. Furthermore, each primer pair needs to have similar annealing temperature preferably close to 60°C since this will significantly reduce mismatch aligning and also the primer pair should not anneal against itself, thus producing primer-dimers. For this a number of online software programs were employed to identify potential primer pairs, amongst which BioEdit, Primer 3 (www.frodo.wi.mit.edu) and Biosearch Technology Primer design (biosearchtech.com)

After choosing the primer sequences that satisfied the aforementioned criteria the next step was to determine which of the primer sets were sensitive enough to detect difference in cDNA copy numbers. This was done by preparing an efficiency plot that consisted of a 1:2 cDNA dilution series ranging from 80ng/μl down to 0.3ng/μl. The efficiency of each primer pair was then calculated by plotting the cycle threshold (CT) (Figure 2.7) value for each of the

cDNA concentrations employed. The efficiency value was then obtained from the equation of the resulting slope where a value ranging between 1.8 and 2 shows that the primer pair displays acceptable sensitivity to changes in cDNA copy number.

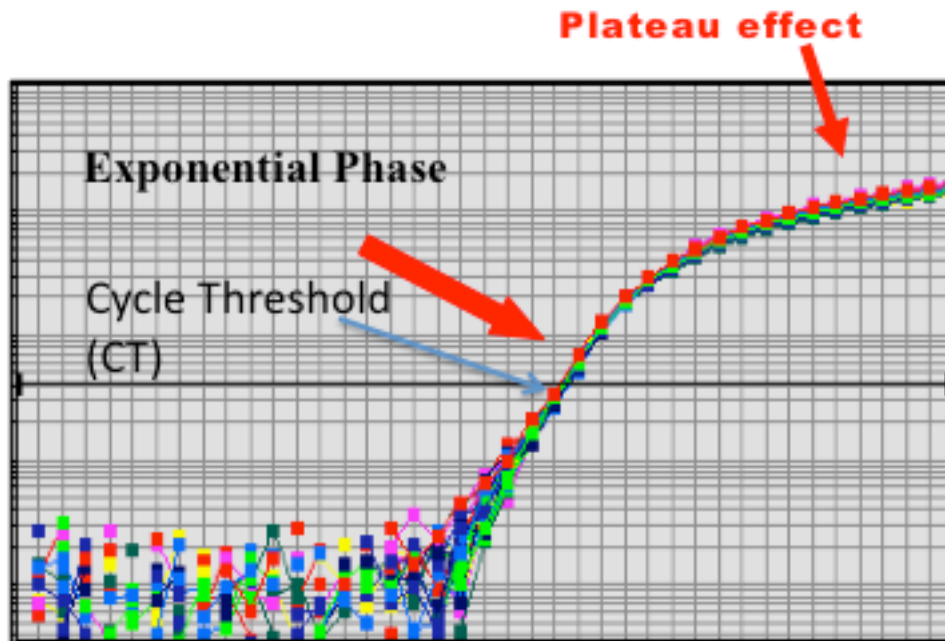


Figure 2-9: Figure outlining a typical expression profile for a real time PCR reaction.

After several attempts I only succeeded in obtaining two primer sets with efficiency values falling between 1.8 and 2, those for GAPDH (Figure 2.8) and those for FPRL1 genes. Thus, I then conducted a literature search, which resulted in identifying a new primer source. This was the Qiagen Quantitec Primer Assay® system that consisted of pre-validated primer pairs which can also be used with the SYBR green detection system. For each of the genes mentioned above, upon purchasing each of these primer pairs I proceeded to validate them in my system by conducting an efficiency analysis, confirming that each of the primer sets was able to detect varying cDNA concentrations.

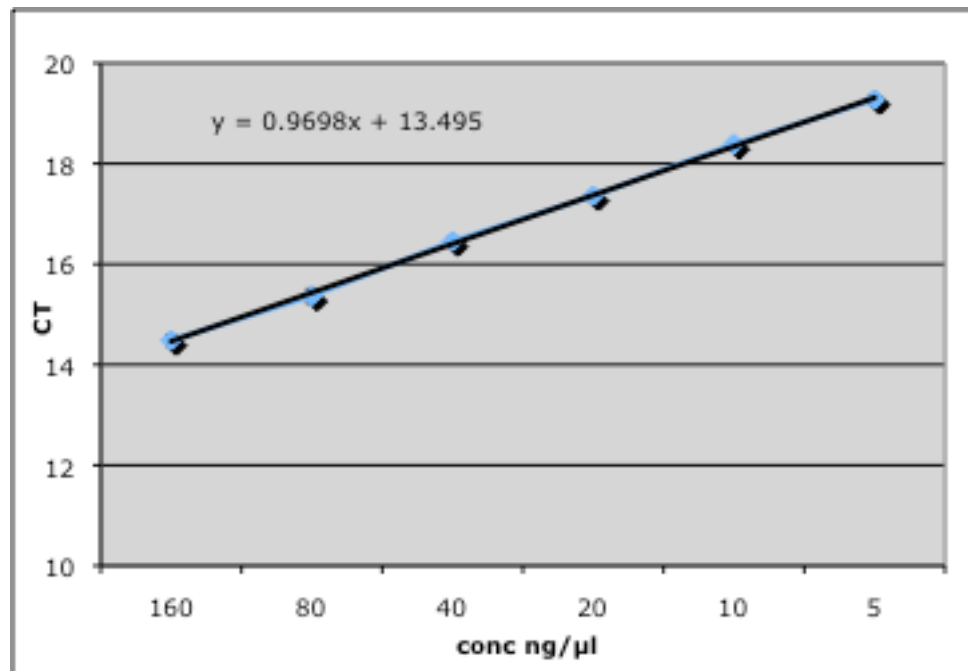


Figure 2-10: Figure outlining the efficiency plot obtained for the GAPDH gene. Representative of 3 distinct experiments.

Thus after identifying the primer sequences to be employed in my study and producing cDNA from each of the patient and control sample under investigation I tested the relative levels of Annexin A1 and FPRL1 levels in these samples using the aforementioned Qiagen Quantitec Primer Assay®. The PCR reaction for determining the efficiency values for each of the primer pairs and subsequently for the detection of the relative gene expressions in the patient and control samples was performed using ABI Prism® 7900 Real Time PCR equipment. A mastermix was made for each gene specific primer, containing 1μl primer, 5μl 2X POWER SYBR Green (ABi biosciences) and 2μl H₂O; a final volume of 8μl was dispensed in each well and 2μl of diluted cDNA (100ng/μl) was added. Each sample was tested in triplicate for each of the four genes. The thermal profile consisted of 50°C for 2min, 95°C for 15min, then 40 cycles of 94°C for 15s, 55°C for 30s and 72°C for 30s. Following which a

dissociation step was added, in order to determine if the PCR reaction was specific to the genes under investigation, with the following thermal profile: 95°C for 15s, 60°C for 15s and 95°C for 15s. SYBR Green binds to newly synthesized double-stranded DNA, emitting fluorescence in direct proportion to the number of amplicons generated. A threshold line of fluorescence detected above background was set in the exponential phase of amplification, and the cycle number at which the samples reached this level was referred to as the cycle threshold value (C_T), thus reflecting the relative abundance of the specific mRNA transcripts. The comparison between samples was performed using GAPDH and 18s ribosomal subunit as internal standards. REST MCS software was utilized for the calculation of the relative difference between the test groups. This software uses a mathematical model that is based on PCR efficiencies and the mean crossing point deviation between the sample and control group. Subsequently, the expression ratio results of the four investigated transcripts are tested for significance by a randomization test (Pfaffl, Horgan et al. 2002).

2.10. Isolation of Microparticles.

2.10.1. From Purified Neutrophils

To determine the functional role of microparticles in the inflammatory response these were isolated from both human and murine PMNs. Whereby after isolation of the PMNs from both species the cells were counted and re-suspended at a concentration of 5×10^6 cells per ml (Gasser and Schifferli 2004). These were then incubated at 37°C for 20 min over an endothelial cell monolayer. In the case of the human PMNs the endothelial monolayer was a HUVEC monolayer, whilst the murine cells were preincubated over an endothelial monolayer isolated from WT lungs as described in section 2.13.1. The cells were then stimulated using fMLP, which aids in a specific priming of the PMNs, the concentrations employed varied between the human and the murine cells due to the varying sensitivity of the FPRL1 or its murine homologue to this ligand. In fact $1 \mu\text{M}$ of fMLP was employed for the human cells and $10 \mu\text{M}$ for the murine cells, in both cases the cells were incubated for a further 20 min at 37°C. Another difference in the murine experiments was that in this case microparticles were produced from both WT and Annexin A1 $-/-$ mice, separately. Following the stimulation, the cells were centrifuged at 2000g for 10 min to remove any cells and debris and then the supernatant was centrifuged at 100,000g for 1 hr to obtain a microparticles pellet. Subsequently the resultant supernatant was removed and the pelleted microparticles were washed and re-suspended in PBS.

In a separate set of experiments microparticles obtained for human PMNs without a pre-incubation over a HUVEC monolayer. In this case PMNs were

stimulated with μM fMLP for 20 min without preincubation with a HUVEC monolayer. After incubation with $1\mu\text{M}$ fMLP for 20 min at 37°C the cells were centrifuged at $2000g$ for 10 min and the microparticles isolated as detailed above.

Microparticles were also generated by stimulating PMN in suspension with either fMLP ($1\mu\text{M}$), LXA_4 (1nM) or AF2 ($10\mu\text{M}$) for 20 min at 37°C in RPMI. Following which the PMNs were removed and the microparticles extracted as outlined above. Furthermore in order to determine if there is an altered release of Annexin A1 in Wegner granulomatosis PMNs, the cells from these patients and aged matched healthy controls were extracted (as outlined in section 2.2) and stimulated for 20 min with $1\mu\text{M}$ of fMLP. The microparticles then extracted as outlined above and both the supernatant and microparticles were blotted for their Annexin A1 content as outlined above.

2.10.2. From whole blood

In order to determine the clinical relevance of Annexin A1 and FPRL1 positive microparticles in rheumatic diseases, blood was obtained from patients suffering from RA, GCA MPO and PR3 ANCA +ve patients along with healthy volunteers; this was done using the gradient centrifugation method outlined in section 2.2. In this protocol after layering the diluted whole blood over the double density Ficoll and centrifugation the plasma fraction was extracted. This was then spun at $4000g$ for 5 min to remove any contaminating platelets, aliquoted and stored at -80°C until required for the analysis of microparticle Annexin A1 and FPRL1 levels as described in section 2.4.2.

In a separate set of experiments blood was obtained from patients recruited to participate in a study to determine the efficacy of a 14 day prednisolone treatment on disease outcome in Rheumatoid arthritis in collaboration with Dr Stefan Kelly, Rheumatology Clinic, Mile End. In this case blood was taken on days 0 (i.e. pre steroid treatment), 1, 7 and 14. The processed as previously described above.

2.11. In-gel Digestion and LC/MS/MS analysis

PMN microparticles were produced as outlined in section 2.5, after which $\sim 5 \times 10^4$ MP were loaded on to an 8% SDS gel run as described in section 2.5 along with an Annexin A1 positive control. After the gel was run, this was cut in two and the proteins found on one half of the gel were transferred on to a PVDF membrane and probed against Annexin A1 as outlined in section 2.5. On the other hand the second half of the gel was stained using Coomassie Blue dye (containing 0.2% Coomassie Blue, 7.5% Acetic Acid and 50% Ethanol) for 1 hour at room temperature and then the excess dye was removed by incubating the gel in destaining solution over night at room temperature on a plate rocker. Following which the band corresponding to the Annexin A1 band (at ~ 37 kDa) was excised.

The excised band was cut into small cubes using a scalpel blade; this was done in order to facilitate the further processing of the sample. In-gel reduction, alkylation and digestion with trypsin were then performed prior to subsequent analysis by mass spectrometry. Cysteine residues were reduced with DTT and

derivatized by treatment with iodoacetamide to form stable carbamidomethyl (CAM) derivatives. Trypsin digestion was carried out overnight at room temperature after an initial 1hr incubation at 37°C.

Peptides were extracted from the gel pieces by a series of acetonitrile and ammonium bicarbonate washes. The extract was pooled and lyophilised. Each sample was then re-suspended in 50mM ammonium bicarbonate and analysed by LC-MS/MS. Chromatographic separations were performed using CapLC system (Waters corporation, UK). Peptides were resolved by reversed phase chromatography on a 75 µm C18 PepMap column. A gradient of acetonitrile in 0.05% formic acid was delivered to elute the peptides at a flow rate of 200 nl/min. Peptides were ionised by electrospray ionisation using a Z-spray source fitted to a QToF-micro (Waters corporation, UK). The instrument was set to run in automated switching mode, selecting precursor ions based on their intensity, for sequencing by collision-induced fragmentation. The MS/MS analyses were conducted using collision energy profiles that were chosen based on the m/z and the charge state of the peptide.

The mass spectral data was processed into peak lists (MS/MS data) and searched against the Swiss Prot and NCBI non-redundant database using Mascot software (Matrix Science, UK). Carbamidomethyl(C) and oxidation (M) were set as variable modifications within the searching parameters. A high level of confidence can be assigned to these protein identities because the results are based on exact matching of MS/MS data for multiple peptides from each protein. Identifications with a score of 30 or above were considered significant

2.12. Assessment of Reactive Oxygen Species (ROS) production by microparticles.

Neutrophil derived microparticles were produced from healthy volunteers by stimulation of these cells with fMLP in the presence or absence of an endothelial monolayer as detailed in section 2.10. These were then re-suspended in HBSS counted (as outlined in section 2.10) and $\sim 1 \times 10^4$ microparticles were loaded into a 96 well plate in a total volume of 150 μ l HBSS containing 15mM of Lucigenin. The plate was then incubated at 37°C in the thermostable chamber of the luminometer (Wallac VICTOR² 1420 Multilabel Counter, Perkin Elmer Life Science, Boston, MA, USA) and allowed to stabilize for 15 min.

After a baseline reading was established, cells were stimulated with 1 μ M fMLP or 16 μ M PMA. Changes in chemoluminescence were measured over a 30 min period. Three separate experiments with triplicates for each test compound were performed. Microparticle generated superoxide was recorded as counts per sec (CPS).

2',7'-Dichlorofluorescein diacetate (DCFDA; Sigma) was also employed to determine ROS production by these microparticle populations. In this case the microparticles were co-incubated with 5 μ M of DCFDA for 50mins at 37°C, they were washed and then re-suspended in PBC. Following which the microparticle ROS production was determined following PMA (16 μ M) stimulation in the FL1 channel of the flow-cytometer.

2.13. Animal experiments

The Annexin A1 $-/-$ mice were bred in house on a homogenous Balb/c background, whilst their age and sex-matched wild type (WT) controls were purchased from B&K Universal. Animals used for all experiments were fed laboratory chow and water *ad libitum* and were housed 6 to a cage under specific pathogen-free conditions. All experiments were performed with male animals (body weight \sim 22-25g) strictly following Home Office regulations (Guidance on the Operation of Animals, Scientific Procedures Act 1986).

2.13.1. Murine Lung Endothelial Cell (MLEC) isolation.

Primary mouse endothelial cells were isolated from the lungs of wild-type (WT) Balb/c mice (Reynolds, Reynolds et al. 2004). Lungs were excised and kept in Ham's F-12 media (Gibco, UK) on ice until isolation. Lungs were briefly rinsed in 70% ethanol, transferred to a Petri dish and chopped into small pieces using a scalpel blade. Tissue was digested with 1mg/ml collagenase type I-S (Gibco, UK) in PBS for 2h at 37°C. The digest was taken up in a syringe, passed through a 19-gauge needle 5 times and sieved through a 70 μ m-pore size cell strainer (BD Falcon, Bedford, MA). The cell suspension was then centrifuged at 300g for 5min and re-suspended in 10ml of complete media (50:50 mix of Ham's F-12:DMEM medium supplemented with 20% FCS, 20 μ g/ml endothelial cell mitogen Biogenesis, Poole), 1 μ g/ml heparin, penicillin (100U) and streptomycin (100mg/ml)). All culture flasks/dishes were coated for 30min with 0.1% gelatine and 10 μ g/ml fibronectin in PBS prior to cell seeding. Cells were plated in a T75 flask and incubated in a humidified chamber in 5% CO₂ at

37°C. After 24h, cells were washed 5 times with PBS to remove unbound cells and cultured for 2-4 days before purifying.

Endothelial cells were purified by positive selection from contaminating fibroblasts using magnetic Dynabeads (DynaL Biotech, UK). The principal of this procedure is outlined in Figure 2-9 Cell culture media was removed from the flask and replaced with cold complete media and cells were put in the fridge for 20min. Media was then aspirated and cells were incubated with 3µg/ml of the primary Ab; rat anti-mouse CD102 (clone 3C4 (mIC2/4); BD Pharmingen) in PBS for 30min at 4°C. The PBS/Ab mix was removed, cells were rinsed once with PBS and then incubated with 10µl (approximately 4×10^6) sheep anti-rat IgG magnetic dynabeads in 3ml of PBS for 5min at 4°C.

Flasks were rinsed 3 times with PBS to remove unbound beads, and then cells were detached using 1x trypsin (Sigma). Detached cells were transferred to a pre-coated T25 flask and positive cells were selected by placing the flask on a flat magnet and leaving for 5min. Contaminating cells were removed by aspiration, being careful not to disturb bead-bound cells. Flasks were rinsed and placed back on the magnet for 5min for two more rinse steps until only positive cells remained. 5ml of complete media was then added and cultures were grown to confluence. At least two positive sorts for ICAM-2-positive endothelial cells were performed before using in subsequent experiments in order to ensure a high purity endothelial culture.

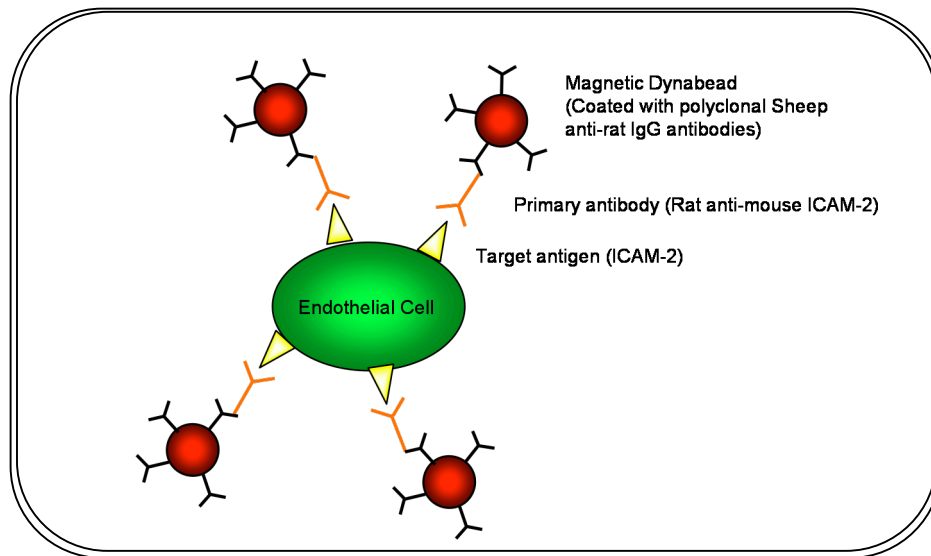


Figure 2-11: Endothelial cell positive selection using magnetic Dynabeads.

2.13.2. Bone Marrow Neutrophil Extraction and Purification

Mice were killed by CO₂ asphyxiation before each animal was sterilized by immersion in 70% ethanol. The femur of each leg was exposed and removed without crushing the bone. Briefly, this involved pulling back the skin from the ankle and then removing the muscle with fine pointed scissors. The lower art of the leg was then removed by cutting at the knee joint in order to facilitate easier access to the hip joint. The femur was removed with the ball joint intact, allowing both ends of the bone to be gently cut to expose the marrow without crushing the bone itself. Using a 2ml syringe with a 25 gauge needle attached, HBSS was flushed through both ends of the bone to remove the marrow. Complete removal was determined when the bone became translucent. The process was repeated for both femurs. The cells were then centrifuged at 500g for 7 minutes at 4°C before being re-suspended in PBS + 0.25% BSA for purification. Neutrophils were purified by a discontinuous Percoll gradient using the following protocol: 75% (7ml) of a 90% isotonic Percoll solution

diluted with PBS was gently overlaid with a 65% Percoll layer (7ml). A 55% (7ml) solution was then overlaid in a similar manner on to the 65% layer. The cell suspension (3ml) was then carefully overlaid onto the 55% layer. The gradient was subsequently centrifuged at 1500g for 30 minutes at 4°C. The cells at the cell/55% interface and the 55%/65% interface were removed to minimize contamination of the neutrophil layer at the interface between the 65%/75% layers (Figure 2-10). These cells were carefully removed, washed and differentially counted as previously described in section 2.2. The resultant yield was approximately 3.5×10^6 - 5×10^6 per mouse. Following the purification step, microparticles were produced from both the WT and Annexin A1 $-/-$ mice as previously described in section 2.10.

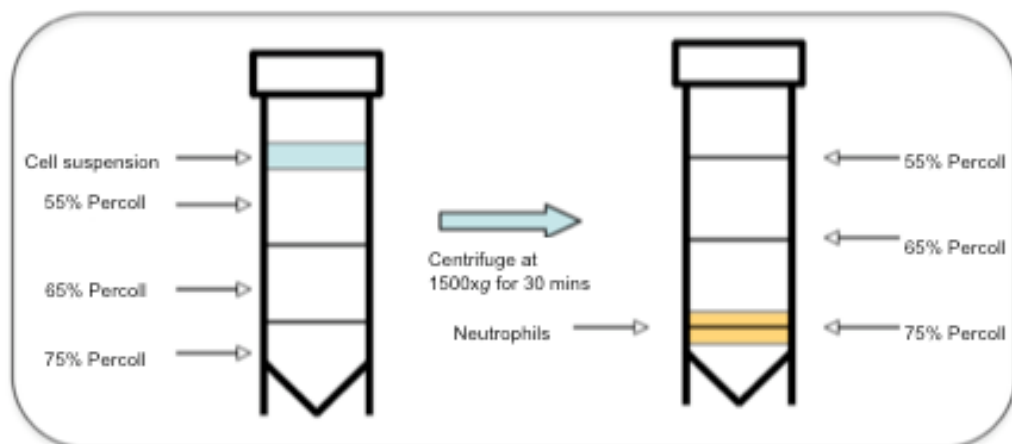


Figure 2-12: Neutrophil isolation from mouse bone marrow cells using a Percoll gradient.

2.13.3. AirPouch Model of Inflammation

Male Balb/c mice (24 to 26 g; B&K, Essex, UK) were used for all the following experiments. Dorsal subcutaneous (S.C.) air-pouches were prepared by injection of 2.5 ml of air on day 0 and day 3. Six days after the initial injection of air, mice received 10 ng of mouse IL-1 β diluted in a volume of 500 μ l of 0.5%

CMC (BDH, Dorset, UK) in PBS directly into the pouch. Control mice received the vehicle only. Four hours after IL-1 β administration mice were killed by exposure to CO₂ and the pouches washed thoroughly with 2 ml of PBS containing 50 U/ml heparin. Total and differential leukocyte counts were performed after staining in Turk's solution (crystal violet 0.01 % in 3% acetic acid) by counting in an improved Neubauer haemocytometer and stained with Gr1 (clone rb6-8c5; eBioscience, Wembley, UK), by co-incubation of the cell suspension with the antibody for 30 min on ice following a 30 min blocking step with rat serum (Sigma, Poole, UK) and FC block (BD Pharmingen). After which the antigen expression was assessed on a FACSCalibur as previously outlined in section 2.4 and from which the number of PMN recovered from the pouch was then calculated.

The effect of microparticles and specifically Annexin A1 as an inhibitor and/or antagonists in an inflammatory setting was assessed in two ways. First of all microparticles derived from human neutrophils were injected intra-venously (i.v.) 10mins prior to IL1 β injection at the following 2 doses: 40x10³ and 90x10³; more over hr-Annexin A1 was injected at 20ng per mouse as a positive control. Subsequently microparticles previously produced from the WT and Annexin A1 -/- mice, as outlined in section 2.10, were injected i.v. 10mins prior to IL1 β injection at the following 2 doses: 40x10³ and 70x10³.

In a distinct set of experiments after the airpouches were setup the mice were injected i.v. 10mins prior to IL1 β injection with 50ng of Pep57, Pep59, Pep84 (sequences illustrated in Table 1.3) or vehicle. After 4h blood was collected

from each group by cardiac puncture following which the cells migrated into the airpouch were recovered as outlined above. Blood cell counts were conducted by diluting the blood 1:10 in Turks solution; whilst the cell counts and Gr1 staining on cells migrated into the airpouch were conducted as previously described in the section 2.4.

2.14. Statistical Analysis

Statistical Analysis was conducted using GraphPad Prism 4 computer software. Values are expressed as mean \pm standard error of mean (SEM) of *n* experiments. Homogeneity of variances was first tested by Bartlett's test to ensure that statistical comparison between groups would be valid. For parametric data when only two variables were being tested statistical differences were analysed by the Student's *t*-test. When comparing multiple groups statistical significance was assessed using a one-way analysis of variance (ANOVA) analysis followed by a Dunnett's post hoc test, with a *P* value ≤ 0.05 considered as significant. In the case of densitometry data, values were either normalized against total protein loaded, against alpha tubulin or total ERK 1/2 and statistical analysis was performed using the Mann-Whitney U test for non-parametric data, *P* value ≤ 0.05 were considered as significant.

3. Results

3.1. The Annexin A1 system and Rheumatic disease, is there a link?

The cause of most types of rheumatic diseases remains unknown and, in many cases, it may vary depending on the type of rheumatic disease. However, it is believed that some if not all of the following factors may play a role in the development or aggravation of one or more types of rheumatic diseases: genetic predisposition and family history; lifestyle choices; trauma; infection; neurogenic disturbances; metabolic disturbances; excessive wear and tear along with stress on a joint(s); environmental trigger and the influence of certain hormones on the body. Increasing evidence is highlighting the role of auto-antibodies in the propagation of at least a subset of rheumatic diseases where there can either reflect organ-specific or generalized autoreactivity.

3.1.1. Role of the Annexin A1 system in Wegener's Vasculitis.

Endogenous anti-inflammatory mediators form a complex network triggered in the host to dampen cell activation and promote resolution of inflammation. Recent data points to the fact that a number of serine proteases expressed on human neutrophils (one such being proteinase 3; PR3), which has also been linked with Wegener granulomatosis) have the ability to cleave Annexin A1 and thus potentially render it inactive. Thus, we hypothesized that alterations in the Annexin A1 pathway in the vasculitis patients' neutrophils could be, at least in part, responsible for the onset and development of this condition; either as a result of an enhanced cleavage of the Annexin A1 protein or in response to their activated phenotype (e.g. frustrated up-regulation).

In collaboration with Prof B. Dasupta and Ms J Hollywood, Wegener granulomatosis patients were stratified in view of their plasma expression of anti-MPO or anti-PR3 ANCA. Blood was collected from age and sex matched healthy volunteers and Wegener patients between 9 and 10 AM, and processed within 2 hours. Gradient-purified neutrophils (PMN) were stained with specific monoclonal antibodies to monitor expression of Annexin A1, FPRL1 or FPR, as previously described in the methods, section 2.4. Annexin A1 levels in the neutrophil cytoplasm and plasma membranes were also gauged by western blotting; furthermore Annexin A1 and FPRL1 mRNA levels were analyzed by Real Time PCR in all patient sample groups. Subsequently, PMN reactivity was assessed by flowing the neutrophils over monolayers of human umbilical vein endothelial cells (HUVEC) for 8 min at 37°C, using 1 dyne/cm² of shear. In some cases, human recombinant (hr) Annexin A1 (10 nM) was incubated with the neutrophils for 10 min prior to flow.

Results obtained from the analysis of the flow-cytometric data points to a significant increase in blood neutrophil surface expression of Annexin A1 in the Wegener (both MPO and PR3 +ve) and GCA patients, with values of 8%, and 13% increase in the number of Annexin A1 positive PMN, respectively (Figure 3.1).

A similar profile was observed for the expression of the Annexin A1 receptor, FPRL1, such that there was a significant increase in cell surface expression of this receptor on neutrophils from Wegener's (MPO +ve: +16%; and PR3 +ve: +34) when compared to the healthy controls (Figure 3.3). Cell surface analysis

of the FPR family prototype receptor illustrated a significant increase in number of FPR +ve cells only in the PR3+ ANCA patients where there was an increased blood cell positivity of 21% (Figure 3.2). Finally, FACS analysis revealed an elevated PR3 membrane expression for both disease groups (Figure 3.4).

Interestingly, in the Wegener patients there is also a possible difference in the mechanism by which the Annexin A1 protein is incorporated into the cell membrane as evidenced by the data generated following the washing of PMNs from these patients and healthy volunteers in an EDTA solution. In fact here we observed that this procedure was only able to remove the Annexin A1 in the cells derived from healthy volunteers whilst the Annexin A1 levels were left unaltered or even enhanced in the Wegener patients. The increase in Annexin A1 levels following the EDTA wash in the MPO+ve ANCA patients is possibly due to the externalization of Annexin A1 found on the inner side of the plasma membrane as a result of the wash process caused by a reshuffling of the membrane components and thus the externalization of the Annexin A1 protein. This observation in conjunction with that made for the PMNs derived from PR3 +ve patients in figure 3.1 would suggest that although in these two patient groups there is a deregulation in the Annexin A1 transport to the cell membrane the actual localisation and thus possibly the mechanism leading to this might be dissimilar.

	No Pat	Age	Sex	Treatment
CT	12	61 ± 7.9	8M 4F	n/a
MPO +ve	5	71 ± 7.3	4M 3F	1 Methotrexate 2 Mycophenolate+Pred 2 Pred
PR3 +ve	8	66 ± 4.2	5M 3F	2 Cyclophosphamide+Pred 1 Methotrexate+Pred 3 Pred 1 Mycophenolate+Pred

Table 3-1: Table outlining the demographic parameters for the subjects employed for this study including treatment regimes.

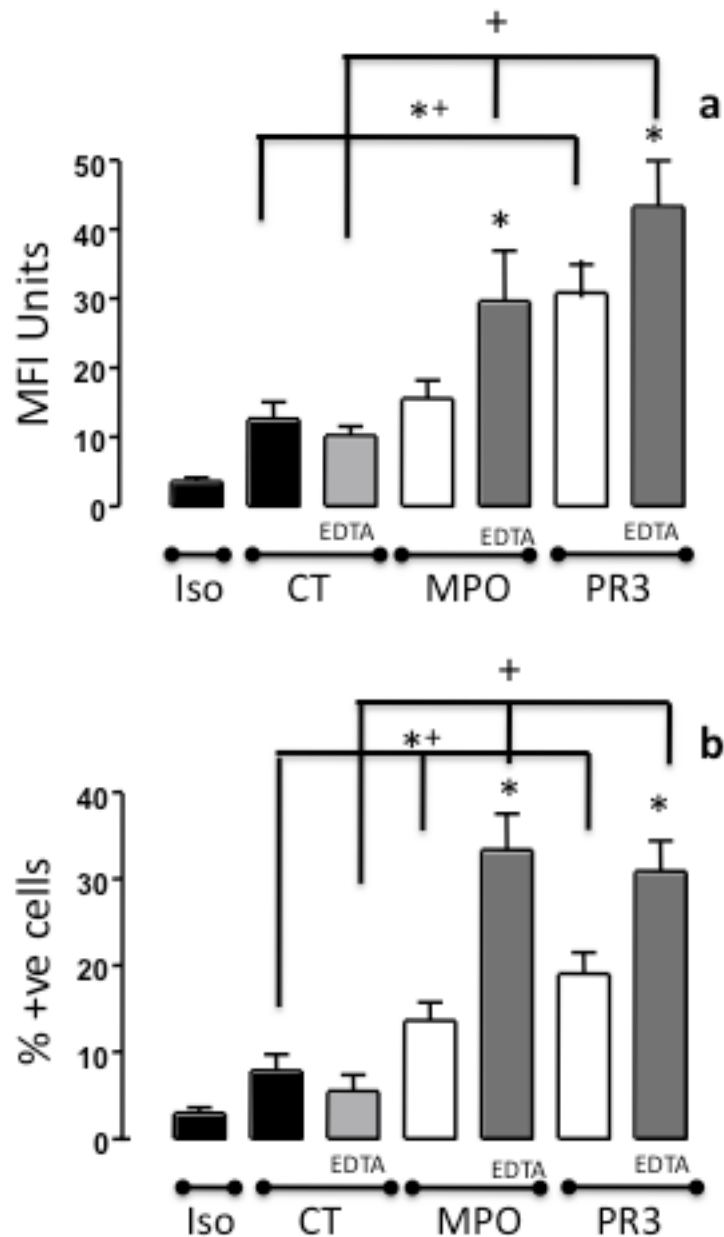


Figure 3-1: Annexin A1 expression on control (CT) and Wegener granulomatosis patients pre and post EDTA wash. PMNs isolated from CT and Wegener patients' whole blood were either washed twice with 1mM EDTA and stained or directly stained using an immunofluorescent anti-Annexin A1 antibody, by incubation for 45 min at 4°C. The results in panel both panels (a) and (b) show that there is a statistically significant increase in Annexin A1 expression on both MPO ANCA and PR3 ANCA patients especially post EDTA wash. Data are mean ± SEM of 5 patients for the MPO ANCA group, 8 for the PR3 ANCA group and 12 for the CT group. ** P<0.05 vs. CT group + P<0.05 vs. CT EDTA group * P<0.05 vs. untreated group.

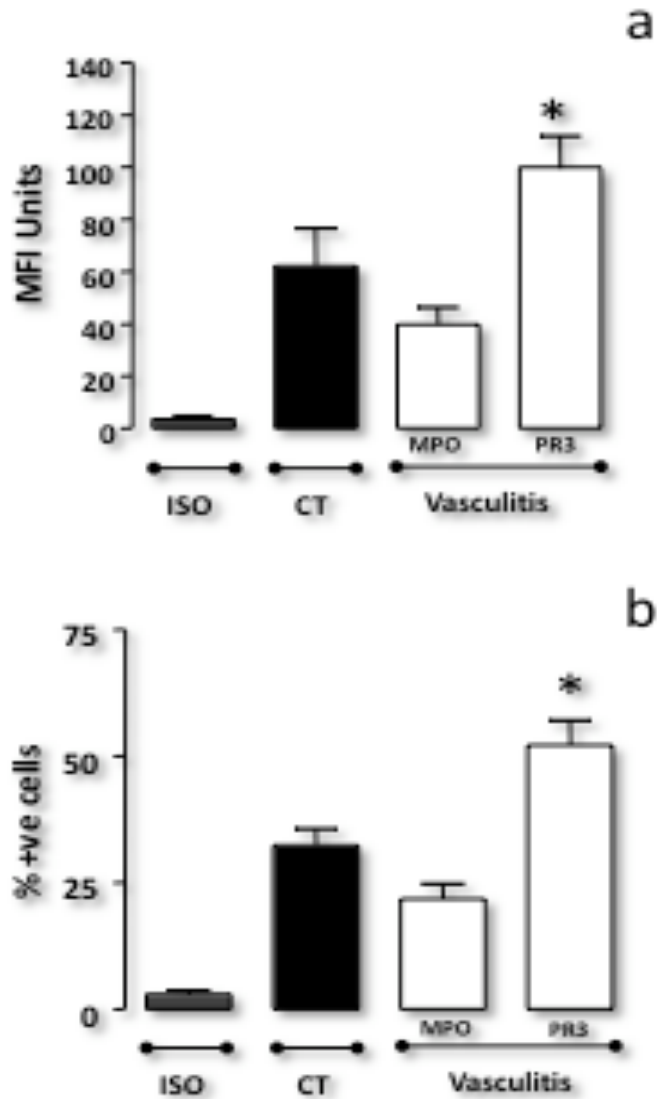


Figure 3-2: FPR expression on control (CT) and Wegener granulomatosis patients. PMNs isolated from Wegener patients' whole blood were stained using an immunofluorescent anti-FPR antibody, by incubation for 45 min at 4°C. These results show that there is a marked although not statistically significant decrease in FPR expression on MPO ANCA patients. On the other hand, there was a statistically significant increase in receptor expression on PR3 ANCA patients. This result is both reflected in the MFI values (a) and the % positive cells (b). Data are mean ± SEM of 5 patients for the MPO ANCA group, 8 for the PR3 ANCA group and 12 for the CT group. * P<0.05 vs. CT group

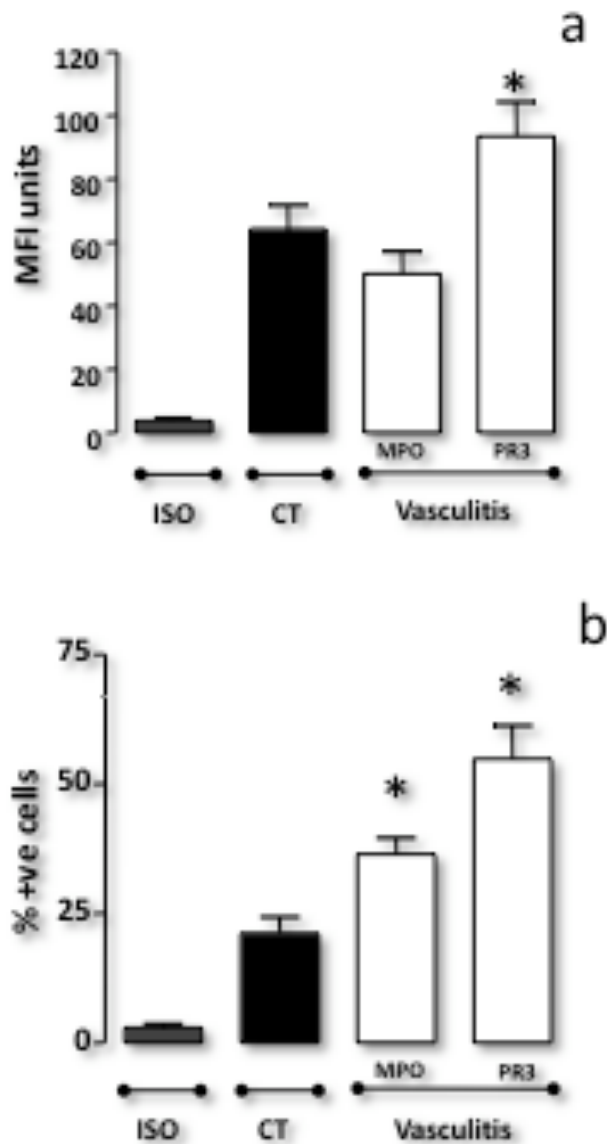


Figure 3-3: FPRL1 expression on control (CT) and Wegener granulomatosis patients. PMNs isolated from Wegener patients' whole blood were stained using an immunofluorescent anti-FPRL1 antibody, by incubation for 45 min at 4°C. The results in panel (a) show that there is a marked although not statistically decrease in FPRL1 expression on MPO ANCA patients whilst on the other hand there was a statistically significant increase of the receptor on PR3 ANCA patients. On the other hand the although the results in panel (b) show that there was an increase FPRL1 receptor in the PR3 ANCA patients concordant with those in panel (a) the results for the MPO ANCA patients show that there is a statistically significant increase in the receptor as opposed to the trend observed in panel (a) Data are mean \pm SEM of 5 patients for the MPO ANCA group, 8 for the PR3 ANCA group and 12 for the CT group. * $P < 0.05$ vs. CT group

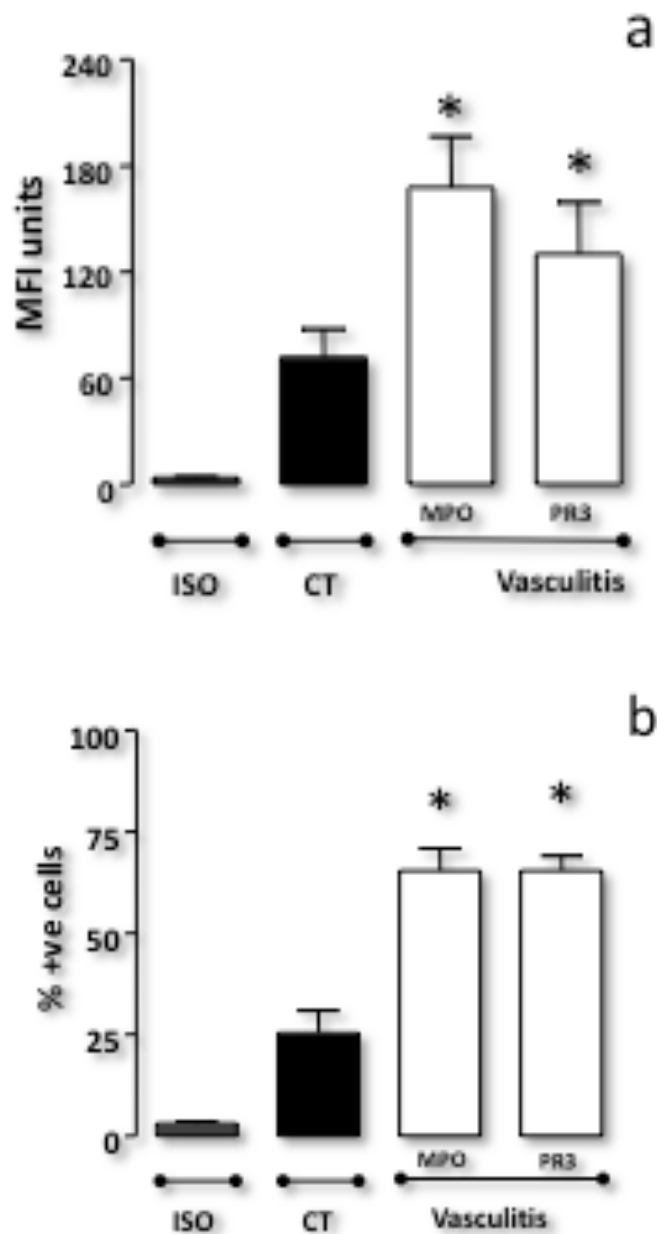


Figure 3-4: Membrane PR3 expression on control (CT) and Wegener granulomatosis patients. PMNs isolated from Wegener patients' whole blood were stained using an immunofluorescent anti-PR3 ANCA antibody, by incubation for 45 min at 4°C. The results in panel both panels (a) and (b) show that there is a statistically significant increase in PR3 expression on both MPO ANCA and PR3 ANCA patients, Data are mean \pm SEM of 5 patients for the MPO ANCA group, 8 for the PR3 ANCA group and 12 for the CT group. * $P < 0.05$ vs. CT group

The western blotting analysis highlights that whilst Annexin A1 levels in the cytoplasm of neutrophils derived from all the three groups of vasculitis patients was not significantly different from those seen in the healthy volunteers, the membrane pool of Annexin A1 was significantly higher (Figure 3.6). This observation corroborates the results obtained in the flow cytometric analysis described above. Even more interesting is the fact that the majority of this membrane pool is in fact found in the cleaved 33 kDa form (Figure 3.6a).

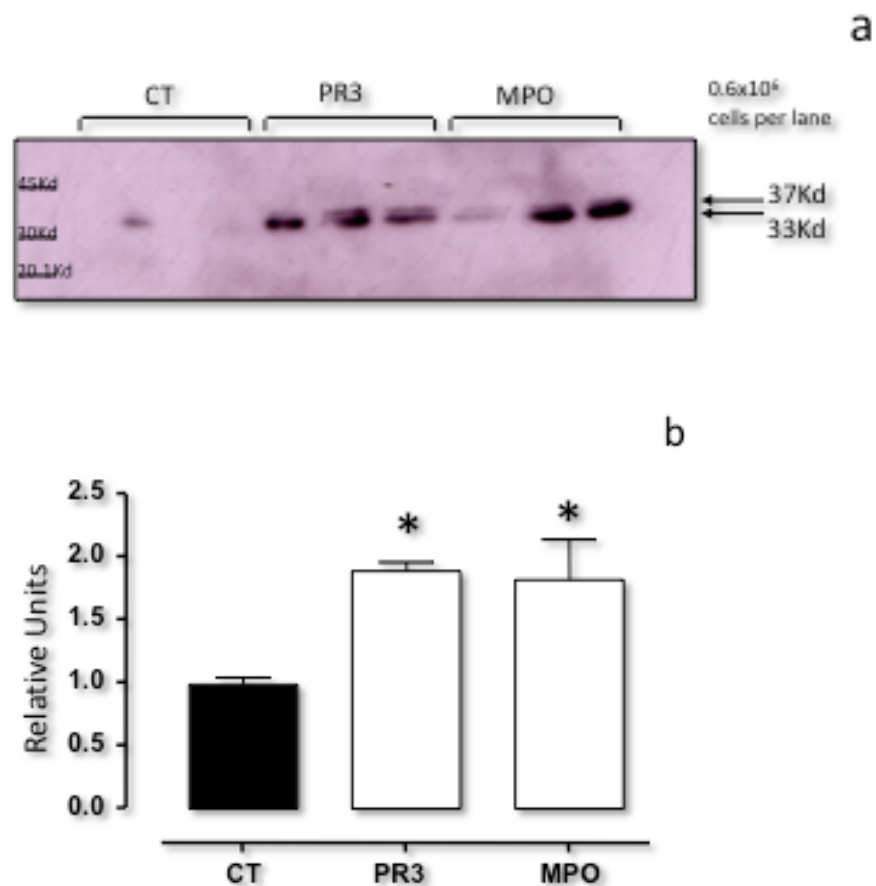


Figure 3-5: Membrane expression of Annexin A1 in PMNs from CT and Wegener vasculitis patients. PMNs were extracted from whole blood, after which the cells were lysed and the membrane fraction was separated by centrifugation and resuspension of the pellet in 1% TritonX. The membrane fraction was then blotted for the expression of Annexin A1 and densitometry was conducted comparing the Annexin A1 expression to β -actin. (a) representative blot of 3 different patients per group. (b) densitometry of 8 individual samples per group. * $P < 0.05$ vs. CT group.

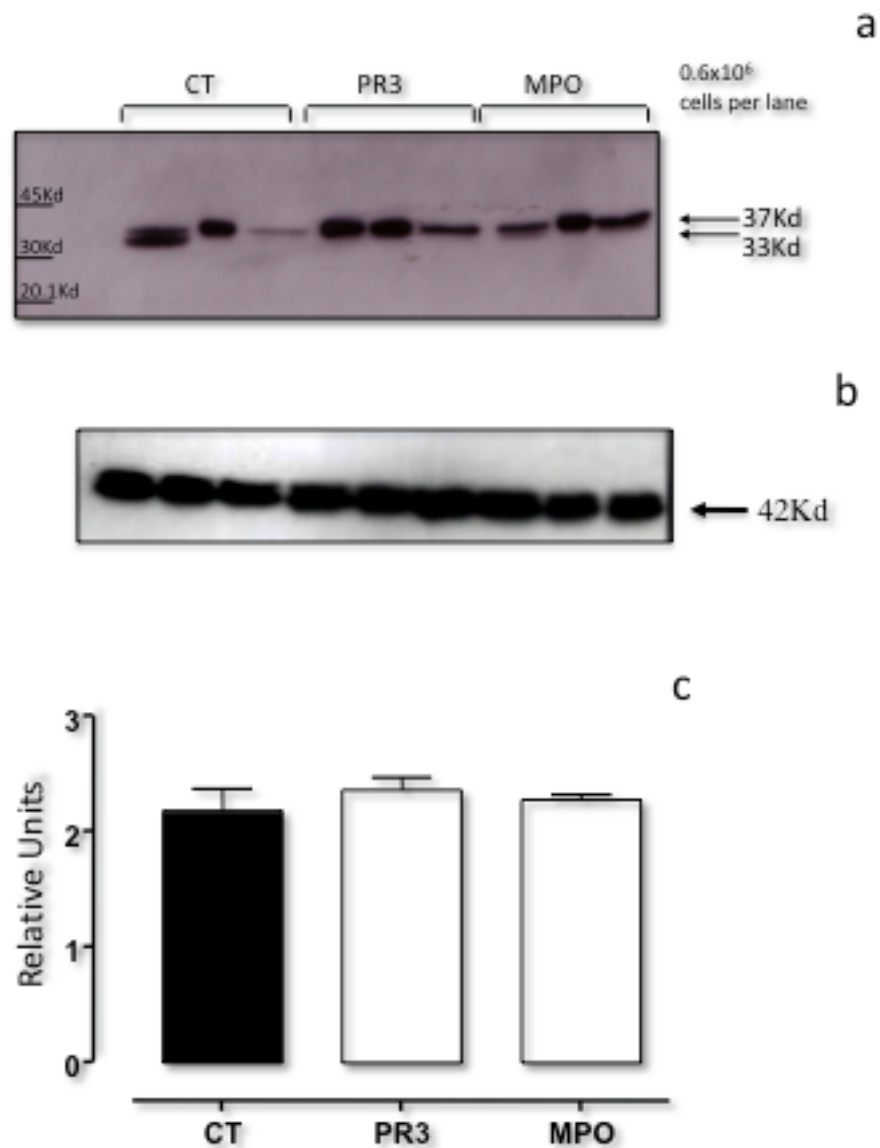


Figure 3-6: Cytosolic expression of Annexin A1 in PMNs from CT and Wegener vasculitis patients. PMNs were extracted from whole blood, after which the cells were lysed and the membrane fraction was centrifuged the supernatant collected in a separate tube, yielding the cytosol fraction. This fraction was then blotted for the expression of Annexin A1 and densitometry was conducting comparing the Annexin A1 expression to b-actin. (a) representative blot of 3 separate patients per group. (b) β -actin blot (c) densitometry of 8 individual samples per group. * $P < 0.05$ vs. CT group.

Following the protein expression analysis we wanted to investigate if there was also an alteration at the genomic level of the Annexin A1 system. Real Time PCR analysis of mRNA extracted from the three vasculitis groups showed that there is no significant difference between the Annexin A1 levels in the Wegener groups and those found in healthy volunteers (Figure 3.8). On the other hand there was 1.5 and 6 fold increase in the FPRL1 mRNA for the MPO +ve ANCA patients over the healthy volunteers (Figure 3.49). Interestingly, the Wegener patients did not show altered mRNA levels when compared to the healthy volunteers (Figure 3.9)

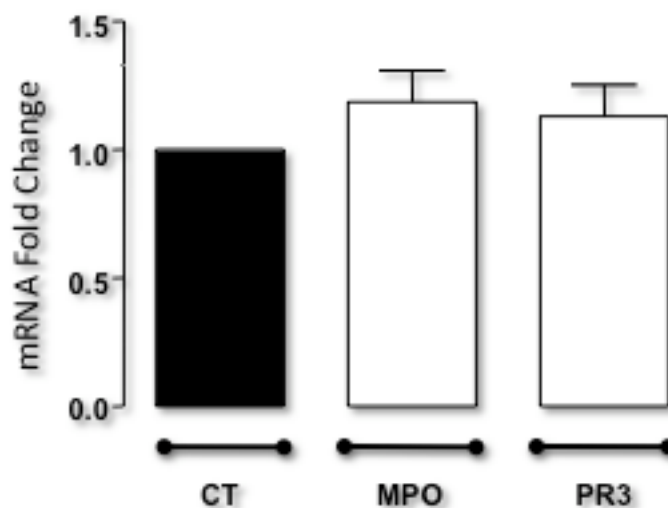


Figure 3-7: mRNA expression of Annexin A1 in Wegener granulomatosis patients versus CT in PMNs. mRNA was extracted from PMNs of CT and Wegener patients and then reverse transcribed, following reverse transcription the expression levels were analysed. The results show that there is no significant change in Annexin A1 expression in both groups of Wegener granulomatosis. Results displayed as a representative blot of 6 different patients per group * P<0.05 vs. CT group.

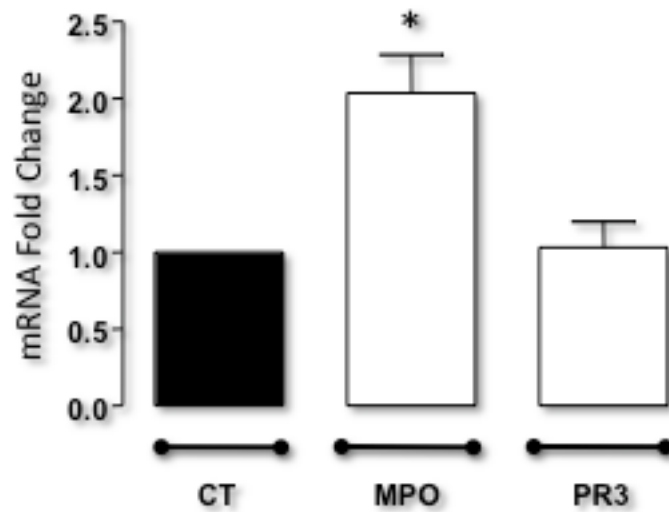


Figure 3-8: mRNA expression of FPRL1 in Wegener granulomatosis patients versus CT in PMNs. mRNA was extracted from PMNs of CT and Wegener patients and then reverse transcribed, following reverse transcription the expression levels were analysed. The results showing that there is a slight but significant elevation in FPRL1 mRNA levels in the MPO ANCA patients however no such elevation was observed in the PR3 ANCA patients. Results displayed as a representative blot of 6 different patients per group *P<0.05 vs. CT group.

After determining the antigen expression levels on these cells, I determined their level of reactivity by measuring the levels of interaction to an activated HUVEC monolayer in the flow chamber model. This analysis revealed that neutrophils derived from vasculitis patients were more reactive than control cells. More in particular, there was a higher number of cells firmly adhering to the endothelial monolayers. Wegener granulomatosis patients showed nearly a 2.5 fold increase in the number of adherent neutrophils (Figure 3.10). Interestingly, there was no real difference in the number of rolling cells highlighting the possibility that the defect in this disease only affects one part of the leukocyte recruitment cascade. Even more striking was the observation that cell incubation with hr-Annexin A1 *corrected* this phenotype, bringing values of cell adhesion back to those measured with cells from the healthy controls (Figure 3.10).

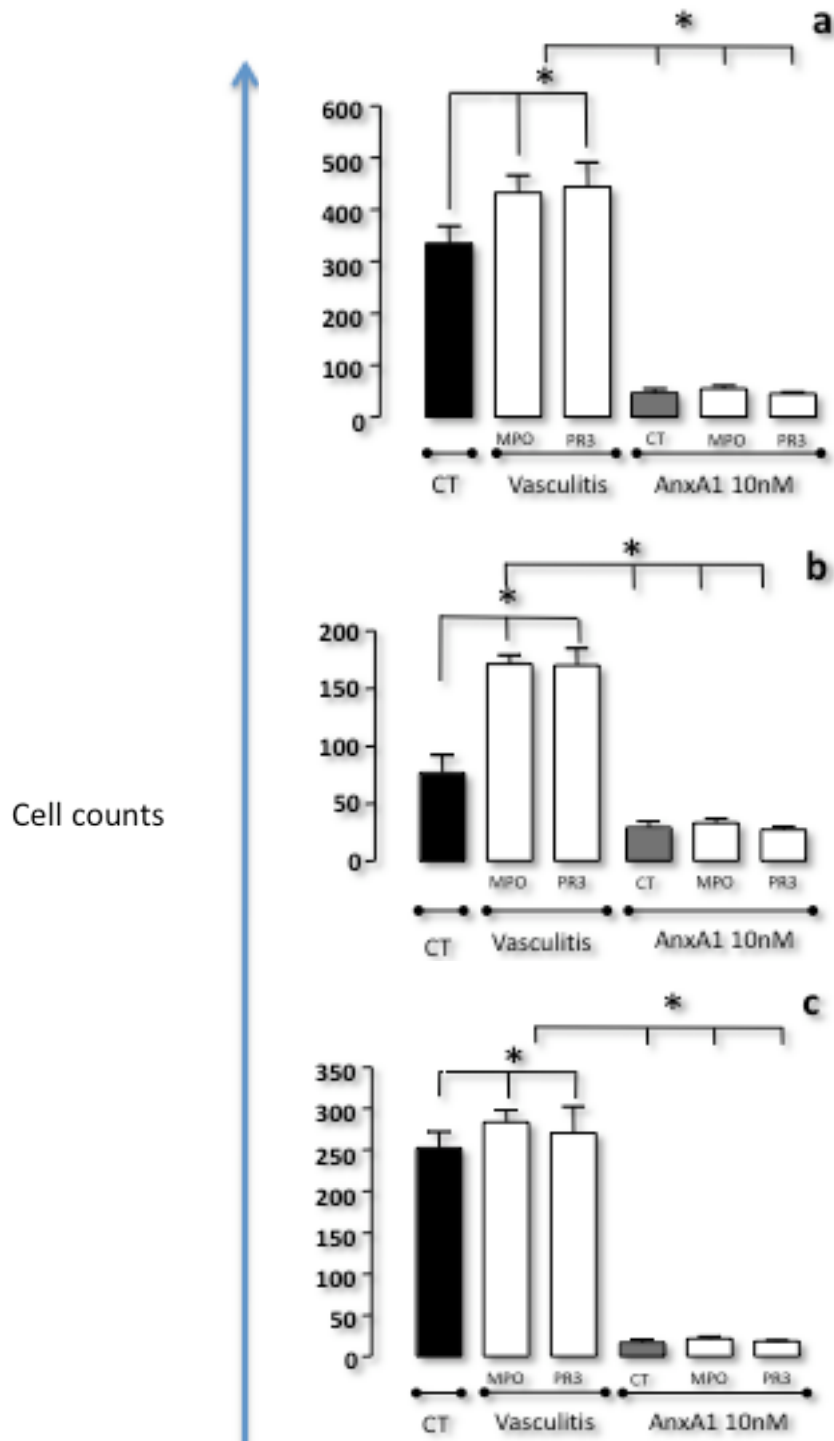


Figure 3-9: Effect of Wegener Vasculitis on activation of PMN's under flow, and the reversal of this effect through the administration of hr-Annexin A1. Confluent HUVEC monolayers were stimulated with TNF- α (10ng/ml) for 4 hours. Neutrophils isolated from CT patients and Wegener patients were incubated for 10 minutes at 37°C with or without 10nM hr-Annexin A1. Neutrophils (1×10^6 /ml) were then perfused over the endothelial monolayers at a constant rate of 1 dyn/cm², prior to quantifying the degree of PMN interaction with the HUVECs, both as PMN capture (a), adhesion (b) and rolling (c). The results depicted Results are plotted as mean + standard error of 3 distinct experiments.

3.1.2. Role of Annexin A1 in Giant Cell Arteritis.

Giant Cell Arteritis (GCA) is an inflammatory vascular disease, most commonly of the large (external carotid arteries) and medium arteries of the head; most common in the elderly. This can result in a wide variety of complications, including jaw pain, blurred vision, scalp sensitivity and headaches. Interestingly this disease is very responsive to glucocorticoid treatment alone, as opposed to Wegener granulomatosis, and thus we set out to explore where the basis of this difference in response could lie, by taking a close look the Annexin A1 system in these patients.

The flow cytometric data showed that there was an elevated expression of all members of the Annexin A1 system on the GCA PMN when compared to the same cells from age matched healthy volunteers. In fact, there is an elevated expression of the FPR receptor in the disease state as shown by an elevated MFI value (Figure 3.11a), along with a trend to an elevated number of FPR positive cells (Figure 3.11b), which however did not reach statistical significance.

An elevation in the Annexin A1 receptor, FPRL1 was also observed both in the quantity per cell, as observed through the increase in the MFI units (Figure 3.12a), and in the number of cells expressing the receptor (Figure 3.12b). A similar result was also obtained for the Annexin A1 expression, where there was an approximate 3-fold increase in the MFI values (Figure 3.13a); the percent positive cells was also approximately a 3 fold increase in the GCA patients when compared to healthy volunteers (CT) (Figure 3.13a).

Interestingly an elevated PR3 expression was also observed in the GCA PMNs as detailed in Figure 3.14a and b, where we see a significant increase in both MFI and percent positive cells.

	No Pat	Age	Sex	Treatment
CT	12	61 ± 7.9	8M 4F	n/a
GCA	8	71 ± 5.7	3 M 5F	5 Pred 3 Methotrexate+Pred

Table 3-2: Table outlining the demographic parameters for the subjects employed for this study including treatment regimes.

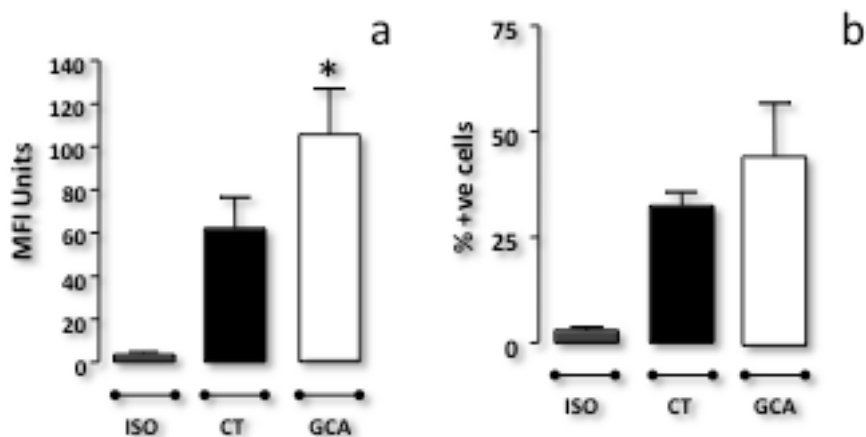


Figure 3-10: FPR expression on control (CT) and GCA patients. PMNs isolated from GCA patients' whole blood were stained using an immunofluorescent anti-FPR antibody, by incubation for 45 min at 4°C. These results show that there is a marked increase in FPR expression on GCA PMNs. This result is reflected in the MFI values (a) but not the % positive cells (b). Data are mean \pm SEM of 8 patients for the GCA group and 12 for the CT group. * P<0.05 vs. CT group

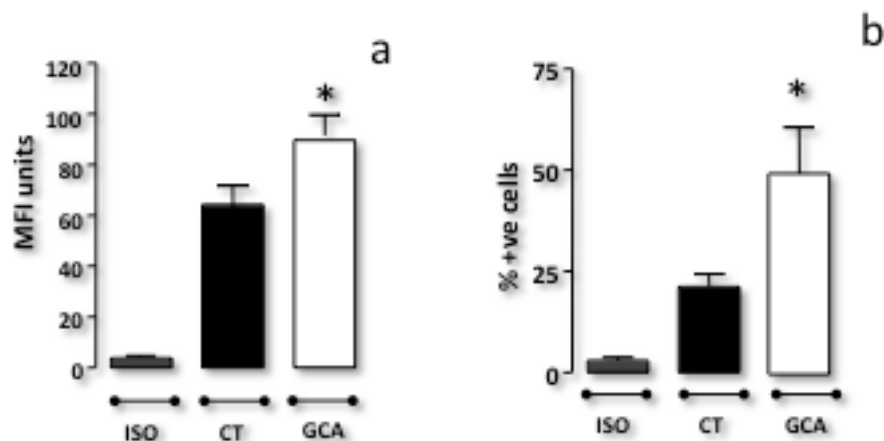


Figure 3-11: FPRL1 expression on control (CT) and GCA patients. PMNs isolated from GCA patients' whole blood were stained using an immunofluorescent anti-FPRL1 antibody, by incubation for 45 min at 4°C. These results show that there is a marked increase in FPRL1 expression on GCA PMNs. This result is both reflected in the MFI values (a) and the % positive cells (b). Data are mean \pm SEM of 8 patients for the GCA group and 12 for the CT group. * P<0.05 vs. CT group

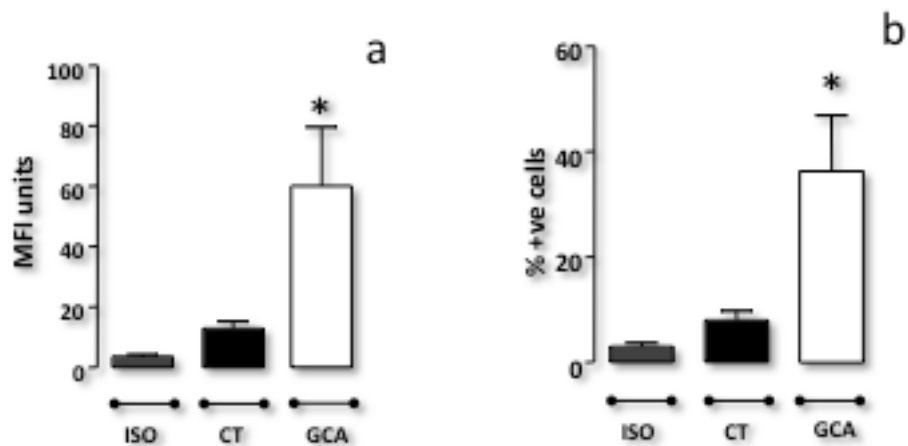


Figure 3-12: Annexin A1 expression on control (CT) and GCA patients. PMNs isolated from GCA patients' whole blood were stained using an immunofluorescent anti-Annexin A1 antibody, by incubation for 45 min at 4°C. These results show that there is a marked increase in Annexin A1 expression on GCA PMNs. This result is both reflected in the MFI values (a) and the % positive cells (b). Data are mean \pm SEM of 8 patients for the GCA group and 12 for the CT group. * $P < 0.05$ vs. CT group

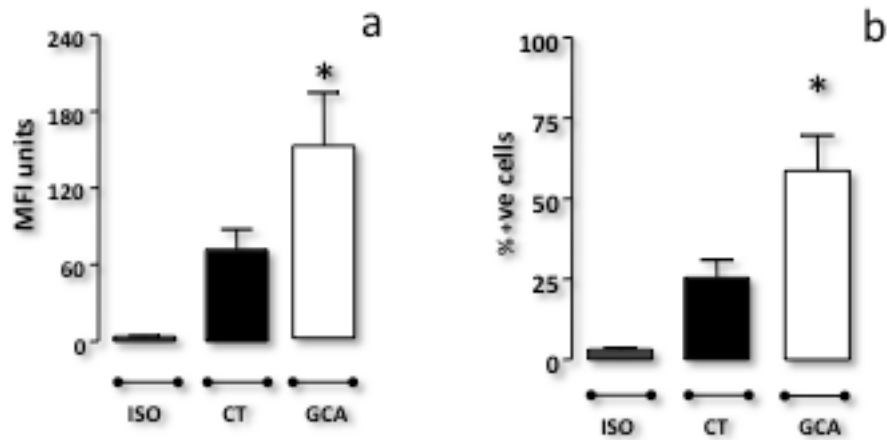


Figure 3-13: PR3 expression on control (CT) and GCA patients. PMNs isolated from GCA patients' whole blood were stained using an immunofluorescent anti-PR3 antibody, by incubation for 45 min at 4°C. These results show that there is a marked increase in PR3 expression on GCA PMNs. This result is both reflected in the MFI values (a) and the % positive cells (b). Data are mean \pm SEM of 8 patients for the GCA group and 12 for the CT group. * $P < 0.05$ vs. CT group

The western blotting analysis highlights that whilst Annexin A1 levels in the cytoplasm of neutrophils derived from both the healthy volunteers and GCA patients were not significantly different from those seen in the healthy volunteers (Figure 3.17), the membrane pool of Annexin A1 was significantly higher (Figure 3.16). This observation corroborates the results obtained in the flow cytometric analysis described above. Similarly to the analyses conducted with PMN taken from Wegener's patients, the majority of this membrane pool is in fact found in the cleaved 33 kDa form (Figure 3.16).

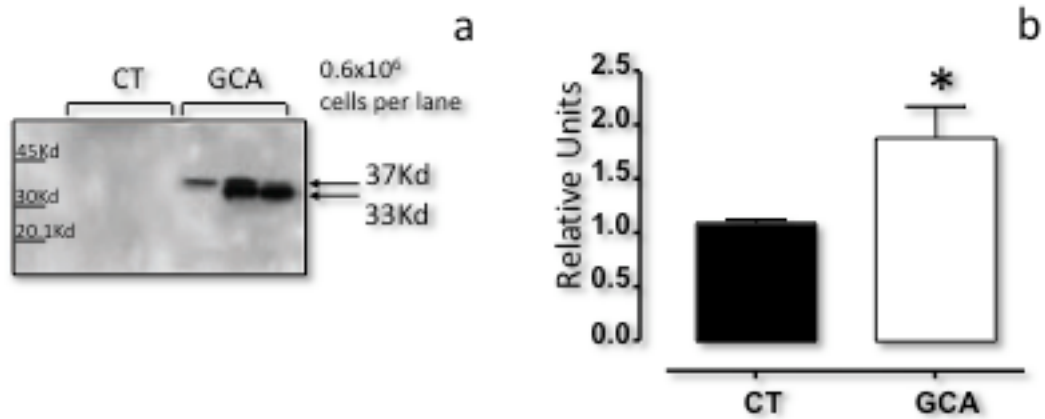


Figure 3-14: Membrane expression of Annexin A1 in PMNs from CT and GCA patients. PMNs were extracted from whole blood, after which the cells were lysed and the membrane fraction was separated by centrifugation and resuspension of the pellet in 1% TritonX. The membrane fraction was then blotted for the expression of Annexin A1 and densitometry was conducting comparing the Annexin A1 expression to β -actin. (a) representative blot of 3 different patients per group. (b) densitometry of 8 individual samples per group. * $P < 0.05$ vs. CT group.

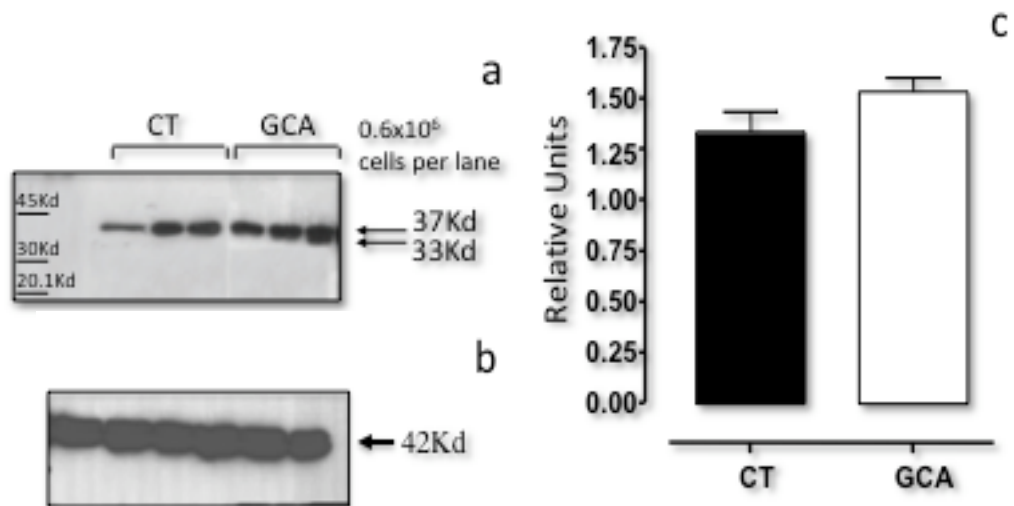


Figure 3-15: Cytosolic expression of Annexin A1 in PMNs from CT and GCA patients. PMNs were extracted from whole blood, after which the cells were lysed and the membrane fraction was centrifuged the supernatant collected in a separate tube, yielding the cytosol fraction. This fraction was then blotted for the expression of Annexin A1 and densitometry was conducting comparing the Annexin A1 expression to β -actin. (a) representative blot of 3 separate patients per group. (b) β -actin blot (c) densitometry of 8 individual samples per group. * $P < 0.05$ vs. CT group.

Following the protein expression analysis I wanted to determine if the alterations observed above at the protein level for the Annexin A1 system were also present at the genomic level. Real-Time PCR analysis of mRNA extracted from PMN of the healthy volunteers and GCA patients groups showed remarkable changes, with a 10-fold increase in Annexin A1 mRNA (Figure 3.18), over the control group whilst there was a 6-fold increase in the FPRL1 mRNA (Figure 3.19).

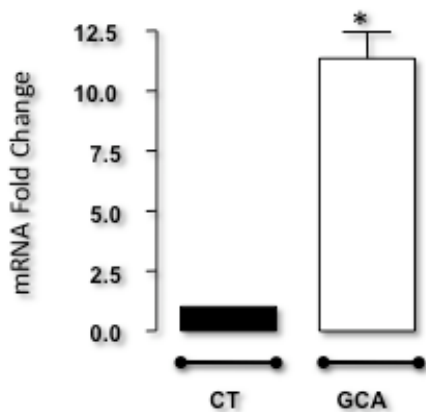


Figure 3-16: mRNA expression of Annexin A1 in GCA patients versus CT in PMNs. mRNA was extracted from PMNs of CT and Wegener patients and then reverse transcribed, following reverse transcription the expression levels were analysed. The results show that there is a significant upregulation of Annexin A1 mRNA expression for the patients studies Results displayed as a representative blot of 6 different patients per group * P<0.05 vs. CT group.

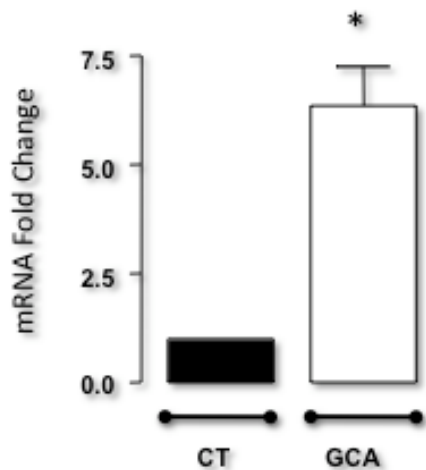


Figure 3-17: mRNA expression of FPRL1 in GCA patients versus CT in PMNs. mRNA was extracted from PMNs of CT and Wegener patients and then reverse transcribed, following reverse transcription the expression levels were analysed. The results showing that there is a slight but significant elevation in FPRL1 mRNA levels in the GCA patients. Results displayed as a representative blot of 6 different patients per group *P<0.05 vs. CT group.

After determining the status of the Annexin A1 system at both the protein and the genomic level in GCA PMNs, the next step was to ascertain the level of reactivity that these cells possess in an *in vitro* system of leukocyte adhesion, the flow chamber model. In this model cells are flowed and a shear stress of 1 dyne/cm² over an activated HUVEC monolayer for 8 min prior to recording and then offline analysis of the leukocyte interaction, primarily capture-total cells, adherent and rolling cells to the endothelial monolayer.

This analysis highlighted a higher level of reactivity of the PMN isolated from the GCA patients when compared to healthy volunteers. In fact, there is an increased number of cells captured over the endothelial monolayer which is mainly the result of an increased number of adherent cells, approximately 3 fold more (Figure 3.20) Interestingly, there was no real difference in the number of rolling cells highlighting the possibility that the defect in this disease affects one element of the leukocyte recruitment cascade selectively. Further supporting the notion that there is a de-regulation in the Annexin A1 axis in these patients was the observation that upon incubation of the PMNs, both CT and those obtained from the GCA patients, with hr-Annexin A1 there was a striking reduction in the number of cells interacting with the endothelium, bringing the numbers of the GCA-derived cells down to those observed in the CT conditions (Figure 3.20)

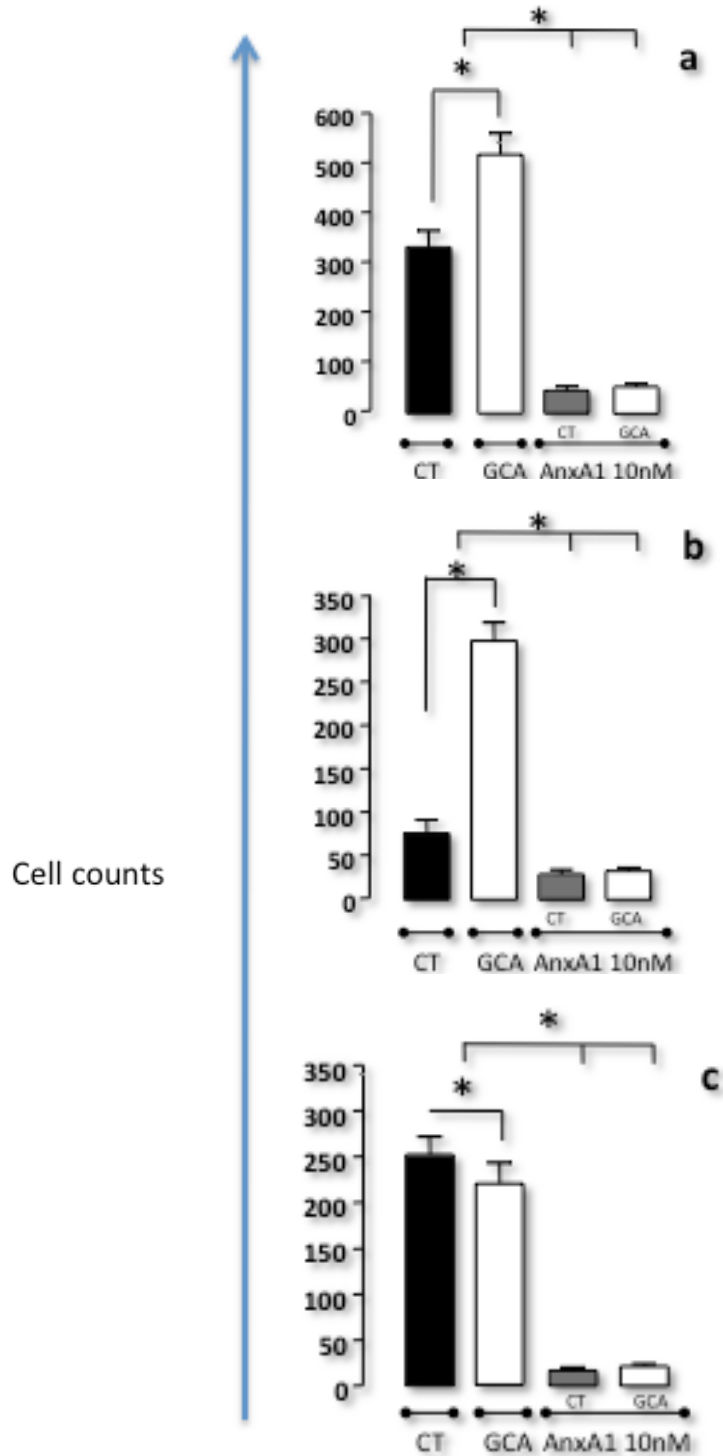


Figure 3-18: Effect of GCA on PMN activation under flow, and the reversal of this effect through the administration of hr-Annexin A1 (Annexin A1). Confluent HUVEC monolayers were stimulated with TNF- α (10ng/ml) for 4 hours. Neutrophils isolated from CT patients and Wegener patients were incubated for 10 minutes at 37°C with or without 10nM hr-Annexin A1. Neutrophils (1×10^6 /ml) were then perfused over the endothelial monolayers at a constant rate of 1 dyn/cm², prior to quantifying the degree of PMN interaction with the HUVECs, both as PMN capture (a), adhesion (b) and rolling (c). The results depicted Results are plotted as mean + standard error of 3 distinct experiments.

3.1.3. Understanding the influence of an acute glucocorticoid treatment on the Annexin A1 system in patients with Rheumatoid Arthritis.

Rheumatoid arthritis (RA) is a chronic, systemic inflammatory disorder that may affect many tissues and organs, but principally attacks the joints producing a inflammatory synovitis that often progresses to destruction of the articular cartilage and ankylosis of the joints (van den Berg, van Lent et al. 2007). RA can also produce diffuse inflammation in the lungs, pericardium, pleura, and sclera, and also nodular lesions, most common in subcutaneous tissue under the skin (Brent 2009). Although the cause of rheumatoid arthritis has been very pinpoint however the pivotal role played by the immune system in the onset and propagation of the disease is beyond discussion.

About 1% of the world's population is afflicted by rheumatoid arthritis, women three times more often than men. Onset is most frequent in 40 to 50 years, but no age is immune. It can be a disabling and painful condition, which can lead to substantial loss of functioning and mobility. It is diagnosed chiefly on symptoms and signs, but also with blood tests (the gold standard being rheumatoid factor) and X-rays.

Currently there is no cure for this disease thus the goal of treatment is mainly alleviation of the current symptoms, and prevention of future destruction of the joints, with the resulting handicap if the disease is left unchecked. These two goals may not always coincide: while pain relievers may achieve the first goal, they do not have any impact on the long-term consequences. For these reasons,

most authorities believe that RA should be treated by at least one specific anti-rheumatic medication, also named Disease modifying anti-rheumatic drugs (DMARD), to which other medications and non-medical interventions can be added as needed.

Glucocorticoid therapy has offered relief in the past, but its long-term effects, amongst which osteoporosis, have been deemed undesirable. However, cortisone injections can be valuable adjuncts to a long-term treatment plan, and using low dosages of daily glucocorticoid (e.g., prednisone or prednisolone, 5-7.5 mg daily) can also have an important benefit if added to a proper specific anti-rheumatic treatment (Strand and Simon 2003).

In my experiments I used blood samples taken from patients between 9 and 11 am, on days 0 (i.e. prior to initiation of a daily dose of 15mg of prednisolone orally), 1, 7 and 14. The blood was immediately processed and PMNs and PBMCs were isolated and stained using a number of immunofluorescent antibodies. The purpose of the study was to determine the effects of an acute glucocorticoid therapy on the disease progression by monitoring cellular markers of activation and also to determine the effect of this therapy on the expression of elements of the Annexin A1 system during this treatment regime.

The initial sets of data comparing the PMN (Figure 3.21) and monocyte (Figure 3.22) populations in the blood versus the synovial fluid, which were identified in view of their scatter profile (i.e. on their physical properties such as granularity and size) as outlined in Figure 3.20 below, at day 0 prior to

glucocorticoid treatment, point to the fact that both subsets of cells display a more activated phenotype in the synovial compartments. Interestingly I could see a difference in the expression of the various members of the Annexin A1 system between the two compartments: Annexin A1 was elevated in both cellular subsets, whilst FPR was only elevated for the monocyte group. Furthermore, even though not reaching statistical significance there is also a trend towards an elevated FPRL1 expression in the synovial over the blood compartment.

	No Pat	Age	Sex	Treatment
RA	7	56 ± 10.1	5 M 2 F	15 mg Pred oral for 14 days

Table 3-3: Table outlining the demographic parameters for the subjects employed for this study including treatment regimes.

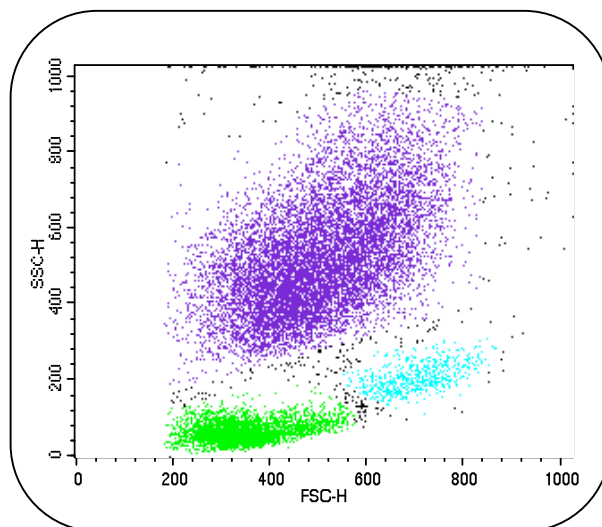


Figure 3-19: Representative dot plot of human blood leukocytes as employed for monitoring of antigen expression during this study. Granulocytes (purple), lymphocytes (green) and monocytes (light blue) are gated according to size and granularity.

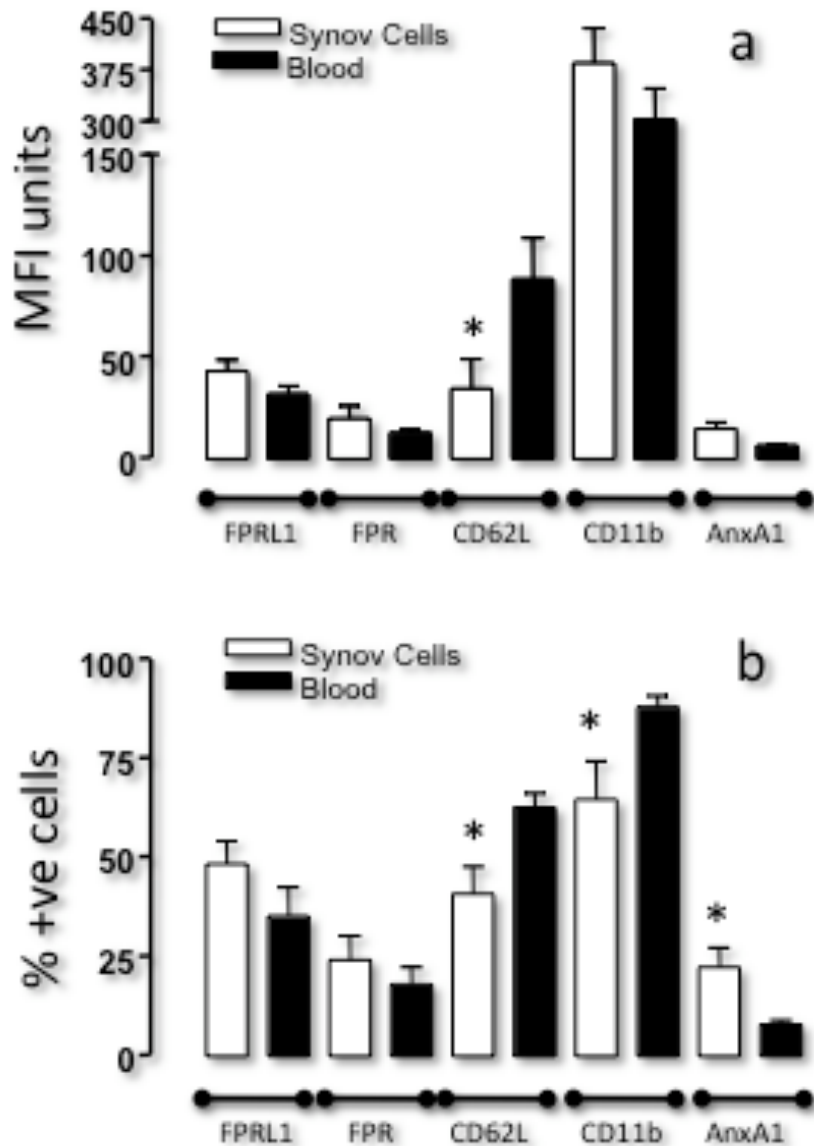


Figure 3-20: Flow cytometric analysis of blood and synovial PMNs CD11b derived from Rheumatoid Arthritis (RA) patients prior to steroid treatment. PMNs isolated from RA patients' whole blood and from synovial fluid following which they were stained using an immunofluorescent antibodies by incubation for 45 min at 4°C. These results show that there is a marked decrease in CD62L expression in the synovial PMNs (a). There is also a decreased number of CD11b and CD62L expressing PMNs in the synovial fluid. (b). * P<0.05 vs. Blood PMN group (n=7 patients)

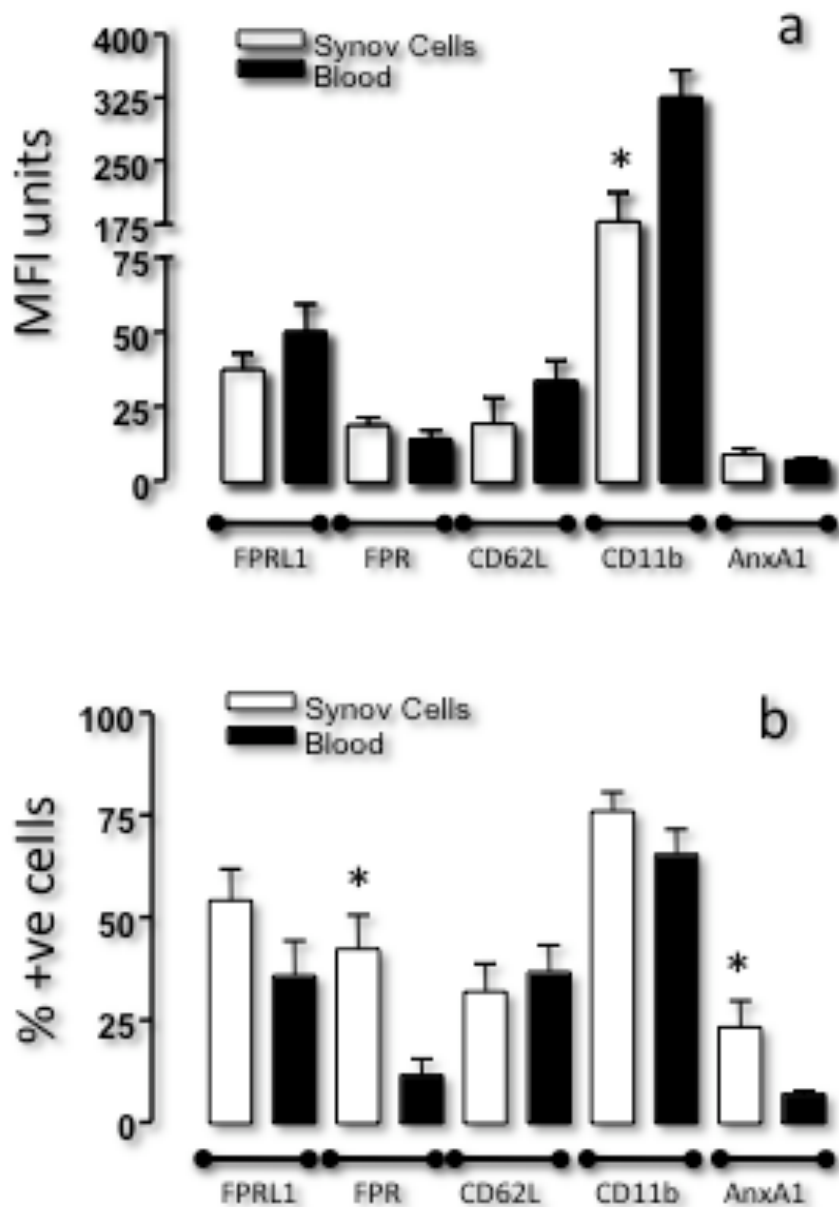


Figure 3-21: Flow cytometric analysis of blood and synovial Monocytes CD11b derived from Rheumatoid Arthritis (RA) patients prior to steroid treatment. Monocytes isolated from RA patients' whole blood and from synovial fluid following which they were stained using immunofluorescent antibodies by incubation for 45 min at 4°C. These results show that there is a marked decrease in CD11b expression in the synovial Monocytes (a). There is also an increased number of FPR and Annexin A1 expressing cells in the synovial fluid (b). * P<0.05 vs. Blood Monocyte group (n=7 patients)

After comparing the difference in basal antigen expression between the synovial and blood compartment for the RA patients, the next step was to determine the effect of the treatment on the propagation of the disease and the potential associated changes in the Annexin A1 system.

The results show that the 14-day treatment led to an increase in the number of cells circulating in the blood, a process of leukocytosis, which has been previously described in other studies looking at the effect of glucocorticoid administration *in vivo* (Figure 3.23) (Dale, Fauci et al. 1975; Fauci and Dale 1975). Interestingly, although there was an increase in the circulating cell counts the flow cytometric analysis showed a reduction in CD11b expression on both cell types which was observed to return back to basal levels, this observation was also mirrored by the number of CD11b expressing cells, in both cell types after the 14 day treatment (Figure 3.24). Similarly a decrease in CD62L expression after the glucocorticoid treatment was measured, where both the CD62L expression per cell and the number of CD62L positive cells was decreased after the first day of treatment, this suggesting a deactivation of both cell types following glucocorticoid treatment and thus a possible shift of these cells to a more quiescent phenotype (Figure 3.25).

Interestingly, in both cell types FPR expression is elevated, so that there is a significant increase in both abundance of the protein per cell and in the number of FPR positive cells (Figure 3.26). This increase is observed at the very beginning of the treatment and returns back to basal levels towards the end

of the study, suggesting that any potential role that regulation of this receptor afforded by the treatment might only be important during the initial stages.

Equally to FPR, FPRL1 cell surface expression is also de-regulated in both cell types, where we see both an increase in abundance of the receptor per cell and also an increase in the number of cells expressing the receptor in the PMN population, an upregulation that becomes more pronounced by day 14. On the other hand the abundance of the receptor per cell for the monocyte group seems only to increase after day 14, however similar to the PMNs there is an increase in the number of cells expressing the receptor from day 1 post treatment (Figure 3.27).

These observations might help provide an insight into the activity of insight into the activity of the glucocorticoids in reducing inflammation. Especially when one also looks at the Annexin A1 expression on these cells, where we see an increase in Annexin A1 levels on the surface of PMNs and monocytes as early as 1 day post treatment (Figure 3.28) which subsequently is reduced, showing that glucocorticoids have only a transient effect in the upregulation of surface Annexin A1 expression on these cells, at least in this condition. However, this transient increase could lead to the observed elevation in the FPRL1 levels previously described very most likely through an autologous feedback mechanism previously described by our lab.

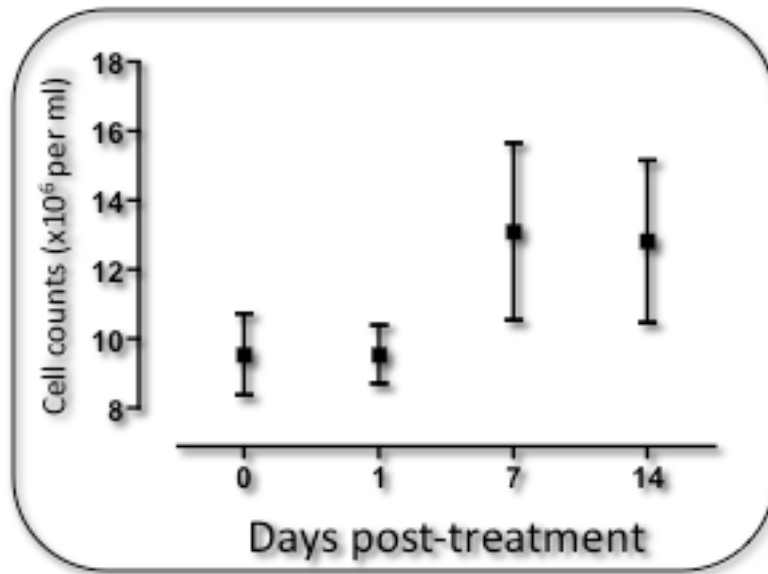


Figure 3-22: White blood profile during a 14-day steroid treatment. Results are Mean and SEM of n=7 patients.

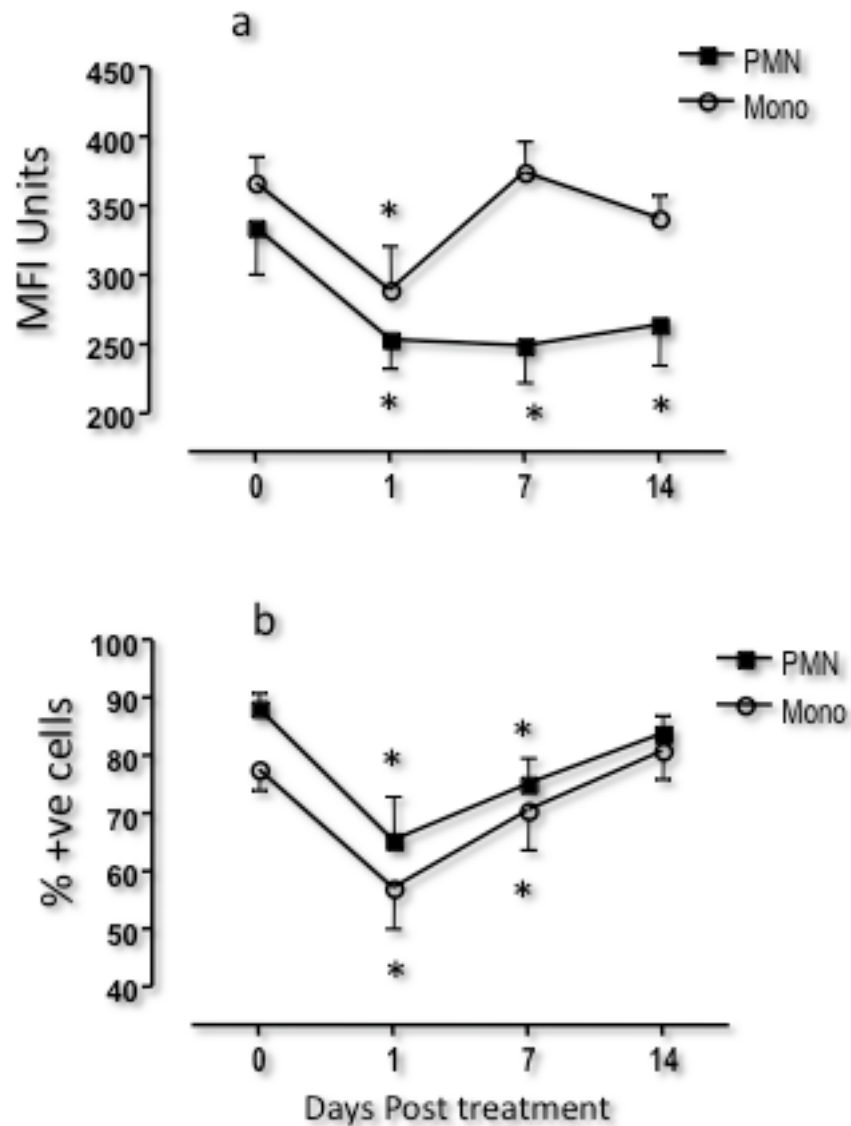


Figure 3-23: CD11b expression on monocytes and PMNs derived from Rheumatoid Arthritis (RA) patients during a 14-day steroid treatment. Monocytes and PMNs isolated from RA patients' blood were stained using an immunofluorescent anti-CD11b antibody, by incubation for 45 min at 4°C. Results are Mean and SEM of n=7 patients; * P<0.05 vs. Day 0 group, One way ANOVA.

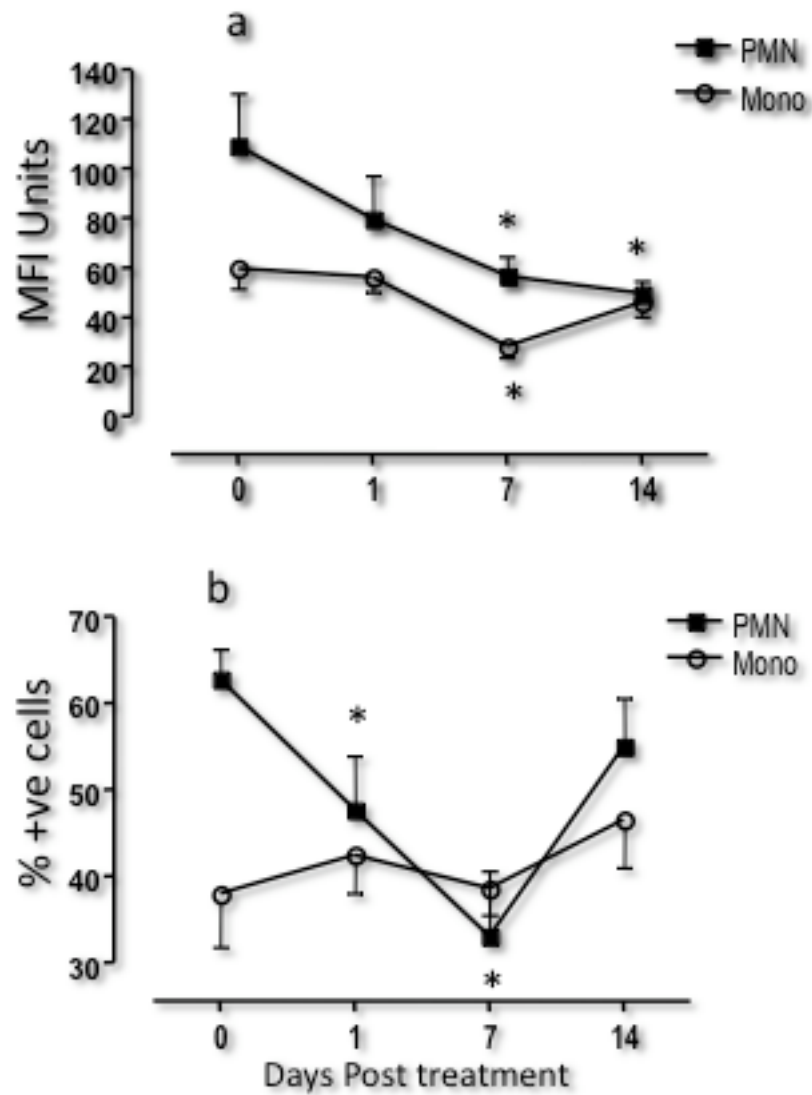


Figure 3-24: CD62L expression on monocytes and PMNs derived from Rheumatoid Arthritis (RA) patients during a 14-day steroid treatment. Monocytes and PMNs isolated from RA patients' blood were stained using an immunofluorescent anti-CD62L antibody, by incubation for 45 min at 4°C. Results are Mean and SEM of n=7 patients; * P<0.05 vs. Day 0 group, One way ANOVA.

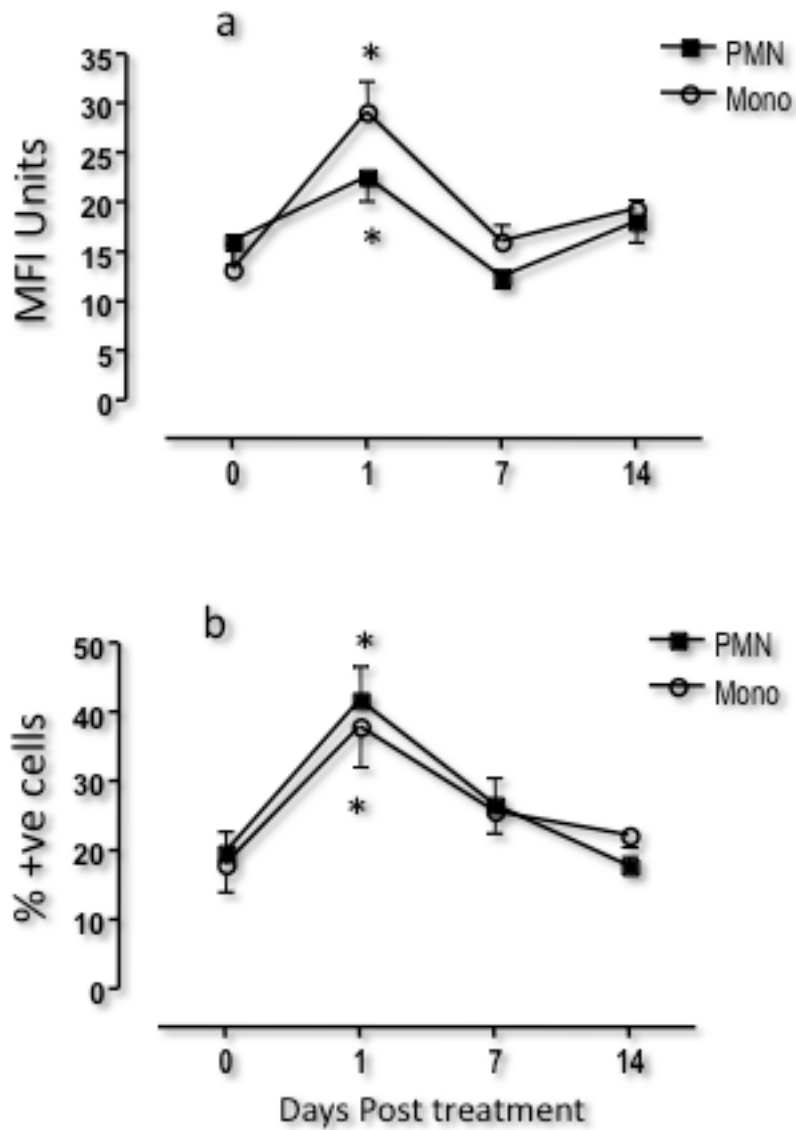


Figure 3-25: FPR expression on monocytes and PMNs derived from Rheumatoid Arthritis (RA) patients during a 14-day steroid treatment. Monocytes and PMNs isolated from RA patients' whole blood were stained using an immunofluorescent anti-FPR antibody, by incubation for 45 min at 4°C. Results are Mean and SEM of n=7 patients; * P<0.05 vs. Day 0 group, One way ANOVA.

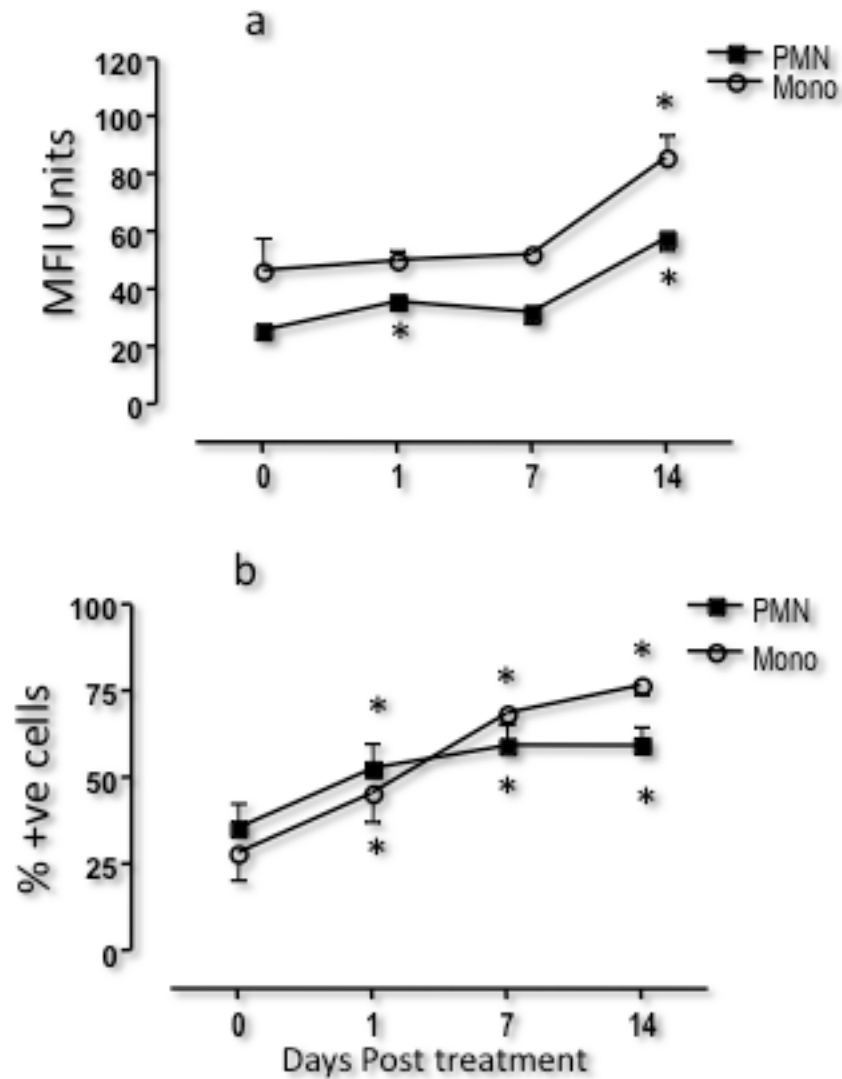


Figure 3-26: FPR1 expression on monocytes and PMNs derived from Rheumatoid Arthritis (RA) patients during a 14-day steroid treatment. Monocytes and PMNs isolated from RA patients' whole blood were stained using an immunofluorescent anti-FPR1 antibody, by incubation for 45 min at 4°C. Results are Mean and SEM of n=7 patients; * P<0.05 vs. Day 0 group, One way ANOVA

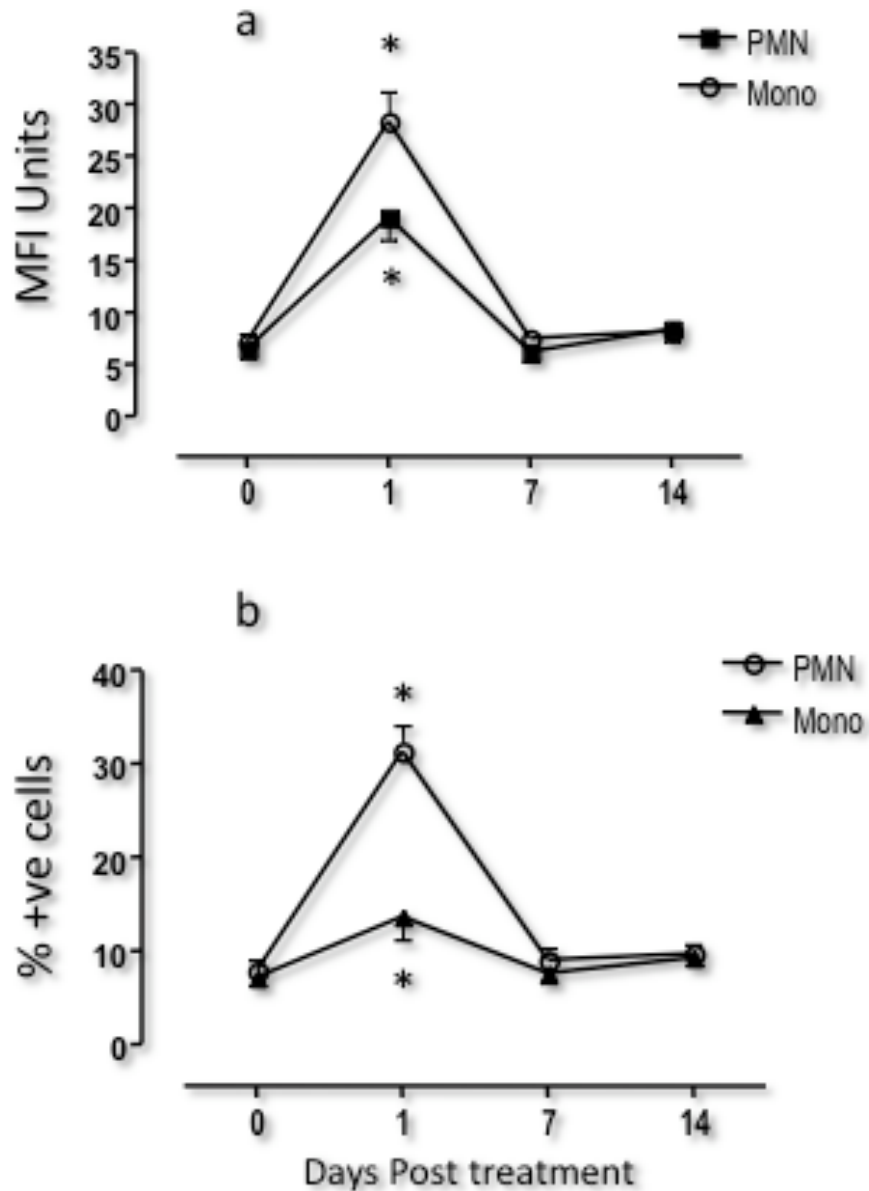


Figure 3-27: Annexin A1 expression in on monocytes and PMNs derived from Rheumatoid Arthritis (RA) patients during a 14-day steroid treatment. Monocytes and PMNs isolated form RA patients' whole blood were stained using an immunofluorescent anti-Annexin A1 antibody, by incubation for 45 min at 4°C. Results are Mean and SEM of n=7 patients; * P<0.05 vs. Day 0 group, One way ANOVA.

3.2. Annexin A1 in microparticles and its potential role as biomarker.

3.2.1. Exploring a novel mechanism for Annexin A1 release

3.2.1.1. Extraction and determination of Annexin A1 presence in PMN-derived microparticles

In order to fulfil the aim of this part of the project, it was important to establish a microparticle extraction technique along with a method to determine the production of microparticles. After extraction using a pre-established technique detailed in the Methods section, the forward and side scatter parameters of the flow cytometer were set using 1 μ M beads, once the instrument was calibrated the microparticle containing solution was analysed using the flow cytometer (Figure 3-29).

This initial determination was only based on the forward and side scatter parameters, therefore size and granularity, along with comparison to the calibration beads. Using these parameters it was established that the population under analysis had similar characteristics to those published for neutrophil microparticles. In order to confirm whether this population was in fact composed of microparticles, staining was performed where first these microparticles were co-incubated with Annexin V, to detect phosphatidylserine (PS) serine exposed on the outer surface of these microstructures (Figure 3-30a). This marker is employed since in the process of microparticle production, phosphatidylserine is exposed on the outer surface of the cell membrane following membrane flip-flop. Furthermore, so as to establish the cellular origin of these microparticles, immunohistochemical staining for CD62L, a PMN

specific antigen, was conducted the result of which confirmed these structures to be neutrophil derived (Figure 3-30b).

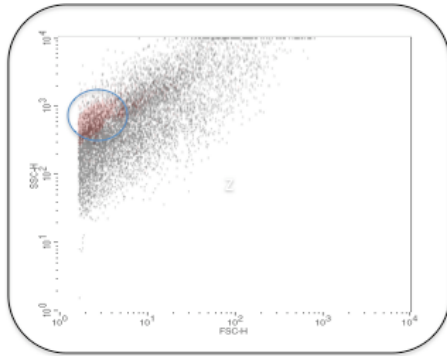


Figure 3-28: Determining the presence of Microparticles following instrument calibration. Following the calibration by 1 μ m beads (in red) microparticles (M.P.) were flowed through the flow cytometer to confirm their presence based on their physical properties, since the literature defines these entities as having a size ranging between 1.5 μ m and 0.2 μ m.

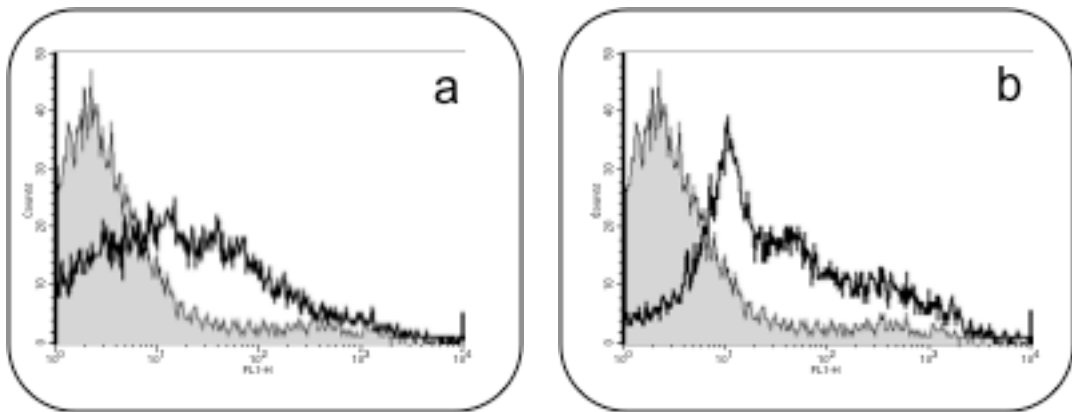


Figure 3-29: FACS analysis on microparticles derived from adherent PMN. Flow cytometry analysis of adherent PMN (to HUVEC monolayers)-derived microparticles, with acquisition of 5-10,000 events per sample. a) Histograms demonstrating detection of Phosphatidylserine L-selectin b) CD62L Data are representative from ≥ 3 independent microparticle preparations.

After confirming that the microstructures isolated from the PMN supernatant were in fact PMN derived microparticles it was now important to establish the presence of Annexin A1 in these microparticles. For this purpose PMN microparticles were isolated and immediately lysed in lysis buffer following which they were loaded on to a 10% polyacrylimide gel, after electrophoresis and transfer the blot was probed against Annexin A1 which showed the presence for the first time of this protein in PMN derived microparticles (Figure 3-31). This result was then confirmed using another analytic tool, mass spectrometry, where the 37kDa band corresponding to the Annexin A1 band was excised from the polyacrylamide gel previously stained with Coomassie blue and analysed as highlighted in the previous section (Figure 3.32). Once the peptide sequences identified from this band were analysed the presence of Annexin A1 was confirmed.

After confirming the presence of Annexin A1 in these microstructures I wanted to determine if this protein was located on the extracellular surface of these structures. For this purpose, I employed flow cytometric analysis, staining microparticles with both anti-CD62L (as a positive control) and anti-Annexin A1 antibodies (Figure 3.33 b and c). The result of this analysis showed that Annexin A1 is present on the outer surface of microparticles and is expressed on their surface. Thus all three experimental methods confirmed the presence of Annexin A1 on PMN derived microparticles, all, or at least a significant pool, being on their membrane. Furthermore, I observed that membrane Annexin A1 bound in a calcium dependent manner, since upon washing the microparticles

with a 1 μ M EDTA solution removed over 95% of the Annexin A1 found on the surface of these microstructures as verified through the flowcytometric analysis depicted in Figure 3.36.

In order to determine if there were any contaminating microparticles derived from other cell sources, PMN-derived microparticles were also stained with anti P-selectin and anti CD14, to identify platelet and monocyte sources, respectively Figure 3.34 (b and c).

An important control, for this part of my study, was to stain microparticles obtained from non-stimulated PMN. Firstly, it was interesting to note that even in this very mild, or null, culturing condition, I could find microparticles; these could be identified by CD62L and phosphatidylserine expression (Figure 3-35 b and c). Of interest, these microparticles were not immuno-reactive for the anti-Annexin A1 antibody (Figure 3-35 d).

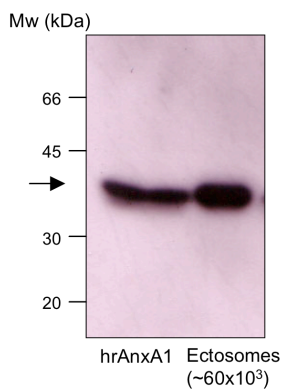


Figure 3-30: Western Blot showing the presence of Annexin A1 in PMN derived microparticles. Following microparticle extraction, western blot analysis was conducted comparing human recombinant Annexin A1 (0.1 ng) to extracts from $\sim 60 \times 10^3$ microparticles. Following gel electrophoresis and transfer the blot was probed with an anti-Annexin A1 antibody, showing the presence of Annexin A1 in the microparticles (arrow).



Figure 3-31: LC/MS/MS analysis of the 37kDa immunoreactive band. Following gel electrophoresis the gel was Coomassie stained and the 37kDa immunoreactive band was excised and digested. The resulting peptides were analysed against the SwissProt database and Annexin A1 resulted as the most abundant protein in this band.

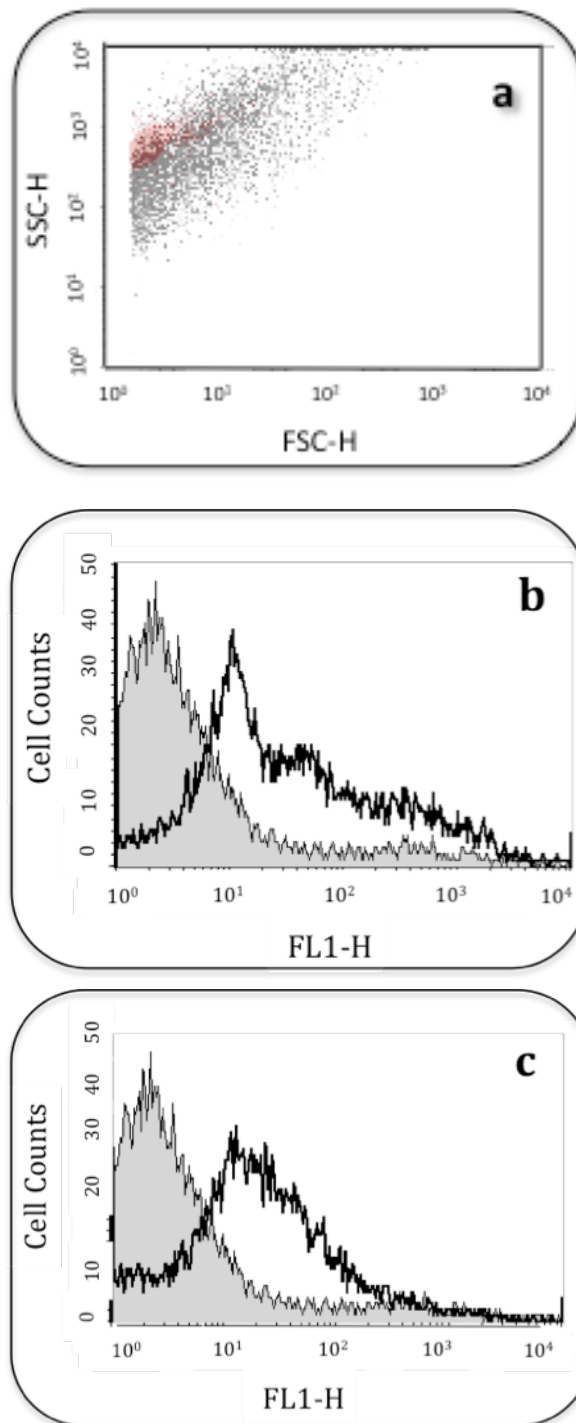


Figure 3-32: FACS analysis on microparticles derived from adherent PMN. Flow cytometry analysis of adherent PMN (to HUVEC monolayers)-derived microparticles, with acquisition of 5-10,000 events per sample. A) Dot-plot showing the heterogeneity in microparticle sizes (a); Histograms demonstrating detection of L-selectin (CD62L) (b), Annexin A1 (c) Data are representative from ≥ 3 independent microparticle preparations.

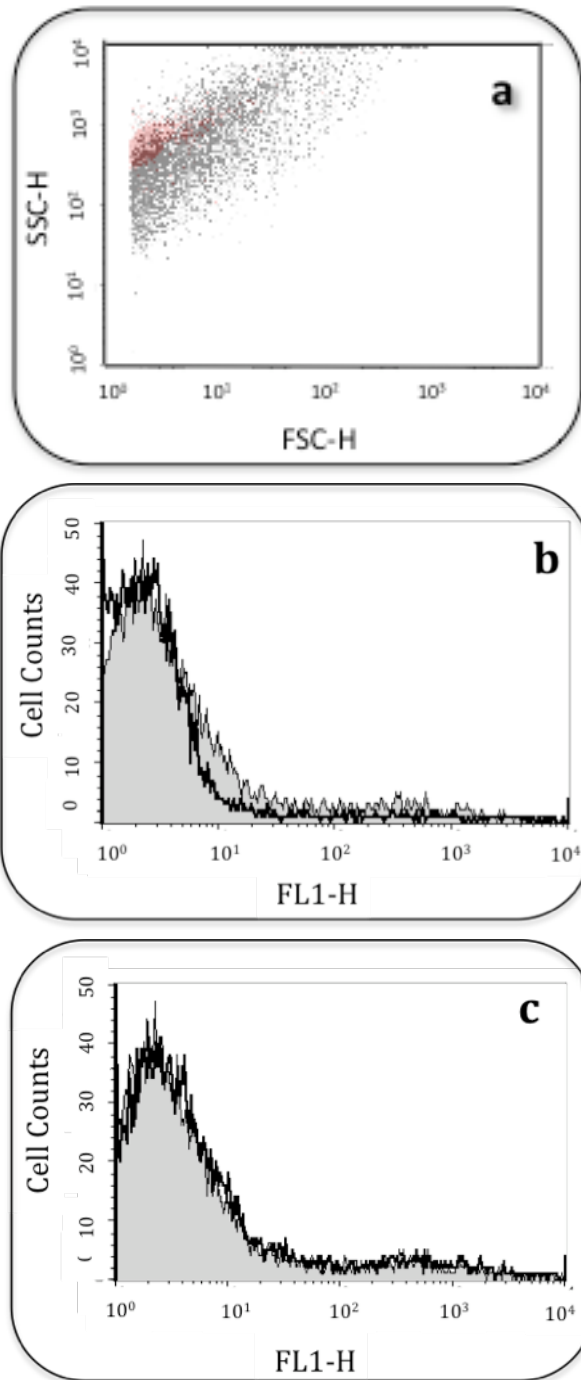


Figure 3-33: FACS analysis on microparticles derived from adherent PMN. Flow cytometry analysis of adherent PMN (to HUVEC monolayers)-derived microparticles, with acquisition of 5-10,000 events per sample. A) Dot-plot showing the heterogeneity in microparticle sizes (a); Histograms demonstrating detection of P-selectin (CD62P) (b), CD14 (c) Data are representative from ≥ 3 independent microparticle preparations.

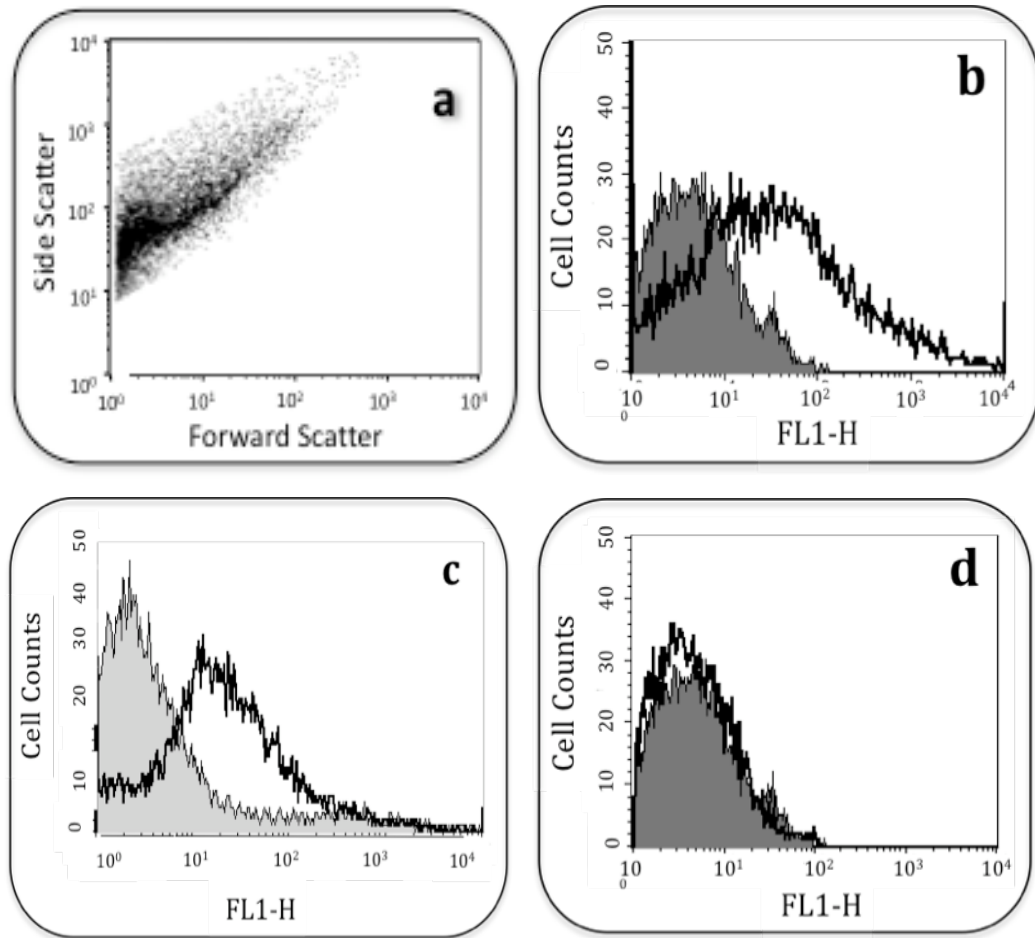
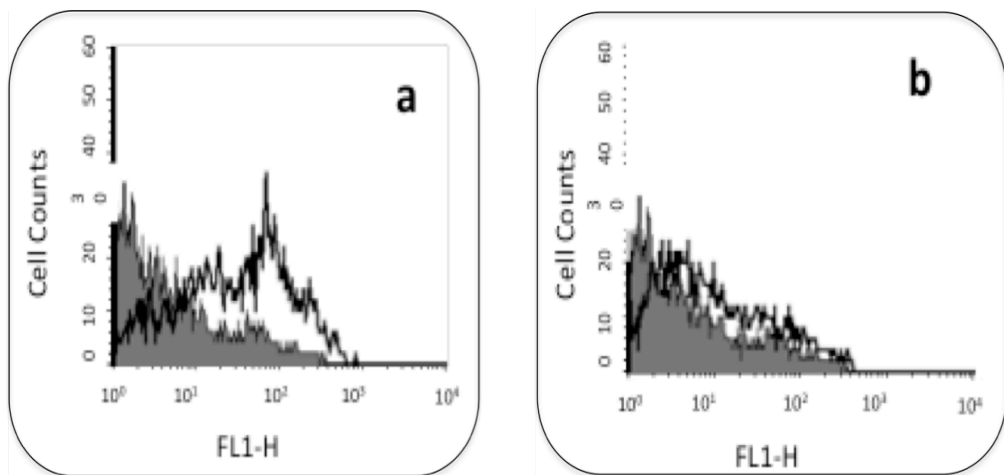


Figure 3-34: Staining for microparticles derived from unstimulated PMNs. Following extraction the microparticles were stained by incubation with for 30 minutes at room temperature with FITC conjugated Annexin V and an immunofluorescent anti-CD62L antibody. The positive shift when compared to the isotype control for both CD62L (b) and phosphatidylserine (c) confirms the presence of PMN derived microparticles, whilst figure (d) outlines the absence of Annexin A1 in this microparticle population



C

	Annexin 1	CD62L
Unwashed M.P.	72 ± 7.2	102 ± 5.9
EDTA washed M.P.	7.8 ± 2.3	112 ± 9.4

Figure 3-35: Flow-cytometric analysis of Annexin A1 +ve M.P following EDTA wash. Following the ultracentrifugation step, microparticles (M.P.) were either washed with 1mM EDTA or just PBC, following this wash step, these M.P. were ultracentrifuged resuspended in PBC and incubated with either an anti-Annexin A1 ab or an isotype control. The figure (a) represents the PBC washed M.P. whilst figure (b) the M.P. washed with the EDTA following which the M.P. Annexin A1 expression Annexin A1 expression was quantified by flow-cytometry, table (c) is a summary of the MFI values obtained in 3 independent microparticle preparations, with results expressed as mean and SEM.

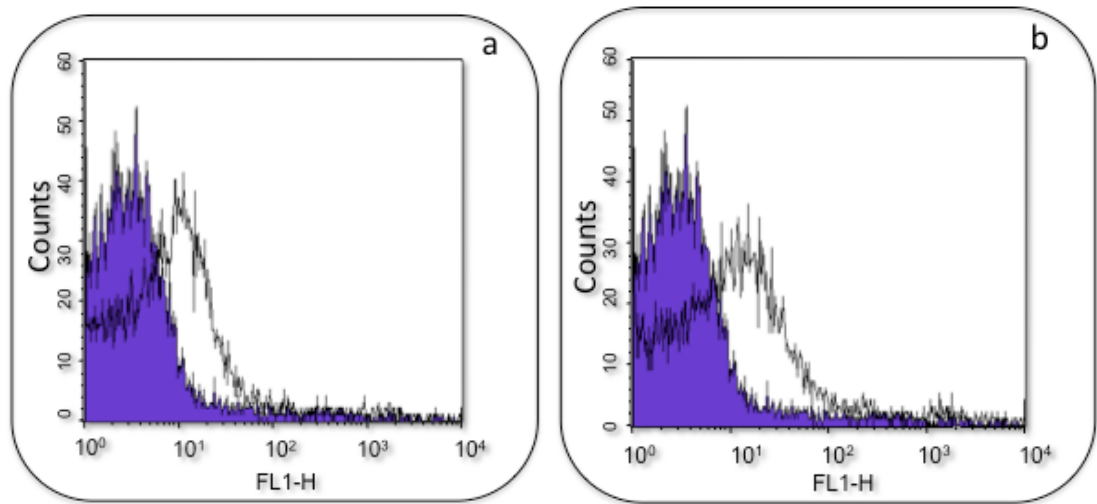
3.2.2. The *in vitro* anti-inflammatory role on Annexin A1 in PMN derived microparticles

After showing presence of Annexin A1 in PMN derived microparticles, the next step was to determine if they might be of any biological relevance. Since hr-Annexin A1 is known to elicit inhibitory and anti-adhesion effects, I tested these microparticles in an adhesion assay. This was done by co-incubating microparticles with recipient PMNs for 10 min and then flowing the mixture of cells and microvesicles over an activated HUVEC monolayer. These results showed that in fact Annexin A1 +ve microparticles do possess anti-inflammatory properties since whether pre-incubated with the HUVECs or with the PMN, the number of cells recruited to the endothelium was significantly reduced. In particular, incubation of these microstructures with PMN reduced significantly both their extent of rolling and adhesion (Figure 3-37).

To elucidate the role of Annexin A1 on the observed inhibition of leukocyte recruitment underflow, neutralising monoclonal antibodies against either the Annexin A1 protein or its receptor were employed, applying them in the microparticle/PMN incubation phase. The results show that by blocking either component of the Annexin A1 pathway, the anti-inflammatory effects exerted by these microparticles was reverted, with values of cell recruitment returning to control levels (Figure 3-40). Interestingly incubation of the microparticles/PMNs with either neutralising antibody was only able to reverse part of the recruitment cascade, that is adhesion. In fact these microparticles were still observed to inhibit PMN rolling over the activated endothelial

monolayer suggesting that an alternative pathway might be at least in part also responsible for the observed reduction in the number of rolling cells.

I finally wanted to determine whether the mode of production of these microparticles was important in the conferring the observed anti-inflammatory properties to these structure and whether there were other components on these microparticle which could also confer anti-inflammatory properties. The results point out that only microparticles produced by co-incubating PMNs over a HUVEC monolayer possessed inhibitory properties, whereas microparticles harvested from un-stimulated PMN were without any evident effect. As the latter type of microparticles are Annexin A1 -ve, these results strongly suggest that presence of Annexin A1 on these microparticles is responsible for some of the observed effects (Figure 3-42).



c

	CD62L	Annexin 1
MFI units	289 ± 22	122 ± 14

Figure 3-36: Characterization of PMN derived M.P. prior to use in flow chamber. M.P. were stained with an anti-Annexin A1 (a) and anti-CD62L (b) both of which confirmed the presence of PMN derived Annexin A1 positive microparticles. The table (c) provides a summary of the MFI values obtained in 3 independent microparticle preparations, with results expressed as mean and SEM

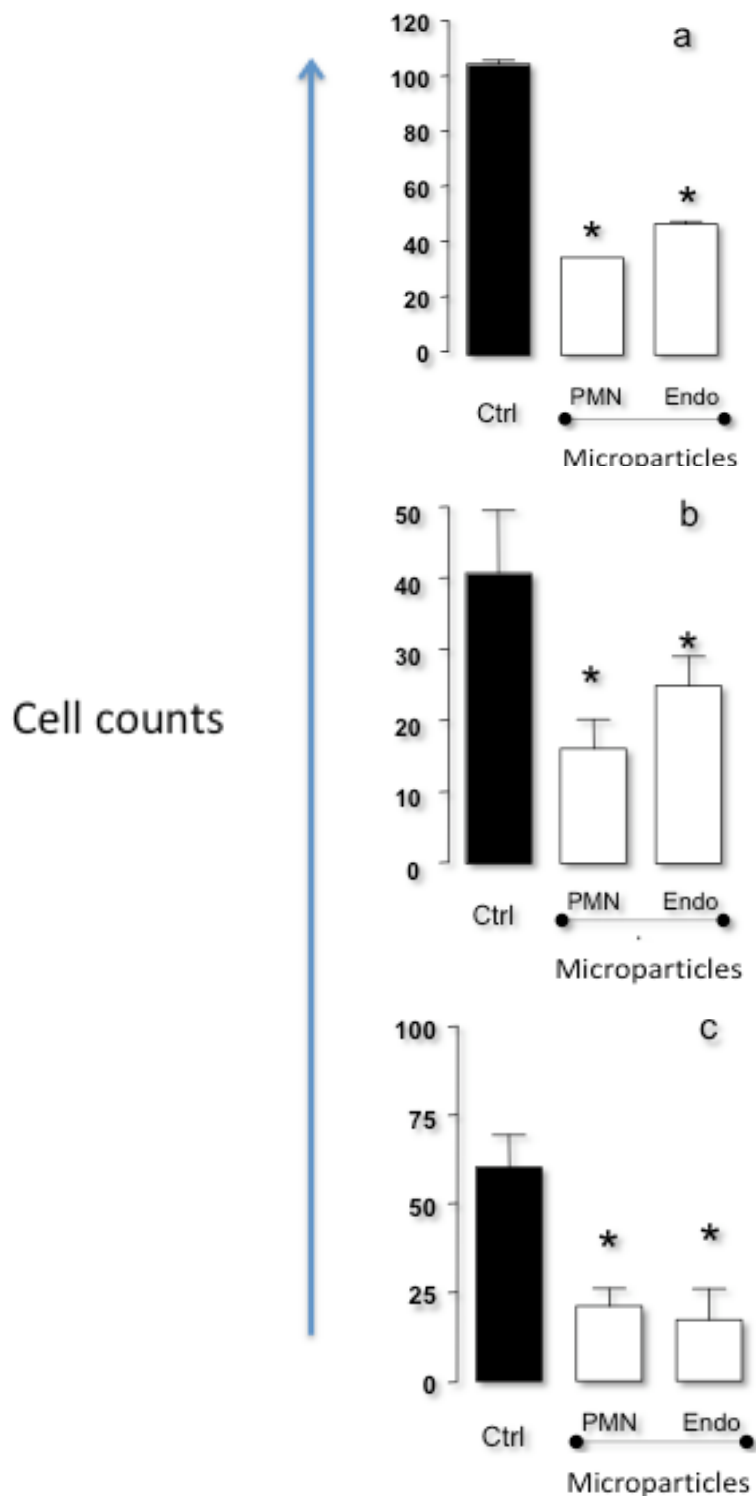
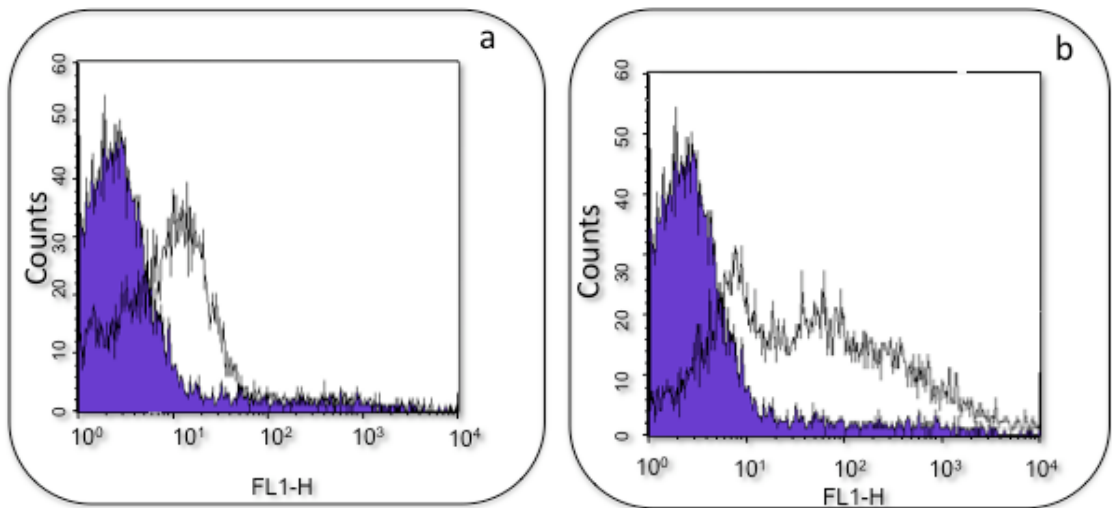


Figure 3-37: Annexin A1 rich microparticles inhibit PMN/HUVEC interaction under flow. PMN were incubated with microparticles, microparticles + anti-FPRL1 neutralizing antibody, Microparticles + anti-Annexin A1 or microparticles + Isotype CT prior to flow over TNF- α stimulated (10 ng/ml, 4 h) HUVEC. PMN-endothelium interactions were quantified off-line. (a) Number of PMN captured. (b) Number of firmly adherent PMN. (c) Number of rolling PMN. Data are presented as mean \pm SEM of 4 independent experiments. * = P<0.05 vs. control group, One way ANOVA.



c

	CD62L	Annexin 1
MFI units	312 ± 31	162 ± 27

Figure 3-38: Characterization of PMN derived M.P. prior to use in flow chamber. M.P. were stained with an anti-Annexin A1 (a) and anti-CD62L (b) both of which confirmed the presence of PMN derived Annexin A1 positive microparticles. The table (c) provides a summary of the MFI values obtained in 3 independent microparticle preparations, with results expressed as mean and SEM.

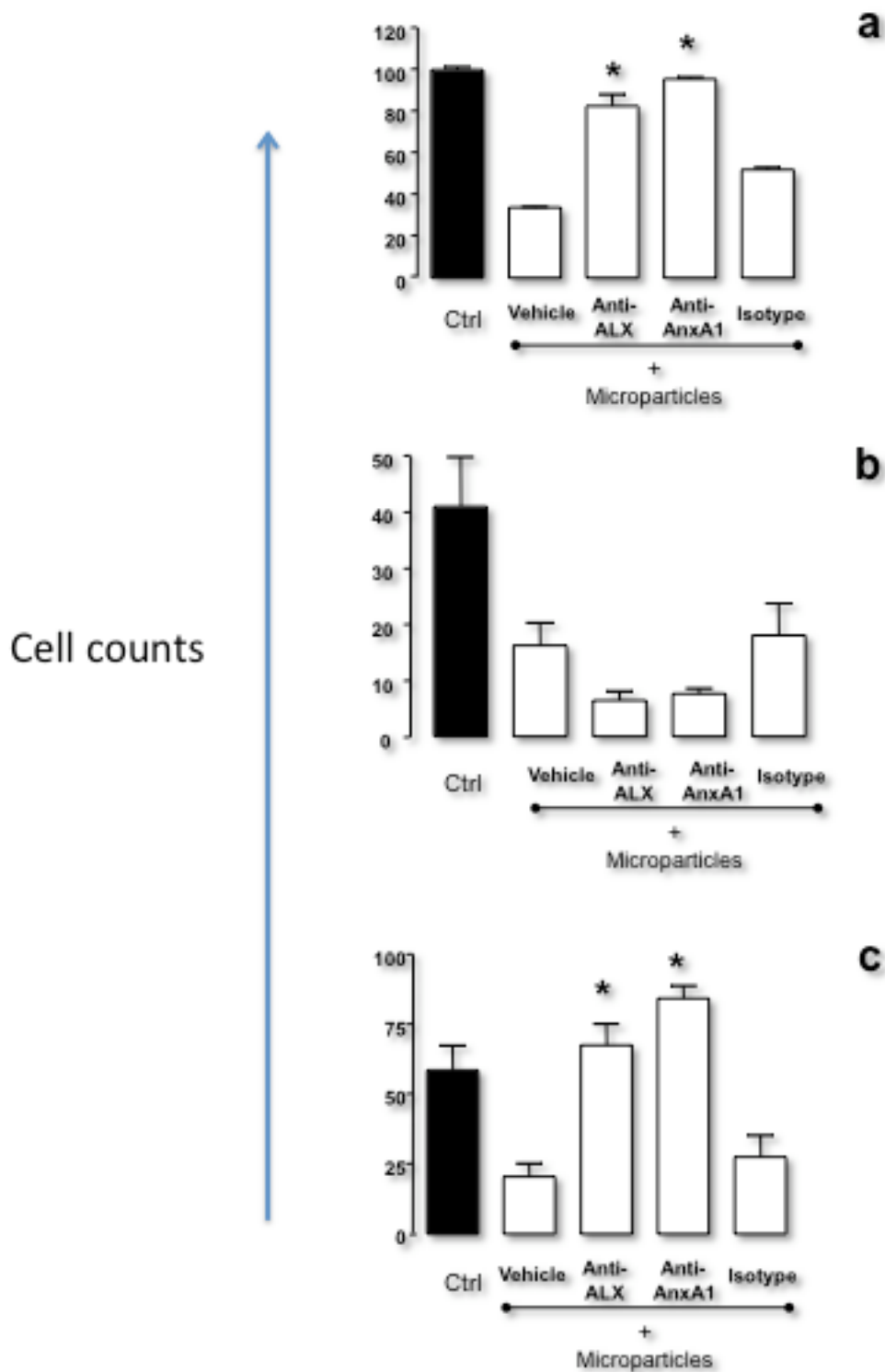
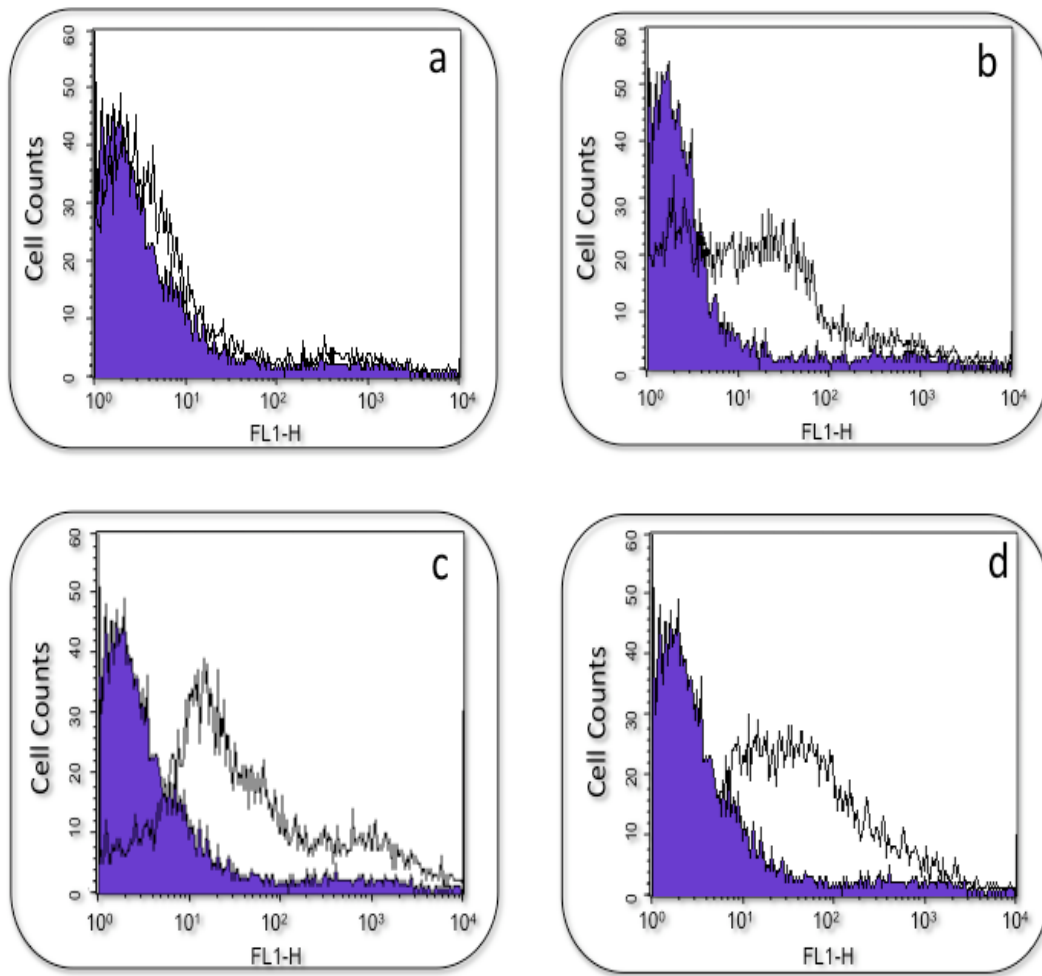


Figure 3-39: Role for Annexin A1 in the inhibitory property of PMN-derived microparticles. PMNs (5×10^6) were incubated with microparticles (between 30 and 50×10^3) for 10 min at 37°C . In some tubes, isotype control Ab, or neutralizing anti-Annexin A1 or anti-ALX mAb were also added. PMN (5×10^6) were then flowed for 8 min at 1 dyne/cm^2 , prior to quantifying the degree of PMN interaction with the HUVECs, both as PMN capture (a), rolling (b) and adhesion (c). Data are mean \pm SEM of from 4 to 5 independent experiments (with distinct microparticles, PMN and HUVEC preparations); $P < 0.05$ vs. microparticles treated group, data analysed using One way ANOVA



e

	CD62L	Annexin 1
Resting M.P.	212 ± 31	6 ± 2.7
Adherent M.P.	294 ± 27	145 ± 19

Figure 3-40: Characterization of PMN derived M.P. prior to use in flow chamber. M.P. from resting and adherent PMN were stained with an anti-Annexin A1 and anti-CD62L the latter confirmed the presence of PMN derive M.P. (b, and d), whilst the former stain showed that Annexin A1 was only found on the M.P. derived from adherent PMNs (c) with the M.P. derived from resting PMN showing no shift in the staining (a). The table (e) provides a summary of the MFI values obtained from in 3 independent microparticle preparations, with results expressed as mean and SEM.

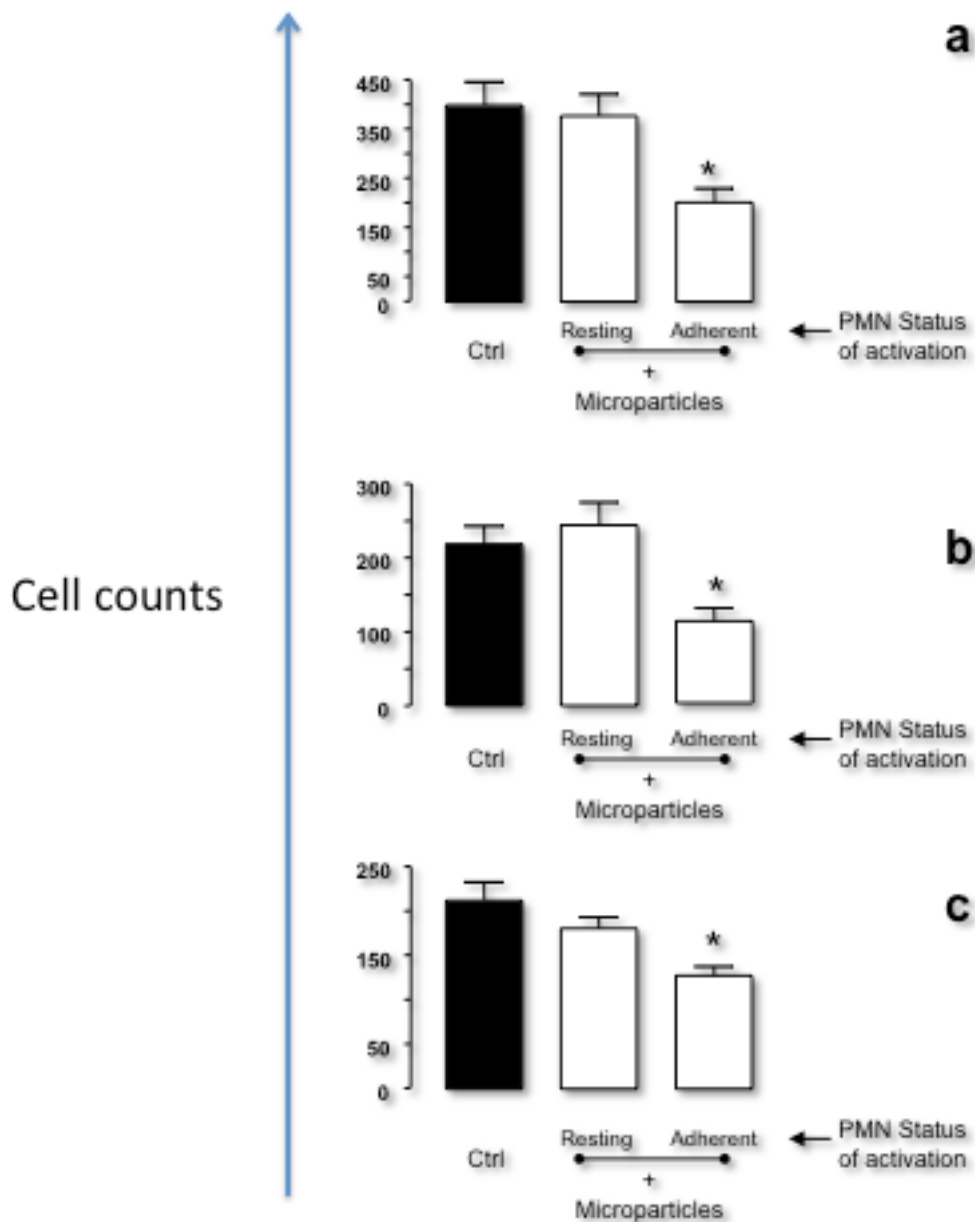


Figure 3-41: Confirming that only microparticle from fMLP stimulated PMN possess inhibitory properties. PMNs (5×10^6) were incubated with M.P. (between 30 and 50×10^3) for 10 min at 37°C . In some tubes PMNs were incubated with microparticles obtained from non-stimulated PMN that had been incubated for 20mins at 37°C or with microparticles obtained from fMLP stimulated PMN. PMN (5×10^6) were then flowed for 8 min at 1 dyne/cm^2 , prior to quantifying the degree of PMN interaction with the HUVECs, both as PMN capture (a), adhesion (b) and rolling (c). Data are mean \pm SEM of from 5 independent experiments (with distinct M.P PMN and HUVEC preparations); $P < 0.05$ vs. M.P. treated group, data analysed using one way ANOVA.

3.2.3. The *in vivo* anti-inflammatory role on Annexin A1 in PMN derived microparticles

A way to extend the inhibitory actions of PMN derived microparticles in the flow chamber assay was to determine if this observation would also hold true in an *in vivo* setting. I set out to determine this by testing these microparticles into a pre-clinical model of PMN recruitment, the mouse air-pouch model.

I injected two doses of microparticles which resulted in a decreased in GR1+ve cell recruitment to the site of inflammation (Figure 3-43). Therefore, the anti-inflammatory actions reported *in vitro* are also translatable to the *in vivo* scenario. However, this observation does not conclusively determine the role that Annexin A1 might be playing in these conditions. In order to address this question, neutrophils were extracted from murine bone marrows of both WT and Annexin A1 *-/-* animals following which the microparticles were produced by co-incubation of these cells over a mouse endothelial layer and stimulation with fMLP. Following production and extraction, microparticles were stained with Annexin V and anti-CD62L in order to confirm the presence and origin (Figure 3-44). Their anti-inflammatory properties were then tested in the murine air-pouch model. As observed for human derived microparticles, there was a dose dependent reduction in the number of GR1+ve cells recruited to the site of inflammation for the WT microparticles whilst, on the other hand, this effect was lost when the animals were injected with similar doses of the Annexin A1 *-/-* PMN-derived microparticles (Figure 3-45). These observations further underscore the anti-inflammatory role played by the Annexin A1 found on PMN derived microparticles.

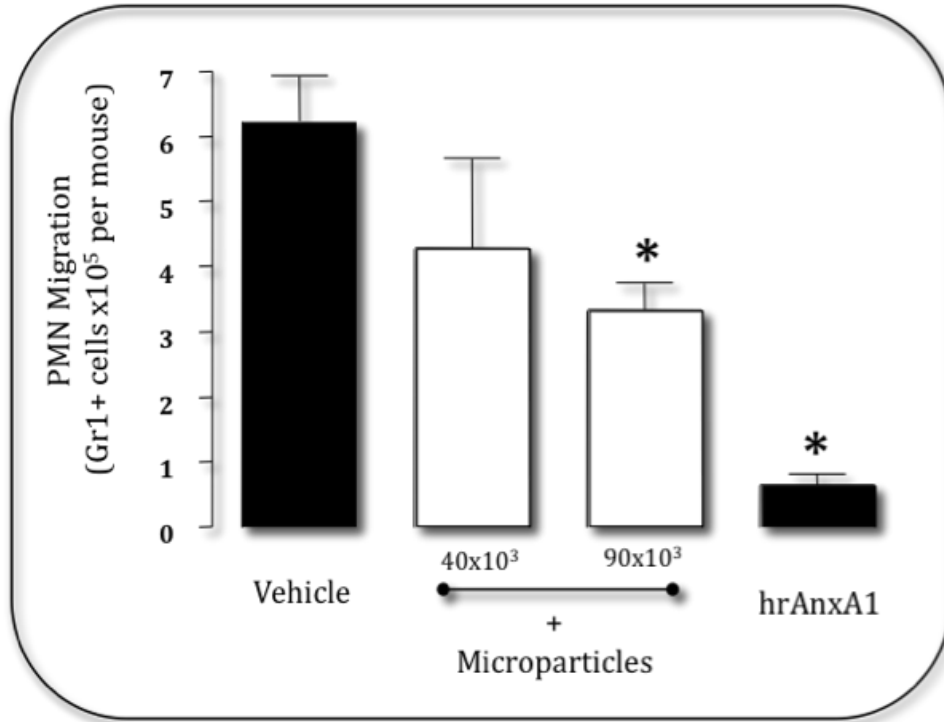
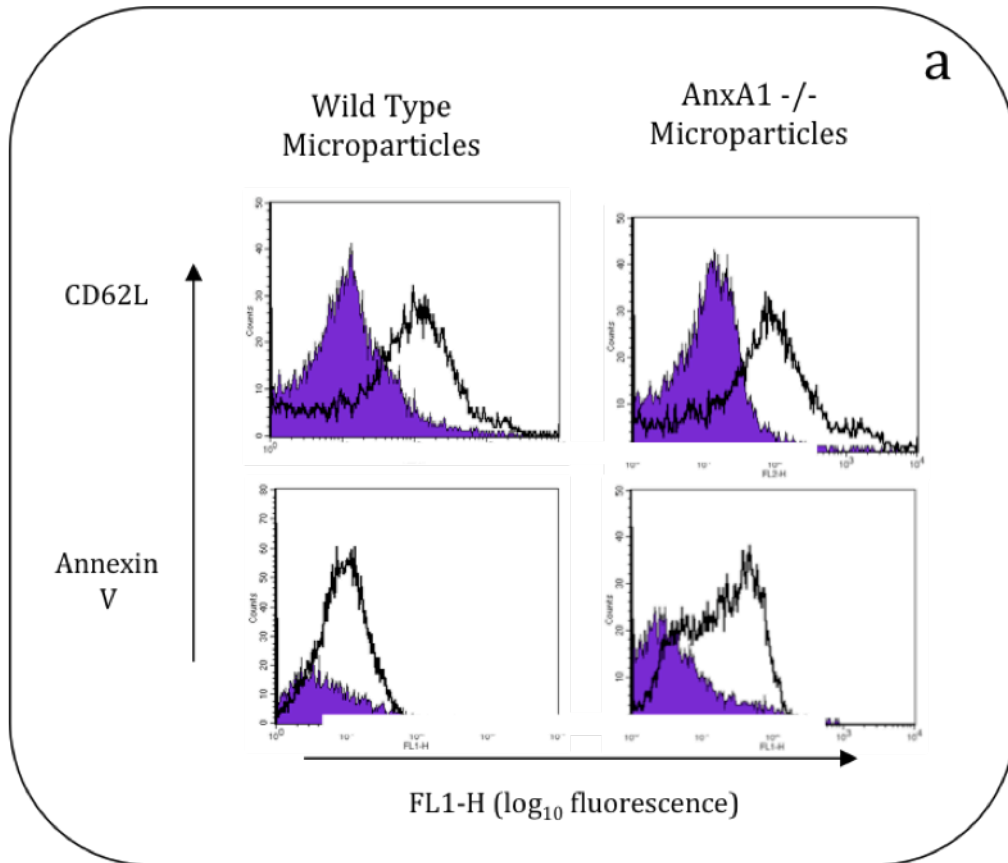


Figure 3-42: Anti-inflammatory effects of human PMN-derived microparticles. Mice received 200 μ l i.v. of saline or two doses of human PMN-derived ectosomes, or human recombinant Annexin A1 (20 μ g; positive control), immediately before the local injection of mouse IL-1 β into 6-day-old airpouches. The extent of cell migration was determined 4 h later, following airpouch washing and staining of migrated cells with Gr1 marker. Data are mean \pm SEM of 5 mice per group. *= $P < 0.05$ vs. vehicle group, statistical analysis was conducted by one way ANOVA.



b

	WT MP	Annexin 1 ^{-/-} M.P.
Phosphatidylserine	18 ± 1.2	22 ± 1.4
CD62L	69 ± 2.3	59 ± 4.2

Figure 3-43: Positive identification of the murine PMN-derived microparticles. Using flow cytometric techniques the microparticles were stained with anti-CD62L and Annexin V, where for both the WT and the Annexin A1 ^{-/-} PMN derived microparticles there was a strong positive signal. Table (b) summarises the MFI values obtained for each animal group (n=5 mice per group), data is expressed as a mean and SEM.

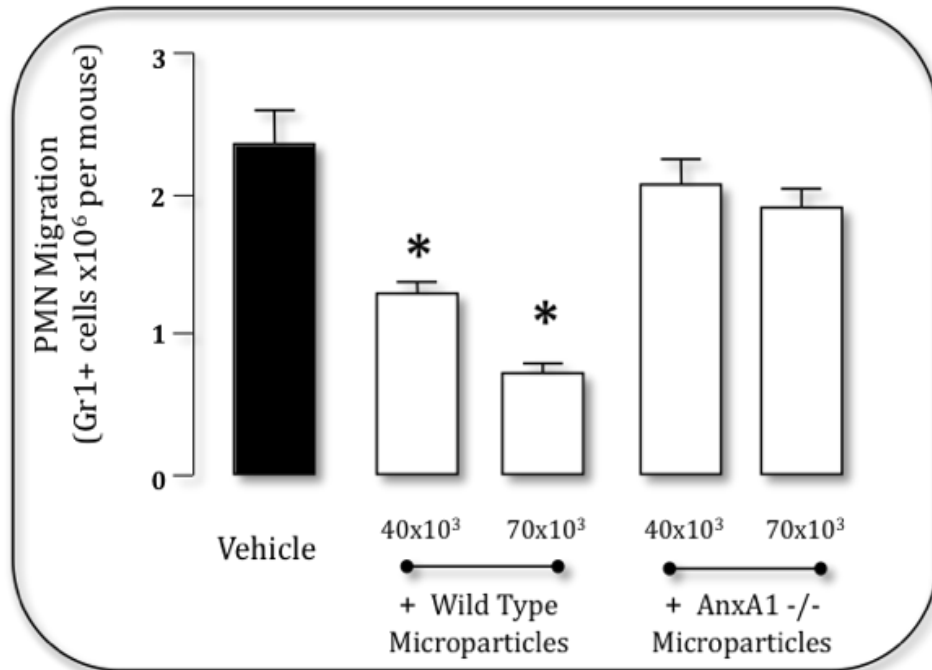


Figure 3-44: Anti-inflammatory effects of murine PMN-derived microparticles. Mice received 200 μ l i.v. of saline or two doses of WT, or Annexin A1 -/- microparticles, immediately before the local injection of mouse IL-1 β into 6-day-old airpouches. The extent of cell migration was determined 4 h later, following airpouch washing and staining of migrated cells with Gr1 marker. Data are mean \pm SEM of 5 mice per group. * P <0.05 vs. vehicle group, data was analysed using one way ANOVA.

3.2.4. Reactive Oxygen Species production by human PMN-derived Microparticles.

As discussed in chapter 1.3 microparticles have been described to possess both pro and anti-inflammatory functions, which can vary depending on the cells of origin or even the stimulus applied to the cell for their generation. For instance, as highlighted above, Annexin A1 loaded PMN-derived microparticles possess anti-inflammatory functions; however, PMN derived microparticles have also been described as having a pro-inflammatory role. Thus, I set out to determine what lead to this dichotomy. One of the approaches I took was to change the stimulus provided, and then determining if these microparticles were capable of producing ROS.

Following incubation of PMNs either in suspension or over a HUVEC monolayer, microparticles were isolated and analysed using a flow cytometer, where it was observed that a distinct, larger population emerged in those samples obtained from PMNs stimulated in suspension (Figure 3-46a). This subset of microstructures was confirmed to be microparticles through the analysis of the antigen expression, which showed that they were both CD62L and were PS (Figure 3-47a) positive, whilst being CD62P negative (Figure 3-47b).

ROS production was assessed by employing a simple technique, where the microparticles were loaded in lucigenin and then stimulated with a direct synthetic NADPH oxidase activator we could detect the presence of ROS (Figure 3-48). Interestingly this ROS production was not observed when I used microparticles obtained from PMNs adherent to a HUVEC monolayer (Figure

3-48), this suggesting a stimulus specific response to the microparticle production and possibly content.

In order to establish whether in fact the larger microparticle population was responsible for the ROS production this population was isolated employing FACS techniques. Following isolation the ability of the two populations gated below as R1 and R2 to produce ROS was assessed employing a DCFDA assay that confirmed that the larger microparticle population (R2) was in fact able to produce ROS (Figure 3-49b) whilst the population gated in R1 was unable to produce these chemical entities (Figure 3-49c).

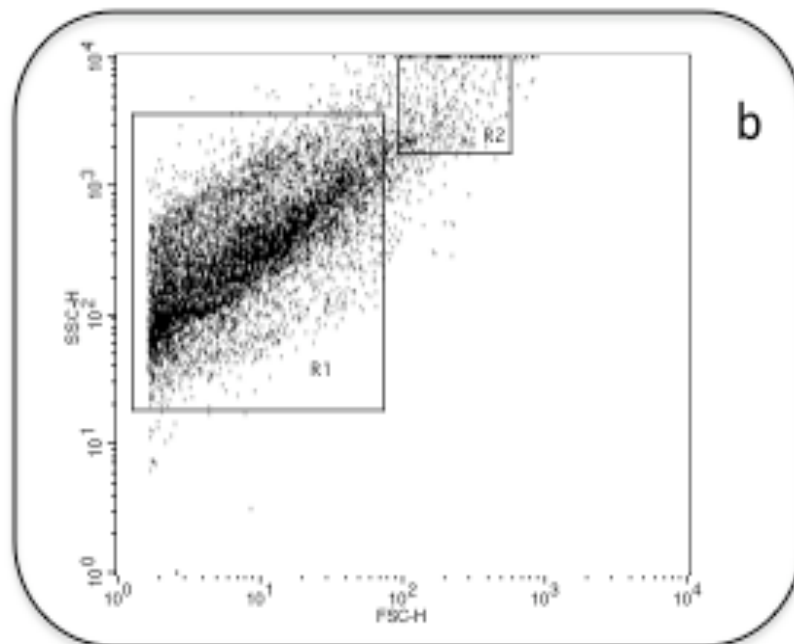
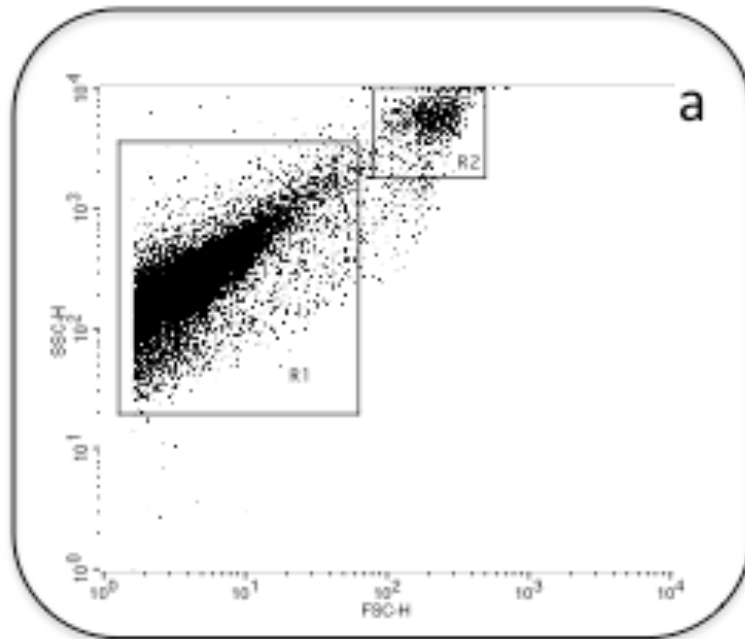


Figure 3-45: Analysis of the microparticle populations produced by differential stimulation using flow cytometry. PMN were incubated either in suspension (a) over a HUVEC monolayer (b) for 20 min, then stimulated for 20 min with 1 μ M fMLP. The analysis of the populations produced a new microparticle population in the PMNs stimulated in suspension highlighted in box R2. Scatterplots are representative of 5 independent microparticle preparations.

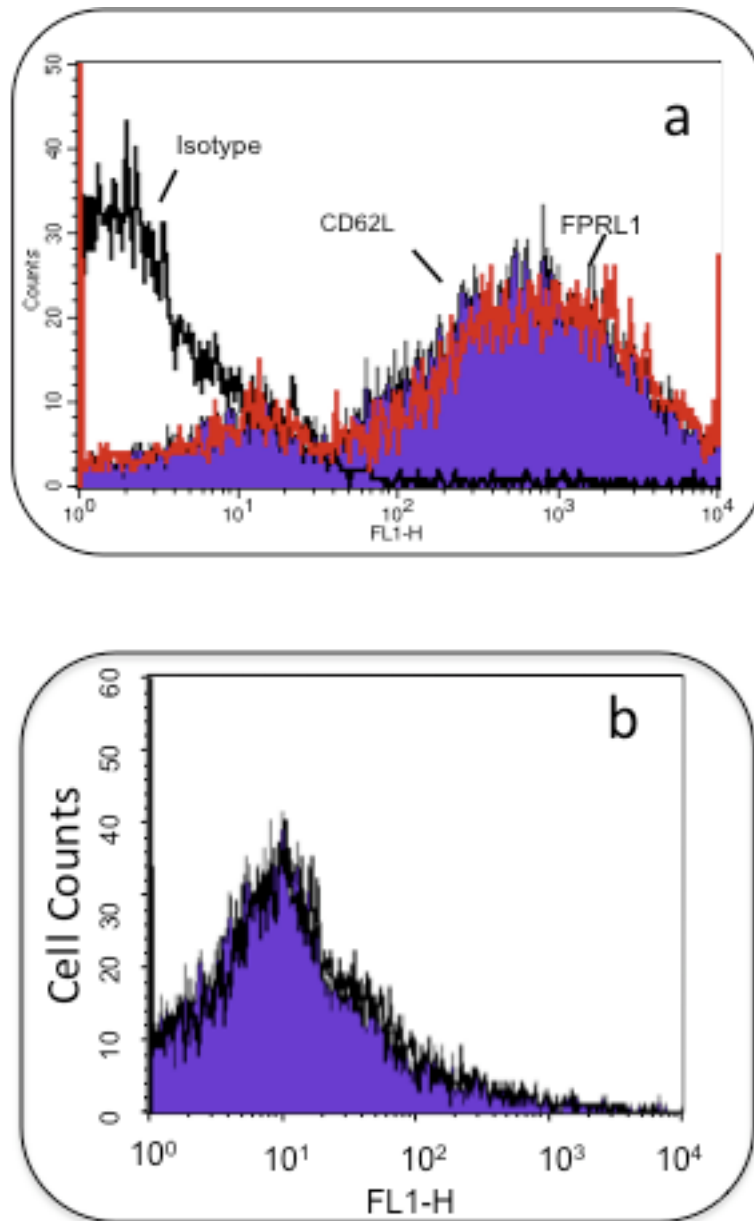


Figure 3-46: Flow cytometric determination of FPRL1 in ROS producing PMN derived microparticles. The microparticles were stained with immunofluorescent anti-CD62L, anti-FPRL1 (a) and anti-CD62P (b) antibodies. The microparticle CD62L, CD62P and FPRL1 expression was quantified by flow cytometry. Histograms are representative of 5 distinct experiments.

Stimulus	R1	R2
Post Adherent M.P.	86.7 ± 1.5	1.9 ± 0.9
In Suspension M.P.	73.9 ± 8.7	20.1 ± 7.5

Table 3-4: Table outlining the abundance of the different microparticle populations produced upon differential stimulation. Results are presented as mean and SEM percentages out of the total population and are representative of 6 distinct preparations.

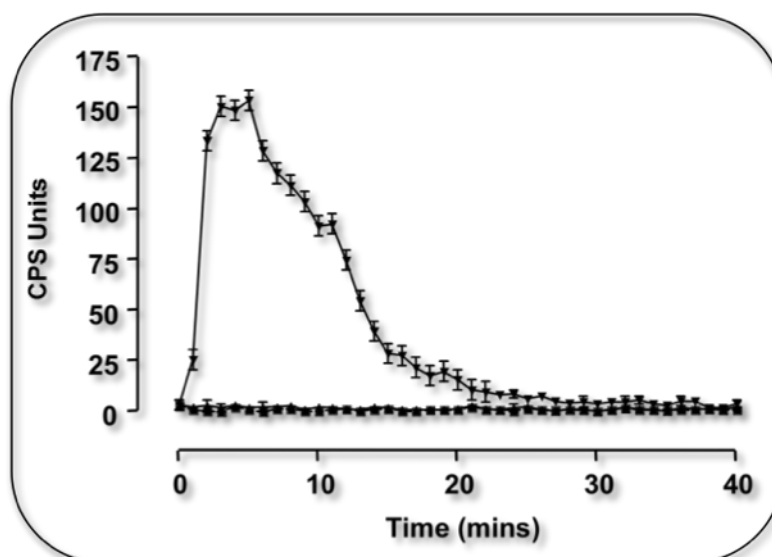


Figure 3-47: Reactive Oxygen Species Production by PMN derived microparticles
 The potential for ROS production was analysed by co-incubation of the two sets of microparticles i.e. microparticles produced by direct stimulation (▼) or following co-cubation over a HUVEC monolayer (■). This showed that only the latter set of microparticles were able to produce ROS. Data are mean ± SEM of 5 distinct preparations.

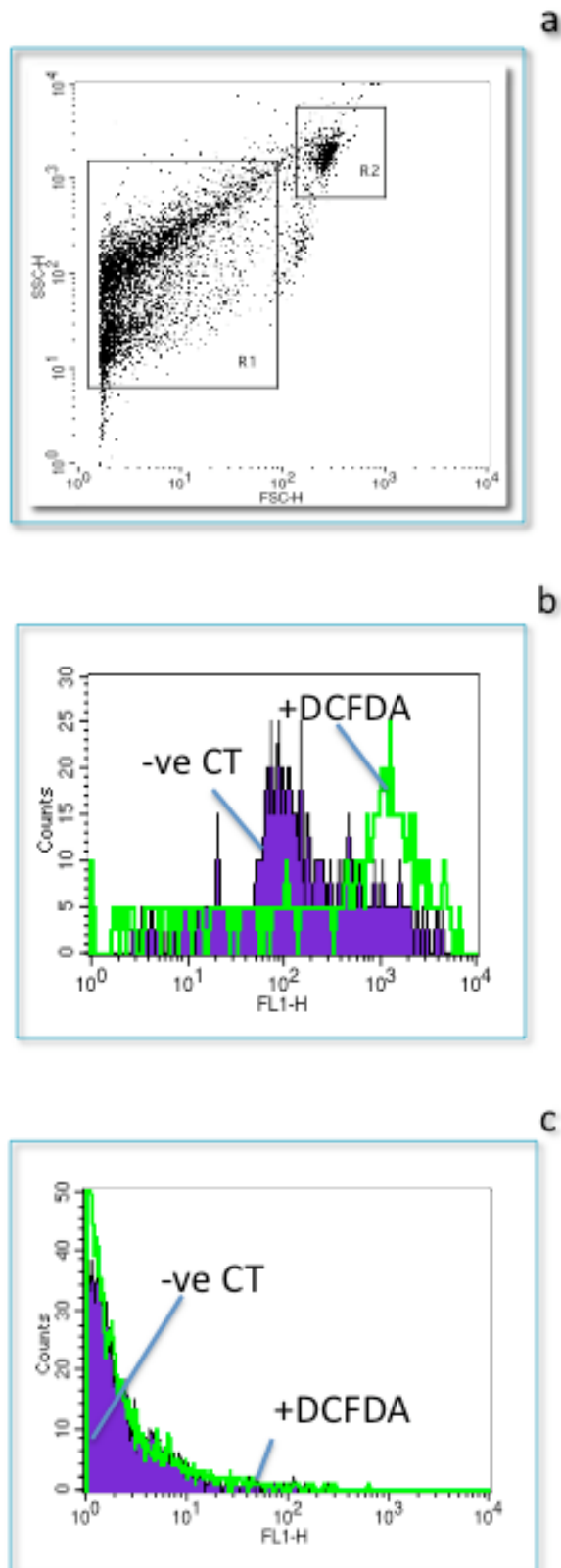


Figure 3-48: Reactive Oxygen Species analysis using the DCFDA assay. Following microparticle isolation, these microstructures were incubated in DCFDA for 20 min at room temperature following which they were stimulated with PMA and the ROS production was determined in the FL1 channel. Figures (b) and (c) show that only the larger microparticle gated in R2 was able to produce ROS. Histograms are representative of 3 distinct preparations.

	R1 M.P. POPULATION	R2 M.P. POPULATION
Non Stimulated	2.1 ± 0.24	112 ± 10
Stimulated	2.4 ± 0.16	982 ± 48

Table 3-5 Quantification results for Reactive Oxygen Species determination in PMN derived microparticles. The MFI values confirm that only the R2 population has the ability to produce reactive oxygen species in this assay. The results are a summary of 3 distinct preparations. Data is expressed as mean and SEM.

	CT M.P.	PMN+HUVEC M.P.	PMN M.P. (R1)	PMN M.P. (R2)
PS	114 ± 33	123 ± 23	178 ± 31	123 ± 51
CD14	3 ± 0.2	3 ± 1.1	7 ± 2.1	14 ± 2.3
CD62L	242 ± 23	362 ± 36	331 ± 41	423 ± 61
CD62P	3 ± 0.6	3 ± 1.4	7 ± 2.2	12 ± 2.9
Annexin 1	4 ± 1.1	132 ± 46	77 ± 12	15 ± 3.2
FPRL1	35 ± 4.1	272 ± 31	221 ± 41	189 ± 23

Table 3-6 Table summarising the MFI values for the 3 distinct M.P. preparations. The data shown above highlights the fact that in each of these conditions PMN derived M.P. were not contaminated by other M.P. present from platelets (CD62P) or monocytes (CD14). Furthermore the M.P. obtained from resting PMN did not have any Annexin A1 as did the larger M.P. (R2) obtained from stimulated PMN in suspension. However all the M.P. populations expressed the FPRL receptor. Data is expressed as mean and SEM

3.2.5. Stimulus specific expression of the Annexin A1 system in M.P.

Previously conducted studies have shown that microparticles from one cell type can be heterogeneous expressing different antigens on their surface. Furthermore opposing roles for microparticles derived from a specific cell type, such as the PMN, have been described. I have previously described that microparticles obtained from PMNs in suspension have the ability to produce ROS, whilst those PMN adhesion to a HUVEC monolayer do not. This prompted us to explore if different stimuli can influence expression of Annexin A1 in PMN derived microparticles.

The flow-cytometric analysis confirmed previously outlined results that fMLP stimulated microparticles express Annexin A1 on their outer surface, furthermore it also showed that LxA₄ and AF2 stimulation produce microparticles which contain similar levels of Annexin A1 (Figure 3-50). On the other hand, there is a stark difference in FPRL1 expression between the various treatments, where in all three cases the expression was above that observed in the control unstimulated levels. This data also shows that the microparticles obtained following LxA₄ stimulation are richer in the receptor than the other three sources whilst AF2 stimulation produced a higher percentage of microparticles containing this receptor (Figure 3-50).

Interestingly western blotting analysis revealed that the majority of the Annexin A1 detected in the incubation medium was in fact contained in the microparticles with very low levels of this protein being detected in the concentrated microparticle depleted supernatant (Figure 3-51).

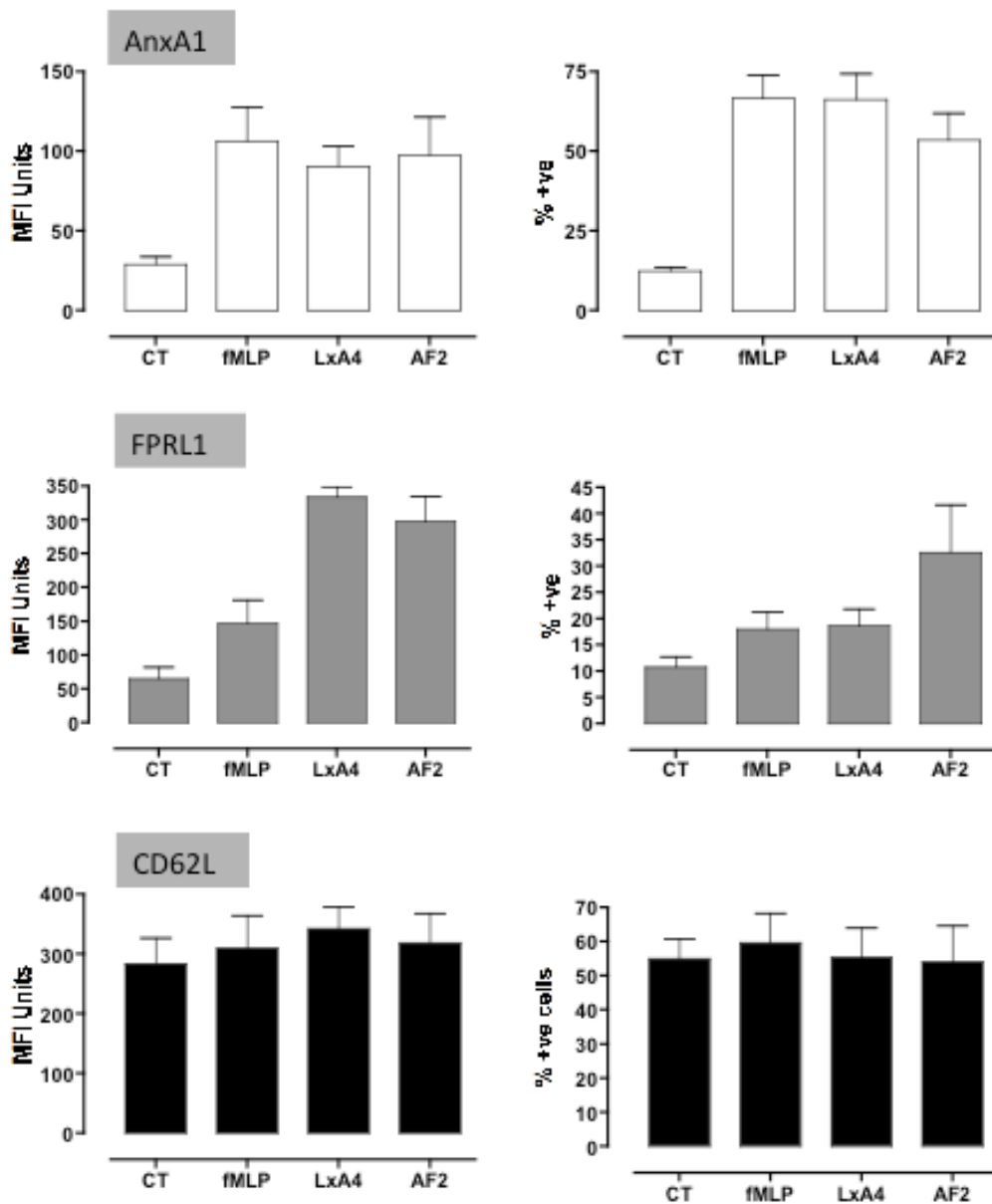


Figure 3-49: Flow cytometric determination of Annexin A1, FPRL1, and CD62L PMN derived M.P. M.P. were produced by coincubation of PMN with fMLP, LxA₄, AF2 or from CT PMN. The M.P. were the stained with anti-Annexin A1, anti-FPRL1 or anti-CD62L ab followed by a 2^o ab. The M.P. were also incubated with an isotype control and a straight secondary control. The microparticle antigen expression was quantified by flow cytometry. Data are mean ± SEM of 3 independent preparations. **P*<0.05 vs. vehicle group, data was analysed using one way ANOVA.

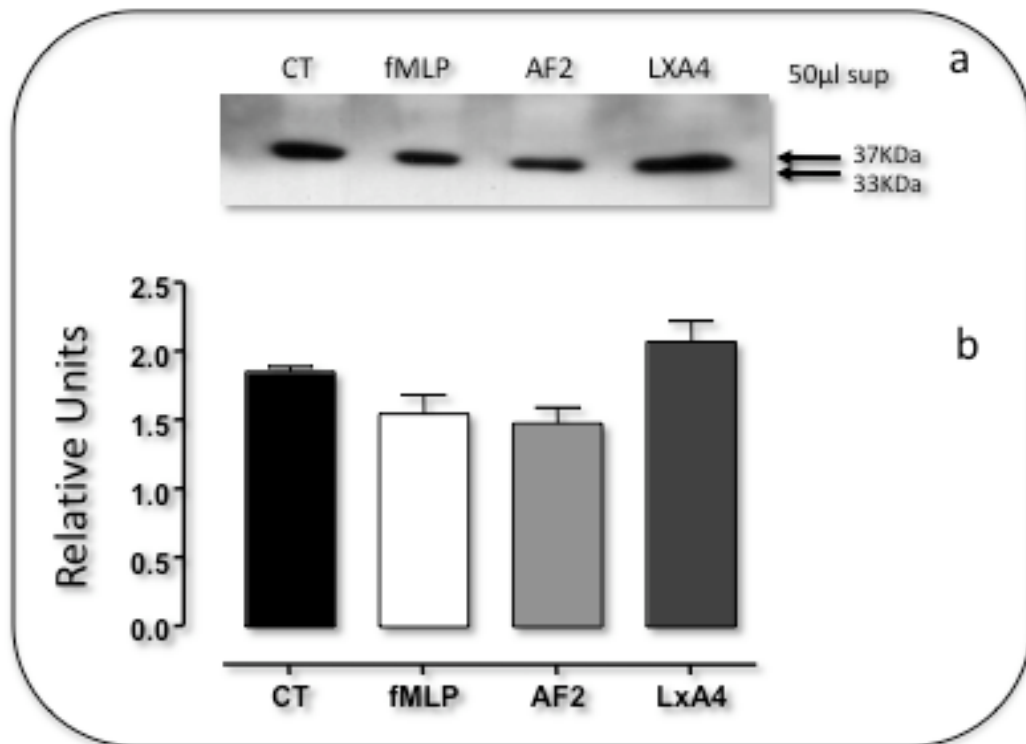


Figure 3-50: Western Blot analysis of M.P. rich supernatant After cell stimulation the cells were centrifuged and the supernatant was loaded on to a 10 % gel. Following gel electrophoresis and transfer the blot was probed with an anti-Annexin A1 antibody, showing the presence of Annexin A1 in the microparticles. (a) representative blot showing the presence of Annexin A1 in the PMN supernatant (b) densitometry results for the microparticles blots (n=3 distinct preparations). Data represented as mean and SEM and analysed using one way ANOVA.

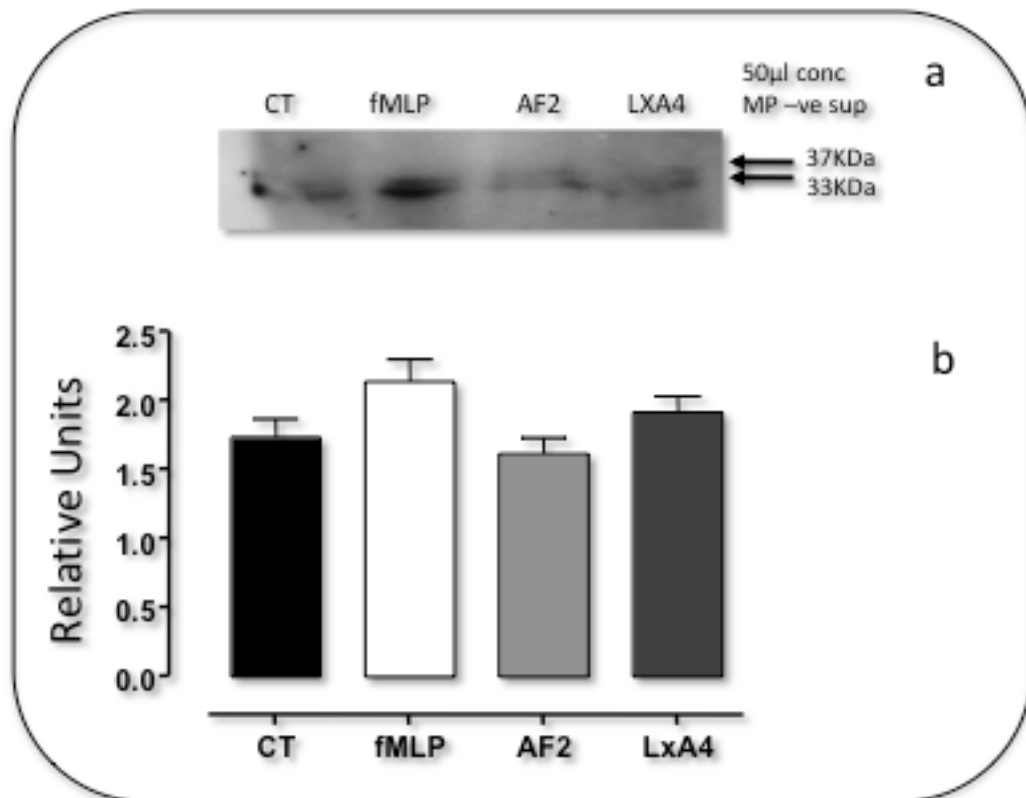


Figure 3-51: Western Blot analysis of microparticles depleted supernatant. Following microparticles extraction, the supernatant from each condition was concentrated down from 2ml to 40 µl using 10kDa cut-off centrifugation columns. The concentrated supernatant was loaded in on to 10% gel. Following gel electrophoresis and transfer the blot was probed with an anti-Annexin A1 antibody, showing the presence of Annexin A1 in the microparticles. (a) a representative blot showing minimal Annexin A1 presence in the microparticles supernatant for all 4 conditions with the fMLP condition showing a slightly elevated Annexin 1 presence; (b) densitometry results for the microparticles blots (n=3 distinct preparations). Data presented as mean and SEM and analysed using one way ANOVA.

3.2.6. Determining the role of the Annexin A1 and FPRL1 positive M.P. in Rheumatic Diseases

Alterations of microparticle populations in the plasma of patients suffering from a number of rheumatic diseases have been reported in the literature. In light of my observations that Annexin A1 positive microparticles play an important role in the resolution of inflammation and that both Annexin A1 and FPRL1 levels can be altered, in a stimulation dependent manner, I decided to explore if there were any differences in their expression in three rheumatic conditions RA, Wegener Vasculitis (MPO and PR3 +ve ANCA) and GCA.

Flow-cytometric analysis highlighted a significant reduction in the Annexin A1 positive microparticles in all 3 conditions, with the largest decrease being in the PR3+ve ANCA patients where we see 15% reduction (Figure 3-53).

On the other hand in all the conditions studied there was an elevated number of FPRL1 positive microparticles with the Wegener Patients displaying the largest increase (Figure 3-53).

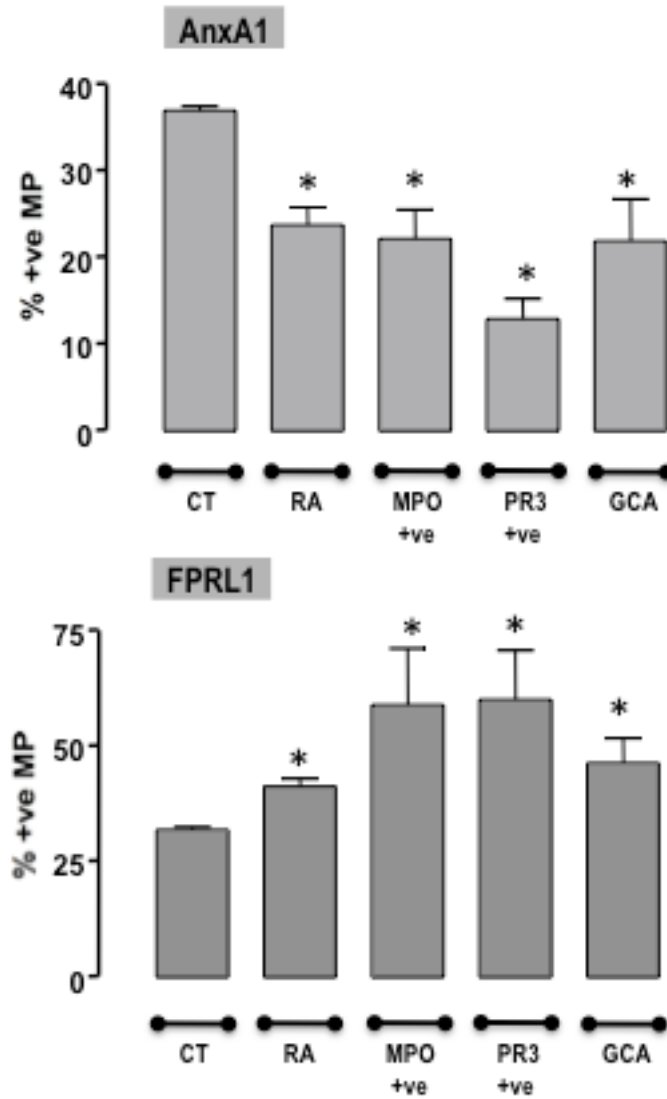


Figure 3-52: Flow cytometric determination of Annexin A1 and FPRL1 +ve M.P. in plasma from patients suffering from Rheumatic diseases. Plasma was obtained from patients suffering from RA, Wegener granulomatosis (MPO +ve and PR3 +ve) and GCA by differential centrifugation. This plasma was then incubated with 1^o antibodies against Annexin A1 and FPRL1 and then a 2^o ab that was FITC conjugated. The microparticle antigen expression was quantified by flow cytometry. Data are mean \pm SEM of 8 patients per group. * $P < 0.05$ vs. CT group. Data analysed using one way ANOVA.

3.2.7. Exploring the potential of monitoring microparticle populations as biomarkers during disease treatment in Rheumatoid Arthritis.

Microparticles have over the last few years gained in importance as biomarkers of disease where elevated levels of specific subsets of microparticles have been linked with a number of systemic conditions, such as atherosclerosis and RA (Erdbruegger, Grossheim et al. 2008; Umekita, Hidaka et al. 2009). However little data is available on the effect of therapeutic treatment on these microparticle populations. Therefore I took advantage of the RA study employing prednisolone treatment to investigate whether I could detect changes in the microparticle profile.

Blood was collected from RA patients in collaboration with Dr. Stephen Kelly between 9 and 11am and the plasma was immediately separated to avoid contamination by further cellular activation. The plasma was centrifuged again to remove any contaminating platelets and stained using immunofluorescent antibodies against a number of antigens described in the literature to correspond to the cell of origin of the microparticles. Furthermore, the level of expression of Annexin A1 and FPRL1 on these microparticles was also determined.

The results I produced indicate that there is a significant reduction in the PMN (CD62L positive) (Figure 3.54), platelet (CD62P positive) (Figure 3.55) and monocyte (CD14 positive) (Figure 3.57) derived microparticle population upon a two week glucocorticoid treatment in these patients. On the other hand, an increase in endothelial (CD54 positive) (Figure 3.56) derived microparticles, both in the MFI and percentage positive events. Even more interestingly, there was a decrease in the number of FPRL1 (Figure 3.58) positive microparticles,

mirrored by an increase in Annexin A1 (Figure 3.59) positive microparticles, suggesting that distinct effects of the prednisolone treatment.

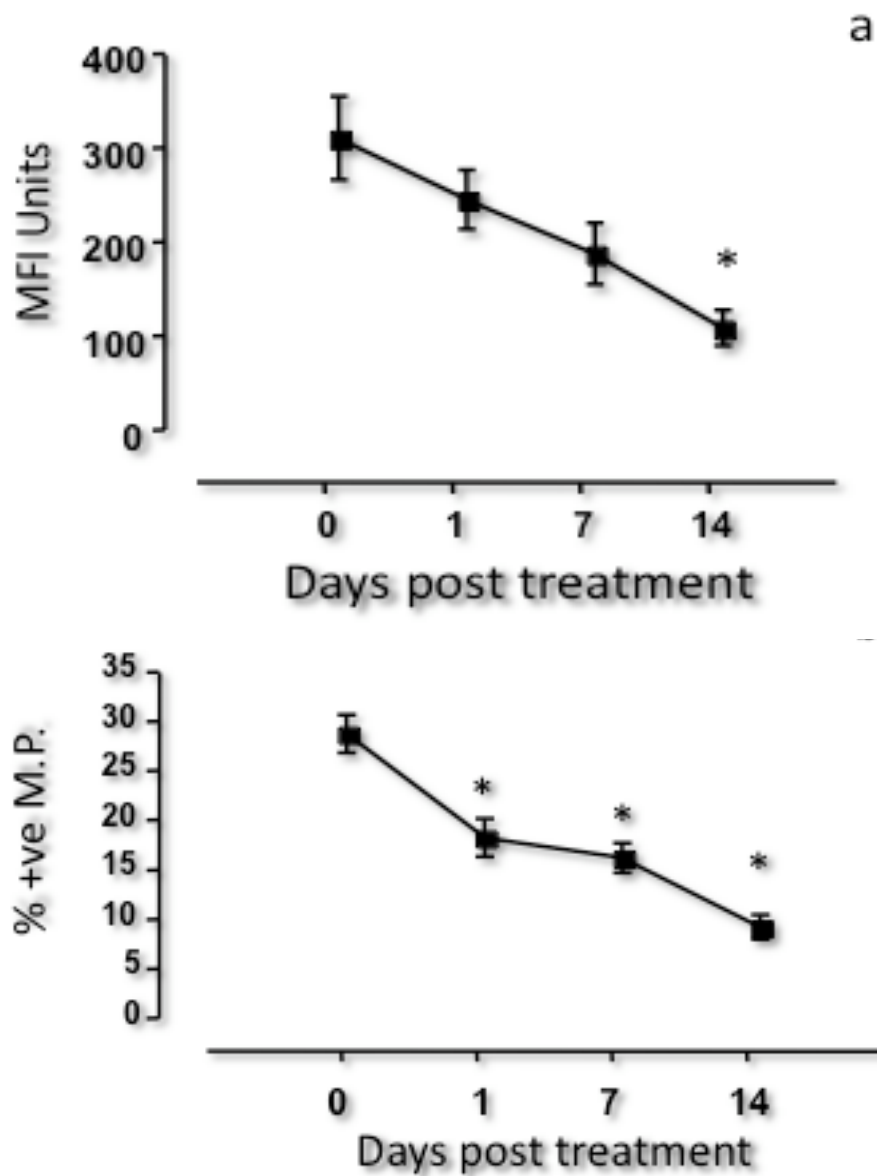


Figure 3-53: CD62L expression on plasma microparticles derived from Rheumatoid Arthritis (RA) patients during a 14-day steroid treatment. Microparticles were isolated and stained by incubation with immunofluorescent anti-CD62L antibody, by incubation for 60 min at 4°C. These results show that there is a marked decrease in CD62L positive microparticles over the 14-day treatment as highlighted by both a reduction in MFI units (a) and number of CD62L positive microparticles (b). * P<0.05 vs. Day 0 group (n=7 patients). Data presented as mean and SEM and analysed by one way ANOVA.

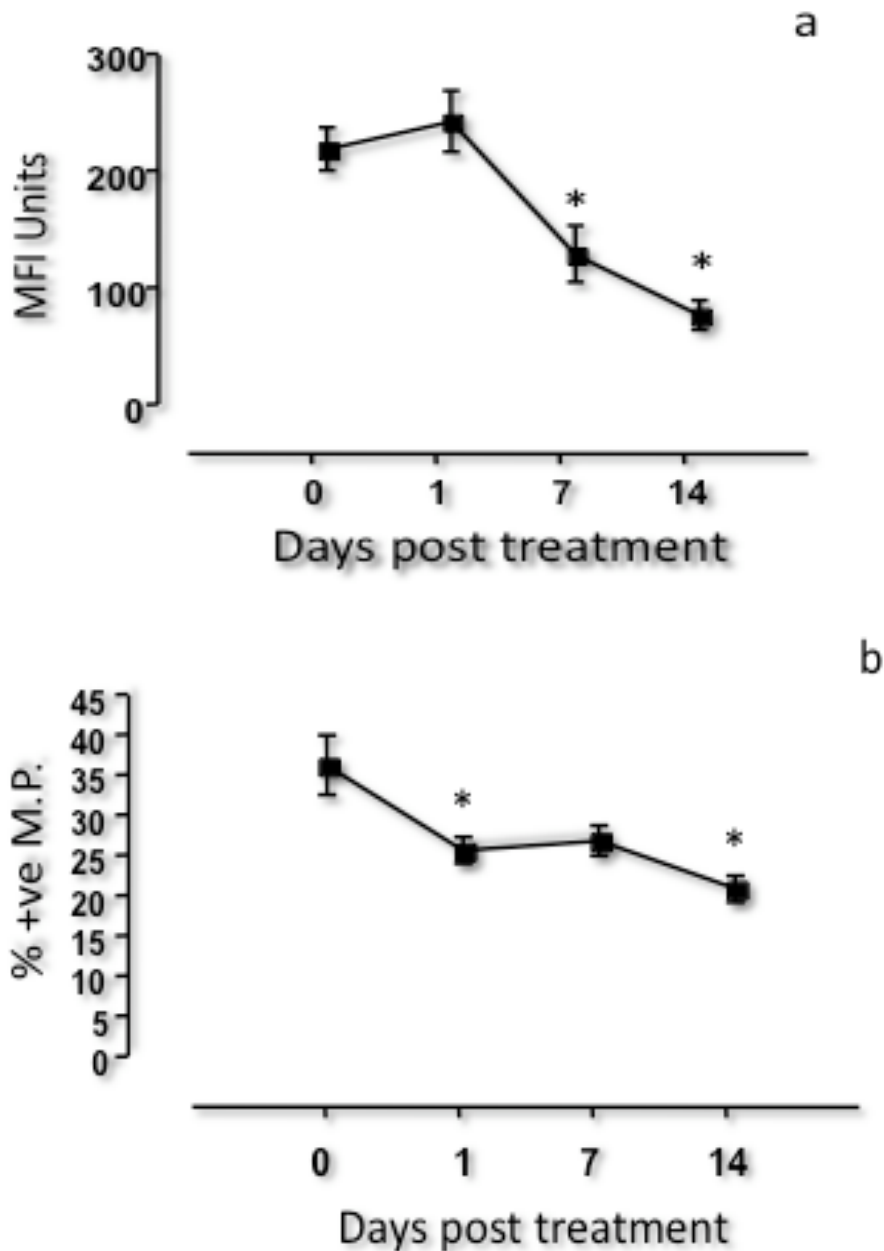


Figure 3-54: CD62P expression on plasma microparticles derived from Rheumatoid Arthritis (RA) patients during a 14-day steroid treatment. Microparticles were isolated and stained by incubation with immunofluorescent anti-CD62P antibody, by incubation for 60 min at 4°C. These results show that there is a marked decrease in CD62P positive microparticles over the 14-day treatment as highlighted by both a reduction in MFI units (a) and number of CD62L positive microparticles (b). * P<0.05 vs. Day 0 group (n=7 patients). Data presented as mean and SEM and analysed by one way ANOVA.

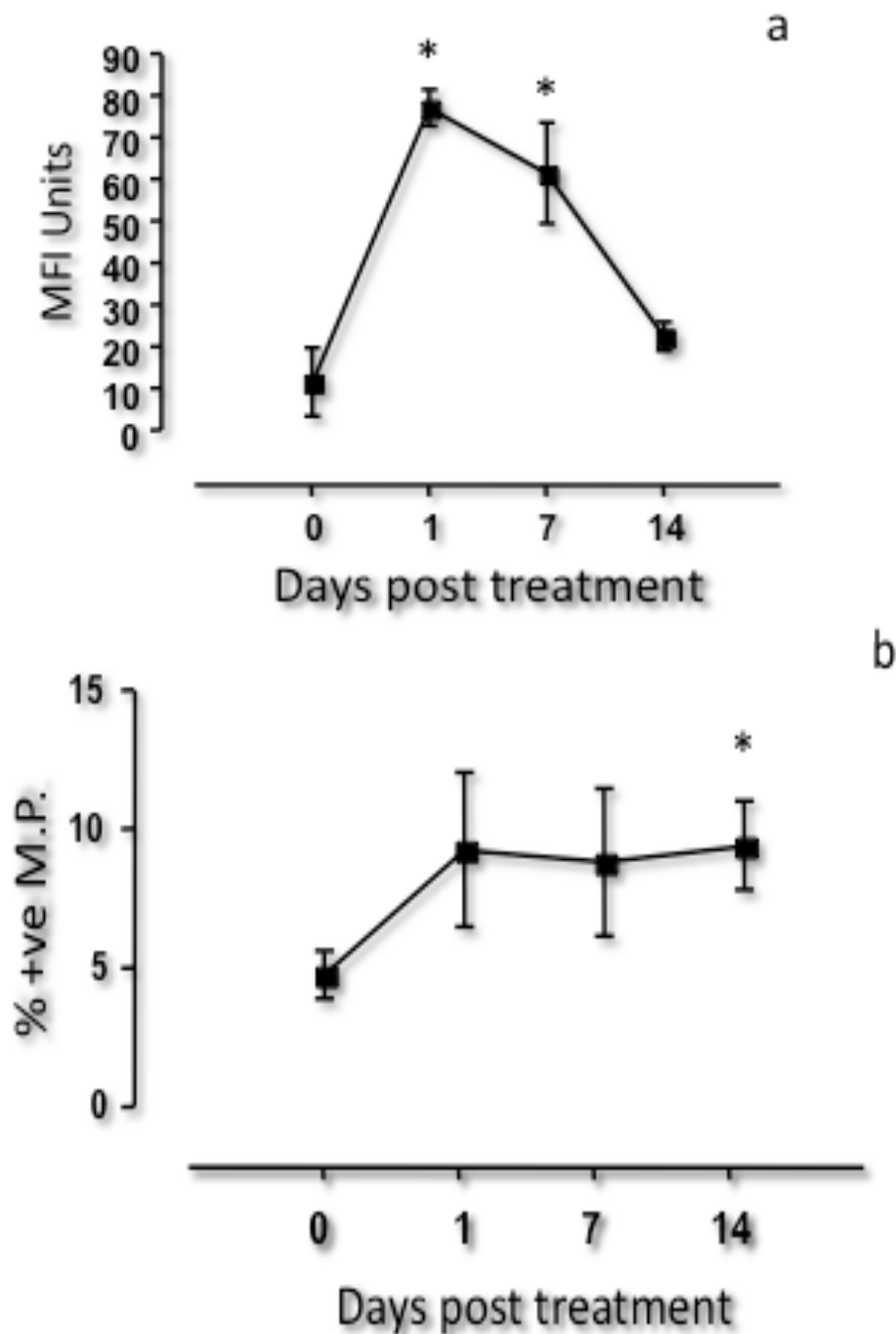


Figure 3-55: CD54 expression on plasma microparticles derived from Rheumatoid Arthritis (RA) patients during a 14-day steroid treatment. Microparticles were isolated and stained by incubation with immunofluorescent anti-CD54 antibody, by incubation for 60 min at 4°C. These results show that there is a marked increase in CD54 positive microparticles over the 14-day treatment as highlighted by both a reduction in MFI units (a) and number of CD54 positive microparticles (b). * P<0.05 vs. Day 0 group (n=7 patients). Data presented as mean and SEM and analysed by one way ANOVA.

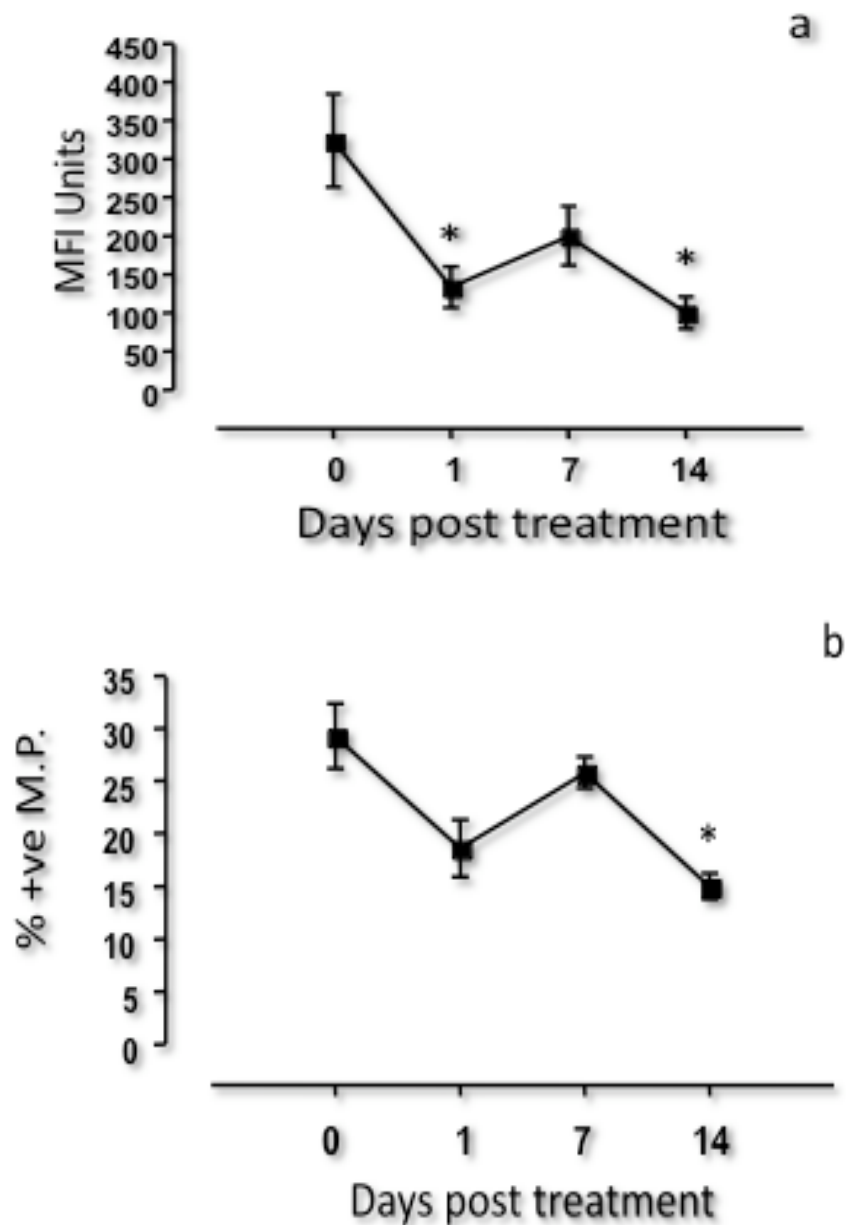


Figure 3-56: CD14 expression in on plasma microparticles derived from Rheumatoid Arthritis (RA) patients during a 14-day steroid treatment. Microparticles were isolated and stained by incubation with immunofluorescent anti-CD14 antibody, by incubation for 60 min at 4°C. These results show that there is a marked decrease in CD14 positive microparticles over the 14-day treatment as highlighted by both a reduction in MFI units (a) and number of CD14 positive microparticles (b). * P<0.05 vs. Day 0 group (n=7 patients). Data presented as mean and SEM and analysed by one way ANOVA.

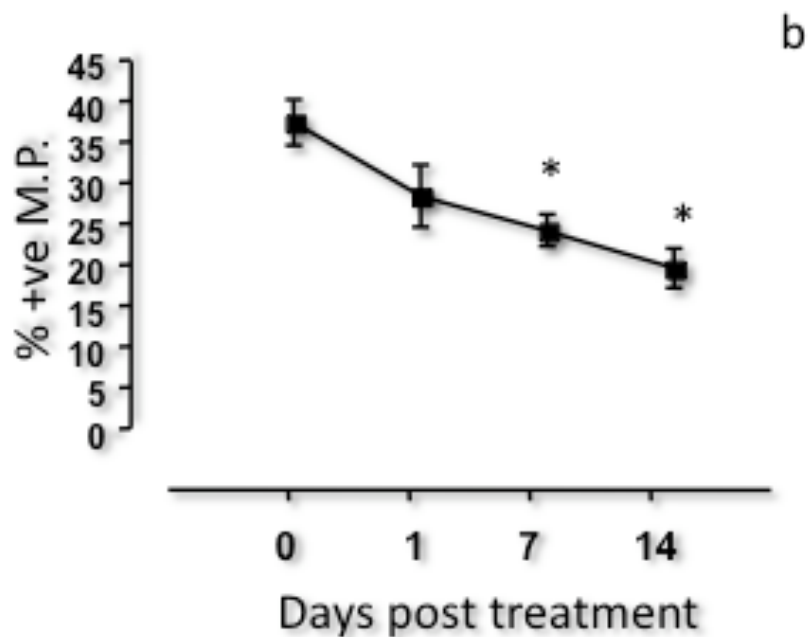
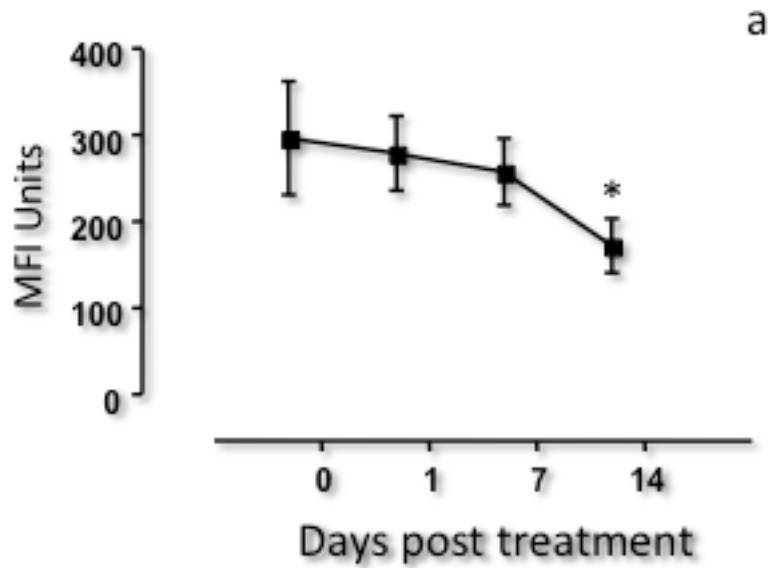


Figure 3-57: FPRL1 expression on plasma microparticles derived from Rheumatoid Arthritis (RA) patients during a 14-day steroid treatment. Microparticles were isolated and stained by incubation with immunofluorescent anti-FPRL1 antibody, by incubation for 60 min at 4°C. These results show that there is a marked decrease in FPRL1 positive microparticles over the 14-day treatment as highlighted by both a reduction in MFI units (a) and number of FPRL1 positive microparticles (b). * P<0.05 vs. Day 0 group (n=7 patients). Data presented as mean and SEM and analysed by one way ANOVA.

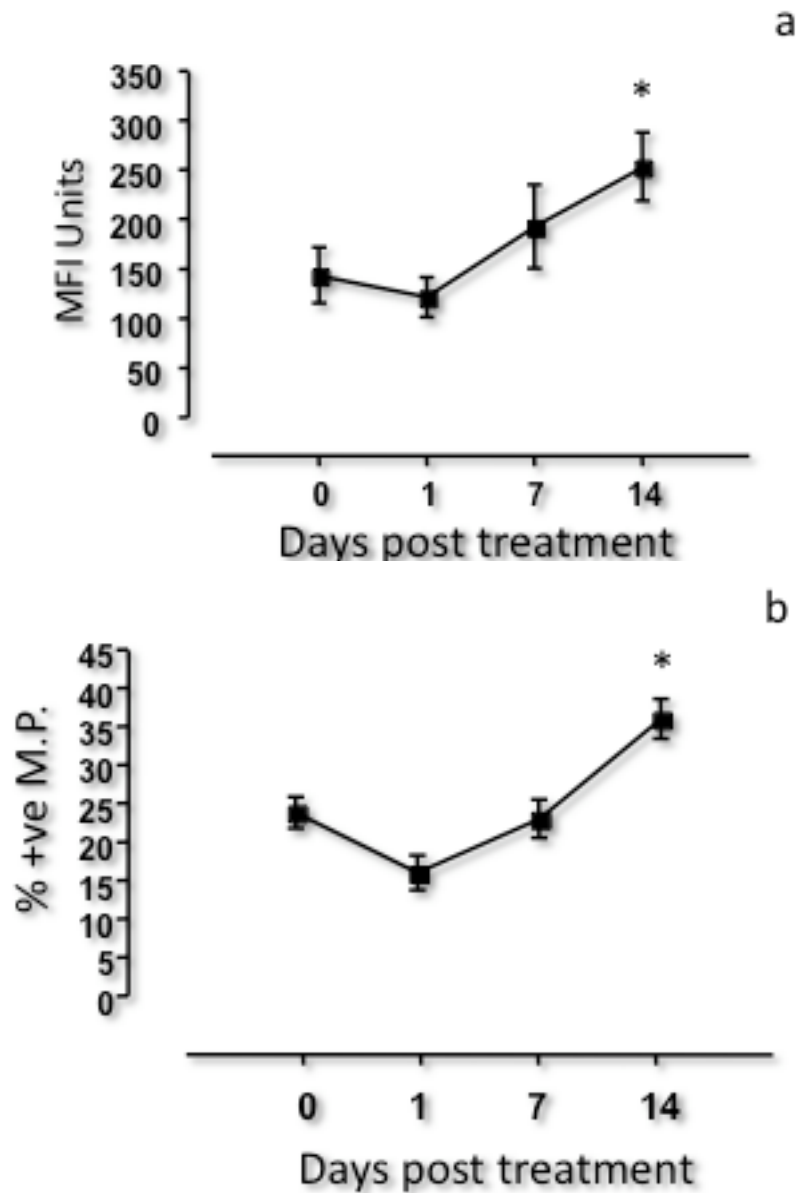


Figure 3-58: Annexin A1 expression in on plasma microparticles derived from Rheumatoid Arthritis (RA) patients during a 14-day steroid treatment. Microparticles were isolated and stained by incubation with immunofluorescent anti-Annexin A1 antibody, by incubation for 60 min at 4°C. These results show that there is a marked increase in Annexin A1 positive microparticles over the 14-day treatment as highlighted by both a reduction in MFI units (a) and number of Annexin A1 positive microparticles (b). * P<0.05 vs. Day 0 group (n=7 patients). Data presented as mean and SEM and analysed by one way ANOVA.

3.3. Development of novel Ac2-26 derived peptides

In the quest to assess the potency of the novel Ac2-26 derived peptides a number of properties were assessed in order to determine their potential as anti-inflammatory drugs. Previous studies conducted in our group and by others has show the Ac2-26 peptide has the ability to bind three of the FPR family members, namely FPR, FPRL1 and FPRL2 leading to the down stream activation of p-ERK, however only the former two receptors have been shown to be important in conveying its anti-inflammatory properties. Therefore, in order to assess the activity of the novel peptides it was deemed important to evaluate their potential for activating these two receptors. For this purpose three transfected HEK cell lines were employed. These cell lines were transfected with either an empty vector and termed HEK-CMV, a vector over expressing FPR, and thus termed HEK-FPR, or a vector over expressing the FPRL1 gene and consequently termed HEK-FPRL1. Before embarking on experiments with the novel Annexin A1 peptides I checked whether the cellines in culture were expressing the expected receptors. As outlined in Figure 3.60 all the HEK-FPR and the HEK-FPRL1 cell expressed the FPR and FPRL1 receptors respectively, with the latter cell line showing a strong receptor expression whilst there seems to be a weaker staining for the FPR receptor. The latter result can be explained in the light of the fact that the FPR antibody possesses lower affinity to the receptor. The second important conclusion that could be deduced from this data was the lack of cross contamination between the cell lines containing the receptors; furthermore, the HEK-CMV cell line was devoid of the two receptors.

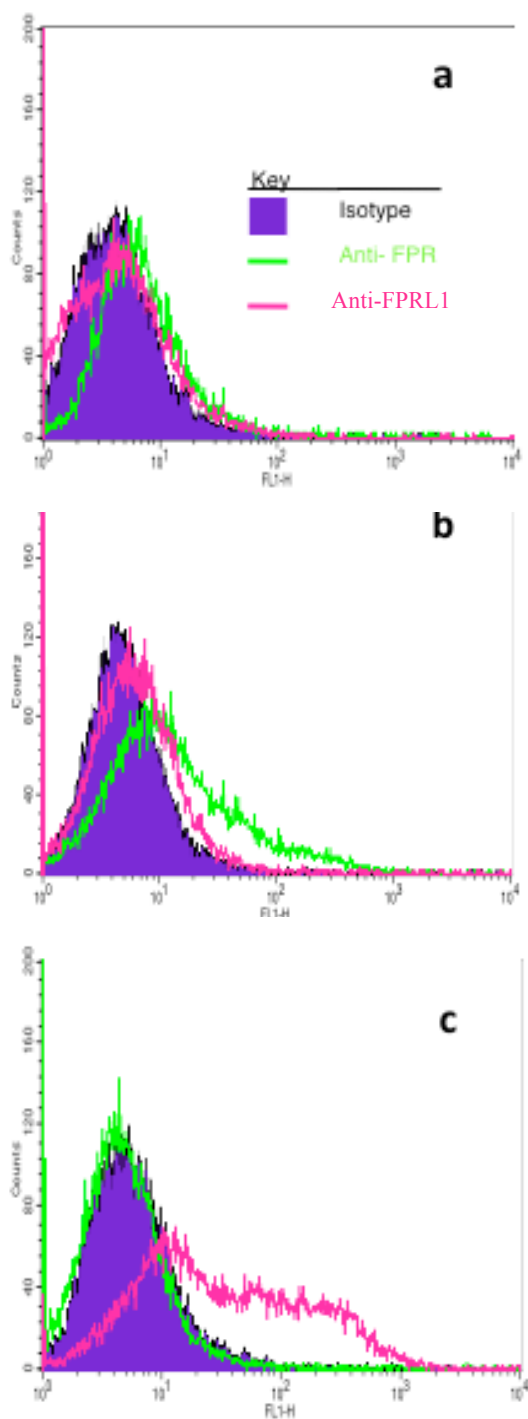


Figure 3-59: Flow cytometric analysis of the three transfected HEK cell lines. The three transfected HEK cell lines, (a) HEK-CMV, (b) HEK FPR and (c) HEK-FPRL1 immunofluorescently stained with 1^o abs against FPR, FPRL1 or an isotype control, followed by a 2^o FITC conjugated ab. The results show that in the CMV cell line, neither of the two receptors is expressed, whilst there is an expression of the FPR receptor in the HEK-FPR cells and FPRL1 in the HEK-FPRL1 cell line.

	HEK-CMV	HEK-FPR	HEK-FPRL1
Negative Staining	1	1	1
FPR Staining	4 ± 0.2	14 ± 0.9	4 ± 0.1
FPRL1 Staining	4 ± 0.2	4 ± 0.1	24 ± 1.1

Table 3-7 Summary of the flow cytometric analysis conducted on the HEK cell lines. The MFI units outlined above confirm that the CMV cell line does not contain any of the two receptors whilst there is no cross contamination between the other two cell-lines (n=3 distinct experiments). Data presented as mean and SEM (PMT value=548).

After the generation of this basic yet fundamental data I was ready to use these cell lines for testing the novel peptide sequences obtained from Unigene. The starting point was to use the p-ERK assay for screening the agonistic activity to the FPRL1 receptors of these novel peptides. Firstly I compared two sources of the Ac2-26 peptide in order to determine if there was a difference in their ability activate the FPLR1 receptor and thus determine which would be more appropriate to use as positive control. As depicted in Figure 3.61, the Ac2-26 obtained from Cambridge Research Biochemicals (CRB) was more effective at activating p-ERK than the peptide supplied by Unigene. Therefore it was decided that the CRB peptide was to be employed in subsequent experimentation.

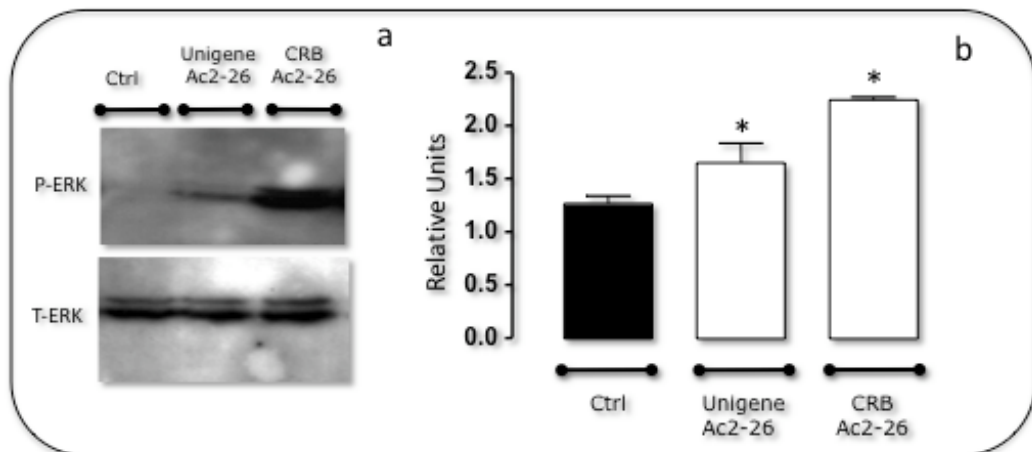


Figure 3.60: Western blotting analysis comparing the activation potency of p-ERK by the two Ac2-26 peptides. The HEK-FPRL1 cells were co-incubated for 8mins with the respective peptides, or just DMSO and then transferred to the -80°C . The cells were then lysed using a lysis solution and 100ng of total protein were loaded on to a 10% polyrylamide gel. Following electrophoresis, transfer and blocking the membrane was first probed with an anti p-ERK anti-body and then stripped and reprobed with and anti t ERK anti-body. Whilst the t-ERK blot shows equal amounts of ERK in all the samples, the CRB peptide was the one that activated p-ERK. (a) a representative blot (b) densitometry results highlighting the ratio between the p-ERK and t-ERK bands. Data presented as mean and SEM of 3 distinct experiments with one way ANOVA employed for statistical analysis. (*= $P < 0.05$ vs. CT)

The next step was to identify which of the novel peptides activated the p-ERK through the FPRL1 receptor, similarly to the parent peptide. The western blot analysis pointed out that Pep57, Pep59 and Pep84 were the more potent ERK activators (Figure 3-62).

However, in order to confirm which of the five Ac2-26 derived peptides showed the highest potential for further analysis another set of experiments was conducted. In this assay the capability of these amino acid sequences to reduce the PMN interaction to an activated HUVEC monolayer was assessed and compared to the inhibitory properties of the parent Ac2-26 peptide. Pep57 and Pep84 were observed to display inhibitory properties similar to those observed in the parent Ac2-26 peptide confirming the p-ERK data (Figure 3-63). Interestingly Pep59, which also showed a very high p-ERK activation potential, did not display any inhibitory properties whilst, on the other hand, Pep60 which was unable to phosphorylate ERK, displayed potent inhibitory properties similar to those displayed by the parent Ac2-26 peptide.

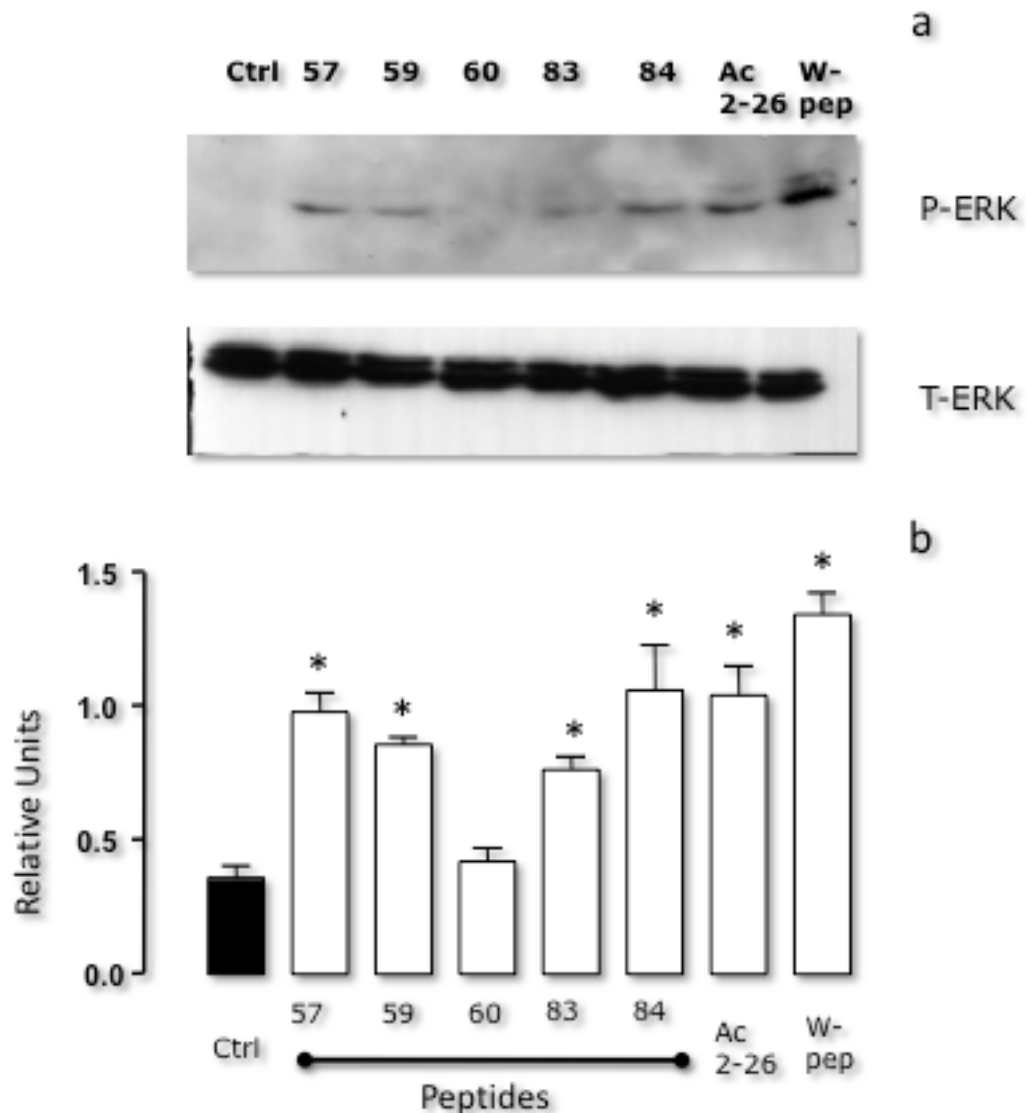


Figure 3-61: Western blotting analysis comparing the activation potency of novel Annexin A1 n-terminally derived peptides. The HEK-FPRL1 cells were co-incubated with 10 μ M of the novel Ac2-26 peptides for 8mins following which the cell were lysed and resuspended in cell lysis solution. Then 100ng of total protein were loaded on to 10% polyacrylamide gel. Following electrophoresis, transfer and blocking the membrane was first probed with an anti p-ERK antibody and then stripped and reprobred with and anti total ERK antibody. Whilst the t-ERK blot shows equal amounts of ERK in all the samples the p-ERK activated was observed to be highest with Pep57, 59 and 84, similar to the activation caused by the parent Ac2-26 and less then the second control, the W-peptide. (a) representative blots for p-ERK and t-ERK (b) densitometry results relating the p-ERK to the t-ERK levels. Data presented as mean and SEM of 3 distinct experiments with one way ANOVA employed for statistical analysis. (*= $P < 0.05$ vs. CT)

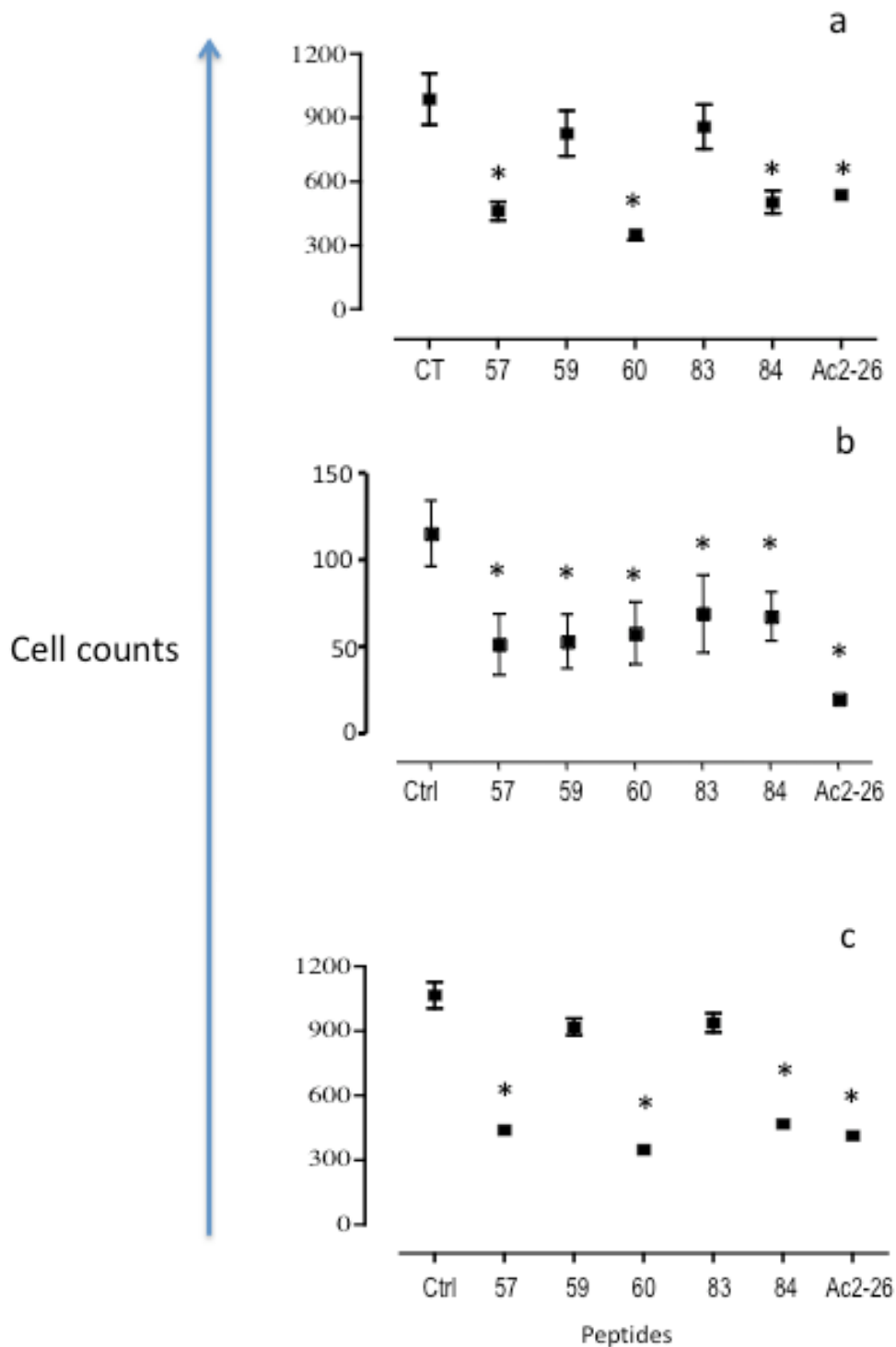


Figure 3-62: Flow chamber analysis determining the inhibitory potency of the novel Ac2-26 peptides. PMNs (5×10^6) were incubated with $10 \mu\text{M}$ of the various peptides for 10 min at 37°C . The PMNs were then flowed for 8 min at $1 \text{ dyne}/\text{cm}^2$, prior to quantifying the degree of PMN interaction with the HUVECs, both as PMN capture (a), adhesion (b) and rolling (c). The results highlights the fact that only Pep57, 60 and 84 display inhibitory properties in this assay. Data are mean \pm SEM of 3 independent experiments (with distinct PMN and HUVEC preparations); * = $P < 0.05$ vs. CT group, data analysed using one way ANOVA.

Following the results obtained in the initial experiments I concluded that out of a panel of 5 peptides only Pep57 (Figure 3-64) and Pep84 (Figure 3-65) displayed properties similar to those observed for Ac2-26 under the same conditions. Thus I extended the investigation on these two peptides whereby both Pep57 and Pep84 were observed to activate ERK even at concentrations as low as 0.1nM. This activity was also observed in the flow chamber model where both peptides significantly reduced the number of cells interacting with the endothelium down to a concentration of 0.01nM (Figure 3-70).

The flow chamber analysis also showed there are a number of distinct differences between the two peptides, the first one is that Pep84 (Figure 3-71) produced a dose response inhibition in the number of PMNs interacting with the endothelium. On the other hand Pep57 showed similar potency throughout the entire concentration range (Figure 3-70). The second difference is that Pep84 was observed to inhibit rolling more significantly than adhesion as was observed for the parent peptide. On the other hand Pep57 was observed to have a higher effect on adhesion over rolling.

The ability of these two peptides to activate ERK through the FPR receptor was also assessed. The results highlight that even in this case the two peptides have the ability to activate ERK at concentrations as low as 0.1nM (Figure 3-66; 3-67) even though this seems to be to a somewhat lower extent as that observed through FPRL1. Importantly no ERK activation was observed in the HEK-CMV (Figure 3-68; 3-69) highlighting that ERK phosphorylation observed in the other two cell lines were consequent to sensitization of either receptor.

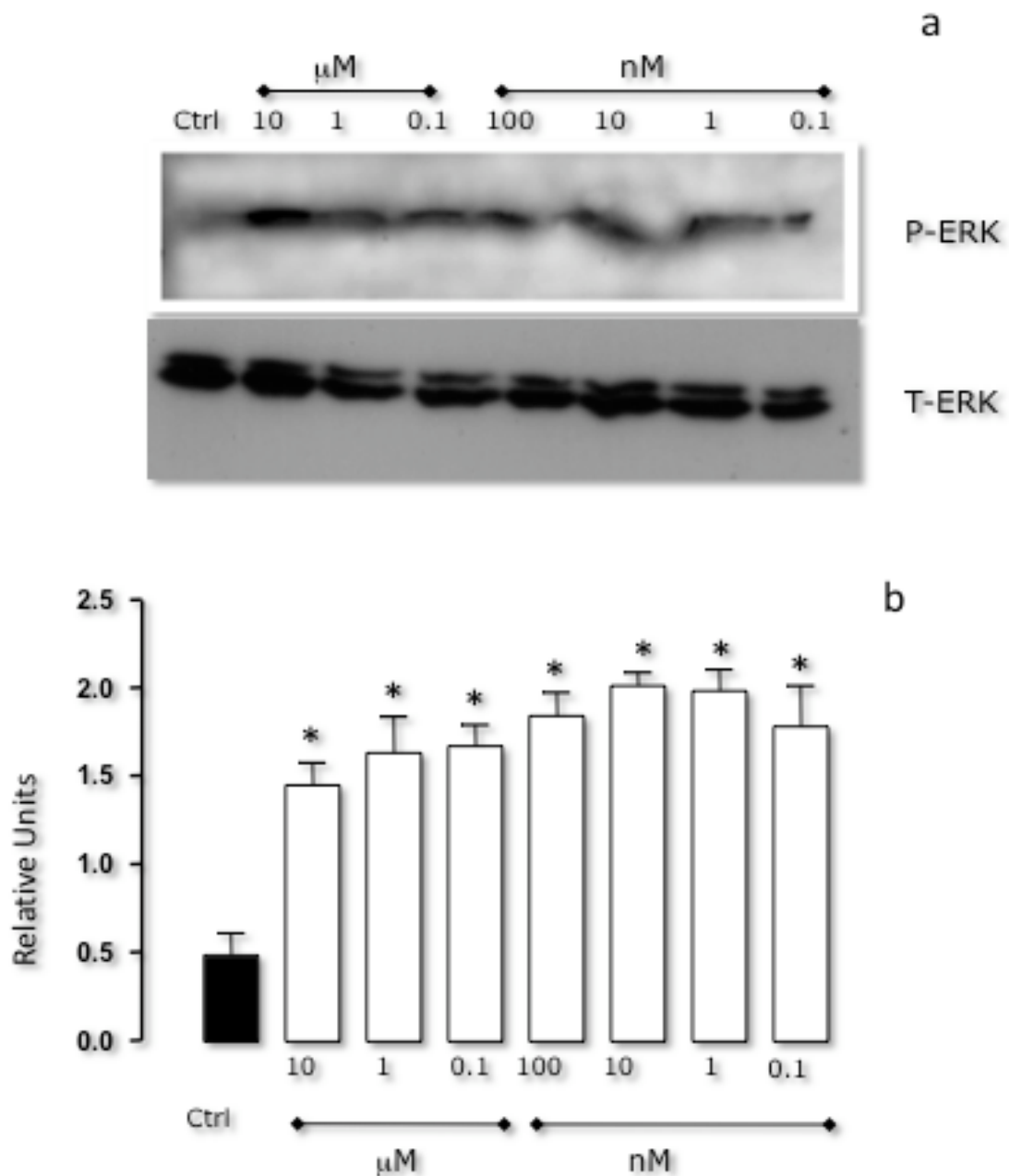


Figure 3-63: Western blotting analysis of the Pep57 dose response highlighting its p-ERK activation potency through the FPRL1 receptor. The HEK-FPRL1 cells were co-incubated with the varying concentrations of Pep57 for 8mins following which the cell were lysed and resuspended in cell lysis solution. Then 100ng of total protein were loaded on to 10% polyacrylamide gel. Following electrophoresis, transfer and blocking the membrane was first probed with an anti p-ERK antibody and then stripped and reprobred with and anti total ERK antibody. The t-ERK blot shows equal amounts of ERK in all the samples. The p-ERK blot also shows a significant activation above basal level for all the Pep57 concentrations employed showing a high affinity of this peptide to the FPRL1 receptor (a) representative blots for -ERK and t-ERK (b) densitometry results relating the p-ERK to the t-ERK levels Data presented as mean and SEM of 3 distinct experiments with one way ANOVA employed for statistical analysis. (*= P<0.05 vs. CT). Data analysis was conducted using one way ANOVA.

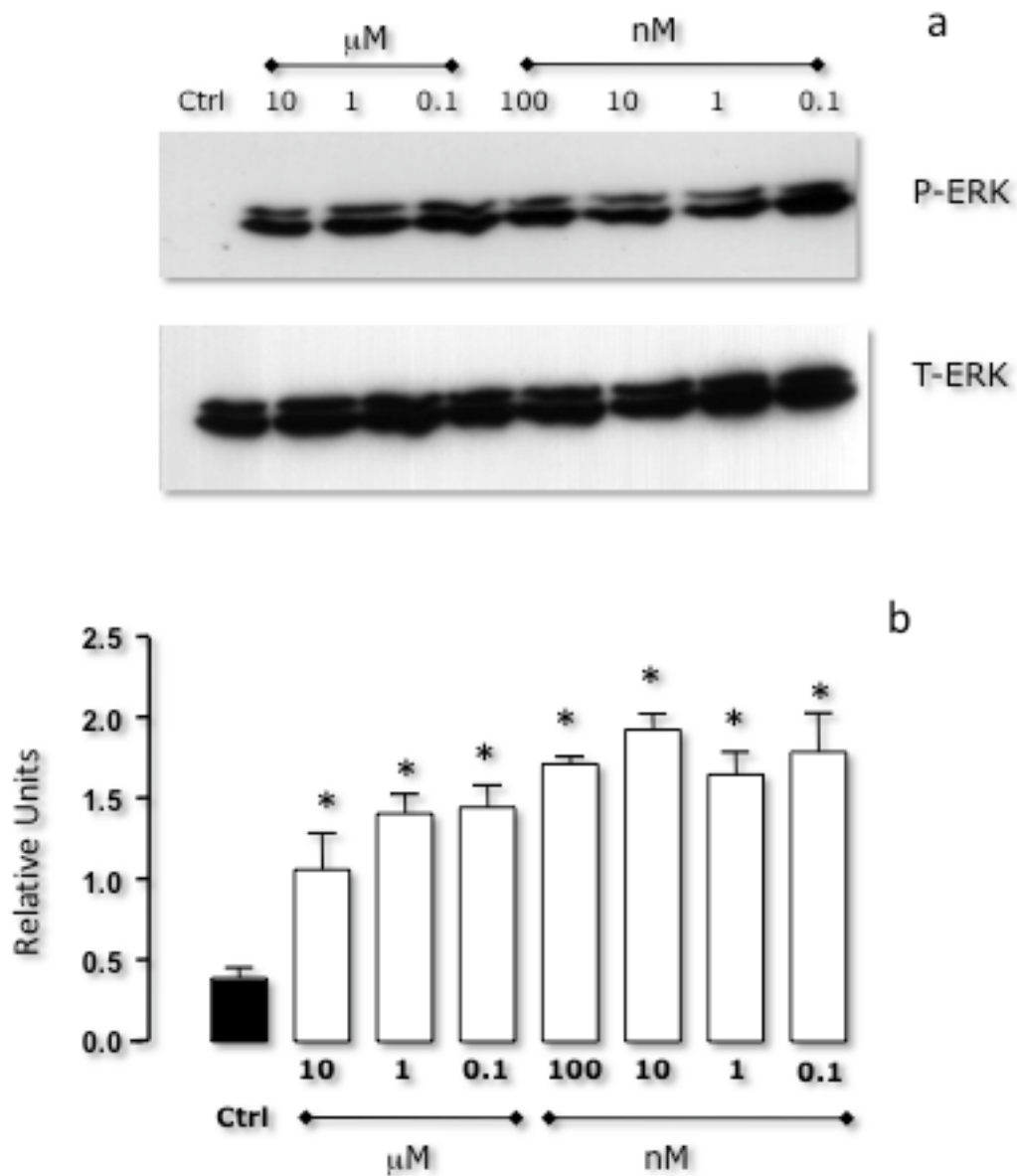


Figure 3-64: Western blotting analysis of the Pep84 dose response highlighting its p-ERK activation potency through the FPRL1 receptor. The HEK-FPRL1 cells were co-incubated with the varying concentrations of Pep84 for 8mins following which the cell were lysed and resuspended in cell lysis solution. Then 100ng of total protein were loaded on to 10% polyacrylamide gel. Following electrophoresis, transfer and blocking the membrane was first probed with an anti p-ERK antibody and then stripped and reprobred with and anti total ERK antibody. The t-ERK blot shows equal amounts of ERK in all the samples. The p-ERK blot also shows a significant activation above basal level for all the Pep84 concentrations employed showing a high affinity of this peptide to the FPRL1 receptor. (a) representative blots for -ERK and t-ERK (b) densitometry results relating the p-ERK to the t-ERK levels. Data presented as mean and SEM of 3 distinct experiments with one way ANOVA employed for statistical analysis. (*= P<0.05 vs. CT). Data analysis was conducted using one way ANOVA.

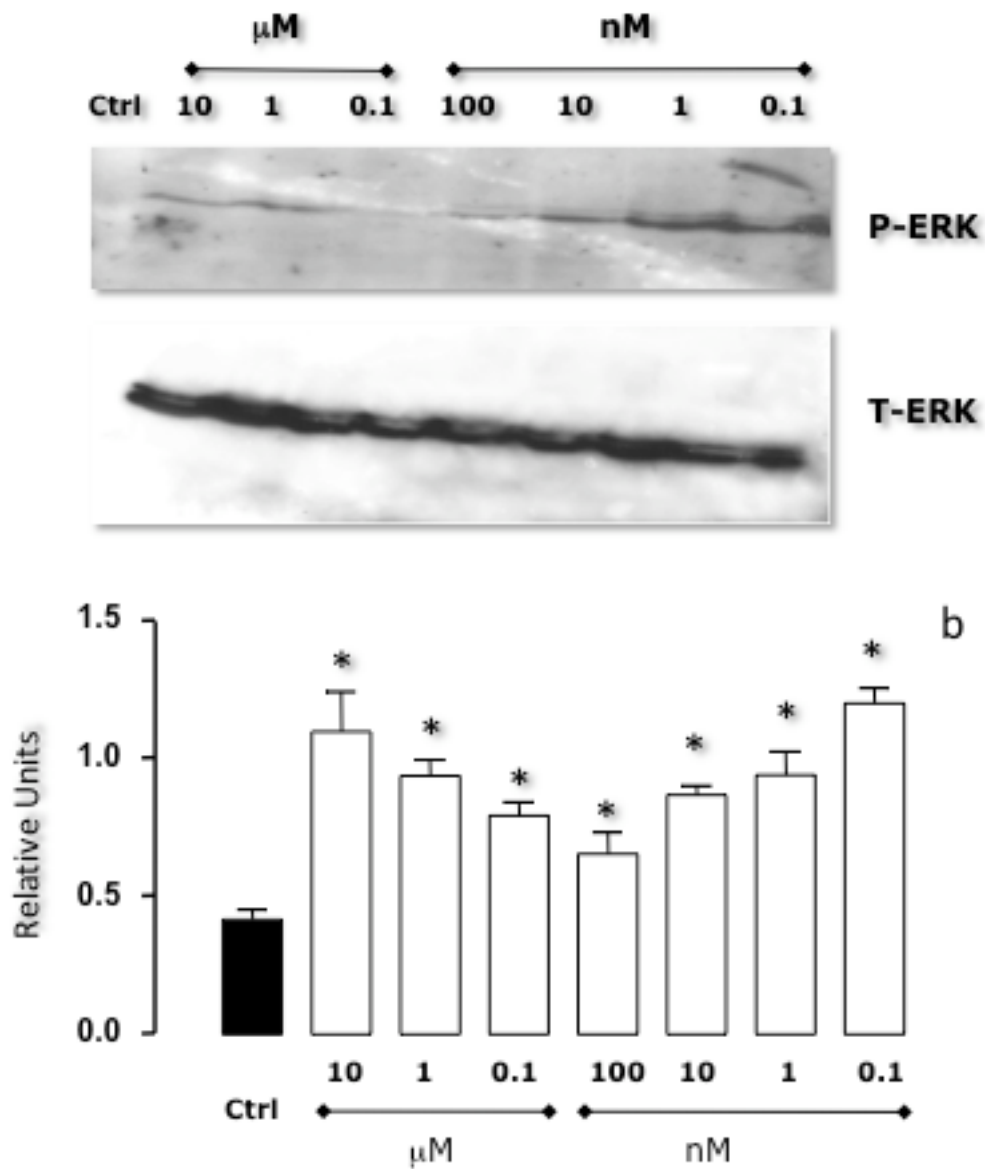


Figure 3-66: Western blotting analysis of the Pep84 dose response highlighting its p-ERK activation potency through the FPR receptor. The HEK-FPR cells were co-incubated with the varying concentrations of Pep84 for 8mins following which the cell were lysed and resuspended in cell lysis solution. Then 100ng of total protein were loaded on to 10% polyacrylamide gel. Following electrophoresis, transfer and blocking the membrane was first probed with an anti p-ERK antibody and then stripped and reprobred with and anti total ERK antibody. The t-ERK blot shows equal amounts of ERK in all the samples. The p-ERK blot also shows a significant activation above basal level for all the Pep84 concentrations employed showing a high affinity of this peptide to the FPR receptor. (a) representative blots for -ERK and t-ERK (b) densitometry results relating the p-ERK to the t-ERK levels. Data presented as mean and SEM of 3 distinct experiments with one way ANOVA employed for statistical analysis. (*= $P < 0.05$ vs. CT). Data analysis was conducted using one way ANOVA.

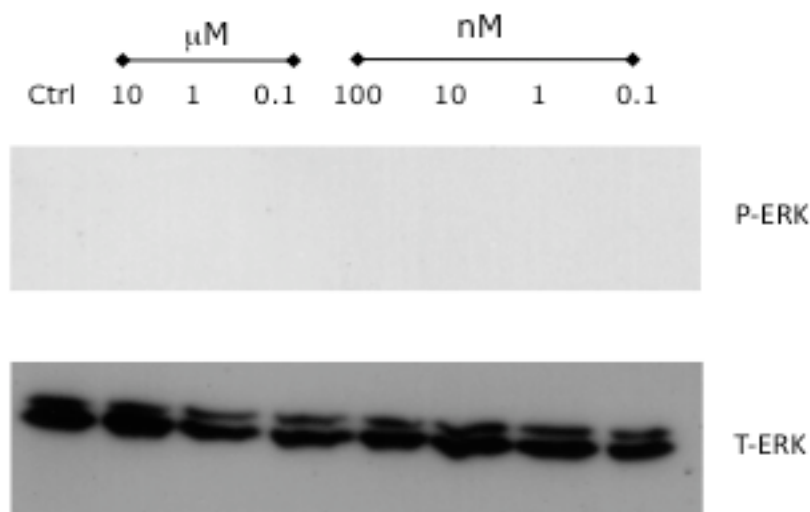


Figure 3-67: Western blotting analysis determine if p-ERK activation by Pep57 is being activated by other receptors apart from the FPR family in the HEK cells. The HEK-CMV cells were co-incubated with the varying concentrations of Pep57 for 8mins following which the cell were lysed and resuspended in cell lysis solution. Then 100ng of total protein were loaded on to 10% polyacrylamide gel. Following electrophoresis, transfer and blocking the membrane was first probed with an anti p-ERK antibody and then stripped and reprobed with and anti total ERK antibody. The t-ERK blot shows equal amounts of ERK in all the samples. However no p-ERK signal was observed confirming that the p-ERK activation observed for Pep57 was solely through the FPR family receptors (representative of 3 indep. exp).

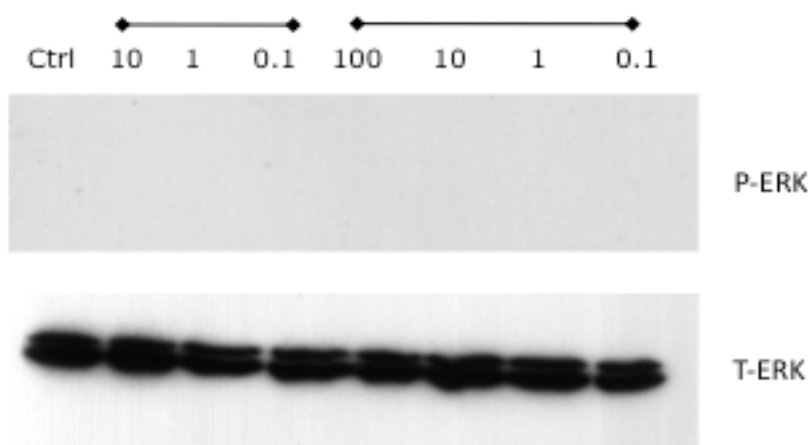


Figure 3-68: Western blotting analysis determine if p-ERK activation by Pep84 is being activated by other receptors apart from the FPR family in the HEK cells. The HEK-CMV cells were co-incubated with the varying concentrations of Pep84 for 8mins following which the cell were lysed and resuspended in cell lysis solution. Then 100ng of total protein were loaded on to 10% polyacrylamide gel. Following electrophoresis, transfer and blocking the membrane was first probed with an anti p-ERK antibody and then stripped and reprobed with and anti total ERK antibody. The t-ERK blot shows equal amounts of ERK in all the samples. However no p-ERK signal was observed confirming that the p-ERK activation observed for Pep84 was solely through the FPR family receptors (representative of 3 indep. exp).

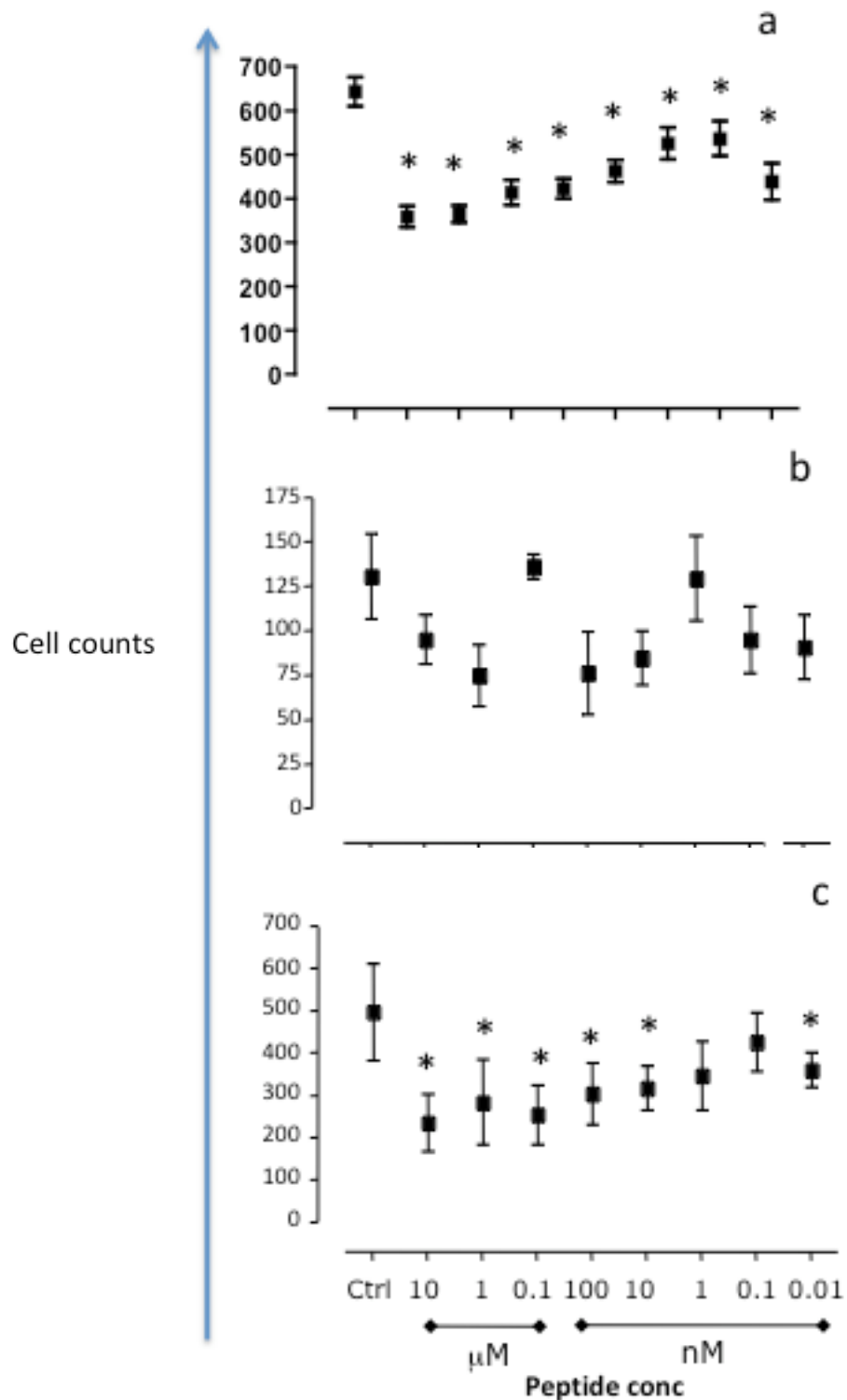


Figure 3-69: Flow chamber analysis determining the inhibitory potency of Pep84. PMNs (5×10^6) were incubated with $10 \mu\text{M}$ of the peptide for 10 min at 37°C . The PMNs were then flowed for 8 min at 1 dyne/cm^2 , prior to quantifying the degree of PMN interaction with the HUVECs, both as PMN capture (a), adhesion (b) and rolling (c). The results highlight the fact that only Pep84 has a dose dependent inhibitory effect on PMN recruitment to the activated endothelial cells. Data are mean \pm SEM of 3 independent experiments (with distinct PMN and HUVEC preparations); $P < 0.05$ vs. CT group. Data analysed using one way ANOVA.

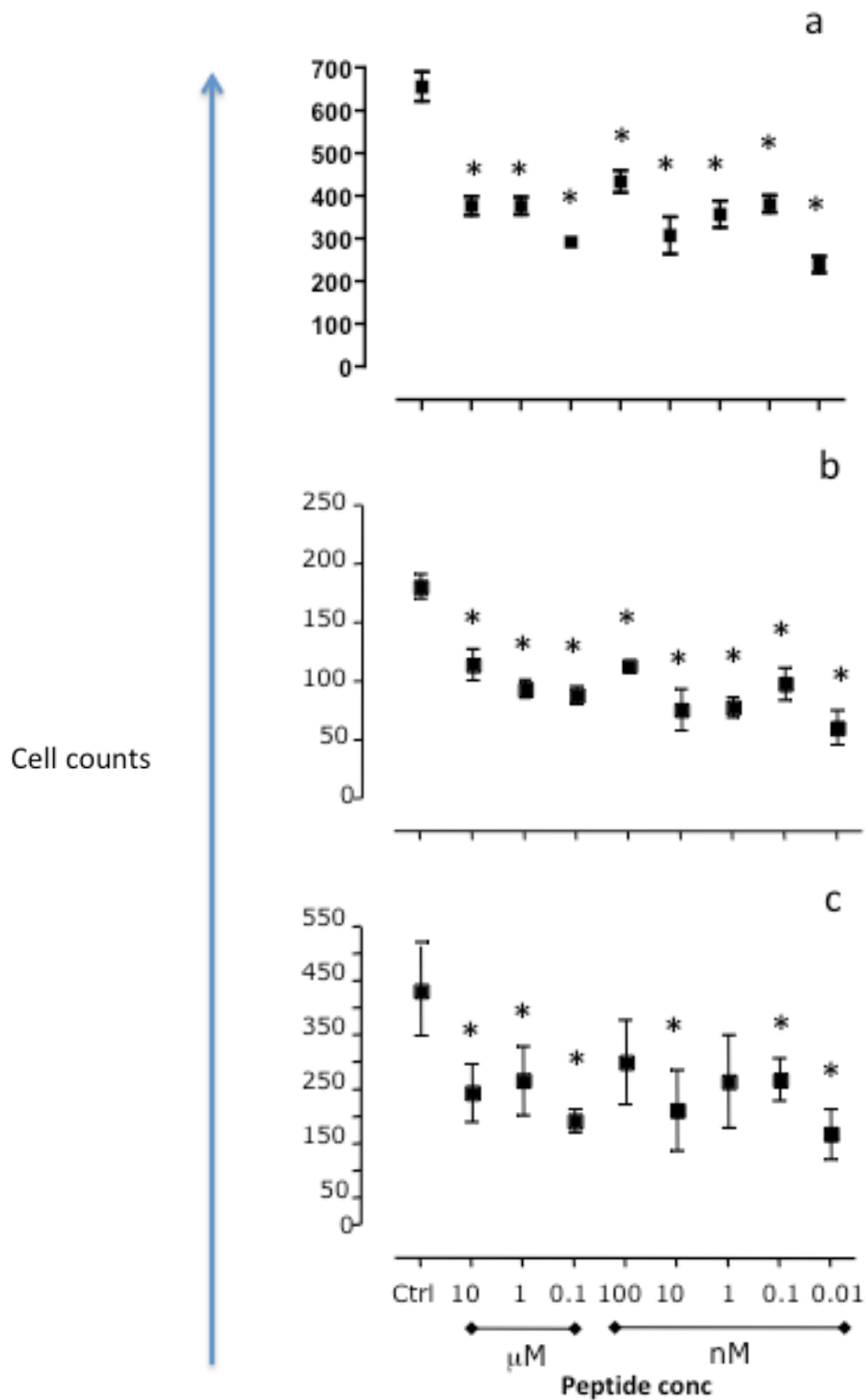


Figure 3-70: Flow chamber analysis determining the inhibitory potency of Pep57 PMNs (5×10^6) were incubated with $10 \mu\text{M}$ of the peptide for 10 min at 37°C . The PMNs were then flowed for 8 min at $1 \text{ dyne}/\text{cm}^2$, prior to quantifying the degree of PMN interaction with the HUVECs, both as PMN capture (a), adhesion (b) and rolling (c). The results highlight the fact that Pep57 does not have the a classical dose response inhibitory effect on PMN recruitment to the activated endothelial cells. Data are mean \pm SEM of 3 independent experiments (with distinct PMN and HUVEC preparations); $P < 0.05$ vs. CT group. Data analysed using one way ANOVA.

I then proceeded to determine the affinity of these novel peptides to the FPRL1 receptor by performing radioligand binding assays. Firstly I determined the concentration of tracer and cold peptide to employ. Basing myself on previously conducted analysis I employed a concentration range between 82pM and 0.82fM and a cold peptide concentration of 1μM. These results highlight that the optimal concentration of tracer to be employed is of 82pM (Figure 3-72). Next step was to determine the optimal cold peptide concentration to be employed, where three concentrations were employed, 0.1, 1 and 10μM. This determined that the optimal concentration of cold peptide to be employed for this set of experiments was of 10μM (Figure 3-73). Following, which the binding affinities of Pep57 (Figure 3-74a) and Pep84 (Figure 3-74b) to the FPRL1 was assessed, this showed that these peptides have a similar binding affinity with an IC₅₀ of approximately 3μM. On the other hand the binding affinity for Pep84 to the FPR receptors was determined to be of about 6μM (Figure 3-75a) whilst that for Pep57 could not be determined as observed in Figure 3-75b.

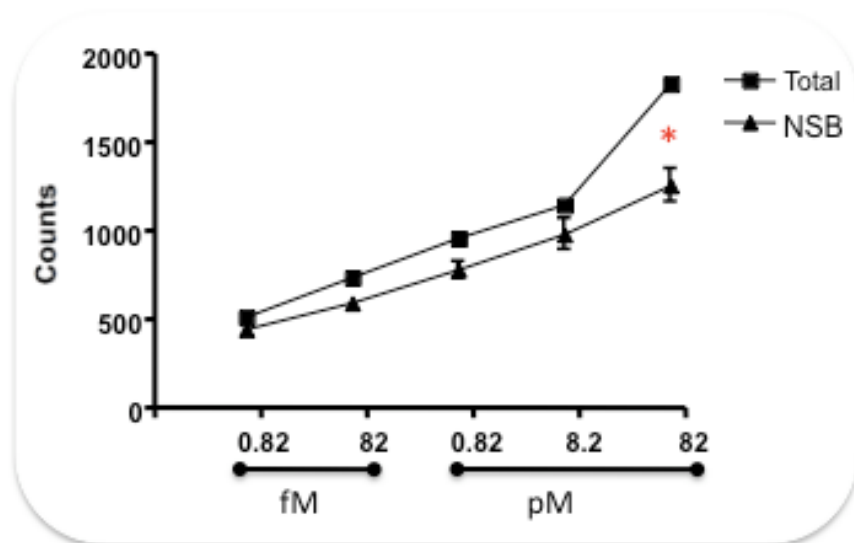


Figure 3-71: Determining the optimal concentration of tracer to be employed in Radioligand Binding assay. Following the resuspension of the HEK-FPRL1 cells at a concentration of 1×10^6 cells were incubated with $10 \mu\text{M}$ of cold peptide and various concentrations of tracer. The highest concentration of tracer is the one that shows a significant difference between Total and nonspecific binding (NSB). Data are mean \pm SEM of 3 independent experiments. * = $P < 0.05$ vs. CT group

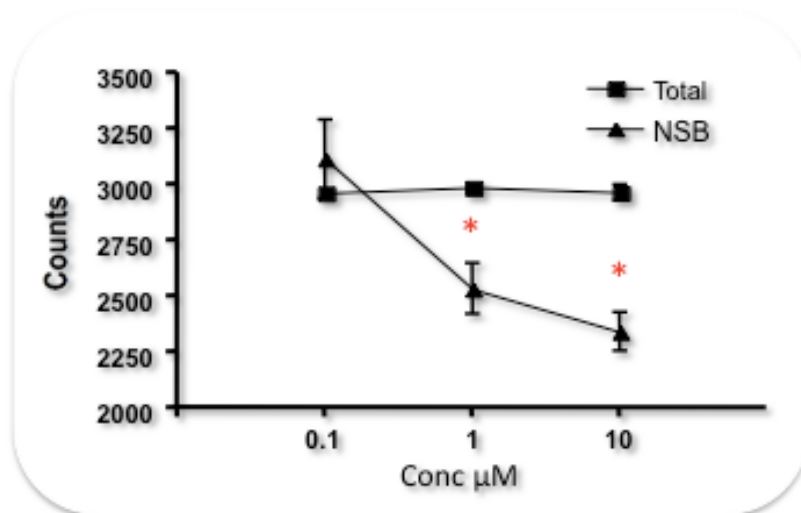


Figure 3-72: Determining the optimal concentration of cold peptide to be employed in Radioligand Binding assay. Following the resuspension of the HEK-FPRL1 cells at a concentration of 1×10^6 cells were incubated with 7pM of cold peptide and 10, 1 or $0.1 \mu\text{M}$ of cold peptide. In this set of experiments the highest concentration of cold peptide was shown to be the most effective at displacing the tracer from the FPRL1 receptor. Data are mean \pm SEM of 3 independent experiments * = $P < 0.05$ vs. CT group

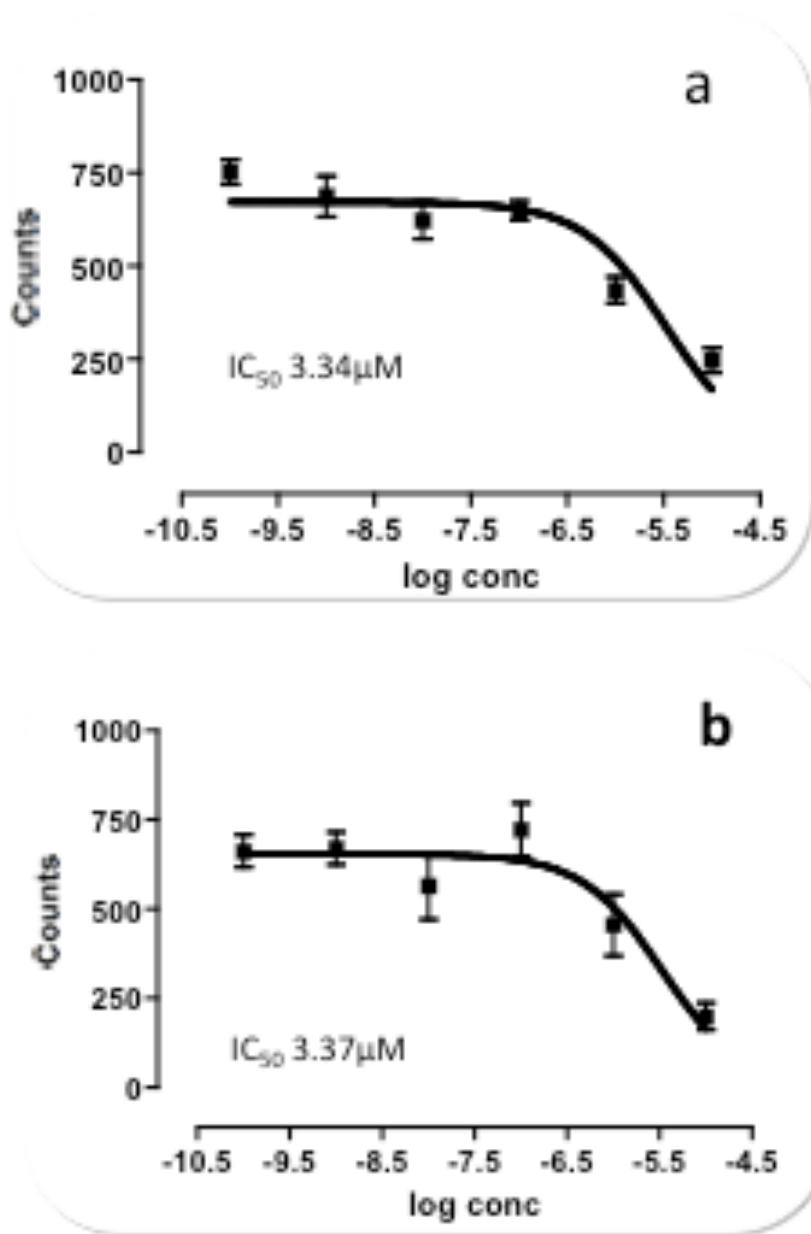


Figure 3-73: Radioligand binding assays determining the affinity of Pep84 and Pep57 to the FPRL1 receptor. HEK-FPRL1 cells were incubated on ice with varying concentrations of Pep84 (a), Pep57 (b) and 82pM of 125 I labelled W-peptide for 1h at 4°C, following which the cells were collected over a filter paper and washed to remove any unbound tracer. The counts were then measured on a gamma counter (SB=specific binding where the cells were incubated with tracer only). The results outline that both peptides exhibit similar affinities for the FPRL1 receptor. Data are mean \pm SEM of 3 independent experiments. Analysis was conducted using a non-linear regression.

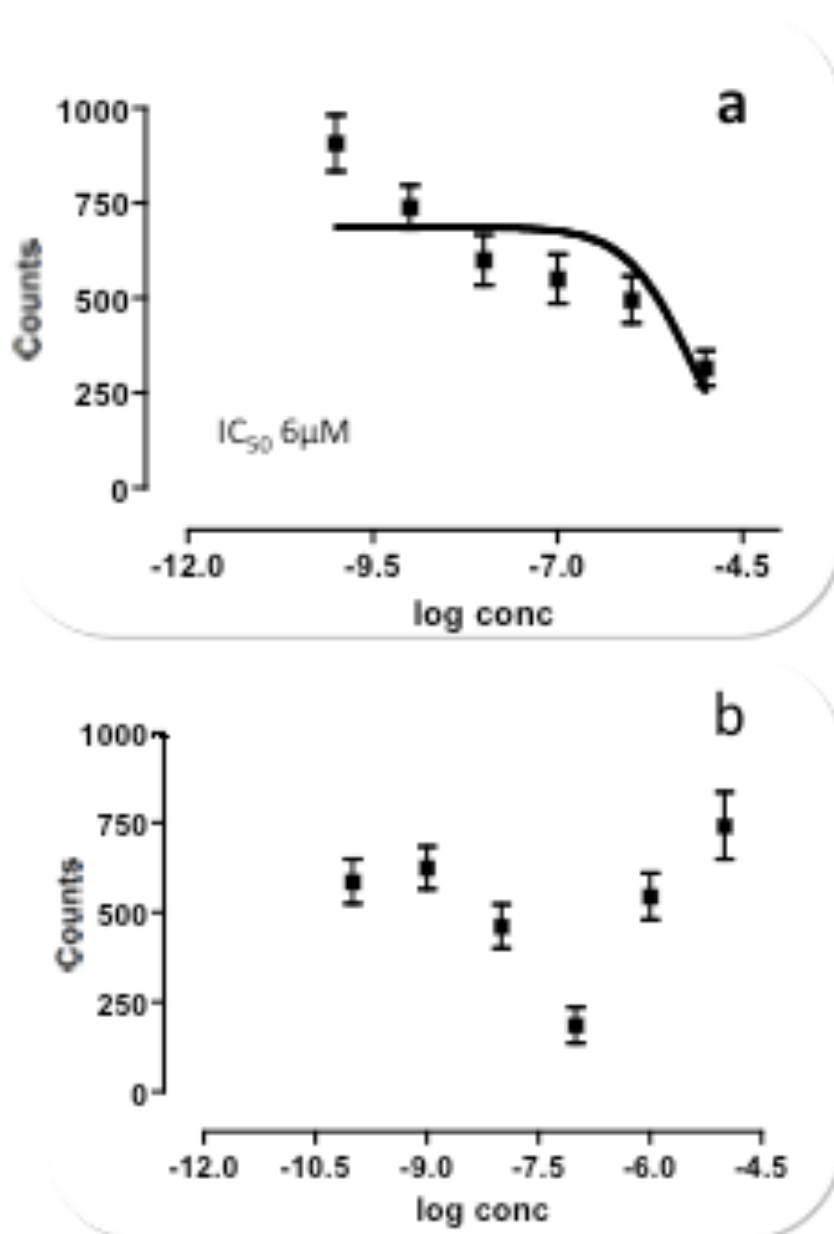


Figure 3-74: Radioligand binding assays determining the affinity of Pep84 and Pep57 to the FPR receptor. HEK-FPR cells were incubated on ice with varying concentrations of Pep84 (a), Pep57 (b) and 82pM of ^{125}I labelled W-peptide for 1h at 4°C , following which the cells were collected over a filter paper and washed to remove any unbound tracer. The counts were then measured on a gamma counter (SB=specific binding where the cells were incubated with tracer only). The results outline that Pep84 has an approximately 10 fold less affinity to the FPR as to the FPRL1. On the other hand Pep57 seems to maximally displace the tracer even to at the lower concentrations thus not providing a classical dose response. Data are mean \pm SEM of 3 independent experiments.

After determining that both Pep57 and Pep84 displayed inhibitory properties *in vitro* the next step was to determine if these peptides were active *in vivo*. For this purpose preclinical model of inflammation was employed where it was observed that Pep84 displayed a higher anti-inflammatory effect than Pep57 *in vivo* (Pep59 was employed as a negative control) (Figure 3-76). The anti-inflammatory effect was further confirmed through the blood cell counts, where it was observed that there was no reduction in circulating neutrophil counts (Figure 3.77), confirming that the reduction in cell recruitment into the airpouch was in fact due to an inhibition of cell recruitment rather than a toxic effect on the circulating cells.

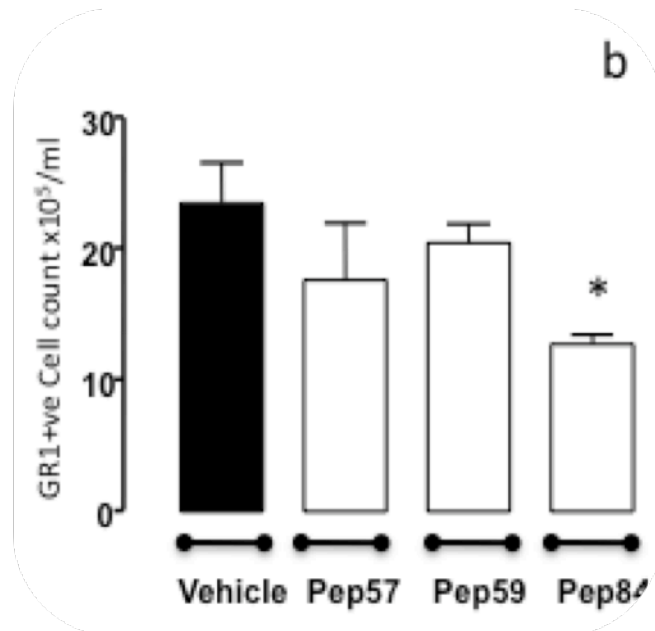
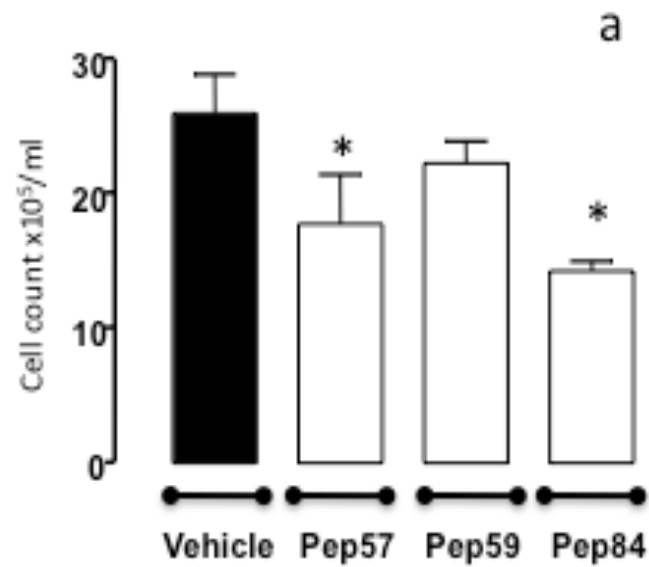


Figure 3-75: Anti-inflammatory effects of three novel Ac2-26 derived peptides. Mice received 200µl i.v. of saline+DMSO or a dose of 50µg per animal of one of the three Ac2-26 derived peptides, immediately before the local injection of mouse IL-1β into 6-day-old airpouches. The extent of cell migration was determined 4 h later, following airpouch washing and staining of migrated cells with Gr1 marker. When cells were counted Pep57 and 84 were observed to display anti-inflammatory properties, with Pep57 losing this observed effect when the GR1+ve cells were taken into account. Data are mean ± SEM of 5 mice per group. **P*<0.05 vs. vehicle group. Data was analysed using one way ANOVA

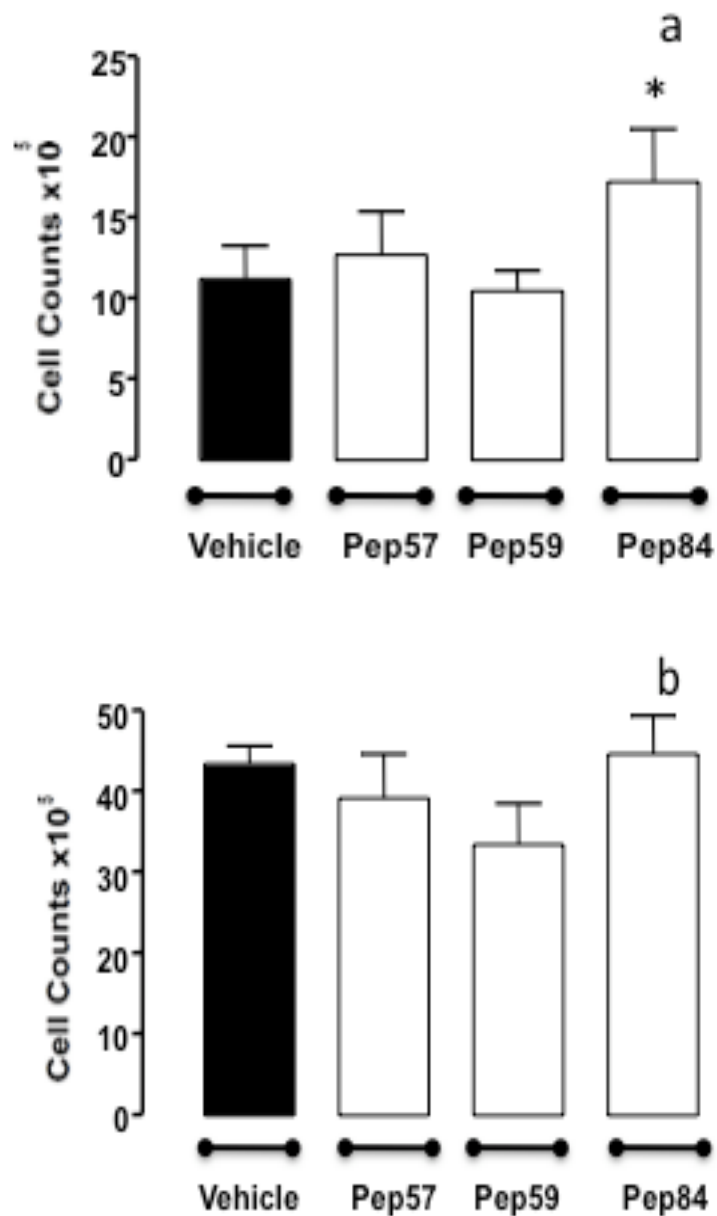


Figure 3-76: The effects the novel Ac2-26 derived peptides on blood leukocyte populations. Blood was taken via cardiac puncture from anaesthetised mice, 4h after peptide and IL1 β immediately prior to culling and washing the pouch. A differential cell count for PMN (a) and PBMC (b) was conducted where it was observed that there were no statistical significant changes in cell counts upon treatment except for the Pep84 treated group where the PMN populations were observed to be elevated. Data are mean \pm SEM of 5 mice per group. * $P < 0.05$ vs. vehicle group. Data was analysed using one way ANOVA

In order to shed novel insights into potential mechanisms of activation, I explored the possibility that FPRL1 receptor internalization could be differently modulated by established and novel agonists. Moreover, FPRL1 internalisation would represent another way to demonstrate agonistic activity by these peptides. From this analysis in the HEK-FPRL1 cells, it emerged that the overall profile for the 3 peptides was similar, where there was an initial down-regulation, and possibly internalization, with levels being reconstituted two hours by the 2 hour time point. Thus, highlighting that following the initial signalling the receptor is generally internalized, with over the first 30 minutes, following which the process starts being reversed and the receptor returned to the cell surface Figure 3-78.

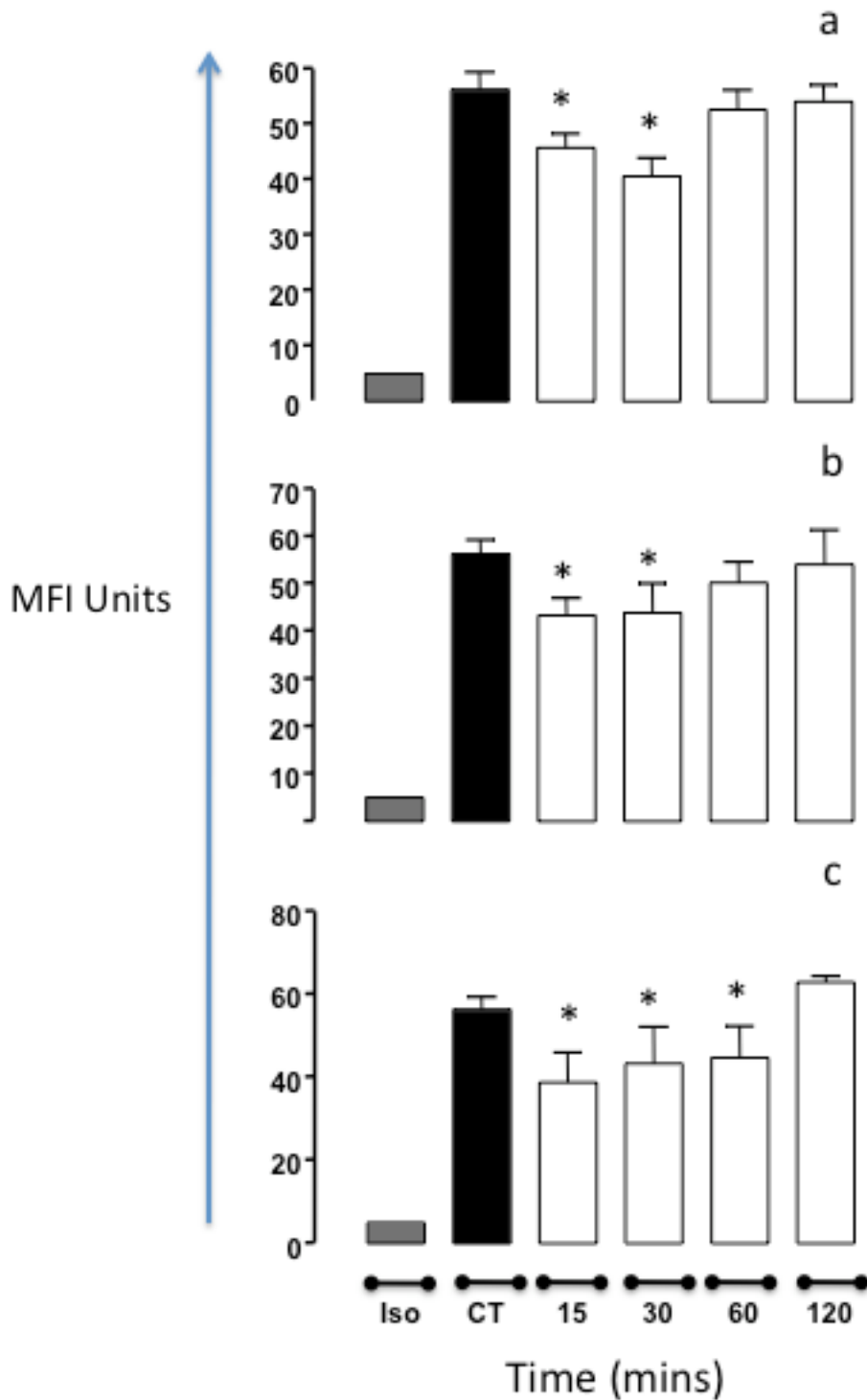


Figure 3-77: Flow cytometric analysis on FPRL1 expression on HEK-FPRL1 cells following co incubation with peptide Ac2-26, Pep57 or Pep 84. HEK-FPRL1 cells were co incubated for various time points with either Pep 84 (a) Pep57 (b) or Ac2-26 (c) following which the cells' metabolism was stopped and the cells stained using an anti-FPRL1 1° ab followed by a 1° ab. Results outline that all 3 peptides cause initial internalization of the receptor, which then recycles back to the cell surface. Data are mean \pm SEM of 3 independent experiments (with distinct PMN and HUVEC preparations); $P < 0.05$ vs. CT group. Data was analysed using one way ANOVA

4. Discussion

4.1. The Annexin A1 circuit and Rheumatic disease, is there a link?

4.1.1. Evidence for a dysregulated Annexin A1 pathway Wegener Granulomatosis and Giant Cell Arteritis

The cause of most rheumatic diseases remains unknown and in many cases may vary depending on the type of disease. Increasing evidence highlights the role of auto-antibodies in the propagation of at least a subset of such diseases where they can either reflect organ-specific or generalized auto-reactivity (Roitt, Hutchings et al. 1992). Glucocorticoids have proved over the years (Combe 2007; Morand 2007), to be an effective treatment for many of these rheumatic conditions with some of these conditions, such as Giant Cell Arteritis (GCA,) being more responsive to this treatment regime (Wang, Hu et al. 2008).

As described in Chapter 1, Annexin A1 was initially identified as a glucocorticoid inducible protein with the ability to downregulate phospholipase A2 (PLA2) and thus arachidonic acid synthesis (Cirino, Peers et al. 1989). Since then studies conducted by a number of laboratories have shown that this protein, at least in part, exerts its anti-inflammatory effects by regulating cell recruitment to the site of inflammation (Errasfa, Rothhut et al. 1985; Perretti and Flower 1993; Lim, Solito et al. 1998; Hayhoe, Kamal et al. 2006). Subsequent studies, have highlighted that the anti-inflammatory effects of Annexin A1 extend beyond inhibition of cell recruitment to the site of the inflammatory insult. In fact, various works have shown that this protein also has

an influence on the crucial pro-resolving process of apoptosis: exogenous administration of Annexin A1 can promote cell apoptosis (see below). Moreover, addition of the Annexin A1 mimetic peptide Ac2-26 to macrophages increments the rate of phagocytosis of apoptotic PMN (MADERNA, Yona et al. 2005), an effect which is coupled to TGF- β 1 release and to changes in F-actin reorganization suggesting that this peptide primes the macrophages to a more phagocytic phenotype leading to the enhanced rate of phagocytosis. This effect reproduces genuine actions of endogenous Annexin A1 as highlighted by the incubation of naive human monocyte derived macrophages in the presence of conditioned medium, produced following a 5 day culture of macrophages in the presence of dexamethasone, which enhanced their ability to engulf apoptotic PMNs. Furthermore this effect was blocked any of the following treatments: an Annexin A1 blocking antibody, by immunodepletion of the supernatants, or by the formyl peptide receptor family antagonist Boc1. It can be concluded that the final effect observed upon Annexin A1 administration may vary depending on the target cell (Goulding, Euzger et al. 1998; Scannell, Flanagan et al. 2007).

The treatment of PMNs with human recombinant Annexin A1 leads to increased PMN apoptosis through a BAD dependent pathway (Solito, Kamal et al. 2003). On the other hand, a diametrically opposite effect is reported on prostate cancer cells and monocytes where Annexin A1 has been shown to exert a protective effect by reducing the rate of apoptosis induced by etoposide and TNF- α respectively (Carollo, Parente et al. 1998; Solito, de Coupade et al. 2001).

Coupled by the fact that glucocorticoids play such an important role as disease modifying drugs in rheumatic conditions, and that both endogenous and exogenous Annexin A1 have been shown to possess very strong immunomodulatory actions, it was deemed important to investigate if there was a deregulation in the Annexin A1 pathway. Furthermore, proof of a deregulated Annexin A1 pathway could provide a pharmacological target for the development of safer treatments, thus eliminating the problems linked with prolonged glucocorticoid administration.

The analyses I conducted on patients suffering from either Wegener granulomatosis or GCA provide the first direct body of evidence that there is in fact an underlying deregulation in the Annexin A1 pathway in these conditions. Initial flow-cytometric analysis illustrated elevated Annexin A1 levels on the cell membranes of patients suffering from either disease. This observation was further corroborated by Western blotting analysis, where in both patient groups Annexin A1 levels in the membrane pool of PMNs, were elevated when compared to the levels found in healthy volunteers. Conversely, real time PCR analysis showed an up-regulation in mRNA levels for Annexin A1 in the GCA group only. This observation suggests that although at the protein level the deregulation in Annexin A1 protein levels seems to be similar for both the Wegener and GCA conditions, the underlying mechanism leading to this deregulation might be different. This is even more interesting in the light of fact that both patient groups were receiving similar glucocorticoid treatment regimes, furthermore it is a well accepted fact that GCA patients respond much better to this treatment regime than Wegener patients (Dasgupta, Hutchings et al. 2006;

Subrahmanyam and Dasgupta 2006; Dasgupta and Hassan 2007) further underlining the importance of the Annexin A1 pathway in the treatment of this condition.

The observed elevation in membrane Annexin A1 levels seems to be in contrast with the current literature, where Annexin A1 has been shown to play a tonic inhibitory role on leukocyte recruitment; blocking the signalling of Annexin A1 by neutralizing antibodies to its receptor FPRL1 increases interactions between PMN and the activated endothelial cells *in vitro* (Hayhoe, Kamal et al. 2006). However, the Western blotting analysis sheds light on this apparent contradiction, as in conjunction to an elevation of the full length (37kDa) protein on the cell membrane of PMNs from the patient groups a second, smaller band of 33kDa corresponding to the N-terminal cleaved form of Annexin A1 was observed.

The 13 members of the Annexin superfamily show a high degree of structural homology, with each including four (or 8 in the case of ANXA6) repeated units of approximately 70 amino acids within the core and C-terminal regions; these units are believed to confer the Ca^{2+} and phospholipid binding properties of the proteins. On the other hand the N-terminal region of each family member is unique and thus is considered to confer the biological specificity to the individual proteins. Therefore cleavage of the N-terminal region, as observed in the membrane pools of these patients, might void Annexin A1 of its unique functions, providing a plausible explanation for the observations made: higher Annexin A1 in inflamed PMN (Gerke and Moss 2002; Rescher and Gerke

2004). The emerging model I wish to propose is that the activation status of the patients' PMN determined membrane localization of intracellular Annexin A1, perhaps in an attempt to counteract the aberrant stimulation, yet the protein is largely cleaved hence inactive.

Consistent with this, the flow-cytometric analysis conducted on neutrophils obtained from these patients, showed elevated proteinase 3 (PR3) expression on the cell surface, an observation that provides us with a possible mechanism for Annexin A1 cleavage in the cell membrane compartment. PR3 is a proteinase that has been linked with the development of Wegener granulomatosis (Witko-Sarsat, Lesavre et al. 1999). The analysis of PR3 membrane expression on circulating resting neutrophils revealed the existence of two distinct subsets of neutrophils, one expressing membrane PR3 (mPR3+) and the other devoid of mPR3 (mPR3-). The proportion of these two subsets is a stable feature of a given subject, not related to age or gender. It was shown that the distribution of the mPR3+ neutrophil subset among healthy individuals corresponds to three discrete phenotypes, mPR3^{low}, mPR3^{inter}, and mPR3^{high}, present in 9, 36, and 55% of the healthy individuals respectively (Witko-Sarsat, Lesavre et al. 1999). Furthermore, the frequency of the mPR3^{high} phenotype is strikingly higher in patients with ANCA-related vasculitis than in the healthy control population. The proportion of mPR3+ neutrophils in a given patient is remarkably stable during follow-up studies and is not influenced by relapses or by therapy, in spite of variations in ANCA titers (Witko-Sarsat, Lesavre et al. 1999). Furthermore, the mPR3+/total neutrophil ratio is not modified after *in vitro* activation of patients' neutrophils. This suggests the possibility that a high proportion of

membrane PR3+ neutrophils might be a more general risk factor for autoimmune responses (Kantari, Pederzoli-Ribeil et al. 2007). Interestingly, the Wegener granulomatosis patients were not the only group presenting with elevated PR3 levels, in fact the flow cytometric analysis conducted on neutrophils from GCA patients revealed that the PR3 levels on these cells were also elevated to similar levels as those observed for the Wegener granulomatosis patients.

Work done by Vong et al (2007) showed that this proteinase enzyme has the ability to cleave Annexin A1 at 3 distinct loci on the N-terminal portion of the protein thus leading to its inactivation. As a result, it could be hypothesized that the translocation of Annexin A1 on to the cell membrane possibly following the activation of the cells by the ANCA antibodies exposes this protein to cleavage by PR3 and other serine proteases present on the cell membrane consequently leading to its inactivation.

Flow chamber analyses further confirm this hypothesis since a significantly higher number of adherent PMNs were observed for all three patient groups when compared to aged matched healthy volunteers, suggesting that these cells are in fact activated and thus providing the driving stimulus for the translocation of Annexin A1 to the cell surface (Perretti, Croxtall et al. 1996). Nonetheless, Annexin A1 is anti-adhesive in this assay (Hayhoe et al., 2006), yet the fact that the large majority of the protein is cleaved fits well with the higher PMN reactivity (quantified as adhesion to HUVEC) I measured.

It must also be noted that elevated mPR3 levels do not reflect an overt over-activation of neutrophils since Wegener granulomatosis patients were shown to present normal levels of CD62L or of CD11b on their circulating PMN (Kantari, Pederzoli-Ribeil et al. 2007). However, in this study the Authors did not evaluate the levels of CD11b in its active conformation, which in turn has been shown to be involved in the process of firm adhesion (Montoya, Luscinskas et al. 1997). Moreover the superfusion of ANCA IgG over rolling cells in an *in vitro* flow chamber model resulted in conversion to stationary adhesion accompanied by shape change, a process shown to be CD11b mediated (Radford, Luu et al. 2001), leaving open the possibility that peculiar, yet relevant, mode(s) of activations could be experienced by these cells *in vivo*. This could provide a possible explanation for the discrepancy in observations between the current study and that by Kantari and colleagues (2007), since an elevation in active CD11b would lead to an increase in PMN firm adhesion, as I have observed in the flow chamber analysis. PMN adhesion in this model relies on CD11a and CD11b so that blockade by specific antibodies directed to either CD11a/CD18 (LFA-1, a ICAM-1 counter-receptor), CD11b/CD18 (Mo-1), or CD18 (common β_2 -integrin) also blocked greater than 90% of PMN transmigration (Luscinskas, Cybulsky et al. 1991). Interestingly, there was no observed difference in the number of neutrophils recorded rolling over the activated endothelial monolayer in my assays; this would be in line with previously published data which show no changes in CD62L levels in Wegener PMNs (Kantari, Pederzoli-Ribeil et al. 2007).

A further deregulation in the Annexin A1 pathway was observed when levels of the Annexin A1 receptor, FPRL1, and its prototype receptor FPR, were assessed. The FPR family of receptors forms part of the GPCR superfamily of receptors. Formyl peptide receptors (FPRs) are a small group of seven-transmembrane domain, G protein-coupled receptors that are expressed mainly by mammalian phagocytic leukocytes and are known to be important in host defense and inflammation (Ye, Boulay et al. 2009).

The FPR receptor was originally identified by cloning the high affinity-binding site for fMLP on the surface of PMNs from a differentiated human myeloid leukaemia-cell (HL-60) cDNA library (Boulay, Tardif et al. 1990). Subsequent work led to the isolation of two additional human genes with high sequence homology (Murphy, Ozcelik et al. 1992) clustered with the prototype FPR on chromosome 19.3.3; these genes encode the GPCRs FPR-Like 1 (FPRL1) and FPR Like-2 (FPRL2) (Ye, Boulay et al. 2009).

Studies have demonstrated that Annexin A1 binds specifically to the FPRL1 (Perretti, Chiang et al. 2002) whilst its N-terminal peptides (Annexin A1 peptido-mimetics) are able to bind and activate - at concentrations in the low micromolar range - all three members of the FPR family (Ernst, Lange et al. 2004). Moreover, recent data showed that this protein and its peptides exert the majority of their anti-inflammatory actions through the FPRL1 (Hayhoe, Kamal et al. 2006). In fact, it was demonstrated, through the use of competitive binding assays, that both Annexin A1 and the N-terminal derived peptides Ac2-26 and Ac2-12 competed for specific [³H]LXA₄, with the full length protein showing a

higher affinity (~30 fold) towards displacement of tracer from FPRL1, than the shorter N-terminal derived peptides (Perretti, Chiang et al. 2002; Hayhoe, Kamal et al. 2006). The direct interaction between Annexin A1 and FPRL1 was further substantiated via immunoprecipitation of both the proteins from activated human polymorphonuclear (PMN) cell lysates (Perretti, Chiang et al. 2002).

Flow cytometric analysis of neutrophils extracted from the three patient groups showed an elevated expression of both the FPR and FPRL1 on their cell surface. The rationale behind this observation is not as clear as that for the Annexin A1 protein, however this enhanced expression could be a result of cell priming which would once again lead to the translocation of the receptor from the cytoplasm to the cell surface. In line with this hypothesis studies conducted on human PMNs have pointed out that both FPR and FPRL1 share a very similar sub-cellular localization: they are found in cytoplasmic vesicles (primarily gelatinase granules but also secretory vesicles), so that mild activation of PMNs would lead to their mobilization resulting in an increased cell membrane expression (Sengelov, Boulay et al. 1994; Bylund, Karlsson et al. 2002). Of interest, a great proportion (~60-70%) of intracellular Annexin A1 in the neutrophil, is contained in gelatinase granules (Perretti, Christian et al. 2000), leading me to hypothesise that ligand and receptor might be in close vicinity also inside the cell; however, externalization onto the cell surface will be associated with Annexin A1 change of structure, with exposure of the N-terminus (Rosengarth and Luecke 2003), a conformational change provoked by the presence of high concentration of Ca^{2+} (Gerke, Creutz et al. 2005)

A process of controlled degranulation – as proposed by Borregaard (Borregaard and Cowland 1997) - would not fully explain the observed increase in cell surface expression of these receptors, since analysis of FPRL1 mRNA levels highlighted a significant up-regulation in the gene expression in both MPO ANCA and GCA patient groups. A model whereby the initial increase in receptor levels could occur through a non-genomic pathway leading to an initial hyper-activation of the cells, which would become a sustained phenotype through up-regulation of gene transcription, could be put forward. What could control FPRL1 gene transcription is scarcely known, though below I will discuss the link between this receptor and glucocorticoids. There are no published studies on the FPRL1 promoter, neither in terms of identification of the right sequence(s) hence even less in terms of factors that would modulate it.

The aim of my study was to determine if the Annexin A1 system was deregulated in these conditions and thus provide a new pharmacological target to treat these conditions. The first aim was achieved as outlined by the discussion above. The next step was to determine if pharmacological treatment with hr-Annexin A1 could prove to be a potential treatment for these conditions.

The flow chamber analysis confirmed that pharmacological treatment of PMNs from the different patient groups with hr-Annexin A1 was able to reverse their activated profile, initially observed through an increased level of adhesion of these cells to the activated endothelium, when compared to healthy control cells. This modulation in fact confirms that Annexin A1, and possibly its N-terminal

derivatives, could be an attractive alternative to glucocorticoid treatment in these conditions, restoring a status demonstrated by a basal degree of PMN activation.

4.1.2. Modulation of the Annexin A1 system upon glucocorticoid administration in Rheumatoid Arthritis

RA is a chronic systemic inflammatory disorder that may affect many tissues and organs, but principally attacks the joints producing inflammatory synovitis that often progresses to destruction of the articular cartilage and ankylosis of the joints. RA can also produce diffuse inflammation in the lungs, pericardium, pleura, and sclera, and also nodular lesions, most common in subcutaneous tissue under the skin (Scott and Steer 2007). Although the cause of rheumatoid arthritis has been very hard to pinpoint the pivotal role played by the immune system in the onset and propagation of the disease is beyond discussion.

Currently there is no cure for this disease thus the goal of treatment is mainly to alleviate the symptoms, preventing the future destruction of the joints with the resulting handicap if the disease is left unchecked. These two goals may not always coincide: while pain relievers may achieve the first goal, they do not have any impact on the long-term consequences (Walker-Bone and Farrow 2007). For these reasons, most authorities believe that the majority of RA patients should be treated by at least one specific anti-rheumatic medication, also named Disease modifying anti-rheumatic drugs (DMARD), to which other medications and non-medical interventions can be added as needed (Dougados, Combe et al. 1999; Sizova 2008; Braun and Rau 2009).

Understanding the influence of an acute glucocorticoid treatment on the Annexin A1 pathway in patients with Rheumatoid Arthritis (RA) is a topic only partially investigated in the past with most of the efforts being concentrated on cells found in the synovial compartments. Work conducted by Sampey and colleagues (2000) showed that there is reduced detection of Annexin A1 binding sites on fibroblast-like synoviocytes obtained from RA patients when compared to age and sex matched cells from osteoarthritis (OA) patients. Furthermore, dexamethasone treatment of these cells *in vitro* showed a modulation of Annexin A1 expression, with an increase in protein translocation to the cell membrane and mRNA expression (Morand, Hall et al. 2006). On the other hand in a study monitoring Annexin A1 induction following the administration of hydrocortisone it was reported that the acute administration of 100-mg of the steroid was unable to induce Annexin A1 production in monocytes extracted from RA patients when compared to those obtained from healthy controls (Morand, Jefferiss et al. 1994). Interestingly raised levels of auto-antibodies to Annexin A1 have also been reported in the plasma of patients suffering from Systemic Lupus Erythematosus (SLE) levels which in turn were observed to be associated with active inflammatory disease but were independent of corticosteroid treatment. Conversely, in patients suffering from RA the levels of anti-Annexin A1 antibodies, were low in for those patients which had not received any glucocorticoid treatment, however subsequent to chronic glucocorticoid administration these levels were observed to elevate, suggesting the that treatment in this case is responsible for the elevation of these auto-antibody levels (Goulding, Podgorski et al. 1989)

Glucocorticoid therapy offers relief, but its long-term side effects, such as osteoporosis and hypertension, are deemed undesirable. Nonetheless, steroid injections can be valuable adjuncts to a long-term treatment plan, and using low dosages of daily glucocorticoid can also have an important benefit if added to a proper specific anti-rheumatic treatment (Da Silva, Jacobs et al. 2006). In order to determine the effect of acute prednisolone treatment (15mg daily), would have on the expression profile of the Annexin A1 system in both PMNs and monocytes, blood samples were taken from patients between 9 and 11 am, on day 0 (i.e. prior to initiation of a daily dose of 15mg of prednisolone), and then day 1, 7 and 14. The blood was immediately processed, PMNs and PBMC's were isolated and stained using a number of immunofluorescent antibodies against L-selectin (CD62L) and CD11b (as markers of activation); (Smith 1993) and FPR, FPRL1 and Annexin A1.

CD62L is a highly glycosylated protein of 95-105 kDa (on PMN) containing lectin, epidermal growth factor (EGF) like, and multiple short consensus repeat (SCR) domains. It is constitutively expressed on almost all leukocytes, including neutrophils, monocytes, NK cells and lymphocytes. The prominent surface localization of CD62L, which is clustered on the tips of leukocyte microvilli, is thought to facilitate its cellular interaction under flow. CD62L has been shown to bind several ligands on high endothelial venules (HEV) including mucosal addressin cell adhesion molecule-1 (MAdCAM-1), glycosylation-dependent cell adhesion molecule-1 (GlyCAM-1) and haematopoietic progenitor cell antigen-1 (HPCA-1; CD34) (Tedder, Penta et al.

1990), whilst it has been shown to bind PSGL1 on HUVECs (Paschall and Lawrence 2008). The CD62L ligands so far identified share similarities to sL^x and sL^a and all are sialylated, fucosylated and sulphated (Hiraoka, Petryniak et al. 1999). This molecule plays a vital role in neutrophil recruitment, with impaired responses in CD62L null mice in a number of models.

CD62L is rapidly shed from PMN surface upon activation, a process that leaves the proteolytically cleaved extracellular portion of the molecule still retaining the functional lectin and EGF domains, present in the plasma (Smalley and Ley 2005). This soluble form of CD62L (sCD62L) retains functional activity by inhibiting PMN recruitment to the activated endothelium. A number of studies have attempted to identify the molecule(s) responsible for this cleavage process. CD62L sheddase was the first protein identified: this is a cell surface metalloproteinase that is resistant to common protease inhibitors including tissue inhibitor of metalloproteinase (TIMP) (Preece, Murphy et al. 1996). Studies have identified CD165b, a disintegrin and metalloproteinase (ADAM-17) protein that sheds TNF- α from the cell surface, and hence is otherwise known as TNF- α converting enzyme (TACE), as an enzyme capable of cleaving CD62L from the surface of thymocytes (Walcheck, Alexander et al. 2003). However more recent evidence has show that, in the absence of ADAM17, such as in ADAM17 null mice, ADAM10 is able to cleave CD62L from the surface of mouse embryonic fibroblasts; the same holds true for CHO cells where the disintegrin is silenced (Le Gall, Bobe et al. 2009). Interestingly, the process of CD62L shedding is elicited by molecules that are both pro-inflammatory, such as PAF and fMLP (Filep, Zouki et al. 1999; Asimakopoulos, Taylor et al. 2000)

and anti-inflammatory, including Ac2-26 (Hayhoe, Kamal et al. 2006) and NSAIDs (Gomez-Gavira, Dominguez-Jimenez et al. 2000; Aktas, Pozgajova et al. 2005).

A number of studies have attempted to shed light onto the biological significance of CD62L shedding. Walcheck and colleagues (1996) have shown that inhibiting CD62L shedding results in a decrease in PMN rolling and an increased PMN accumulation in an *in vitro* flow adhesion assay. Furthermore by using a MECA-79 antigen (the peripheral node addressin carbohydrate epitope found on CD62L ligands) as an adhesion substrate in the flow chamber assay, it was concluded that CD62L shedding represented a de-adhesive event in PMN rolling, thereby decreasing leukocyte accumulation at sites of inflammation. However more recent results, from another flow chamber study, provided conflicting results, showing no evidence for a regulatory role of CD62L shedding on neutrophil recruitment to an activated HUVEC monolayer (Allport, Ding et al. 1997). This later result can be explained in the light of the observations made by Hafezi-Moghadam and colleagues (1999) who showed that the expected reduction in rolling velocity after blocking of CD62L does not occur when CD62E is also expressed, suggesting the existence of at least some degree of redundancy in this system. *In vivo* data produced using the mouse cremaster model have shown that in this model there is in fact a decrease in rolling velocity and an increase in the number of rolling leukocytes per unit time after CD62L blockade using a hydroxamic acid-based metalloprotease (KD-IX-73-4) (Hafezi-Moghadam and Ley 1999), confirming the initial observations made by Walcheck and colleagues (1996).

On these bases, (Hafezi-Moghadam, Thomas et al. 2001) and colleagues (2001) have proposed two mechanisms for the involvement of CD62L in leukocyte recruitment. Firstly the observed decrease in rolling velocity observed upon blockade of CD62L shedding increases the time that the leukocyte is exposed to the activated endothelium which in turn increases the likelihood that the leukocyte is activated thus increasing the likelihood of a successful arrest. Furthermore this process also leads to an increase in the contact time of the leukocyte with the endothelium, since CD62L blockade reduces the degree of jerkiness of the rolling (fewer microjumps along the endothelial surface) thus leading to an elevated contact time with the endothelium. Moreover they suggest that CD62L acts as a signalling molecule activating the Ras pathway via src-like tyrosine kinases and the small G-protein Rac, leading to integrin activation, binding to ICAM-1 and subsequent adhesion (Brenner, Gulbins et al. 1996; Brenner, Weinmann et al. 1997). Thus blockade of CD62L shedding also leads to enhanced signalling and thus an elevated integrin activation, which can be expected to lead to an elevated 'stickiness' of these cells.

The implications of CD62L shedding can be viewed in two opposing ways: this process could either mediate the detachment of the leukocytes from the activated endothelial surface or on the other hand promote transmigration through the endothelium. A number of studies have tried to address the modulation of CD62L expression in disease, where CD62L expression on peripheral blood monocytes and granulocytes in patients on continuous ambulatory peritoneal dialysis (Dadfar, Lundahl et al. 2004), and those suffering

from asthma (Jahnova, Horvathova et al. 1998) sickle cells disease (Lard, Mul et al. 1999) and Cohen syndrome (Olivieri, Lombardi et al. 1998), was observed to be significantly lower when compared to those found in healthy volunteers. Interestingly, the CD62L levels in patients suffering from asthma were significantly elevated following disodium chromoglycate treatment (Jahnova, Horvathova et al. 1998). On the other hand, when CD62L levels were measured in peripheral blood PMNs in patients suffering from cystic fibrosis (Russell, McRedmond et al. 1998), chronic obstructive pulmonary disease (COPD) (Noguera, Busquets et al. 1998), Kawasaki disease (Kobayashi, Kimura et al. 2007) and SLE (Molad, Buyon et al. 1994) no significant differences were observed compared to levels measured in healthy volunteers. Conflicting results were also obtained when CD62L levels were monitored in PMNs derived from Wegener granulomatosis patients. In fact whilst Muller and colleagues (1998) did not report any significant differences but Riecken and colleagues (1994) observed an elevated CD62L expression in the patient derived cells when compared to healthy volunteers, a discrepancy, which was, attributed to the different PMN extraction methods. Thus, although conflicting data exists, so to not confirm CD62L expression as a universal marker of cell activation in systemic disease, very little data is available on the effect of treatment, in particular glucocorticoid treatment, on the modulation of CD62L expression in RA. Moreover, as highlighted above, since CD62L is important in mediating leukocyte recruitment to the site of inflammation it was deemed important to determine the impact of a glucocorticoid treatment regime on the expression of this surface antigen.

Analysis of antigen expression on PMN and monocytes during the glucocorticoid treatment regimen highlighted the anti-inflammatory properties of an acute glucocorticoid dosing, and provided an insight into the mechanism governing these effects in rheumatoid arthritis. The first protein observed to be modulated following the initiation of treatment is Annexin A1, so that cell membrane levels of the protein are significantly elevated above control (Day 0) levels after the first day of treatment. This observation comes as no surprise since the relationship glucocorticoids—> Annexin A1 is well established. Recent work demonstrates that short-term application of glucocorticoids to cells induces externalization of Annexin A1 from the cytosolic pool through a non-genomic mechanism (Yazid, Solito et al. 2009); longer treatments of cells, in this case HL60 cells, was shown to up-regulate the Annexin A1 gene leading to a more sustained higher degree of protein expression (Sawmynaden and Perretti 2006).

Cell surface expression of the Annexin A1 receptor (FPRL1) on PMN and monocytes was also rapidly modulated after Day 1. This, I believe this is the first study that has monitored FPRL1 (and FPR) modulation on these cell types following clinical administration of glucocorticoids to RA patients. The process leading to the observed up-regulation in membrane expression of this receptor is probably parallel to that observed for Annexin A1 whereby upon cellular activation, following binding of the glucocorticoid to its intra-cellular receptor, there is a mobilization/translocation of the receptor from intracellular compartments, as discussed above. Subsequently the observed sustained up-regulation would result from *de novo* synthesis, an effect that has been

previously described in HL60 and monocytes cells upon incubation with glucocorticoids (Sawmynaden and Perretti 2006). In fact in this study it was observed that in both HL60 cells and monocytes, glucocorticoid treatment led to an initial up-regulation in FPRL1 mRNA followed by protein expression as soon as 2h post treatment, with a second peak at 24 h post treatment. I would think that the initial peak results from cellular activation, as described above, a process that would occur concomitantly to the mobilization of Annexin A1 to the cell membrane. Once the Annexin A1 protein is on the cell membrane it can bind to its receptor leading to *de novo* synthesis of its receptor; though not fully reported in any study as yet, I would not be surprised if a positive loop Annexin A1/FPRL1 will soon be described. Further support to this model derives from the observations made in Annexin A1 *-/-* animals, whereby the Fpr2 (the murine equivalent of human FPRL1) levels were decreased in a model of colitis when compared to wild type littermate controls (Babbin, Laukoetter et al. 2008), supporting the notion of a potential role for Annexin A1 in regulating FPRL1 (or Fpr2 in this case) expression under patho-physiological conditions.

Levels of expression of FPR, the prototype of this family of receptors, were also modified upon glucocorticoid treatment. In line with changes for Annexin A1, the degree of expression of FPR peaked 24h (Day 1) after the initiation of treatment. Such a regulation has already been reported in a recent study conducted with primary monocytes *in vitro* where fluticasone was observed to markedly up-regulate FPR expression and function. Furthermore treatment of an osteosarcoma cell line (Saos-2) also resulted in up-regulation of this receptor, but only at the mRNA level (Giner, Mancini et al. 2007).

However, the link between Annexin A1 and FPR is not as clear as for FPRL1, as no direct binding affinity has been shown between the FPR and full length Annexin A1. I have discussed in the Introduction section that peptide Ac2-26 binds to and activates - to a different extent - all three members of the FPR family FPR, FPRL1 and FPRL2 (Rescher, Danielczyk et al. 2002; Ernst, Lange et al. 2004; Karlsson, Fu et al. 2005). A note of caution, here, is due though: these analyses have always been conducted with transfected cell line, hence with artificial levels of expression of these GCPRs.

The binding of the FPR to this and other Annexin A1 N-terminal derived peptides, suggests that glucocorticoid treatment might lead to the production of these peptides, perhaps downstream the over-production of Annexin A1. The release of these peptides, possibly at the site of inflammation, could in turn lead to deactivation of both PMNs and monocytes through a process involving CD62L shedding, as shown by Hayhoe and colleagues (2006). Altogether, this could be a second mechanism up-regulated by acute glucocorticoid treatment, which is responsible for the mediation of their anti-inflammatory properties through the Annexin A1 pathway.

The observed modulation of the Annexin A1 pathway is seen to coincide with a reduction in CD62L expression on both the PMN and monocyte cell surfaces, thus suggesting that this circuit might be responsible for the 'de-priming' of these cells during this treatment regime. In fact, it has long been established that Annexin A1 is endowed with anti-inflammatory properties leading to reduction

in the extent of PMN recruitment in a number of *in vitro* and *in vivo* (Errasfa, Rothhut et al. 1985; Cirino, Peers et al. 1989; Lim, Solito et al. 1998; D'Amico, Di Filippo et al. 2000; Gavins, Dalli et al. 2007) models. This process might occur, at least in part, through CD62L shedding; for instance, co-incubation of the monocytic cell line U-937 with either dexamethasone or hr-Annexin A1 *in vitro* leads to CD62L shedding (de Coupade, Solito et al. 2003). Furthermore, immuno-precipitation and binding assays supported the suggestion that this effect could be mediated by an interaction between externalized Annexin A1 and CD62L. Such interaction involved the N-terminal domain of Annexin A1 and was calcium-dependent (de Coupade, Solito et al. 2003). Thus, I wish to propose that the observed reduction in CD62L expression might be a consequence of a reduction in the activation profile of the cell following treatment with the glucocorticoid

The second leukocyte adhesion molecule I monitored in this study was CD11b, a heterodimeric integrin composed of integrin alpha M (ITGAM) subunits. It has been shown to form a heterodimer with CD18 and is found on both granulocytes and monocytes, but not lymphocytes. This molecule has been shown to be involved primarily with the leukocyte firm adhesion process, involved in sustaining the adhesion initiated by the interaction of CD11a/CD18 with ICAM-1 on the endothelium (Hentzen, Neelamegham et al. 2000). Experiments conducted in CD11b deficient mice further confirmed this role, as displayed by a significantly impaired neutrophil adhesion to fibrinogen coated-plastic discs implanted into the mouse peritoneal cavity when compared with wild type mice. Furthermore, CD11b deficient neutrophils display defective

degranulation and complement-mediated phagocytosis, thus suggesting that CD11b/CD18 mediated stabilization of adhesive bonds is due, at least in part, to its involvement in the process of neutrophil activation (Lu, Smith et al. 1997).

The results obtained for the CD11b staining also suggest that there is a decrease in the activation profile of both PMNs and monocytes at day 1 post treatment, further suggesting that the Annexin A1 pathway, and in particular the Annexin A1 itself, could be mediating these effects. This observation is corroborated by a number of *in vivo* studies where CD11b protein, but not mRNA, levels were down-regulated in eosinophils post-glucocorticoid treatment (Lim, Flower et al. 2000), an effect that was, at least in part, mediated by Annexin A1 (Das, Lim et al. 1997).

Interestingly, the CD11b levels return back to basal levels at Day 7 remaining stable until the end of the study, suggesting that white blood cells return to their basal status. However, these observations are not conclusive since it is not merely the presence of the integrin that is important but, as I said above, the degree of activation of this protein. This is a point, which will need to be considered when designing future studies in order to determine if there is in fact a reduction in the active conformation of the CD11b antigen upon glucocorticoid treatment.

A further added value for this translational study was to monitor the levels of expression of these proteins on synovial cells and compare them to those seen in the blood pool to determine how the Annexin A1 system is modulated in this

condition, upon extravasation of these cells into the synovium. Comparison of the blood vs. synovial cell populations highlighted that both synovial PMN and PBMC, population had reduced CD62L and CD11b cell membrane levels, possibly suggesting a less activated profile than those found in the blood compartment.

A reduction in CD62L expression also goes hand in hand with the changes of this protein described in the PMN extravasation process (Finn, Strobel et al. 1994; Liu, Kishimoto et al. 1998). Cellular activation along with the transmigration process could also be responsible for the elevated Annexin A1 expression on the cell membranes of these cells, since it has been demonstrated in a number of studies that PMN activation and adhesion leads to the translocation of gelatinase granules containing Annexin A1, causing the increased localization of the protein in the membrane compartment. Moreover, studies in a mouse peritonitis model showed up-regulation of Annexin A1 gene promoter activity (measured with a LacZ gene reporter assay) in PMN extravasated into the mesenteric tissue as early as 4h post zymosan injection, with protein levels increasing soon after and being still elevated at the 24h time-point (Damazo, Yona et al. 2006).

This result suggests that following the initial up-regulation elicited by the extravasation process through granule mobilization, *de novo* synthesis is possibly elicited either by an autocrine/paracrine effect or through priming by the pro-inflammatory environment found in the synovium. Furthermore I could also measure elevated FPR and FPRL1 levels in the synovial monocyte

subgroup, as compared to matched blood cells, an observation that could be explained again by cellular activation resulting from the transmigration process. I would repeat, though, that I am aware the CD11b levels measured here do not reflect the activated status of the cell since only the total antigen population was analysed, as opposed to the levels of active CD11b proportion. Thus, overall this analysis in RA patients subjected to glucocorticoid treatment suggests a strong modulation of elements of the Annexin A1 pathway upon cellular transmigration into the synovium; I believe this is the first study in man to report so.

4.2. The biological functions of Annexin A1 in PMN derived microparticles

4.2.1. The anti-inflammatory action of Annexin A1 in PMN-derived microparticles

Microparticles, which were first described by Wolf in 1967, are membrane-derived vesicles produced by a number of cells as a result of activation or apoptosis. Originally described as platelet dust, they have been shown to possess pro-thrombotic properties. Since their discovery they have been implicated in a number of processes, including cardiovascular function and inflammation. However, to date very few microparticle components have been shown to be directly responsible for these effects, amongst these we find receptors such CCR5 and CXCL7. These receptors have been reported to be responsible for the increase in susceptibility of cells to infection by some strains of the HIV virus (Mack, Kleinschmidt et al. 2000).

Interestingly, microparticles have also been attributed a role in the reduction/prevention of inflammation; specifically, PMN-derived microparticles were shown to exert an inhibitory effect on human monocyte derived macrophages, leading to the downregulation of TNF- α and IL8 production when these cells were incubated with these microvesicles and LPS (Gasser and Schifferli 2004). This interesting knowledge prompted the following question: can Annexin A1, a homeostatic pro-resolving protein that is abundantly expressed in PMNs, be mediating this inhibitory effect of microparticles?

As a result of the investigations I conducted it can be concluded that Annexin A1 is at least in part responsible for the anti-inflammatory role attributed to PMN-derived microparticles.

As previously highlighted, the mechanism leading to the incorporation of the Annexin A1 protein is governed by the adhesion of the PMNs to the endothelial cells, a process that leads to the translocation of the Annexin A1 protein from inside the cytoplasm to the plasma membrane (Perretti, Croxtall et al. 1996). However, even though a number of studies have tried to address the mechanism by which Annexin A1 is translocated to the cell membrane, no data is available as to the process by which this protein is exported outside the cell and recovered from supernatants. Thus, my study started by addressing the question whether PMN-derived microparticles contained Annexin A1 and if so, whether this protein could be responsible for the time dependent dampening effect on PMN recruitment to an activated endothelial monolayer *in vitro* and, ideally, to the site of inflammation *in vivo*.

The results I produced provide us with a potential mechanism by which these microstructures, released into the circulation and rich in Annexin A1, could lead to their accumulation and subsequent inactivation of other PMNs, as observed by the reduction in cell recruitment to the activated HUVEC monolayer *in vitro*. This will in turn lead to the inhibition of cell recruitment to the site of inflammation as observed *in vivo* upon administration of Annexin A1+ve PMN microparticles, where there was a significant reduction in the number of cells that extravasated to the mouse air-pouch. This effect was primarily Annexin A1

dependent since microparticles produced from Annexin A1 -/- neutrophils failed to inhibit PMN recruitment into the mouse airpouch.

It is also possible that Annexin A1+ve PMN-derived microparticles might alter the phenotype of endothelial cells, a model perhaps more likely to occur *in vivo*, where longer time-points were applied (4 h) compared to the short time of the flow chamber assay (10 min). Importantly, microparticle components derived from activated/apoptotic human cells have been shown to alter EC phenotype. In a recent study, Agouni and colleagues (2007) demonstrated that microparticles containing sonic hedgehog (a morphogen involved in embryogenesis but also shown modulate angiogenesis under ischaemic conditions) could modulate ECs phenotype. These microparticles were produced from activated/apoptotic T lymphocyte and once incubated with ECs augmented expression and phosphorylation of enzymes related to the NO pathway resulting in increased release of NO from these cells. Furthermore the administration of these microparticles *in vivo* reverted endothelial dysfunction following ischemia reperfusion injury by modulating the release of NO (Agouni, Mostefai et al. 2007).

The hypothesis I put forward above, that microparticles might affect PMN responsiveness of recipient PMN, is indirectly supported by studies conducted in patients suffering from septic shock (Fujimi, Ogura et al. 2003): PMNs derived from these patients are unresponsive to further stimulation. Although these studies did not investigate the presence of Annexin A1+ve microparticles in these patients, from the data generated in my study I can speculate that these

PMN microparticles could contain Annexin A1; in turn, this protein will interact with its receptor leading to desensitization of other GPCR, and the overall outcome would be desensitization of the target cells. In any case, I am aware this model can only explain part of the effects of PMN-derived microparticles, so it may be only a transient effect; in fact when PMNs were obtained from the same patients after several days of the initial insult it was observed that the cells were then hyper-reactive (Fujimi, Ogura et al. 2003).

4.2.2. Reactive oxygen species production by PMN-derived microparticles

Infection by bacteria and other foreign organisms leads to the build up of an inflammatory response. One of the response mechanisms of PMNs and other inflammatory cells to infection is the production of reactive oxygen species. This response plays a very important role within the innate immune system since it is crucial for the destruction of inflammatory agents. Therefore, the further understanding of this type of response is of fundamental importance, especially in addressing problems related to septic shock. Thus, initially I set out to determine whether PMN-derived microparticles were able to generate ROS. Upon stimulation with phorbol 12-myristate 13-acetate (PMA) it was observed that microparticles are in fact able to produce ROS, a process, which is normally related to the onset of inflammation. At this point the question of how can the same PMN-derived microparticles fulfill both a pro- and anti-inflammatory role came naturally. The answer to this, I believe and propose, lies in their mode of production, where in fact ROS producing microparticles were obtained through direct stimulation of the PMNs with a high concentration of fMLP, mimicking perhaps the close encounter of the PMN with the infective agent, whilst microparticles observed to convey the anti-inflammatory effect

reported above (produced by co-incubation of the PMNs with a HUVEC monolayer) were unable to produce ROS even upon subsequent stimulation with PMA. This observation further supports the knowledge that microparticles are not produced through passive processes but are stimulus dependent hence heterogeneous in their content and possibly function(s). Stressing this point further is the fact that the microparticles shown to be responsible for the production of ROS are larger than those observed to contain Annexin A1, possibly as a result of the incorporation of the ROS producing machinery, which is known to be formed by relatively large proteins. Amongst these proteins we find NADPH oxidases, originally thought to be a single enzyme but now known to be a large family of enzymes dedicated to the production of ROS play a major role in their production, although other complexes such as xanthine oxidase, glucose oxidase and enzymes involved in arachidonic acid metabolism probably also contribute here (Morgan, Kim et al. 2008; Dowling and Simmons 2009). Moreover flow cytometric analysis of ROS generating microvesicles show that they are devoid of Annexin A1, further outlining their pro-inflammatory role.

Collectively, these observations support the hypothesis that protein incorporation into microparticles is a tightly regulated process resulting from a complex sequence of events and stimuli. Thus, in the context of pathological conditions like sepsis where ROS production is thought to play a central role in the aetiology of cell dysfunction and tissue damage (Everton Andrades, Ritter et al. 2009), understanding the mechanisms leading to the production of these

microstructures in the vasculature could provide an insight into this very complex, and still elusive, pathological condition.

Interestingly, ROS-producing microparticles were observed to contain the Annexin A1 receptor FPRL1. This result suggests that the modulatory role of these microstructures *in vivo* could be two fold. Firstly as pro-inflammatory agents through the production of ROS, aiding in the destruction of the infectious agent. Secondly, they could play a delayed anti-inflammatory role through the incorporation of the FPRL1 receptor onto 'naive' cells, that is to say cells that do not normally express the receptor at a given time point, thus rendering these cells responsive to the anti-inflammatory actions of Annexin A1 (or other ligands, e.g. Lipoxin A₄), leading to the proposed time dampening effect referred to above. Clearly future studies can address this specific point determining, for instance, the components of ROS-producing microparticles, the ability to transfer elements of the Annexin A1 pathway in recipient cells, and so forth; in any case, I think that my initial data have just opened the lid onto a completely new area of biology, the cell-to-cell cross talk in inflammation.

4.2.3. The potential for use of of Annexin A1 positive PMN-derived microparticles as biomarkers of treatment and disease

Another important aspect that my research has indicated is whether Annexin A1+ve PMN derived microparticles could be used as biomarkers of disease. The use (and need) of disease biomarkers is growing, with a steady stream of products and assays being brought out by the pharmaceutical industry. Some of these assist in diagnosis, others provide a means of monitoring the state of disease progression and the effectiveness of therapeutic options. Identification

of robust disease biomarkers to provide unequivocal disease diagnosis, ideally also easy to quantify, is becoming the prime focus of a large body of research.

Having established that Annexin A1 positive microparticles play an important role in the regulation of cell recruitment both *in vitro* and *in vivo* in a preclinical model of cell recruitment, it was deemed important to determine if these microparticles were also detectable in the plasma of healthy volunteers and then in patients suffering from a number of diseases where PMN-derived microparticle populations have been shown to be significantly elevated. For this purpose, I measured levels of Annexin A1 and FPRL1+ve microparticles in the plasma of patients suffering from rheumatoid arthritis and vasculitis, specifically GCA and Wegener granulomatosis. Captivatingly, observations made from these analyses showed a reduction in the number of Annexin A1+ve microparticles and an increase in the FPRL1+ve microparticles in these disease conditions. This observation further confirms the hypothesis of a deregulation in the Annexin A1 pathway in pathology, coupling alterations at the cellular level with ‘defects’ in specific microparticle levels.

The biological significance of the observed deregulation in the Annexin A1 axis is not clear however one can speculate that the reduction in Annexin A1+ve microparticles could at least in part explain the hyper-reactive profile of PMNs and monocytes obtained from these patients. Furthermore the increase in the number of FPRL1+ve microparticles could either occur through chance incorporation, since it has been shown that this receptor is normally located in lipid rich regions of the cell membrane known as lipid rafts (Tuluc, Meshki et

al. 2003), the same regions which have been indicated to be the site of microparticle production (Horstman, Jy et al. 2004). Thus activation of the parent cell, with the subsequent increase in microparticle production, could lead to an increased presence of the receptor in the plasma of these patients. However this hypothesis is in sharp contrast to the mounting body of evidence that protein incorporation into microparticles is governed by a tightly regulated process (Horstman, Jy et al. 2004; Hugel, Martinez et al. 2005). An alternative hypothesis, more in line with the current literature, is that the observed increase FPRL1 levels are a compensatory mechanism to the reduction in Annexin A1+ve microparticles. An attempt by the cells to re-establish homeostasis in these disease conditions by elevating the levels of the receptor in the absence, or reduction, of the ligand, is an interesting hypothesis which obviously needs further robust testing, but which would be very exciting if confirmed since it would give a better insight into the processes responsible for the reestablishment of homeostasis.

I wish to note that changes in microparticle levels, in a specific cell source manner, have been recently reported, adding inflammatory pathological conditions to the series of studies that have investigated, by and large, cardiovascular diseases (e.g. atherosclerosis). As an example, elevated levels of PMN and platelet-derived microparticles have been reported in the acute phase of vasculitis and dialysis-induced inflammation, where it was suggested that their elevated levels could be important in the modulation of the coagulation and inflammatory processes (Daniel, Fakhouri et al. 2006).

Can Annexin A1+ve PMN derived microparticles be used as biomarkers of treatment effectiveness? After establishing the presence of Annexin A1+ve microparticles in these inflammatory disease states, and the fact that there is a sensible alteration in Annexin A1 content in microparticles obtained from patients suffering from a number of chronic inflammatory conditions, the next question that came to mind was if microparticle populations are modulated during treatment, and whether they could be used as a measure of treatment efficacy. For this purpose I took advantage on a clinical trial conducted by our Musculo-skeletal Clinical Academic Unit (led by Professor Pitzalis) measuring microparticle levels in the plasma of patients suffering from RA, both pre- and post-steroid treatment. The results showed a striking modulation in microparticle populations with a general decrease in the number of microparticles found in the plasma of these patients, where a reduction in CD62L, CD62P and CD14+ve microparticles was measured. Interestingly, the incremented plasma levels of these microparticles was similar to that observed in a number of systemic pathologies including atherosclerosis (Leroyer, Isobe et al. 2007) and sepsis (Mostefai, Meziani et al. 2008). Following the regimen of glucocorticoid treatment of the RA patients, cell-specific microparticle returned to levels similar to those observed in healthy volunteers (Mostefai, Meziani et al. 2008), as also highlighted in the results section above). My data indicates that this process might be concordant with the anti-inflammatory properties of glucocorticoids. However, more interestingly, administration of 15 mg prednisolone daily had an influence on both Annexin A1 and FPRL1+ve microparticles over the course of a 14-day treatment. I wish to note, though, that these changes were significant by day 14, so they may reflect not necessarily

modulation of white blood cell activation, but could also be reflective of changes within the peripheral blood leukocyte populations.

Studies conducted by Dale and colleagues (1975) have shown that an oral dose of prednisolone (even as low 5mg) is able to elicit bone marrow PMN egress into the blood stream with a significant rise in the number of circulating cells as early as 2h post administration. A second study looking at the effect of glucocorticoid administration on lymphocyte recruitment showed that following a single intra-venous hydrocortisone administration lymphocyte recruitment into the blood peaked 28h post administration, following which the lymphocyte levels returned to basal after 48h. There are no controlled studies, to my knowledge that have monitored peripheral blood cells upon glucocorticoid treatment for 1 or 2 weeks.

Altogether, I favour the hypothesis that the changes provoked by glucocorticoid treatment administered to the RA patients derive from a 'deactivating' effect, rather than qualitative and/or quantitative changes in white blood cell types. Importantly, monitoring Annexin A1+ve (and FPRL1+ve) microparticles could be used as an indication of treatment efficiency. In support of this, although the treatment was observed to increase the number of circulating leukocytes, there wasn't an increase in the number of CD62L positive and CD14 positive microparticles; so, cells present in the circulation following the initiation of glucocorticoid treatment have a more quiescent profile, and this is in line with the cell surface expression of CD11b and CD62L discussed above.

Altogether, I think that these observations are exciting and could provide a way of easily monitoring the effectiveness of glucocorticoid, and possibly other treatments, in this and other inflammatory disease conditions.

4.3. Developing and testing of Novel Ac2-26 peptides

Members of the annexin family of proteins are characterized by a highly conserved core region, responsible for the annexins distinctive Ca^{2+} and phospholipid binding properties, and an N-terminal segment unique to each annexin, with this portion of the protein being responsible for the individual function of each member of the annexin family (Gerke and Moss 2002). For this reason a number of Annexin A1 N-terminally derived peptides have been developed over the years that were shown to mimic the anti-inflammatory actions of the full-length protein in several models of inflammation both in vitro and in vivo, albeit at higher molar concentrations than those employed for the parent protein (Relton, Strijbos et al. 1991; Lim, Solito et al. 1998; Perretti, Chiang et al. 2002; Hayhoe, Kamal et al. 2006).

More recent studies conducted in our lab have identified a number of cleavage sites susceptible to proteinase 3 (PR3) in the N-terminal portion of the Annexin A1 protein (Vong, D'Acquisto et al. 2007). Thus, following the rationale whereby cleavage of the N-terminal portion of the full-length protein by this serine proteinase would lead to the loss of its anti-inflammatory properties, it was hypothesized that the same enzyme could also cleave the N-terminally derived peptides rendering them inactive. Thus basing ourselves on one of the more extensively studied N-terminal derived peptide, the Ac-2-26, in collaboration with Unigene Corp. we substituted two cleavage sites, the alanine at position 11 and the valine at position 22 (Vong, D'Acquisto et al. 2007) with a number of amino acids. The amino acids employed in these substitutions were selected based on the impact that their inclusion would produce on the three

dimensional properties of the polypeptide. In this sense amino acid χ (Peptide 59) and amino acid δ (Peptide 60) are charged amino acids thus their inclusion would most likely alter the three dimensional properties of the polypeptide especially at position 11 which might lead to the breakdown of the alpha-helix found in this portion of the protein. The inclusion of amino acid β (Peptide 83), which in contrast to the previous two amino acids is not charged is also likely to lead to the breakdown of the alpha helix due to the steric hindrance produced by the hydrocarbon side chain found on this amino acid. Finally two non-charged, non-bulky amino acids were also employed in the synthesis of the novel N-terminally derived amino acids, these were amino acid α (Peptide 84) and amino acid ϵ (Peptide 57). In this case the substitution of the alanine and valine amino acids with either amino acid α or amino acid ϵ is not expected to cause any significant changes in the 3 dimensional properties of the peptide (Note: clearly, I cannot disclose the precise sequences of these novel Ac2-26 derivatives in view of our commitment with Unigene Corp (furthermore, I am in the dark here); however, the indications given above are sufficient to allow me elaborate on the changes acted upon the Ac2-26 sequence and trying to relate them to biological function).

In the quest to determine the potency of the novel Ac2-26 derived peptides a number of properties were assessed in order to determine their potential as anti-inflammatory drugs. Previous studies conducted in our group, and by others, have shown that peptide Ac2-26 binds to the two FPR receptors expressed by PMN, namely FPR and FPRL1 (Walther, Riehemann et al. 2000; Ernst, Lange

et al. 2004; Hayhoe, Kamal et al. 2006). The classical ligand of the FPR family of GPCRs is the pro-inflammatory chemoattractant fMLP.

The binding of agonist to the FPR receptor leads to a conformational change allowing the interaction of the C-terminal portion of the receptor with the G_i protein family, a process shown to be pertussis toxin sensitive. This interaction leads to the exchange of guanosine diphosphate (GDP) with guanosine triphosphate (GTP) on the α -subunit and dissociation of the $\beta\gamma$ -subunits from the G protein heterotrimer (Selvatici, Falzarano et al. 2006; Gripentrog and Miettinen 2008). This leads to the activation of several signalling pathways and, in human neutrophils, the G_i $\beta\gamma$ -subunits leads to the activation of phospholipase $C\beta$ (PLC β) (Camps, Carozzi et al. 1992), resulting in the hydrolysis of phosphatidylinositol 4,5-bisphosphate (PtIns(4,5)P₂), with the generation of diacylglycerol (DAG) and inositol 1,4,5-trisphosphate (IP₃) as second messengers (Berridge 1993). DAG subsequently leads to the activation of various PI3K isoforms amongst which phosphoinositide 3-kinase (PI3K); the γ isoform of PI3K is also activated by G_i proteins (Stephens, Ellson et al. 2002) and causes actin polymerization and activation of integrins involved in neutrophil migration, although in this respect it is still not clear whether this FPRL1 signalling is positive or negative towards migration. IP₃ mediates the rapid release of Ca^{2+} from intracellular stores, which precedes the longer lasting influx of extracellular Ca^{2+} (Berridge 1993; Davies-Cox, Laffafian et al. 2001). In addition other intracellular effectors including small GTP binding proteins of the Rho family, the mitogen activated protein kinase (MAPK) cascade, tyrosine

kinases and protein phosphatases can also be activated by ligand binding to FPR (Niggli 2003).

The exact signalling pathway for the Ac2-26 peptide is not yet fully understood however a number of studies have shown that its binding to the FPR family of receptors leads to an increase in intracellular Ca^{2+} fluxes, as observed for fMLP (Ernst, Lange et al. 2004). Furthermore, the incubation of cells with the Ac2-26 peptide was shown to down-regulate subsequent cellular responses to fMLP, including generation of respiratory burst by the desensitization of the receptor (Walther, Riehemann et al. 2000).

To assess the activity of the novel peptides, I initially determined their ability to bind to and activate the FPR family of receptors, specifically FPR and FPRL1. For this purpose three transfected HEK cell lines were employed. These cell lines were transfected with either an empty vector and termed HEK-CMV, a vector over expressing FPR and thus termed HEK-FPR or a vector over expressing the FPRL1 gene and consequently termed HEK-FPRL1 (Hayhoe, Kamal et al. 2006). One drawback of using this cell line was that activation of the receptor lead to only a marginal phosphorylation of the extracellular signal-regulated kinases (ERK) 1 and 2, which made it more difficult to determine the ability of the peptides to activate the receptor, however this problem was overcome by loading a high amount of protein (~120 μg) onto the SDS gel, which made the detection of the phospho-ERK 1/2 possible by western blotting.

The results obtained from the initial screening using these cell-lines showed that peptides 57, 59 and 84 had the highest ability to activate ERK 1/2 through the FPRL1 receptor to levels similar to those observed for the parent Ac2-26 peptide. Furthermore the assessment of the novel N-terminal derived peptides showed that peptide 57 and 84 were also able to inhibit PMN interaction with an activated endothelium, similar to that observed for Ac2-26 (Hayhoe, Kamal et al. 2006). Interestingly peptide 59, which has the ability to activate ERK 1/2 to a similar level as the other three peptides, did not display any anti-adhesive property in the flow chamber assay! Therefore, either ERK phosphorylation is only one of the possible downstream signalling events evoked by FPRL1 activation, or this outcome is dissociated from the effects monitored with the flow chamber assay (I discuss this point further below).

Furthermore peptide 60, which did not show any activity in the p-ERK assay when using FPRL1-HEK cells, also displayed anti-inflammatory properties. This result could be due to the observed inhibitory effects transduced by receptor/s other than the FPRL1, possibly the FPR, however this hypothesis merits further investigation since I did not explore the ability of this peptide to interact and activate the FPR receptor due to time constraints. Alternatively, peptide 60 might incite distinct intracellular signaling, in any case, this observation is interesting in itself since it suggests that the amino acid substitutions conducted in the synthesis of this peptide could have created an FPR specific agonist.

Studies conducted in our lab have shown that the Ac2-26 can bind to both the FPR and FPRL1 receptors with a similar affinity and that its inhibitory effects are mediated through both receptors (Hayhoe, Kamal et al. 2006). Thus in line with the aim to determine which from the newly synthesized peptides displayed anti-inflammatory properties similar to those reported for the parent Ac2-26 peptide, I decided to proceed with my analyses focusing on peptides 57 and 84, since these two peptides best mimicked the properties of the parent peptide.

Subsequent analysis of the binding affinities for these two peptides showed that they have similar binding affinities to the FPRL1 receptor (3.34 μ M and 3.37 μ M for peptides 84 and 57 respectively), which is also similar to that reported for Ac2-26 (1.8 μ M) (Hayhoe, Kamal et al. 2006). On the other hand the binding affinity to the FPR receptor for peptide 84 (6 μ M) was two orders of magnitude lower than that observed for the FPRL1 receptor and 6 orders less than that reported for the parent peptide (1.4 μ M) (Hayhoe, Kamal et al. 2006). Furthermore, peptide 57 did not seem to bind in a classical manner to the FPR receptor since no classical dose response was observed however the peptide was still able to activate ERK.

These results highlight that peptide 84 is in fact the one that shares the highest degree of similarity, at least in the experimental assays I conducted, with the native peptide Ac2-26. However, this data is in contrast to the p-ERK data which shows that peptide 57 is able to bind and activate the receptor to a similar extent as peptide 84, suggesting that although not showing a classical binding pattern to the FPR, it is still biologically active through this receptor. It is

plausible that other downstream signaling events are important, and activated, by Ac2-26 and its novel derivatives; moreover, different degree of activity can be present with respect to these 'un-identified' signaling responses. I wish to note that LXA₄, another agonist at FPRL1, activates and recruits SHP-2 (SH2 domain-containing tyrosine phosphatase-2) within a lipid raft microdomain, which in turn leads to the dephosphorylation of PDGFR β diminishing its mitogenic activities (Mitchell, O'Meara et al. 2007). Furthermore, LXA₄ has also been reported to lead to the dephosphorylation of MYH9, a nonmuscle myosin H chain (NMMHC) class IIA protein, which is involved in cytoskeleton rearrangement, a process that was observed to lead to an increase in phagocytosis of apoptotic leukocytes, an observation also reported for the Ac2-26 peptide (Maderna, Yona et al. 2005; Reville, Crean et al. 2006). A Real-time PCR analysis conducted on samples obtained from a animal model of anti-glomerular basement membrane (GBM) glomerulonephritis, where the animals were treated with (15-epi-16-(FPhO)-LXA-Me) or vehicle alone showed that treatment with the stable lipoxin analogue lead to the down regulation of a number of genes amongst which: Interferon regulatory factor 1 (IRF1), proteosome subunit, beta type 9 (PSM β 9), T cell-specific GTPase (TGTP), and IFN- γ -induced GTPase (IGTP) (Ohse, Ota et al. 2004). In light of the diverse effects that can be elicited through the FPRL1 receptor by LXA₄ I can now see how my analyses have been quite basic, aiming at establishing, predominantly, whether these new peptides were endowed with agonistic activity at FPRL1 (and by comparison, FPR). More importantly, my focus was by and large on the biological properties of these peptides.

The inhibitory potential was also assessed for both peptides by conducting a full concentration response analysis in the flow chamber assay. This analysis demonstrated that both peptides showed inhibitory properties down to 0.01 nM, with peptide 84 displaying a classical dose dependent response, whilst peptide 57 retained a similar level of activity down to the lowest concentration tested. An explanation for the observed difference in the ability of the two peptides to inhibit PMN recruitment could be possibly related to a different mode of activation of the FPR and FPRL1. In any case, it is clear that much more work is necessary for these issues to be unravelled to a degree of scientific satisfaction.

Finally when the inhibitory properties of peptides 57 and 84 were assessed *in vivo* in a preclinical model of PMN recruitment, both inhibited PMN recruitment into the air-pouch inflamed with IL-1 β . However, this observed reduction reached statistical significance only for peptide 84. Again, more experiments are required. An important observation I made, though, is that peptide 84 effect genuinely resulted from inhibition of cell recruitment into the air-pouch and was not secondary to a non-specific toxic effect exerted, for instance, on blood cell profiles. This apparent discrepancy between the results obtained from the *in vitro* assay and those obtained *in vivo* especially for peptide 57, could be due to the a difference in the ability of this peptide to activate the murine FPR family of receptors, which have been reported to show a reduced affinity to classical ligands such as fMLP. Moreover, could be influenced by pharmacokinetics issues, which clearly are not explored at all at these early stages of development.

In conclusion, peptide 84 with the α substitution seems to maintain most of the anti-inflammatory properties of the parent Ac2-26. Further work will determine if this new peptide is resistant to cleavage thus resulting in a better pharmacodynamic profile. In any case, I am happy to have contributed to put in motion a 'pharmaceutical project' that could take advantage from over 20 years of research on Annexin A1 and PMN recruitment in inflammation, possibly exploiting this wealth of knowledge for novel therapeutic development.

5. Conclusion

Studies published following the successful cloning of lipocortin-1 and its subsequent renaming to Annexin A1 have provided us with convincing evidence that Annexin A1 is a homeostatic endogenous anti-inflammatory mediator of the innate immune system. Although the link between the Annexin A1 pathway and inflammatory conditions is far from clear, the current study has for the first time provided evidence for a deregulation of this circuit in rheumatic conditions. In particular, I observed that there were elevated levels of cleaved Annexin A1 on the cell membranes of PMNs extracted from both Wegner granulomatosis and GCA patients. Furthermore both FPR and FPRL1 levels were elevated on PMNs and monocytes extracted from these patients. Over and above, my data have provided evidence in support of monitoring specific elements of the Annexin A1 pathway as potential biomarker of disease as well as to determine the efficacy of drug treatment upon effective disease management.

In line with this, the data obtained from flow chamber analysis on PMNs from vasculitis patients has evidenced that the addition of exogenous Annexin A1 was able to reduce leukocyte-endothelial interactions bringing them back to similar levels as those observed with control PMNs. Furthermore evidence was also provided implying Annexin A1 as a mediator of the anti-inflammatory effects observed in RA patients upon acute glucocorticoid treatment.

Furthermore this treatment was also observed to modulate the levels of Annexin A1 and FPRL1 positive microparticles in the plasma of these patients. This was another captivating outcome of my studies, hence the correlation, for the first

time, of Annexin A1 in PMN derived microparticles with their anti-inflammatory properties.

These microstructures inhibited cellular recruitment to an activated endothelial monolayer *in vitro* and reduced the reduction of cell recruitment into the mouse airpouch *in vivo*. Annexin A1 lacks a signal peptide but nonetheless is abundantly released from activated PMN. Thus these novel data indicate that Annexin A1 can be released from activated PMN *via* the ‘microparticle pathway’, hence multiple ways of mobilizing the protein from this cell type might exist. Annexin A1 is not unique in employing this mechanism of release, in fact the FPRL1 was also observed to be contained in these microparticles. Collectively, these observations allow me to hypothesise novel biological functions, so that the receptor contained in the microparticles might have a role in the time-dependent regulation of cell recruitment, though the exact dynamics governing these processes were not investigated during this study fueling scope for future studies.

The current notion is that microparticles are not just a by-product of cellular activation, but distinct entities produced through a highly regulated process. An observation which was in part confirmed by data produced during this study whereby differential stimulation of PMNs in suspension produced microparticles which in contrast to those produced upon co-incubation over an endothelial monolayer were able to produce reactive oxygen species. This ability was subsequently attributed to a distinct subset of the microparticle population, moreover this subset of the microparticle population was also

observed to be Annexin A1 negative.

A number of studies have highlighted altered microparticle populations in a number of systemic diseases, an observation that I corroborated here for patients suffering from Wegner granulomatosis, GCA and Rheumatoid arthritis. However, the published studies have monitored the degree of microparticles generated from the different cell sources (e.g. CD62L+ve or CD14+ve, for PMN and monocytes, respectively). My analyses have evolved around the determination of the levels of Annexin A1 or its receptor on these microstructures, identifying a deregulation in the number of Annexin A1 and FPRL1 positive microparticles in these inflammatory diseases, suggesting a further “mode of alteration” of the Annexin A1 pathway. Interestingly an acute glucocorticoid treatment had profound effects on this subset of microparticles, further corroborating the observation that these microstructures may not be just mere by-products of activation. The observed modulation of microparticle populations in disease, and upon therapeutic management, might suggest that different microparticle subsets could be useful indicators or biomarkers.

The development of safe and effective drugs is the ultimate quest of current major drug discovery programs. Peptides derived from the N-terminal portion of the Annexin A1 have been shown to retain the anti-inflammatory properties of the parent protein in several *in vivo* models. The *in vitro* and *in vivo* analysis conducted on the 5 new Annexin A1 N-terminal derived peptides pointed to peptides 57 and 84 as two potential candidates for use as anti-inflammatory drugs.

Interestingly in both these peptides the amino acid groups used to modify the parent Ac2-26 peptide were neither charged nor bulky suggesting that the three dimensional properties of these peptides, especially the alanine located in the initial alpha helical portion of the peptide, determine the level and extent of binding to the FPR family of receptors, in order to mediate their anti-inflammatory effects. Another interesting observation was that whilst peptide 59 was able to activate ERK to a similar extent to peptides 57 and 84, it did not display any anti-inflammatory properties as observed through both *in vitro* and *in vitro* analyses. On the other hand peptide 60 did not activate ERK through the FPRL1 receptor however it still displayed very strong inhibitory properties as determined by the flow chamber assay. It seems to me I can suggest that that ERK phosphorylation through FPRL1 is not discriminatory for mediating the anti-inflammatory effects of these peptides.

To reiterate and conclude, my results further advanced our understanding of the role of the Annexin A1 and other elements of this circuit (FPRL-1) in disease, providing for the first time a strong indication for a link between Annexin A1 and a number of rheumatic conditions. Furthermore, this study has also provided, for the first time, evidence suggesting that the anti-inflammatory actions of glucocorticoids in rheumatoid arthritis are associated with changes in the Annexin A1 pathway. Moreover this pathway is also important in mediating the anti-inflammatory properties of PMN derived microparticles and it is deregulated in the rheumatic conditions studied, a deregulation which seems to be reversed upon an acute glucocorticoid treatment. It is plausible that novel

Annexin A1 derived peptides could retain some of the anti-inflammatory actions of glucocorticoids and be developed as novel therapeutic tools, possibly effective in controlling the degree of leukocyte activation in the vasculature. Only the future will tell us if this possibility will become real!

6. References

Abid Hussein, M. N., E. W. Meesters, et al. (2003). "Antigenic characterization of endothelial cell-derived microparticles and their detection ex vivo." J Thromb Haemost **1**(11): 2434-43.

- Agouni, A., H. A. Mostefai, et al. (2007). "Sonic hedgehog carried by microparticles corrects endothelial injury through nitric oxide release." *Faseb J* **21**(11): 2735-41.
- Aktas, B., M. Pozgajova, et al. (2005). "Aspirin induces platelet receptor shedding via ADAM17 (TACE)." *J Biol Chem* **280**(48): 39716-22.
- Ali, H., R. M. Richardson, et al. (1999). "Chemoattractant receptor cross-desensitization." *J Biol Chem* **274**(10): 6027-30.
- Allport, J. R., H. T. Ding, et al. (1997). "L-selectin shedding does not regulate human neutrophil attachment, rolling, or transmigration across human vascular endothelium in vitro." *J Immunol* **158**(9): 4365-72.
- Amabile, N., A. P. Guerin, et al. (2005). "Circulating endothelial microparticles are associated with vascular dysfunction in patients with end-stage renal failure." *J Am Soc Nephrol* **16**(11): 3381-8.
- Asimakopoulos, G., K. M. Taylor, et al. (2000). "Inhibition of neutrophil L-selectin shedding: a potential anti-inflammatory effect of aprotinin." *Perfusion* **15**(6): 495-9.
- Babbin, B. A., M. G. Laukoetter, et al. (2008). "Annexin A1 regulates intestinal mucosal injury, inflammation, and repair." *J Immunol* **181**(7): 5035-44.
- Bae, Y. S., H. Y. Lee, et al. (2004). "Identification of peptides that antagonize formyl peptide receptor-like 1-mediated signaling." *J Immunol* **173**(1): 607-14.
- Barry, O. P., M. G. Kazanietz, et al. (1999). "Arachidonic acid in platelet microparticles up-regulates cyclooxygenase-2-dependent prostaglandin formation via a protein kinase C/mitogen-activated protein kinase-dependent pathway." *J Biol Chem* **274**(11): 7545-56.
- Barry, O. P., D. Pratico, et al. (1997). "Transcellular activation of platelets and endothelial cells by bioactive lipids in platelet microparticles." *J Clin Invest* **99**(9): 2118-27.
- Becker, E. L., F. A. Forouhar, et al. (1998). "Broad immunocytochemical localization of the formylpeptide receptor in human organs, tissues, and cells." *Cell Tissue Res* **292**(1): 129-35.
- Bellner, L., F. Thoren, et al. (2005). "A proinflammatory peptide from herpes simplex virus type 2 glycoprotein G affects neutrophil, monocyte, and NK cell functions." *J Immunol* **174**(4): 2235-41.
- Berckmans, R. J., R. Nieuwland, et al. (2005). "Synovial microparticles from arthritic patients modulate chemokine and cytokine release by synoviocytes." *Arthritis Res Ther* **7**(3): R536-44.
- Berridge, M. J. (1993). "Inositol trisphosphate and calcium signalling." *Nature* **361**(6410): 315-25.
- Blanchard, N., D. Lankar, et al. (2002). "TCR activation of human T cells induces the production of exosomes bearing the TCR/CD3/zeta complex." *J Immunol* **168**(7): 3235-41.
- Borregaard, N. and J. B. Cowland (1997). "Granules of the human neutrophilic polymorphonuclear leukocyte." *Blood* **89**(10): 3503-21.
- Boulay, F., M. Tardif, et al. (1990). "Synthesis and use of a novel N-formyl peptide derivative to isolate a human N-formyl peptide receptor cDNA." *Biochem Biophys Res Commun* **168**(3): 1103-9.
- Boulay, F., M. Tardif, et al. (1990). "The human N-formylpeptide receptor. Characterization of two cDNA isolates and evidence for a new

- subfamily of G-protein-coupled receptors." *Biochemistry* **29**(50): 11123-33.
- Braun, J. and R. Rau (2009). "An update on methotrexate." *Curr Opin Rheumatol* **21**(3): 216-23.
- Brenner, B., E. Gulbins, et al. (1996). "L-selectin activates the Ras pathway via the tyrosine kinase p56lck." *Proc Natl Acad Sci U S A* **93**(26): 15376-81.
- Brenner, B., S. Weinmann, et al. (1997). "L-selectin activates JNK via src-like tyrosine kinases and the small G-protein Rac." *Immunology* **92**(2): 214-9.
- Brent, L. H. (2009). "Inflammatory arthritis: an overview for primary care physicians." *Postgrad Med* **121**(2): 148-62.
- Buckingham, J. C. (1996). "Fifteenth Gaddum Memorial Lecture December 1994. Stress and the neuroendocrine-immune axis: the pivotal role of glucocorticoids and lipocortin 1." *Br J Pharmacol* **118**(1): 1-19.
- Bustin, S. A. (2002). "Quantification of mRNA using real-time reverse transcription PCR (RT-PCR): trends and problems." *J Mol Endocrinol* **29**(1): 23-39.
- Bustin, S. A., V. Benes, et al. (2005). "Quantitative real-time RT-PCR--a perspective." *J Mol Endocrinol* **34**(3): 597-601.
- Bustin, S. A. and T. Nolan (2004). "Pitfalls of quantitative real-time reverse-transcription polymerase chain reaction." *J Biomol Tech* **15**(3): 155-66.
- Butikofer, P., F. A. Kuypers, et al. (1989). "Enrichment of two glycosyl-phosphatidylinositol-anchored proteins, acetylcholinesterase and decay accelerating factor, in vesicles released from human red blood cells." *Blood* **74**(5): 1481-5.
- Bylund, J., A. Bjorstad, et al. (2003). "Reactivation of formyl peptide receptors triggers the neutrophil NADPH-oxidase but not a transient rise in intracellular calcium." *J Biol Chem* **278**(33): 30578-86.
- Bylund, J., A. Karlsson, et al. (2002). "Lipopolysaccharide-induced granule mobilization and priming of the neutrophil response to Helicobacter pylori peptide Hp(2-20), which activates formyl peptide receptor-like 1." *Infect Immun* **70**(6): 2908-14.
- Bylund, J., S. Pellme, et al. (2004). "Cytochalasin B triggers a novel pertussis toxin sensitive pathway in TNF-alpha primed neutrophils." *BMC Cell Biol* **5**: 21.
- Camps, M., A. Carozzi, et al. (1992). "Isozyme-selective stimulation of phospholipase C-beta 2 by G protein beta gamma-subunits." *Nature* **360**(6405): 684-6.
- Camussi, G., C. Tetta, et al. (1990). "Antiinflammatory peptides (antiflammins) inhibit synthesis of platelet-activating factor, neutrophil aggregation and chemotaxis, and intradermal inflammatory reactions." *J Exp Med* **171**(3): 913-27.
- Carey, F., R. Forder, et al. (1990). "Lipocortin 1 fragment modifies pyrogenic actions of cytokines in rats." *The American Journal of Physiology* **259**: R266-R269.
- Carollo, M., L. Parente, et al. (1998). "Dexamethasone-induced cytotoxic activity and drug resistance effects in androgen-independent prostate tumor PC-3 cells are mediated by lipocortin 1." *Oncol Res* **10**(5): 245-54.

- Chan, C. C., M. Ni, et al. (1991). "Effects of anti-inflammatories on endotoxin-induced uveitis in rats." *Arch Ophthalmol* **109**(2): 278-81.
- Chen, J., H. S. Bernstein, et al. (1995). "Tethered ligand library for discovery of peptide agonists." *J Biol Chem* **270**(40): 23398-401.
- Chiang, N., I. M. Fierro, et al. (2000). "Activation of lipoxin A(4) receptors by aspirin-triggered lipoxins and select peptides evokes ligand-specific responses in inflammation." *J Exp Med* **191**(7): 1197-208.
- Christophe, T., A. Karlsson, et al. (2001). "The synthetic peptide Trp-Lys-Tyr-Met-Val-Met-NH₂ specifically activates neutrophils through FPRL1/lipoxin A4 receptors and is an agonist for the orphan monocyte-expressed chemoattractant receptor FPRL2." *J Biol Chem* **276**(24): 21585-93.
- Cirino, G., R. J. Flower, et al. (1987). "Recombinant human lipocortin 1 inhibits thromboxane release from guinea-pig isolated perfused lung." *Nature* **328**(6127): 270-2.
- Cirino, G., S. H. Peers, et al. (1989). "Human recombinant lipocortin 1 has acute local anti-inflammatory properties in the rat paw edema test." *Proc Natl Acad Sci USA* **86**: 3428-3432.
- Combe, B. (2007). "Early rheumatoid arthritis: strategies for prevention and management." *Best Pract Res Clin Rheumatol* **21**(1): 27-42.
- Combes, V., A. C. Simon, et al. (1999). "In vitro generation of endothelial microparticles and possible prothrombotic activity in patients with lupus anticoagulant." *J Clin Invest* **104**(1): 93-102.
- Crumpton, M. J. and J. R. Dedman (1990). "Protein terminology tangle." *Nature* **345**(6272): 212.
- Cruz, B. A., J. Ramanoelina, et al. (2003). "Prognosis and outcome of 26 patients with systemic necrotizing vasculitis admitted to the intensive care unit." *Rheumatology (Oxford)* **42**(10): 1183-8.
- Csernok, E., P. Lamprecht, et al. (2006). "Diagnostic significance of ANCA in vasculitis." *Nat Clin Pract Rheumatol* **2**(4): 174-5.
- Cuzzocrea, S., A. Taylor, et al. (1997). "Lipocortin 1 protects against splanchnic artery occlusion and reperfusion injury by affecting neutrophil migration." *The Journal of Immunology* **159**: 5089-5097.
- Czech, M. P. (2000). "Lipid rafts and insulin action." *Nature* **407**(6801): 147-8.
- D'Amico, M., C. Di Filippo, et al. (2000). "Lipocortin 1 reduces myocardial ischaemia-reperfusion injury by affecting local leukocyte recruitment." *FASEB J.* **14**: 1867-1869.
- Da Silva, J. A., J. W. Jacobs, et al. (2006). "Safety of low dose glucocorticoid treatment in rheumatoid arthritis: published evidence and prospective trial data." *Ann Rheum Dis* **65**(3): 285-93.
- Dadfar, E., J. Lundahl, et al. (2004). "Leukocyte CD11b and CD62l expression in response to interstitial inflammation in CAPD patients." *Perit Dial Int* **24**(1): 28-36.
- Dahlgren, C. (1987). "Difference in extracellular radical release after chemotactic factor and calcium ionophore activation of the oxygen radical-generating system in human neutrophils." *Biochim Biophys Acta* **930**(1): 33-8.
- Dahlgren, C., T. Christophe, et al. (2000). "The synthetic chemoattractant Trp-Lys-Tyr-Met-Val-DMet activates neutrophils preferentially through the lipoxin A(4) receptor." *Blood* **95**(5): 1810-8.

- Dale, D. C., A. S. Fauci, et al. (1975). "Comparison of agents producing a neutrophilic leukocytosis in man. Hydrocortisone, prednisone, endotoxin, and etiocholanolone." *J Clin Invest* **56**(4): 808-13.
- Dalpiatz, A., M. E. Ferretti, et al. (2002). "C- and N-terminal residue effect on peptide derivatives' antagonism toward the formyl-peptide receptor." *Eur J Pharmacol* **436**(3): 187-96.
- Dalpiatz, A., R. Pecoraro, et al. (1999). "Formylpeptide receptor antagonists: structure and activity." *Boll Chim Farm* **138**(3): 44-8.
- Damazo, A. S., S. Yona, et al. (2006). "Spatial and Temporal Profiles for Anti-Inflammatory Gene Expression in Leukocytes during a Resolving Model of Peritonitis." *J Immunol* **176**(7): 4410-8.
- Daniel, L., F. Fakhouri, et al. (2006). "Increase of circulating neutrophil and platelet microparticles during acute vasculitis and hemodialysis." *Kidney Int* **69**(8): 1416-23.
- Das, A. M., L. H. Lim, et al. (1997). "Dexamethasone reduces cell surface levels of CD11b on human eosinophils." *Mediators Inflamm* **6**(5-6): 363-7.
- Dasgupta, B. and N. Hassan (2007). "Giant cell arteritis: recent advances and guidelines for management." *Clin Exp Rheumatol* **25**(1 Suppl 44): S62-5.
- Dasgupta, B., A. Hutchings, et al. (2006). "Polymyalgia rheumatica: the mess we are now in and what we need to do about it." *Arthritis Rheum* **55**(4): 518-20.
- Davies-Cox, E. V., I. Laffafian, et al. (2001). "Control of Ca²⁺ influx in human neutrophils by inositol 1,4,5-trisphosphate (IP₃) binding: differential effects of micro-injected IP₃ receptor antagonists." *Biochem J* **355**(Pt 1): 139-43.
- de Coupade, C., E. Solito, et al. (2003). "Dexamethasone enhances interaction of endogenous annexin 1 with L-selectin and triggers shedding of L-selectin in the monocytic cell line U-937." *Br J Pharmacol* **140**(1): 133-45.
- De, Y., Q. Chen, et al. (2000). "LL-37, the neutrophil granule- and epithelial cell-derived cathelicidin, utilizes formyl peptide receptor-like 1 (FPRL1) as a receptor to chemoattract human peripheral blood neutrophils, monocytes, and T cells." *J Exp Med* **192**(7): 1069-74.
- Denzer, K., M. J. Kleijmeer, et al. (2000). "Exosome: from internal vesicle of the multivesicular body to intercellular signaling device." *J Cell Sci* **113 Pt 19**: 3365-74.
- Devauchelle-Pensec, V., S. Jousse, et al. (2008). "Epidemiology, imaging, and treatment of giant cell arteritis." *Joint Bone Spine* **75**(3): 267-72.
- Distler, J. H., L. C. Huber, et al. (2005). "The release of microparticles by apoptotic cells and their effects on macrophages." *Apoptosis* **10**(4): 731-41.
- Distler, J. H., D. S. Pisetsky, et al. (2005). "Microparticles as regulators of inflammation: novel players of cellular crosstalk in the rheumatic diseases." *Arthritis Rheum* **52**(11): 3337-48.
- Dougados, M., B. Combe, et al. (1999). "Combination therapy in early rheumatoid arthritis: a randomised, controlled, double blind 52 week clinical trial of sulphasalazine and methotrexate compared with the single components." *Ann Rheum Dis* **58**(4): 220-5.

- Dowling, D. K. and L. W. Simmons (2009). "Reactive oxygen species as universal constraints in life-history evolution." Proc Biol Sci **276**(1663): 1737-45.
- Durstin, M., J. L. Gao, et al. (1994). "Differential expression of members of the N-formylpeptide receptor gene cluster in human phagocytes." Biochem Biophys Res Commun **201**(1): 174-9.
- Edwards, B. S., C. Bologna, et al. (2005). "Integration of virtual screening with high-throughput flow cytometry to identify novel small molecule formylpeptide receptor antagonists." Mol Pharmacol **68**(5): 1301-10.
- Erdbruegger, U., M. Grossheim, et al. (2008). "Diagnostic role of endothelial microparticles in vasculitis." Rheumatology (Oxford) **47**(12): 1820-5.
- Ernst, S., C. Lange, et al. (2004). "An annexin 1 N-terminal peptide activates leukocytes by triggering different members of the formyl peptide receptor family." J Immunol **172**(12): 7669-76.
- Errasfa, M., B. Rothhut, et al. (1985). "The presence of lipocortin in human embryonic skin fibroblasts and its regulation by anti-inflammatory steroids." Biochim Biophys Acta **847**(2): 247-54.
- Everton Andrades, M., C. Ritter, et al. (2009). "The role of free radicals in sepsis development." Front Biosci (Elite Ed) **1**: 277-87.
- Fauci, A. S. and D. C. Dale (1975). "The effect of Hydrocortisone on the kinetics of normal human lymphocytes." Blood **46**(2): 235-43.
- Ferlazzo, V., P. D'Agostino, et al. (2003). "Anti-inflammatory effects of annexin-1: stimulation of IL-10 release and inhibition of nitric oxide synthesis." Int Immunopharmacol **3**(10-11): 1363-9.
- Fierro, I. M., S. P. Colgan, et al. (2003). "Lipoxin A4 and aspirin-triggered 15-epi-lipoxin A4 inhibit human neutrophil migration: comparisons between synthetic 15 epimers in chemotaxis and transmigration with microvessel endothelial cells and epithelial cells." J Immunol **170**(5): 2688-94.
- Filep, J. G., C. Zouki, et al. (1999). "Anti-inflammatory actions of lipoxin A(4) stable analogs are demonstrable in human whole blood: modulation of leukocyte adhesion molecules and inhibition of neutrophil-endothelial interactions." Blood **94**(12): 4132-42.
- Finn, A., S. Strobel, et al. (1994). "Endotoxin-induced neutrophil adherence to endothelium: relationship to CD11b/CD18 and L-selectin expression and matrix disruption." Ann N Y Acad Sci **725**: 173-82.
- Flower, R. J. (1988). "Lipocortin and the mechanism of action of the glucocorticoids." Br J Pharmacol **94**: 987-1015.
- Forlow, S. B., R. P. McEver, et al. (2000). "Leukocyte-leukocyte interactions mediated by platelet microparticles under flow." Blood **95**(4): 1317-23.
- Francis, J. W., K. J. Balazovich, et al. (1992). "Human neutrophil annexin I promotes granule aggregation and modulates Ca(2+)-dependent membrane fusion." J Clin Invest **90**(2): 537-44.
- Freer, R. J., A. R. Day, et al. (1980). "Further studies on the structural requirements for synthetic peptide chemoattractants." Biochemistry **19**(11): 2404-10.
- Fu, H., J. Bylund, et al. (2004). "The mechanism for activation of the neutrophil NADPH-oxidase by the peptides formyl-Met-Leu-Phe and Trp-Lys-Tyr-Met-Val-Met differs from that for interleukin-8." Immunology **112**(2): 201-10.

- Fu, H., C. Dahlgren, et al. (2003). "Subinhibitory concentrations of the deformylase inhibitor actinonin increase bacterial release of neutrophil-activating peptides: a new approach to antimicrobial chemotherapy." Antimicrob Agents Chemother **47**(8): 2545-50.
- Fujimi, S., H. Ogura, et al. (2003). "Increased production of leukocyte microparticles with enhanced expression of adhesion molecules from activated polymorphonuclear leukocytes in severely injured patients." J Trauma **54**(1): 114-9; discussion 119-20.
- Gabriel, S. E., C. S. Crowson, et al. (2003). "Survival in rheumatoid arthritis: a population-based analysis of trends over 40 years." Arthritis Rheum **48**(1): 54-8.
- Gao, J. L., E. L. Becker, et al. (1994). "A high potency nonformylated peptide agonist for the phagocyte N-formylpeptide chemotactic receptor." J Exp Med **180**(6): 2191-7.
- Gao, J. L., E. J. Lee, et al. (1999). "Impaired antibacterial host defense in mice lacking the N-formylpeptide receptor." J Exp Med **189**(4): 657-662.
- Gasser, O., C. Hess, et al. (2003). "Characterisation and properties of ectosomes released by human polymorphonuclear neutrophils." Exp Cell Res **285**(2): 243-57.
- Gasser, O. and J. A. Schifferli (2004). "Activated polymorphonuclear neutrophils disseminate anti-inflammatory microparticles by ectocytosis." Blood **104**(8): 2543-8.
- Gavins, F. N., J. Dalli, et al. (2007). "Activation of the annexin 1 counter-regulatory circuit affords protection in the mouse brain microcirculation." Faseb J.
- Gavins, F. N., S. Yona, et al. (2003). "Leukocyte antiadhesive actions of annexin 1: ALXR- and FPR-related anti-inflammatory mechanisms." Blood **101**(10): 4140-7.
- Gerke, V., C. E. Creutz, et al. (2005). "Annexins: linking Ca²⁺ signalling to membrane dynamics." Nat Rev Mol Cell Biol **6**(6): 449-61.
- Gerke, V. and S. E. Moss (2002). "Annexins: from structure to function." Physiol Rev **82**(2): 331-71.
- Getting, S. J., R. J. Flower, et al. (1997). "Inhibition of neutrophil and monocyte recruitment by endogenous and exogenous lipocortin 1." British Journal of Pharmacology **120**: 1075-1082.
- Giner, R. M., L. Mancini, et al. (2007). "Uneven modulation of the annexin 1 system in osteoblast-like cells by dexamethasone." Biochem Biophys Res Commun **354**(2): 414-9.
- Gomez-Gaviro, M. V., C. Dominguez-Jimenez, et al. (2000). "Down-regulation of L-selectin expression in neutrophils by nonsteroidal anti-inflammatory drugs: role of intracellular ATP concentration." Blood **96**(10): 3592-600.
- Goulding, N. J., H. S. Euzger, et al. (1998). "Novel pathways for glucocorticoid effects on neutrophils in chronic inflammation." Inflamm Res **47 Suppl 3**: S158-65.
- Goulding, N. J., J. L. Godolphin, et al. (1990). "Anti-inflammatory lipocortin 1 production by peripheral blood leucocytes in response to hydrocortisone." The Lancet **335**: 1416-1418.

- Goulding, N. J., C. M. Jefferiss, et al. (1992). "Specific binding of lipocortin-1 (annexin I) to monocytes and neutrophils is decreased in rheumatoid arthritis." *Arth Rheum* **35**: 1395-1397.
- Goulding, N. J., L. Pan, et al. (1996). "Evidence for specific annexin I-binding proteins on human monocytes." *Biochemical Journal* **316**: 593-597.
- Goulding, N. J., M. R. Podgorski, et al. (1989). "Autoantibodies to recombinant lipocortin-1 in rheumatoid arthritis and systemic lupus erythematosus." *Ann Rheum Dis* **48**(10): 843-50.
- Gripentrog, J. M. and H. M. Miettinen (2008). "Formyl peptide receptor-mediated ERK1/2 activation occurs through G(i) and is not dependent on beta-arrestin1/2." *Cell Signal* **20**(2): 424-31.
- Gross, W. L., W. H. Schmitt, et al. (1993). "ANCA and associated diseases: immunodiagnostic and pathogenetic aspects." *Clin Exp Immunol* **91**(1): 1-12.
- Guler-Yuksel, M., J. Bijsterbosch, et al. (2008). "Changes in bone mineral density in patients with recent onset, active rheumatoid arthritis." *Ann Rheum Dis* **67**(6): 823-8.
- Hafezi-Moghadam, A. and K. Ley (1999). "Relevance of L-selectin shedding for leukocyte rolling in vivo." *J Exp Med* **189**(6): 939-48.
- Hafezi-Moghadam, A., K. L. Thomas, et al. (2001). "L-selectin shedding regulates leukocyte recruitment." *J Exp Med* **193**(7): 863-72.
- Hattori, T., H. Komoda, et al. (1998). "Decline of anti-DP107 antibody associated with clinical progression." *Aids* **12**(12): 1557-9.
- Haviland, D. L., A. C. Borel, et al. (1993). "Structure, 5'-flanking sequence, and chromosome location of the human N-formyl peptide receptor gene. A single-copy gene comprised of two exons on chromosome 19q.13.3 that yields two distinct transcripts by alternative polyadenylation." *Biochemistry* **32**(16): 4168-74.
- Hayhoe, R. P., A. M. Kamal, et al. (2006). "Annexin 1 and its bioactive peptide inhibit neutrophil-endothelium interactions under flow: indication of distinct receptor involvement." *Blood* **107**(5): 2123-30.
- Heit, B., S. Tavener, et al. (2002). "An intracellular signaling hierarchy determines direction of migration in opposing chemotactic gradients." *J Cell Biol* **159**(1): 91-102.
- Hench, P. S. (1950). "Introduction: cortisone and ACTH in clinical medicine." *Proc Staff Meet Mayo Clin* **25**(17): 474-6.
- Hentzen, E. R., S. Neelamegham, et al. (2000). "Sequential binding of CD11a/CD18 and CD11b/CD18 defines neutrophil capture and stable adhesion to intercellular adhesion molecule-1." *Blood* **95**(3): 911-20.
- Hilgenberg, L. and K. Miles (1995). "Developmental regulation of a protein kinase C isoform localized in the neuromuscular junction." *J Cell Sci* **108 (Pt 1)**: 51-61.
- Hiraoka, N., B. Petryniak, et al. (1999). "A novel, high endothelial venule-specific sulfotransferase expresses 6-sulfo sialyl Lewis(x), an L-selectin ligand displayed by CD34." *Immunity* **11**(1): 79-89.
- Hollenberg, M. D., K. A. Valentine-Braun, et al. (1988). "Protein tyrosine kinase substrates: Rosetta stones or simply structural elements?" *Trends Pharmacol Sci* **9**(2): 63-6.
- Horstman, L. L., W. Jy, et al. (2004). "New horizons in the analysis of circulating cell-derived microparticles." *Keio J Med* **53**(4): 210-30.

- Hristov, M., W. Erl, et al. (2004). "Apoptotic bodies from endothelial cells enhance the number and initiate the differentiation of human endothelial progenitor cells in vitro." Blood **104**(9): 2761-6.
- Hu, J. Y., Y. Le, et al. (2001). "Synthetic peptide MMK-1 is a highly specific chemotactic agonist for leukocyte FPRL1." J Leukoc Biol **70**(1): 155-61.
- Hugel, B., M. C. Martinez, et al. (2005). "Membrane microparticles: two sides of the coin." Physiology (Bethesda) **20**: 22-7.
- Hughes, M., C. P. Hayward, et al. (2000). "Morphological analysis of microparticle generation in heparin-induced thrombocytopenia." Blood **96**(1): 188-94.
- Jaffe, E. A., R. L. Nachman, et al. (1973). "Culture of human endothelial cells derived from umbilical veins. Identification by morphologic and immunologic criteria." J Clin Invest **52**(11): 2745-56.
- Jahnova, E., M. Horvathova, et al. (1998). "Expression of adhesion molecules and effect of disodium cromoglycate treatment in asthmatics." Physiol Res **47**(6): 439-43.
- Janmey, P. A. (1994). "Phosphoinositides and calcium as regulators of cellular actin assembly and disassembly." Annu Rev Physiol **56**: 169-91.
- Jayne, D. (2003). "Current attitudes to the therapy of vasculitis." Kidney Blood Press Res **26**(4): 231-9.
- Jennette, J. C., H. Xiao, et al. (2006). "Pathogenesis of vascular inflammation by anti-neutrophil cytoplasmic antibodies." J Am Soc Nephrol **17**(5): 1235-42.
- Jimenez, J. J., W. Jy, et al. (2003). "Endothelial cells release phenotypically and quantitatively distinct microparticles in activation and apoptosis." Thromb Res **109**(4): 175-80.
- Jodo, S., S. Xiao, et al. (2001). "Apoptosis-inducing membrane vesicles. A novel agent with unique properties." J Biol Chem **276**(43): 39938-44.
- John, C., P. Cover, et al. (2002). "Annexin 1-dependent actions of glucocorticoids in the anterior pituitary gland: roles of the N-terminal domain and protein kinase C." Endocrinology **143**(8): 3060-70.
- Joseph, J. E., P. Harrison, et al. (2001). "Increased circulating platelet-leucocyte complexes and platelet activation in patients with antiphospholipid syndrome, systemic lupus erythematosus and rheumatoid arthritis." Br J Haematol **115**(2): 451-9.
- Jy, W., J. J. Jimenez, et al. (2002). "Agonist-induced capping of adhesion proteins and microparticle shedding in cultures of human renal microvascular endothelial cells." Endothelium **9**(3): 179-89.
- Kamal, A. M., R. P. Hayhoe, et al. (2006). "Antiflammin-2 activates the human formyl-peptide receptor like 1." ScientificWorldJournal **6**: 1375-84.
- Kantari, C., M. Pederzoli-Ribeil, et al. (2007). "Proteinase 3, the Wegener autoantigen, is externalized during neutrophil apoptosis: evidence for a functional association with phospholipid scramblase 1 and interference with macrophage phagocytosis." Blood **110**(12): 4086-95.
- Karlsson, J., H. Fu, et al. (2005). "Neutrophil NADPH-oxidase activation by an annexin AI peptide is transduced by the formyl peptide receptor (FPR), whereas an inhibitory signal is generated independently of the FPR family receptors." J Leukoc Biol **78**(3): 762-771.

- Klein, C., J. I. Paul, et al. (1998). "Identification of surrogate agonists for the human FPRL-1 receptor by autocrine selection in yeast." Nat Biotechnol **16**(13): 1334-7.
- Klotz, K. N. and A. J. Jesaitis (1994). "Neutrophil chemoattractant receptors and the membrane skeleton." Bioessays **16**(3): 193-8.
- Knijff-Dutmer, E. A., J. Koerts, et al. (2002). "Elevated levels of platelet microparticles are associated with disease activity in rheumatoid arthritis." Arthritis Rheum **46**(6): 1498-503.
- Kobayashi, T., H. Kimura, et al. (2007). "Increased CD11b expression on polymorphonuclear leucocytes and cytokine profiles in patients with Kawasaki disease." Clin Exp Immunol **148**(1): 112-8.
- La, M., M. D'Amico, et al. (2001). "Annexin 1 peptides protect against experimental myocardial ischemia- reperfusion: analysis of their mechanism of action." Faseb J **15**(12): 2247-56.
- Lacy, M., J. Jones, et al. (1995). "Expression of the receptors for the C5a anaphylatoxin, interleukin-8 and FMLP by human astrocytes and microglia." J Neuroimmunol **61**(1): 71-8.
- Lambert, M. P., A. K. Barlow, et al. (1998). "Diffusible, nonfibrillar ligands derived from Abeta1-42 are potent central nervous system neurotoxins." Proc Natl Acad Sci U S A **95**(11): 6448-53.
- Lard, L. R., F. P. Mul, et al. (1999). "Neutrophil activation in sickle cell disease." J Leukoc Biol **66**(3): 411-5.
- Lawrence, M. B., L. V. McIntire, et al. (1987). "Effect of flow on polymorphonuclear leukocyte/endothelial cell adhesion." Blood **70**(5): 1284-90.
- Le Gall, S. M., P. Bobe, et al. (2009). "ADAMs 10 and 17 represent differentially regulated components of a general shedding machinery for membrane proteins such as transforming growth factor alpha, L-selectin, and tumor necrosis factor alpha." Mol Biol Cell **20**(6): 1785-94.
- Le, Y., W. Gong, et al. (1999). "Utilization of two seven-transmembrane, G protein-coupled receptors, formyl peptide receptor-like 1 and formyl peptide receptor, by the synthetic hexapeptide WKYVM for human phagocyte activation." J Immunol **163**(12): 6777-84.
- Le, Y., S. Jiang, et al. (2000). "N36, a synthetic N-terminal heptad repeat domain of the HIV-1 envelope protein gp41, is an activator of human phagocytes." Clin Immunol **96**(3): 236-42.
- Le, Y., B. Li, et al. (2000). "Novel pathophysiological role of classical chemotactic peptide receptors and their communications with chemokine receptors." Immunol Rev **177**: 185-94.
- Le, Y., P. M. Murphy, et al. (2002). "Formyl-peptide receptors revisited." Trends Immunol **23**(11): 541-8.
- Le, Y., J. J. Oppenheim, et al. (2001). "Pleiotropic roles of formyl peptide receptors." Cytokine Growth Factor Rev **12**(1): 91-105.
- Le, Y., R. D. Ye, et al. (2005). "Identification of functional domains in the formyl peptide receptor-like 1 for agonist-induced cell chemotaxis." Febs J **272**(3): 769-78.
- Leroyer, A. S., H. Isobe, et al. (2007). "Cellular origins and thrombogenic activity of microparticles isolated from human atherosclerotic plaques." J Am Coll Cardiol **49**(7): 772-7.

- Levy, B. D., V. V. Fokin, et al. (1999). "Polyisoprenyl phosphate (PIPP) signaling regulates phospholipase D activity: a 'stop' signaling switch for aspirin-triggered lipoxin A4." Faseb J **13**(8): 903-11.
- Levy, B. D. and C. N. Serhan (2003). "Exploring new approaches to the treatment of asthma: potential roles for lipoxins and aspirin-triggered lipid mediators." Drugs Today (Barc) **39**(5): 373-84.
- Lim, L. H., R. J. Flower, et al. (2000). "Glucocorticoid receptor activation reduces CD11b and CD49d levels on murine eosinophils: characterization and functional relevance." Am J Respir Cell Mol Biol **22**(6): 693-701.
- Lim, L. H., E. Solito, et al. (1998). "Promoting detachment of neutrophils adherent to murine postcapillary venules to control inflammation: effect of lipocortin 1." Proc Natl Acad Sci U S A **95**(24): 14535-9.
- Liu, N. K., Y. P. Zhang, et al. (2007). "Annexin A1 reduces inflammatory reaction and tissue damage through inhibition of phospholipase A2 activation in adult rats following spinal cord injury." J Neuropathol Exp Neurol **66**(10): 932-43.
- Liu, Q., T. K. Kishimoto, et al. (1998). "Dynamic expression of L-selectin in cell-to-cell interactions between neutrophils and endothelial cells in vitro." Exp Cell Res **243**(1): 87-93.
- Lu, H., C. W. Smith, et al. (1997). "LFA-1 is sufficient in mediating neutrophil emigration in Mac-1-deficient mice." J Clin Invest **99**(6): 1340-50.
- Luscinskas, F. W., M. I. Cybulsky, et al. (1991). "Cytokine-activated human endothelial monolayers support enhanced neutrophil transmigration via a mechanism involving both endothelial-leukocyte adhesion molecule-1 and intercellular adhesion molecule-1." J Immunol **146**(5): 1617-25.
- Mack, M., A. Kleinschmidt, et al. (2000). "Transfer of the chemokine receptor CCR5 between cells by membrane-derived microparticles: a mechanism for cellular human immunodeficiency virus 1 infection." Nat Med **6**(7): 769-75.
- MacKenzie, A., H. L. Wilson, et al. (2001). "Rapid secretion of interleukin-1beta by microvesicle shedding." Immunity **15**(5): 825-35.
- Maderna, P., S. Yona, et al. (2005). "Modulation of phagocytosis of apoptotic neutrophils by supernatant from dexamethasone-treated macrophages and annexin-derived peptide Ac2-26." J Immunol **174**(6): 3727-3733.
- Martin, G. R., M. Perretti, et al. (2008). "Annexin-1 modulates repair of gastric mucosal injury." Am J Physiol Gastrointest Liver Physiol **294**(3): G764-9.
- Martinez, M. C., A. Tesse, et al. (2005). "Shed membrane microparticles from circulating and vascular cells in regulating vascular function." Am J Physiol Heart Circ Physiol **288**(3): H1004-9.
- McCoy, R., D. L. Haviland, et al. (1995). "N-formylpeptide and complement C5a receptors are expressed in liver cells and mediate hepatic acute phase gene regulation." J Exp Med **182**(1): 207-17.
- Meerschaert, J. and M. B. Furie (1995). "The adhesion molecules used by monocytes for migration across endothelium include CD11a/CD18, CD11b/CD18, and VLA-4 on monocytes and ICAM-1, VCAM-1, and other ligands on endothelium." J Immunol **154**(8): 4099-112.

- Merrill, J. E., L. J. Ignarro, et al. (1993). "Microglial cell cytotoxicity of oligodendrocytes is mediated through nitric oxide." J Immunol **151**(4): 2132-41.
- Mesri, M. and D. C. Altieri (1998). "Endothelial cell activation by leukocyte microparticles." J Immunol **161**(8): 4382-7.
- Miele, L., E. Cordella-Miele, et al. (1988). "Novel anti-inflammatory peptides from the region of highest similarity between uteroglobin and lipocortin I." Nature **335**(6192): 726-30.
- Migeotte, I., E. Riboldi, et al. (2005). "Identification and characterization of an endogenous chemotactic ligand specific for FPRL2." J Exp Med **201**(1): 83-93.
- Miller, A. F. and J. J. Falke (2004). "Chemotaxis receptors and signaling." Adv Protein Chem **68**: 393-444.
- Mills, J. S., H. M. Miettinen, et al. (2000). "Characterization of the binding site on the formyl peptide receptor using three receptor mutants and analogs of Met-Leu-Phe and Met-Met-Trp-Leu-Leu." J Biol Chem **275**(50): 39012-7.
- Milstein, C., G. G. Brownlee, et al. (1972). "A possible precursor of immunoglobulin light chains." Nat New Biol **239**(91): 117-20.
- Mitchell, D., S. J. O'Meara, et al. (2007). "The Lipoxin A4 receptor is coupled to SHP-2 activation: implications for regulation of receptor tyrosine kinases." J Biol Chem **282**(21): 15606-18.
- Miyazaki, Y., S. Nomura, et al. (1996). "High shear stress can initiate both platelet aggregation and shedding of procoagulant containing microparticles." Blood **88**(9): 3456-64.
- Molad, Y., J. Buyon, et al. (1994). "Intravascular neutrophil activation in systemic lupus erythematosus (SLE): dissociation between increased expression of CD11b/CD18 and diminished expression of L-selectin on neutrophils from patients with active SLE." Clin Immunol Immunopathol **71**(3): 281-6.
- Monleon, I., M. J. Martinez-Lorenzo, et al. (2001). "Differential secretion of Fas ligand- or APO2 ligand/TNF-related apoptosis-inducing ligand-carrying microvesicles during activation-induced death of human T cells." J Immunol **167**(12): 6736-44.
- Montoya, M. C., F. W. Luscinskas, et al. (1997). "Reduced intracellular oxidative metabolism promotes firm adhesion of human polymorphonuclear leukocytes to vascular endothelium under flow conditions." Eur J Immunol **27**(8): 1942-51.
- Morand, E. F. (2007). "Effects of glucocorticoids on inflammation and arthritis." Curr Opin Rheumatol **19**(3): 302-7.
- Morand, E. F., P. Hall, et al. (2006). "Regulation of annexin I in rheumatoid synovial cells by glucocorticoids and interleukin-1." Mediators Inflamm **2006**(2): 73835.
- Morand, E. F., C. M. Jefferiss, et al. (1994). "Impaired glucocorticoid induction of mononuclear leukocyte lipocortin-1 in rheumatoid arthritis." Arthritis Rheum **37**(2): 207-11.
- Morgan, M. J., Y. S. Kim, et al. (2008). "TNFalpha and reactive oxygen species in necrotic cell death." Cell Res **18**(3): 343-9.

- Mostefai, H. A., F. Meziani, et al. (2008). "Circulating microparticles from patients with septic shock exert protective role in vascular function." Am J Respir Crit Care Med **178**(11): 1148-55.
- Moutray, T. N., M. A. Williams, et al. (2008). "Suspected giant cell arteritis: a study of referrals for temporal artery biopsy." Can J Ophthalmol **43**(4): 445-8.
- Movitz, C., C. Sjolín, et al. (1999). "Cleavage of annexin I in human neutrophils is mediated by a membrane-localized metalloprotease." Biochim Biophys Acta **1416**(1-2): 101-8.
- Murphy, P. M. (1994). "The molecular biology of leukocyte chemoattractant receptors." Annu Rev Immunol **12**: 593-633.
- Murphy, P. M. (1997). "Neutrophil receptors for interleukin-8 and related CXC chemokines." Semin Hematol **34**(4): 311-8.
- Murphy, P. M. and D. McDermott (1991). "Functional expression of the human formyl peptide receptor in *Xenopus* oocytes requires a complementary human factor." J Biol Chem **266**(19): 12560-7.
- Murphy, P. M., T. Ozcelik, et al. (1992). "A structural homologue of the N-formyl peptide receptor. Characterization and chromosome mapping of a peptide chemoattractant receptor family." J Biol Chem **267**(11): 7637-43.
- Murphy, P. M., H. L. Tiffany, et al. (1993). "Sequence and organization of the human N-formyl peptide receptor-encoding gene." Gene **133**(2): 285-90.
- Nauta, A. J., L. A. Trouw, et al. (2002). "Direct binding of C1q to apoptotic cells and cell blebs induces complement activation." Eur J Immunol **32**(6): 1726-36.
- Nieuwland, R., R. J. Berckmans, et al. (2000). "Cellular origin and procoagulant properties of microparticles in meningococcal sepsis." Blood **95**(3): 930-5.
- Niggli, V. (2003). "Signaling to migration in neutrophils: importance of localized pathways." Int J Biochem Cell Biol **35**(12): 1619-38.
- Noguera, A., X. Busquets, et al. (1998). "Expression of adhesion molecules and G proteins in circulating neutrophils in chronic obstructive pulmonary disease." Am J Respir Crit Care Med **158**(5 Pt 1): 1664-8.
- Nurden, P. (1997). "Bidirectional trafficking of membrane glycoproteins following platelet activation in suspension." Thromb Haemost **78**(5): 1305-15.
- Ohse, T., T. Ota, et al. (2004). "Modulation of interferon-induced genes by lipoxin analogue in anti-glomerular basement membrane nephritis." J Am Soc Nephrol **15**(4): 919-27.
- Oliani, S. M., H. C. Christian, et al. (2000). "An immunocytochemical and in situ hybridization analysis of annexin 1 expression in rat mast cells: modulation by inflammation and dexamethasone." Lab Invest **80**(9): 1429-1438.
- Oliani, S. M., M. J. Paul-Clark, et al. (2001). "Neutrophil interaction with inflamed postcapillary venule endothelium alters annexin 1 expression." Am J Pathol **158**(2): 603-15.
- Olivieri, O., S. Lombardi, et al. (1998). "Increased neutrophil adhesive capability in Cohen syndrome, an autosomal recessive disorder associated with granulocytopenia." Haematologica **83**(9): 778-82.

- Omer, S., D. Meredith, et al. (2006). "Evidence for the role of adenosine 5'-triphosphate-binding cassette (ABC)-A1 in the externalization of annexin 1 from pituitary folliculostellate cells and ABCA1-transfected cell models." *Endocrinology* **147**(7): 3219-27.
- Pachter, J. S. (1997). "Inflammatory mechanisms in Alzheimer disease: the role of beta-amyloid/glial interactions." *Mol Psychiatry* **2**(2): 91-5.
- Paschall, C. D. and M. B. Lawrence (2008). "L-selectin shear thresholding modulates leukocyte secondary capture." *Ann Biomed Eng* **36**(4): 622-31.
- Patel, K. D. (1999). "Mechanisms of selective leukocyte recruitment from whole blood on cytokine-activated endothelial cells under flow conditions." *J Immunol* **162**(10): 6209-16.
- Peers, S. H., F. Smillie, et al. (1993). "Glucocorticoid- and non-glucocorticoid induction of lipocortins (annexins) 1 and 2 in rat peritoneal leucocytes *in vivo*." *British Journal of Pharmacology* **108**: 66-72.
- Perez, H. D., R. Holmes, et al. (1992). "Cloning of the gene coding for a human receptor for formyl peptides. Characterization of a promoter region and evidence for polymorphic expression." *Biochemistry* **31**(46): 11595-9.
- Perretti, M. (1997). "Endogenous mediators that inhibit the leukocyte-endothelium interaction." *Trends in Pharmacological Sciences* **18**: 418-425.
- Perretti, M., A. Ahluwalia, et al. (1993). "Lipocortin-1 fragments inhibit neutrophil accumulation and neutrophil-dependent edema in the mouse. A qualitative comparison with an anti-CD11b monoclonal antibody." *J Immunol* **151**(8): 4306-14.
- Perretti, M., N. Chiang, et al. (2002). "Endogenous lipid- and peptide-derived anti-inflammatory pathways generated with glucocorticoid and aspirin treatment activate the lipoxin A4 receptor." *Nat Med* **8**(11): 1296-302.
- Perretti, M., H. Christian, et al. (2000). "Annexin I is stored within gelatinase granules of human neutrophils and mobilised on the cell surface upon adhesion but not phagocytosis." *Cell Biol Int* **24**: 163-174.
- Perretti, M., J. D. Croxtall, et al. (1996). "Mobilizing lipocortin 1 in adherent human leukocytes downregulates their transmigration." *Nat Med* **22**: 1259-1262.
- Perretti, M. and R. J. Flower (1993). "Modulation of IL-1-induced neutrophil migration by dexamethasone and lipocortin 1." *J Immunol* **150**: 992-999.
- Perretti, M. and R. J. Flower (1996). "Measurement of lipocortin 1 levels in murine peripheral blood leukocytes by flow cytometry: modulation by glucocorticoids and inflammation." *Br J Pharmacol* **118**(3): 605-10.
- Perretti, M., S. J. Getting, et al. (2001). "Involvement of the receptor for formylated peptides in the *in vivo* anti-migratory actions of annexin 1 and its mimetics." *Am J Pathol* **158**(6): 1969-73.
- Pfaffl, M. W., G. W. Horgan, et al. (2002). "Relative expression software tool (REST) for group-wise comparison and statistical analysis of relative expression results in real-time PCR." *Nucleic Acids Res* **30**(9): e36.
- Philip, J. G., R. J. Flower, et al. (1998). "Blockade of the classical pathway of protein secretion does not affect the cellular exportation of lipocortin 1." *Regul Pept* **73**(2): 133-9.
- Preece, G., G. Murphy, et al. (1996). "Metalloproteinase-mediated regulation of L-selectin levels on leucocytes." *J Biol Chem* **271**(20): 11634-40.

- Ptasznik, A., A. Traynor-Kaplan, et al. (1995). "G protein-coupled chemoattractant receptors regulate Lyn tyrosine kinase. Shc adapter protein signaling complexes." *J Biol Chem* **270**(34): 19969-73.
- Puechal, X. (2007). "Antineutrophil cytoplasmic antibody-associated vasculitides." *Joint Bone Spine* **74**(5): 427-35.
- Quehenberger, O., Z. K. Pan, et al. (1997). "Identification of an N-formyl peptide receptor ligand binding domain by a gain-of-function approach." *Biochem Biophys Res Commun* **238**(2): 377-81.
- Rabiet, M. J., E. Huet, et al. (2005). "Human mitochondria-derived N-formylated peptides are novel agonists equally active on FPR and FPRL1, while *Listeria monocytogenes*-derived peptides preferentially activate FPR." *Eur J Immunol* **35**(8): 2486-95.
- Radford, D. J., N. T. Luu, et al. (2001). "Antineutrophil cytoplasmic antibodies stabilize adhesion and promote migration of flowing neutrophils on endothelial cells." *Arthritis Rheum* **44**(12): 2851-61.
- Rane, M. J., S. L. Carrithers, et al. (1997). "Formyl peptide receptors are coupled to multiple mitogen-activated protein kinase cascades by distinct signal transduction pathways: role in activation of reduced nicotinamide adenine dinucleotide oxidase." *J Immunol* **159**(10): 5070-8.
- Raynal, P. and H. B. Pollard (1994). "Annexins: the problem of assessing the biological role for a gene family of multifunctional calcium- and phospholipid-binding proteins." *Biochim Biophys Acta* **1197**(1): 63-93.
- Relton, J. K., P. J. Strijbos, et al. (1991). "Lipocortin-1 is an endogenous inhibitor of ischemic damage in the rat brain." *J Exp Med* **174**(2): 305-10.
- Rescher, U., A. Danielczyk, et al. (2002). "Functional activation of the formyl Peptide receptor by a new endogenous ligand in human lung a549 cells." *J Immunol* **169**(3): 1500-4.
- Rescher, U. and V. Gerke (2004). "Annexins--unique membrane binding proteins with diverse functions." *J Cell Sci* **117**(Pt 13): 2631-9.
- Rescher, U., V. Goebeler, et al. (2006). "Proteolytic cleavage of annexin 1 by human leukocyte elastase." *Biochim Biophys Acta* **1763**(11): 1320-4.
- Reville, K., J. K. Crean, et al. (2006). "Lipoxin A4 redistributes myosin IIA and Cdc42 in macrophages: implications for phagocytosis of apoptotic leukocytes." *J Immunol* **176**(3): 1878-88.
- Reynolds, A. R., L. E. Reynolds, et al. (2004). "Elevated Flk1 (vascular endothelial growth factor receptor 2) signaling mediates enhanced angiogenesis in beta3-integrin-deficient mice." *Cancer Res* **64**(23): 8643-50.
- Ritchie, R. H., X. Sun, et al. (2003). "Cardioprotective actions of an N-terminal fragment of annexin-1 in rat myocardium in vitro." *Eur J Pharmacol* **461**(2-3): 171-9.
- Roitt, I. M., P. R. Hutchings, et al. (1992). "The forces driving autoimmune disease." *J Autoimmun* **5 Suppl A**: 11-26.
- Rosales, J. L. and J. D. Ernst (1997). "Calcium-dependent neutrophil secretion: characterization and regulation by annexins." *J Immunol* **159**(12): 6195-202.

- Rosengarth, A. and H. Luecke (2003). "A calcium-driven conformational switch of the N-terminal and core domains of annexin A1." J Mol Biol **326**(5): 1317-25.
- Russell, K. J., J. McRedmond, et al. (1998). "Neutrophil adhesion molecule surface expression and responsiveness in cystic fibrosis." Am J Respir Crit Care Med **157**(3 Pt 1): 756-61.
- Salzer, U., P. Hinterdorfer, et al. (2002). "Ca(++)-dependent vesicle release from erythrocytes involves stomatin-specific lipid rafts, synexin (annexin VII), and sorcin." Blood **99**(7): 2569-77.
- Sautebin, L., G. Cirino, et al. (1992). "Selective inhibition by antiinflamrin-2 of thromboxane B(2) release from isolated and perfused guinea-pig lung." Mediators Inflamm **1**(4): 251-4.
- Sawmynaden, P. and M. Perretti (2006). "Glucocorticoid upregulation of the annexin-A1 receptor in leukocytes." Biochem Biophys Res Commun **349**(4): 1351-5.
- Scannell, M., M. B. Flanagan, et al. (2007). "Annexin-1 and peptide derivatives are released by apoptotic cells and stimulate phagocytosis of apoptotic neutrophils by macrophages." J Immunol **178**(7): 4595-605.
- Scott, D. L. and S. Steer (2007). "The course of established rheumatoid arthritis." Best Pract Res Clin Rheumatol **21**(5): 943-67.
- Selvatici, R., S. Falzarano, et al. (2006). "Signal transduction pathways triggered by selective formylpeptide analogues in human neutrophils." Eur J Pharmacol **534**(1-3): 1-11.
- Sengelov, H., F. Boulay, et al. (1994). "Subcellular localization and translocation of the receptor for N-formylmethionyl-leucyl-phenylalanine in human neutrophils." Biochem J **299** (Pt 2): 473-9.
- Sengelov, H., P. Follin, et al. (1995). "Mobilization of granules and secretory vesicles during in vivo exudation of human neutrophils." J Immunol **154**(8): 4157-65.
- Sengelov, H., L. Kjeldsen, et al. (1993). "Control of exocytosis in early neutrophil activation." J Immunol **150**(4): 1535-43.
- Seo, P. and J. H. Stone (2004). "The antineutrophil cytoplasmic antibody-associated vasculitides." Am J Med **117**(1): 39-50.
- Serhan, C. N. (2002). "Lipoxins and aspirin-triggered 15-epi-lipoxin biosynthesis: an update and role in anti-inflammation and pro-resolution." Prostaglandins Other Lipid Mediat **68-69**: 433-55.
- Shin, E. H., H. Y. Lee, et al. (2006). "Trp-Arg-Trp-Trp-Trp-Trp antagonizes formyl peptide receptor like 2-mediated signaling." Biochem Biophys Res Commun **341**(4): 1317-22.
- Simons, K. and E. Ikonen (1997). "Functional rafts in cell membranes." Nature **387**(6633): 569-72.
- Sizova, L. (2008). "Approaches to the treatment of early rheumatoid arthritis with disease-modifying antirheumatic drugs." Br J Clin Pharmacol **66**(2): 173-8.
- Smalley, D. M. and K. Ley (2005). "L-selectin: mechanisms and physiological significance of ectodomain cleavage." J Cell Mol Med **9**(2): 255-66.
- Smith, C. W. (1993). "Leukocyte-endothelial cell interactions." Semin Hematol **30**(4 Suppl 4): 45-53; discussion 54-5.
- Sohn, J., T. I. Kim, et al. (2003). "Novel transglutaminase inhibitors reverse the inflammation of allergic conjunctivitis." J Clin Invest **111**(1): 121-8.

- Solito, E., H. C. Christian, et al. (2006). "Post-translational modification plays an essential role in the translocation of annexin A1 from the cytoplasm to the cell surface." *Faseb J* **20**(9): 1498-500.
- Solito, E., C. de Coupade, et al. (2001). "Transfection of annexin 1 in monocytic cells produces a high degree of spontaneous and stimulated apoptosis associated with caspase-3 activation." *Br J Pharmacol* **133**(2): 217-28.
- Solito, E., A. Kamal, et al. (2003). "A novel calcium-dependent proapoptotic effect of annexin 1 on human neutrophils." *Faseb J* **17**(11): 1544-6.
- Solito, E., I. A. Romero, et al. (2000). "Annexin 1 binds to U937 monocytic cells and inhibits their adhesion to microvascular endothelium: involvement of the alpha 4 beta 1 integrin." *J Immunol* **165**(3): 1573-81.
- Stegeman, C. A., J. W. Tervaert, et al. (1994). "Anti-neutrophil cytoplasmic antibodies: tools for diagnosis and follow-up in systemic vasculitis." *Ann Med Interne (Paris)* **145**(8): 523-32.
- Stein, J. M. and J. P. Luzio (1991). "Ectocytosis caused by sublytic autologous complement attack on human neutrophils. The sorting of endogenous plasma-membrane proteins and lipids into shed vesicles." *Biochem J* **274** (Pt 2): 381-6.
- Stephens, L., C. Ellson, et al. (2002). "Roles of PI3Ks in leukocyte chemotaxis and phagocytosis." *Curr Opin Cell Biol* **14**(2): 203-13.
- Strand, V. and L. S. Simon (2003). "Low dose glucocorticoids in early rheumatoid arthritis." *Clin Exp Rheumatol* **21**(5 Suppl 31): S186-90.
- Strausbaugh, H. J. and S. D. Rosen (2001). "A potential role for annexin 1 as a physiologic mediator of glucocorticoid-induced L-selectin shedding from myeloid cells." *J Immunol* **166**(10): 6294-300.
- Su, S. B., W. Gong, et al. (1999). "A seven-transmembrane, G protein-coupled receptor, FPRL1, mediates the chemotactic activity of serum amyloid A for human phagocytic cells." *J Exp Med* **189**(2): 395-402.
- Subrahmanyam, P. and B. Dasgupta (2006). "Polymyalgia rheumatica and giant cell arteritis." *Br J Hosp Med (Lond)* **67**(5): 240-3.
- Tato, F. and U. Hoffmann (2008). "Giant cell arteritis: a systemic vascular disease." *Vasc Med* **13**(2): 127-40.
- Tedder, T. F., A. C. Penta, et al. (1990). "Expression of the human leukocyte adhesion molecule, LAM1. Identity with the TQ1 and Leu-8 differentiation antigens." *J Immunol* **144**(2): 532-40.
- Teixeira, M. M., A. M. Das, et al. (1998). "The role of lipocortin-1 in the inhibitory action of dexamethasone on eosinophil trafficking in cutaneous inflammatory reactions in the mouse." *Br J Pharmacol* **123**(3): 538-44.
- They, C., M. Boussac, et al. (2001). "Proteomic analysis of dendritic cell-derived exosomes: a secreted subcellular compartment distinct from apoptotic vesicles." *J Immunol* **166**(12): 7309-18.
- Tiffany, H. L., M. C. Lavigne, et al. (2001). "Amyloid-beta induces chemotaxis and oxidant stress by acting at formylpeptide receptor 2, a G protein-coupled receptor expressed in phagocytes and brain." *J Biol Chem* **276**(26): 23645-52.
- Tsao, F. H., K. C. Meyer, et al. (1998). "Degradation of annexin I in bronchoalveolar lavage fluid from patients with cystic fibrosis." *Am J Respir Cell Mol Biol* **18**(1): 120-8.

- Tuluc, F., J. Meshki, et al. (2003). "Membrane lipid microdomains differentially regulate intracellular signaling events in human neutrophils." Int Immunopharmacol **3**(13-14): 1775-90.
- Turesson, C., W. M. O'Fallon, et al. (2003). "Extra-articular disease manifestations in rheumatoid arthritis: incidence trends and risk factors over 46 years." Ann Rheum Dis **62**(8): 722-7.
- Umekita, K., T. Hidaka, et al. (2009). "Leukocytapheresis (LCAP) decreases the level of platelet-derived microparticles (MPs) and increases the level of granulocytes-derived MPs: a possible connection with the effect of LCAP on rheumatoid arthritis." Mod Rheumatol **19**(3): 265-72.
- van den Berg, W. B., P. L. van Lent, et al. (2007). "Amplifying elements of arthritis and joint destruction." Ann Rheum Dis **66 Suppl 3**: iii45-8.
- VanWijk, M. J., E. VanBavel, et al. (2003). "Microparticles in cardiovascular diseases." Cardiovasc Res **59**(2): 277-87.
- Vergnolle, N., C. Comera, et al. (1997). "Expression and secretion of lipocortin 1 in gut inflammation are not regulated by pituitary-adrenal axis." Am J Physiol **273**(2 Pt 2): R623-9.
- Vong, L., F. D'Acquisto, et al. (2007). "Annexin 1 cleavage in activated neutrophils: a pivotal role for proteinase 3." J Biol Chem **282**(41): 29998-30004.
- Vostal, J. G., A. B. Mukherjee, et al. (1989). "Novel peptides derived from a region of local homology between uteroglobin and lipocortin-1 inhibit platelet aggregation and secretion." Biochem Biophys Res Commun **165**(1): 27-36.
- Walcheck, B., S. R. Alexander, et al. (2003). "ADAM-17-independent shedding of L-selectin." J Leukoc Biol **74**(3): 389-94.
- Walker-Bone, K. and S. Farrow (2007). "Rheumatoid arthritis." Clin Evid (Online) **2007**.
- Walther, A., K. Riehemann, et al. (2000). "A novel ligand of the formyl peptide receptor: annexin I regulates neutrophil extravasation by interacting with the FPR." Mol Cell **5**(5): 831-40.
- Wang, X., Z. P. Hu, et al. (2008). "Giant cell arteritis." Rheumatol Int **29**(1): 1-7.
- Weaver, A. L., R. L. Lautzenheiser, et al. (2006). "Real-world effectiveness of select biologic and DMARD monotherapy and combination therapy in the treatment of rheumatoid arthritis: results from the RADIUS observational registry." Curr Med Res Opin **22**(1): 185-98.
- White, J. M. (1993). "Merging minds on membrane merger." Trends Cell Biol **3**(3): 99-101.
- Wiedmer, T. and P. J. Sims (1991). "Participation of protein kinases in complement C5b-9-induced shedding of platelet plasma membrane vesicles." Blood **78**(11): 2880-6.
- Witko-Sarsat, V., P. Lesavre, et al. (1999). "A large subset of neutrophils expressing membrane proteinase 3 is a risk factor for vasculitis and rheumatoid arthritis." J Am Soc Nephrol **10**(6): 1224-33.
- Wolf, P. (1967). "The nature and significance of platelet products in human plasma." Br J Haematol **13**(3): 269-88.
- Wu, C. C., J. D. Croxtall, et al. (1995). "Lipocortin 1 mediates the inhibition by dexamethasone of the induction by endotoxin of nitric oxide synthase in the rat." Proc Natl Acad Sci U S A **92**(8): 3473-7.

- Yang, Y., M. Leech, et al. (1997). "Antiinflammatory effect of lipocortin 1 in experimental arthritis." Inflammation **21**(6): 583-96.
- Yazid, S., E. Solito, et al. (2009). "Cromoglycate drugs suppress eicosanoid generation in U937 cells by promoting the release of Anx-A1." Biochem Pharmacol **77**(12): 1814-26.
- Ye, R. D., F. Boulay, et al. (2009). "International Union of Basic and Clinical Pharmacology. LXXIII. Nomenclature for the formyl peptide receptor (FPR) family." Pharmacol Rev **61**(2): 119-61.
- Zaffran, Y., H. Lepidi, et al. (1993). "F-actin content and spatial distribution in resting and chemoattractant-stimulated human polymorphonuclear leucocytes. Which role for intracellular free calcium?" J Cell Sci **105** (Pt 3): 675-84.